

Conformation of the Aryl Amine DNA Adduct 2-Amino-3-methylimidazole-
[4,5-f]quinoline *N*²-deoxyguanine in the NarI Endonuclease Recognition
Sequence as Determined by NMR Spectroscopy

By

Kallie Marie Stavros

Dissertation

Submitted to the Faculty of the
Graduate School of Vanderbilt University
in partial fulfillment of the requirements

for the degree of

DOCTOR OF PHILOSOPHY

In

Chemical and Physical Biology

May, 2015

Nashville, Tennessee

Approved:

Michael Stone, Ph.D.

Brandt Eichman, Ph.D.

Frederick Guengerich, Ph.D.

Carmelo Rizzo, Ph.D.

Charles Sanders, Ph.D.

ACKNOWLEDGEMENTS

I would like to acknowledge everyone who provided support and assistance that made my Ph.D. possible. First of all, I want to thank Dr. Michael Stone for all of his patience and guidance throughout the last five years. I would also like to thank each of my committee members for their time and effort: Dr. Carmelo Rizzo, Dr. Fred Guengerich, Dr. Charles Sanders, and Dr. Brandt Eichmann.

Many members of the lab, both past and present, were instrumental in helping me along the way. Dr. Ewa Kowal and Dr. Marta Szulik were always available for help and advice for NMR calculations and sample preparation. Dr. Markus Voehler and Dr. Donald Stec were very willing to provide their assistance with NMR experiments. Dr. Amritaj Patra taught me how to loop crystals. Dr. Surajit Banerjee spent much of his time over the phone and email to troubleshoot the crystallography as well as collecting diffraction data. I also really appreciate the encouragement I received from the rest of the Stone lab, who have made the journey a pleasant one: Dr. Liang Li, Dennis Kuo, Drew Kellum, and Dustin Politica. I worked with several undergraduate students that have been very helpful, including Patrick Donahue and Reneisha Franklin, who assisted with protein expression, and Ruidan Ma and Sam Lazaroff for help with setting up many, many crystal trays. Amy Millsap taught me to run the extension assays and gel polymerization as well as providing good conversation as a collaborator. I would especially like to remember Ed Hawkins, who synthesized my NMR samples and was always a great resource for really getting me started with the IQ project.

I would also like to acknowledge the National Institutes of Health and Center for Molecular Toxicology for funding my project.

Finally, I want to thank my parents, sister, and Ryan who have been enormously supportive and full of encouragement throughout my graduate career.

TABLE OF CONTENTS

	Page
ACKNOWLEDGEMENTS	ii
LIST OF TABLES	vii
LIST OF FIGURES	viii
LIST OF SCHEMES	xi
LIST OF CHARTS	xii
LIST OF ABBREVIATIONS	xiii
Chapter	
I. Introduction	1
Deoxyribonucleic Acid (DNA).....	1
DNA Replication	4
DNA Damage, Repair and Bypass	5
Heterocyclic Amines	10
2-Amino-3-methylimidazo-[4,5-f]quinoline and metabolism	12
NarI Recognition Sequence	14
Structural Biology Techniques for Macromolecules.....	15
X-ray Crystallography of Biological Molecules	17
Using NMR to Understand Oligonucleotides	22
Circular Dichroism	33
Dissertation Statement.....	33
II. Materials and methods	35
Sample Preparation	35
Thermal Melting Experiments.....	37
Circular Dichroism.....	38
NMR Spectroscopy	38
Distance Restraints	39
Restrained Molecular Dynamics Calculations	39
Expression and Purification of Dpo4.....	40
Activity Assay.....	44
Crystallization of DNA:Dpo4 Complexes.....	45
X-Ray Diffraction Data Collection and Processing.....	46
Structure Determination and Refinement	46
III. Solution Structure of N^2 -dG-IQ at the mutagenic hotspot G^3 position in the <i>NarI</i> sequence context.....	48

Introduction	48
Results.....	48
Oligodeoxynucleotide Containing the N^2 -dG-IQ Adduct.....	48
NMR.....	49
Conformational Refinement.....	56
Conformation of the N^2 -dG-IQ Adduct.....	62
Discussion	63
Comparison to the N^2 -Acetylaminofluorene-dG Adduct	65
Comparison to the C8-dG-IQ Adduct.....	66
Structure-Activity Relationships.....	69
Summary	72
 IV. Solution Structure of N^2 -dG-IQ at the mutagenic hotspot G ¹ position in the <i>NarI</i> sequence context.....	 73
Introduction	73
Results.....	73
Circular Dichroism	73
NMR.....	75
IQ Proton Assignments.....	77
Exchangeable Protons	79
Structure Refinement.....	81
Conformation of N^2 -dG-IQ at G ¹	84
Discussion	86
Sequence Dependence of N^2 -dG-IQ in <i>NarI</i>	90
N^2 vs. C8-dG-IQ	91
Summary	92
 V. Conclusions and Future Directions	 94
Conclusions.....	94
Introduction	95
Results.....	96
Activity Assay	96
Crystal Structures of Dpo4:8-oxoG	97
Discussion	98
Future Directions	100
 Appendix	
A. RMD Input Files	101
B. PDB Output Files	104
C. Partial Charges for Modified Base	170
D. Chemical Shifts	171
E. Distance Restraints Files.....	177

LIST OF TABLES

Table	Page
1-1. Characteristic parameters for A, B, and Z DNA	3
1-2. Characteristics for each crystal system	21
3-1. Summary of NOEs observed between <i>N2-dG-IQ</i> adduct protons and oligodeoxynucleotide protons, and their intensities	56
3-2. NMR restraints used for the <i>N2-dG-IQ</i> structure calculations	57
3-3. Structural statistics for the <i>N2-dG-IQ</i> modified duplex.....	61
3-4. Thermal melting temperatures (<i>T_m</i> measurements) of <i>NarI</i> duplexes containing the <i>N2-dG-IQ</i> adducts	70
4-1. Summary of observed NOEs from IQ to DNA and their intensities	79
4-2. Refinement statistics for <i>N2-dG-IQ</i> at G1 position in the <i>NarI</i> sequence	82

LIST OF FIGURES

Figure	Page
1-1. Watson-Crick hydrogen bonding for A) adenine: thymine and B) guanine: cytosine base pairs.....	2
1-2. Structural comparison of A) A-type DNA, B) B-type DNA, and C) Z-type DNA	3
1-3. Types of DNA damage and possible cellular response pathways	6
1-4. Steps by which lesions are recognized and removed in the nucleotide excision repair pathway	9
1-5. Examples of identified HCA compounds	12
1-6. Streisinger slippage mechanism.....	15
1-7. Stages of solutions in relation to the drop concentration and precipitating agent.....	18
1-8. Hanging drop vapor diffusion where the precipitant in the well is more concentrated than the drop	19
1-9. X-ray diffraction pattern	20
1-10. Chemical shifts for unmodified oligonucleotides	26
1-11. The walking region consists of the NOESY walk from aromatic base proton to H1' sugar proton.....	27
1-12. Exchangeable protons observable in NOESY experiments due to participation in hydrogen bonding	30
2-3. Dpo4 elution on HisTrap column	42
2-4. MonoS elution profile of Dpo4.....	43
2-5. SDS-PAGE gel of Dpo4 after final purification step showing intended band at about 41 kDa	44
2-6. Typical crystals of Dpo4 with 8-oxoG modified oligonucleotide.....	46
3-1. Expanded plot of the 250 ms NOESY spectrum showing NOEs between the base aromatic and deoxyribose anomeric protons of the N2-dG-IQ <i>modified</i> duplex	50
3-2. Expanded plots of the NOESY spectrum, showing the NOEs between the exchangeable imino and amino protons of the N2-dG-IQ- <i>modified</i> duplex	51
3-3. 1-D spectra of imino exchangeable region at different temperatures	52

3-4. Expanded tile plot of the 250 ms NOESY spectrum showing the assignments of the IQ ring protons.....	53
3-5. Chemical shift perturbations of the deoxyribose H1' protons (grey) and the pyrimidine H6 or purine H8 aromatic protons (black), for the <i>N2-dG-IQ</i> modified duplex.....	54
3-6. Superposition of ten potential energy minimized structures emergent from the rMD calculations of the <i>N2-dG-IQ</i> modified duplex, using distance restraints from the 250 ms NOESY data.....	58
3-7. Sixth root residuals (R1x) calculated using complete relaxation matrix calculations from the average of ten structures emergent from the rMD calculations of the <i>N2-dG-IQ</i> modified duplex.....	60
3-8. Expanded view of the average structure calculated from ten structures emergent from the rMD calculations of the <i>N2-dG-IQ</i> modified duplex, showing base pairs C6:G19, X7:C18, and C8:G17.....	62
3-9. Expanded views of the average structure calculated from ten structures emergent from the rMD calculations of the <i>N2-dG-IQ</i> modified duplex.....	68
4-1. A) UV and B) CD spectra for <i>N2-dG-IQ</i> at G1 and G3 as well as the unmodified <i>NarI</i> sequence.....	75
4-2. Plot of NOESY spectrum with 150 ms mixing time showing connectivities between base aromatic protons to deoxyribose anomeric protons for adduct <i>N2-dG-IQ</i> located at G1 position.....	77
4-3. Plot of NOESY spectrum showing IQ ring proton assignments.....	78
4-4. 1-D spectrum of imino region from 5 °C – 15 °C showing the assignment of X4 N1H proton.....	80
4-5. NOESY plot with exchangeable proton assignments for <i>N2-dG-IQ</i> modified duplex at position G1.....	81
4-6. Sixth root residuals (R1x) calculated using complete relaxation matrix calculations from the average of ten structures emergent from the rMD calculations of the <i>N2-dG-IQ</i> modified duplex.....	83
4-7. Ten best fitting structures calculated from NOESY data with 150 ms mixing time superimposed.....	84
4-8. Expanded view of calculated structure from major groove, showing base pairs C3:G22, X4:C21, G5:C20.....	85
4-9. View from top of duplex looking at base-stacking interactions.....	88
5-1. Extension of unmodified oligonucleotide by Dpo4.....	97

5-2. The active site of Dpo4 containing an 8-oxoG modified DNA sequence (modified base shown in red) paired opposite dC. The arrow highlights residue R332.....98

LIST OF SCHEMES

Scheme	Page
1-1. Sugars and amino acids react at high temperatures through the Maillard reaction	11
1-2. Metabolism pathway for IQ	13
1-3. Diagram of how the energy states of spin-up and spin-down depend on the magnetic field	24
1-4. Strategy for refining oligonucleotide structures using solution NMR	32
2-1. Synthesis schematic for <i>N2-dG-IQ</i> phosphoramidite	35

LIST OF CHARTS

Charts	Page
3-1. Adduct structures: A. Structure of 2-amino-3-methylimidazo[4,5-f]quinolone (IQ). B. Structure of the <i>N2-dG-IQ</i> adduct, showing the numbering of guanine base and IQ protons. C. Structure of the C8-dG-IQ adduct. D. Structure of the <i>N2-dG-AAF adduct</i> . E. The duplex containing the <i>NarI</i> sequence, showing the numbering of the nucleotides. The <i>N2-dG-IQ</i> adduct is positioned at X7, which corresponds to the G3 frameshift-prone position of the <i>NarI</i> sequence.....	65

LIST OF ABBREVIATIONS

1-D	1-dimensional
2-D	2-dimensional
3-D	3-dimensional
8-oxoG	8-dihydro-8-oxoguanine
AAF-dG	N-(2-deoxyguanosin-8-yl)-2-acetylaminofluorene
AF-dG	N-(2-deoxyguanosin-8-yl)-2-aminofluorene
CORMA	complete relaxation matrix analysis
COSY	correlated spectroscopy
dA	deoxyadenosine
dC	deoxycytosine
DNA	deoxyribose nucleic acid
dNTP	deoxyribonucleic triphosphate
Dpo4	<i>Sulfolobus solfataricus</i> P2 DNA polymerase IV
dT	deoxythymidine
EDTA	ethylenediaminetetraacetic acid
FPLC	fast protein liquid chromatography
HCA	heterocyclic amine
HPA	hydroxypicolinic acid
hpol	human DNA polymerase
IPTG	Isopropyl β -D-1-thiogalactopyranoside
IQ	2-amino-3-methylimidazo-[4,5-f]quinoline
LB	Luria-Bertani
MAD	multiple-wavelength anomalous dispersion
MALDI-TOF	matrix-assisted laser desorption ionization- time of flight
MIR	multiple isomorphous replacement

MR	molecular replacement
NaCl	sodium chloride
NER	nucleotide excision repair
NMR	nuclear magnetic resonance spectroscopy
NOESY	nuclear Overhauser effect spectroscopy
PEG	polyethylene glycol
ppm	parts per million
rMD	restrained molecular dynamics
rmsd	root mean-square deviation
RP-HPLC	reverse phase- high performance liquid chromatography
RPA	replication protein A
SAD	single-wavelength anomalous dispersion
SDS-PAGE	sodium dodecyl sulfate polyacrylamide gel electrophoresis
TFIIH	transcription factor IIH
T_m	melting temperature
UV	ultraviolet
XP	xeroderma pigmentosum

Chapter I

INTRODUCTION

Deoxyribonucleic Acid (DNA)

DNA is the genetic material responsible for coding for proper functioning and development of all living organisms. It does this through a genetic alphabet composed of four nitrogenous bases: adenine (A), cytosine (C), guanine (G), and thymine (T). These bases are attached to a deoxyribose ring and polymerized through a phosphodiester backbone. DNA is typically found in a double helix, where the two antiparallel strands form Watson-Crick hydrogen bonding and coil around each other about an axis¹. Hydrogen bonding typically occurs between two sets of base pairs, A-T and G-C, shown in Figure 1-1. James Watson and Frances Crick first proposed this structure in 1953^{2,3}, followed by evidence from H.R. Wilson that it does exist in living organisms⁴. The canonical structure led them to believe that it “suggests a possible copying mechanism for genetic material.”²

Three forms of DNA shown in Figure 1-2 have been identified. The typical right-handed helix discovered by Watson and Crick is known as B DNA. This is the most common type found in organisms at neutral pH and physiological salt concentrations. However, A-DNA⁵ and Z-DNA^{5,6} have also been observed in organisms. A form DNA differs by the sugar conformation where it adopts a C3' endo conformation instead of a C2' endo like B-DNA⁷, which results in shorter linkages of the phosphate backbone and a more compact helix compared to B-DNA⁸. This form is more favorable at high salt concentrations⁹. Z-DNA is the only left-handed helix and tends to be found in CpG islands and involved in transcription regulation¹⁰. The alternating purine-pyrimidine pattern creates a zig-zag pattern. The conformation of Z-DNA is drastically different from either A or B in that guanine bases are

typically found in the syn conformation¹¹. A comparison of duplex geometries can be found in Table 1-1.

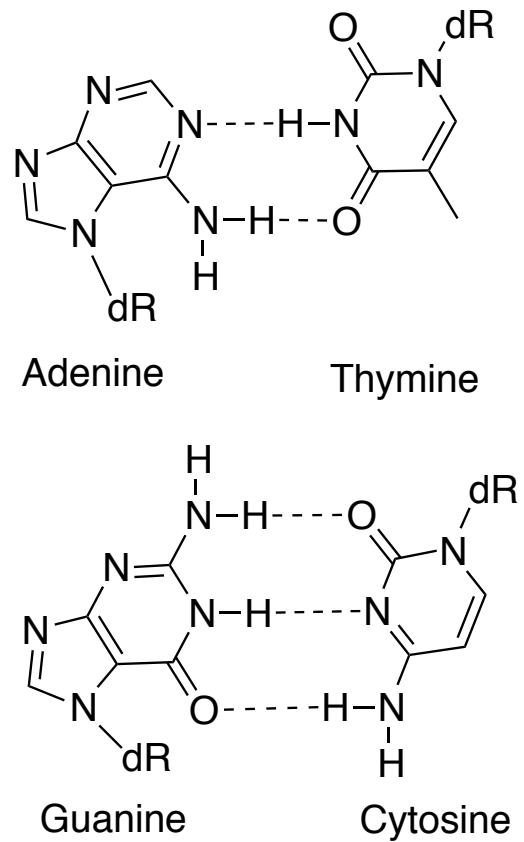


Figure 1-1. Watson-Crick hydrogen bonding for A) adenine: thymine and B) guanine: cytosine base pairs.

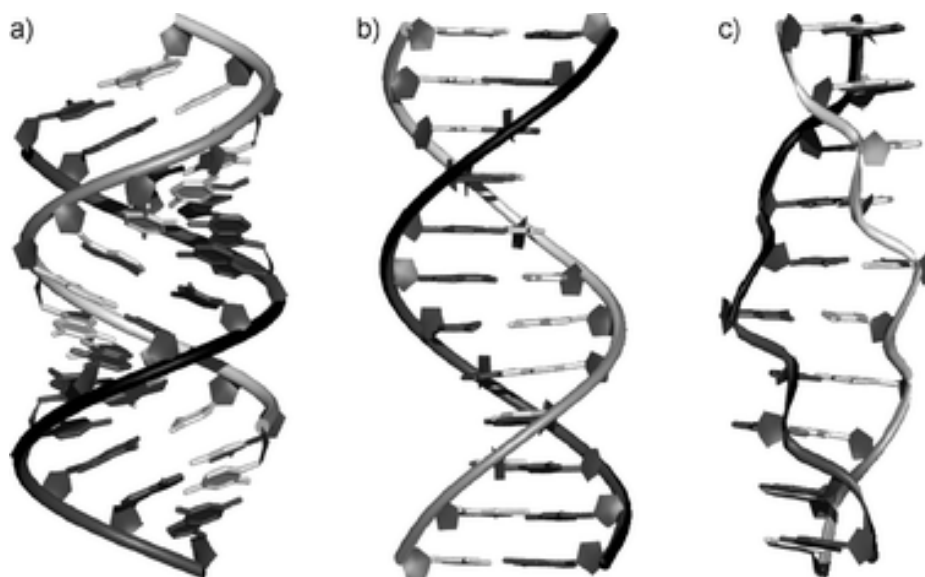


Figure 1-2. Structural comparison of A) A-type DNA, B) B-type DNA, and C) Z-type DNA (Reprinted with permission from reference ¹², Copyright (2010) Royal Society of Chemistry).

B-DNA has a number of characteristics that are important for interactions with other biological molecules. The double helical structure results in a wider major groove and a narrower minor groove. The major groove is easily accessible for many DNA binding proteins, while the minor groove provides a more hydrophobic environment that is less solvent exposed

Table 1-1. Characteristic parameters for A, B, and Z DNA¹³.

	A DNA	B DNA	Z DNA
Handedness	Right	Right	Left
BP per turn	11	10	12
Rise per pair (Å)	2.56	3.4	3.7
Rotation per pair (°)	33	36	-30
Helical diameter (Å)	23	19	18
Propeller twist (°)	18	16	0

DNA Replication

The order of these bases create a genetic code, where an open reading frame can be transcribed into mRNA and later translated into proteins, required for functioning of living organisms. Three bases are required to code for each amino acid.

In order for cells to divide, proper replication of the genetic code must occur for biological functions to be conserved. This process typically requires high fidelity polymerases that strongly favor insertion of correct nucleotide. Errors for these polymerases are rare, making a mistake an estimated one for every one million bases that are copied^{14,15}. Several polymerases are also equipped with a 3'-5' exonuclease activity which can remove incorrect nucleotides in the event of misincorporation. These polymerases are members of the B family of polymerases, including δ , and ϵ as well as α , but lacks exonuclease activity, and are responsible for the bulk of DNA replication. During the process of replication in eukaryotes, an MCM2-7 helicase complex¹⁶ must separate the two strands into lagging and leading ssDNA. Synthesis is then initiated by the pol α -primase complex. A polymerase can subsequently bind to the leading strand, inserting the new complementary code in a continuous fashion. The lagging strand, however, is replicated in a series of discontinuous patches of approximately 250 base pairs known as Okazaki fragments. Each fragment must be initiated by pol α -primase activity¹⁷.

There are also other polymerases with more specialized roles important for replication of the nuclear genome. These include a B-family polymerase, ζ , as well as Y-family polymerases η , ι , κ , and Rev1. These polymerases are responsible for bypassing DNA lesions that block the replicative polymerases. The active sites for these polymerases are

much larger, in order to accommodate the extra bulk of the lesions, which this also makes the active site more solvent accessible and lack exonuclease activity. These characteristics make the polymerases more error prone.

Replication fidelity seems to be facilitated by hydrogen bonding ability between the template and incoming dNTP¹⁸. One idea to explain this is enthalpy-entropy compensation¹⁹, which requires water molecules that are hydrogen-bonded to the base of the dNTP to be desolvated before hydrogen bonding to the template can occur, thus decreasing the entropy of the system. This is consistent with the solvent accessible, error-prone active sites of Y-family polymerases, which behave as though enthalpy-entropy compensation does not contribute to selectivity as demonstrated by kinetic insertion analysis of non-polar base analogs by yeast pol η ²⁰.

Nucleotide selectivity also results from the shape complementarity of the newly formed base-pair in the binding pockets^{21,22}. Mismatches would likely alter the geometry of the base pair^{23,24}, which would otherwise fit snugly in the active site. However, the mismatch is presumed to result in steric clashes that would reduce the binding affinity of the incorrect dNTP and reduce the catalysis for proper phosphodiester bond formation.

DNA Damage, Repair and Bypass

DNA is subjected to damaging agents on a daily basis. Sources of damage include endogenous factors, such as oxidative damage or deamination, and exogenous causes, including toxic chemicals and radiation²⁵. Damaging agents are generally metabolized, resulting in a reactive species that subsequently react with DNA. On average, somewhere between 10,000 to 1,000,000 lesions may form on any given day, where approximately

10,000 lesions alone could be the result of various cellular processes²⁶. DNA damage can lead to mutations, which is the initial step in carcinogenesis. Organisms have developed systems to prevent carcinogenesis from occurring. There are a number of pathways in mammalian cells designed to remove potentially dangerous lesions. These pathways include mismatch repair²⁷, base excision repair²⁸, and nucleotide excision repair²⁹. Some pathways are specialized for specific types of DNA damages; however, proteins involved in each repair process may have overlapping functions in other pathways.

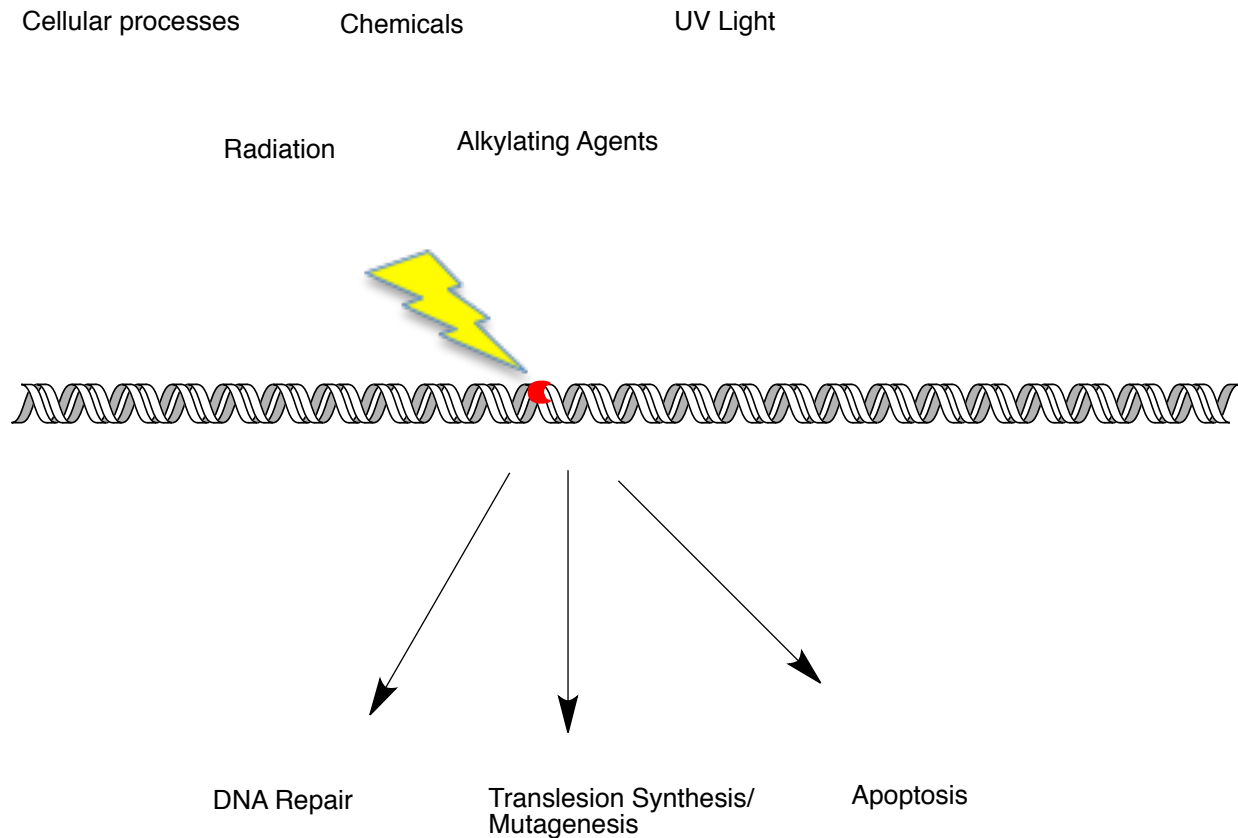


Figure 1-3. Types of DNA damage and possible cellular response pathways.

UV radiation DNA damage products are known substrates of the nuclear excision repair pathway (NER). This was discovered from studies of people diagnosed with

xeroderma pigmentosum, or a disease involving deficient activity of one or more of the proteins involved in the NER pathway, are highly sensitive to UV exposure and become prone to skin cancer³⁰. This pathway is involved in removing much larger adducts that other pathways may not be able to repair. Human NER requires the orchestration of many proteins to recognize, remove, and repair the damaged DNA. There are two types of NER pathways: transcription coupled repair and global genome repair, which only differ in the initial recognition process.

There are a number of characteristics induced by DNA lesions that are believed to recruit NER proteins to the lesion site. These include DNA unwinding, loss of hydrogen bonding or change in base-pairing geometry, and/or thermal instabilities due to reduced base stacking. The XPC, RAD23B, and centrin 2 protein complex is thought to recognize distortions in the helix induced by a wide array of damage^{31,32}, while XPE-binding factor more likely recognizes UV radiation damage³³ and stimulates binding of XPC^{34,35}. The XPC complex binds to the lesion site and recruits more proteins to verify the presence of the lesion³⁶. It does this by associating with transcription initiation factor IIH (TFIIH) complex³⁷, which is comprised of ten protein subunits. The complex consists of two DNA helicases and TFIIH basal transcription factor complex helicase subunits XPB and XPD that extend the distorted lesion area and likely verify the lesion³⁸, while XPA is thought to be able to identify altered chemical structures of bases³⁹. When the TFIIH complex is loaded on XPC, it performs a 5'→3' scan of the ssDNA⁴⁰ and the archaeal orthologue of XPD appears to form an internal channel, where undamaged ssDNA can slide through but damage does not^{41,42}. When TFIIH binds to XPC on the damaged DNA, the CDK-activating

kinase subcomplex (CAK) dissociates from TFIIH, which is only essential for the transcription activity of TFIIH but not necessary for repair⁴³.

Once the lesion has been verified, it must be excised in order to be repaired. The excision is conducted by structure-specific endonucleases, XPF-ERCC1 and XPG, that are able to remove about 22-30 nucleotides around the site of damage, leaving a single-stranded gap⁴⁴. Proper excision is coordinated by the XPA, XPG and replication protein A (RPA)⁴⁵ at the location identified by XPC and verified by TFIIH. XPF-ERCC1 is recruited through interactions with XPA⁴⁶ and activated by the presence of XPG to make the 5' excision⁴⁷. Before the XPG-mediated 3' excision is made, gap filling begins in order to prevent DNA-damage signaling⁴⁸. The gap-filling synthesis can be done by a high fidelity DNA polymerase, usually determined by the proliferative status of the cell⁴⁹. Once repaired, replication and normal cell functioning can continue. Figure 1-3 depicts the series of steps involved in the NER pathway. The NER pathway recognizes the widest variety of DNA damage. It does not detect a specific lesion but instead recognizes changes to the DNA induced by the lesion, such as unwinding and bending, and is probably the most accurate method of repair due to the extensive lesion verification process before removal.

If a repair pathway does not recognize the damage, the cell must have a way to replicate the damaged DNA base, or replication will stall and apoptosis will be induced. Y-family polymerases are typically recruited to bypass lesions, since replicative polymerases cannot accommodate large adducts in their active site. Y-family polymerases can often bypass the lesion; however, many times it will insert an incorrect base opposite the adducted base. When the misinsertion occurs, this results in a mutation. If a mutation

occurs in a critical gene, such as one that regulates cell proliferation, carcinogenesis may be induced if the function of the gene is affected.

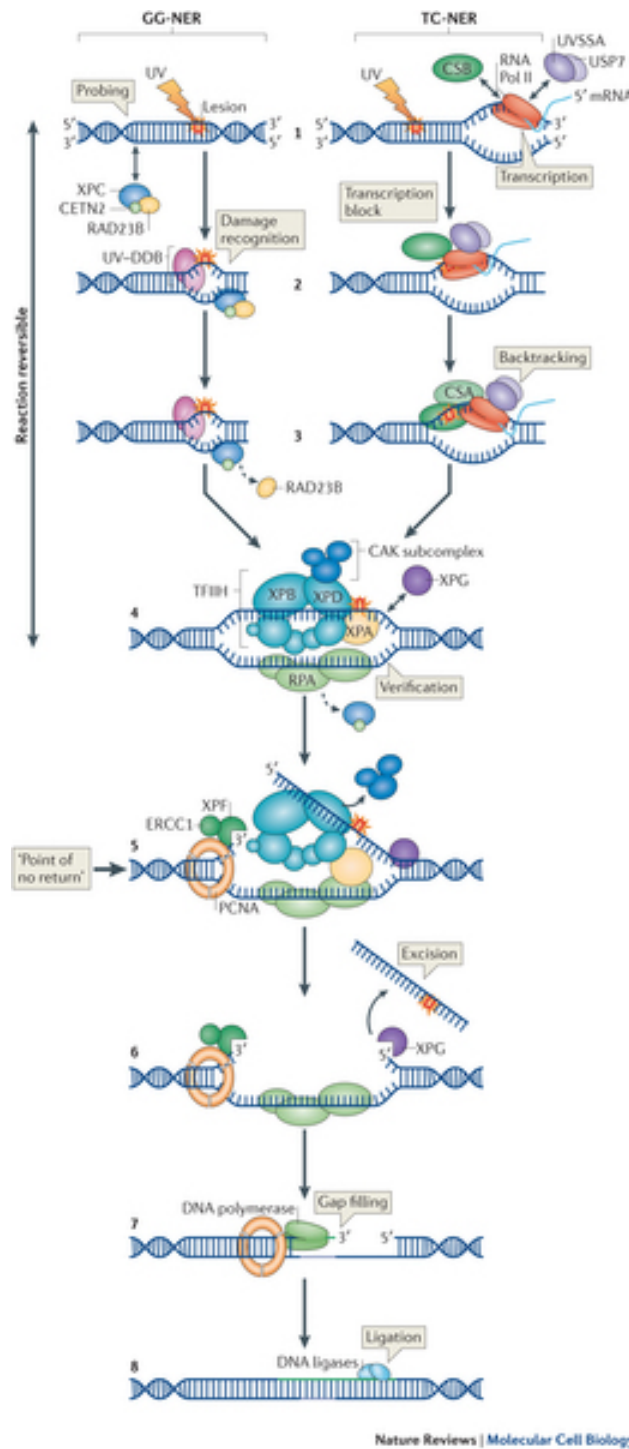
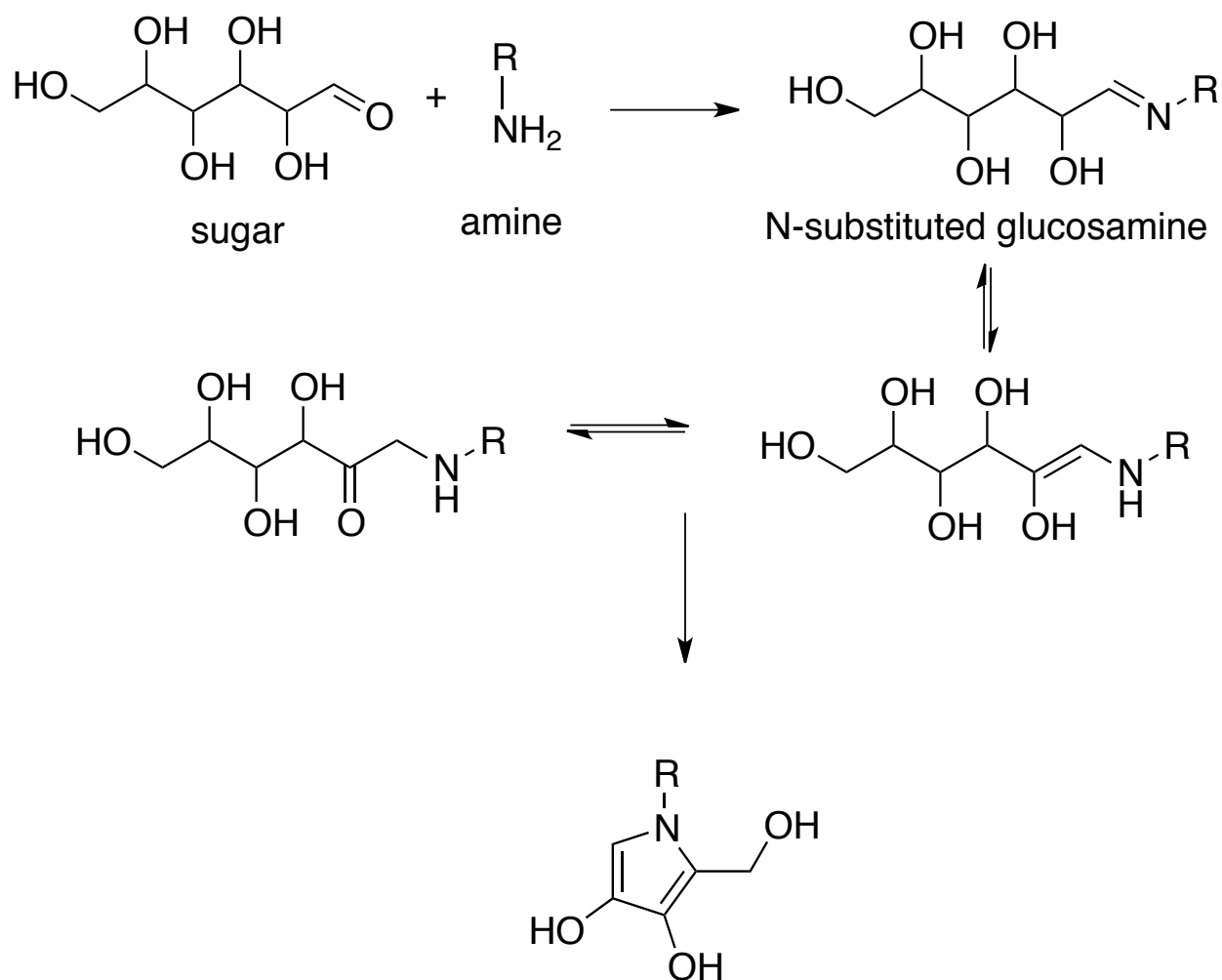


Figure 1-4. Steps by which lesions are recognized and removed in the nucleotide excision repair pathway. Reprinted with permission from reference⁵⁰, Copyright (2014) Nature Publishing Group.

Heterocyclic Amines

Heterocyclic amines (HCA) are a class of compounds that form in high temperatures when cooking meat through the Maillard reaction^{51,52}. The reaction causes amino acids to react with sugars, which is typically induced at high temperatures above 300 °C. However, the reaction could occur at lower temperatures in meats with higher concentrations of amino acids and sugars. Incidentally, the Maillard reaction is also responsible for the browning that occurs during cooking as well as the enticing aroma that emanates from the cooking meat⁵² (Scheme 1-1). Approximately more than twenty HCA compounds have been identified. As a class of compounds, they have proved to be mutagenic in Ames assays as well as mammalian *in vitro* and *in vivo* studies. About 25-30% of cancers result from inflammation, smoking, and dietary factors^{53,54}. While HCA are difficult to definitively link to human carcinogenesis, they are believed to play a role in pancreatic⁵⁵, colon⁵⁶, breast⁵⁷ and prostate⁵⁸. Studies evaluating HCA formation in meats have been ongoing for over twenty years. Many HCA are classified as either 2A (probable human carcinogens) or 2B (possible human carcinogens) compounds by the International Agency for Research on Cancer (IARC), though many believe these should be upgraded to 1A carcinogens. Methods to reduce HCA intake have already been suggested, such as avoiding cooking meat over an open flame⁵⁹, flipping meat often⁶⁰ or microwaving⁶¹ as well as marinades or cooking agents rich in polyphenols^{57,62,63} have all been shown to reduce the formation of HCAs.



Scheme 1-1. Sugars and amino acids react at high temperatures through the Maillard reaction. The carbonyl group on a sugar can react with the amino group to form an N-substituted glycosylamine. The glycosamine undergoes Amadori rearrangement to produce a ketosamine. The ketosamine can react in many possible ways. The products of these reactions can also undergo further reactions for many possible products.

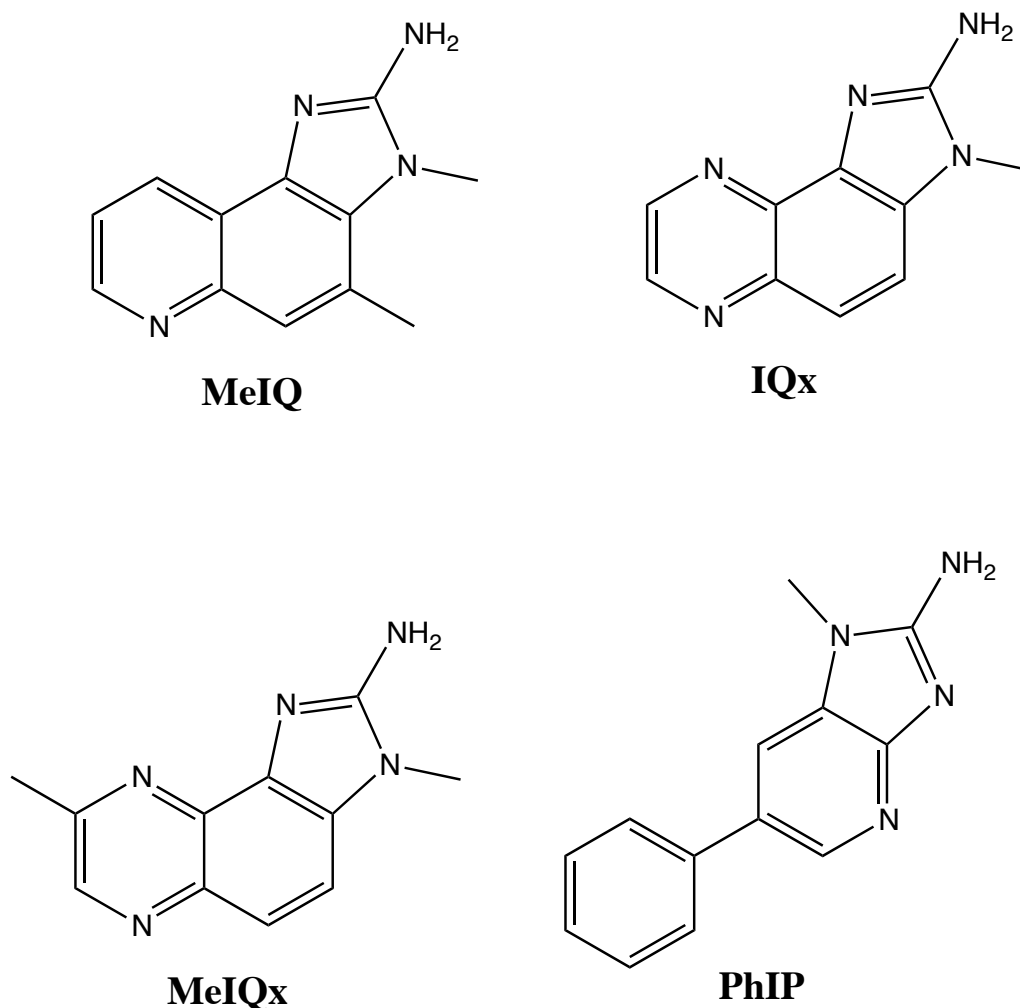
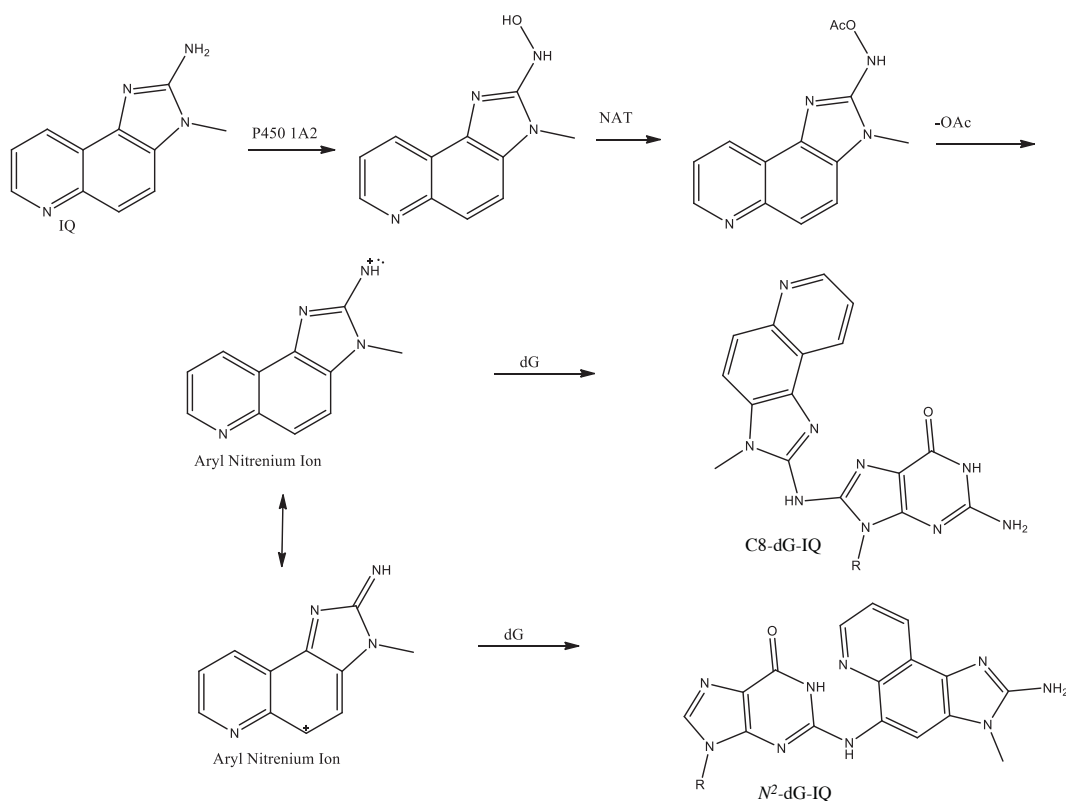


Figure 1-5. Examples of identified HCA compounds.

2-Amino-3-methylimidazo-[4,5-f]quinoline and metabolism

2-Amino-3-methylimidazo-[4,5-f]quinoline (IQ) is one of the most mutagenic of the characterized HCA compounds. IQ is classified as a class 2A carcinogen by the IARC⁶⁴, the highest classification of any HCA. Many animal studies have been done that indicated IQ is carcinogenic in animals. One study exposed rats through intragastric intubation and found formation of tumors in mammary glands, liver and ear ducts⁶⁵. Another study fed cynomolgus monkeys IQ and observed hepatocellular carcinomas⁶⁶.

IQ is metabolized by cytochrome P450, primarily 1A2, while cytochromes P450 1A1, 1B1, and 3A4 may be involved to a lesser extent⁶⁷. P450 enzymes oxidize the exocyclic amino group to a hydroxylamine. Tissues with active N-acetyltransferase (NAT1 and NAT2) and sulfotransferase enzymes⁶⁸ catalyze the acetylation of the hydroxyl group. The reaction can continue without transferase enzymes under acidic conditions. The hydroxylamine may also become protonated, resulting in the loss of this group through solvolysis, resulting in a reactive aryl nitrenium ion. However, the reaction is much more efficient with transferase enzyme catalysis; thus tissues with active NAT2 activity tend to be more prone to IQ adduction.



Scheme 1-2. Metabolism pathway for IQ.

NarI Recognition Sequence

The *NarI* recognition DNA sequence has been frequently used in relationship to understanding mutagenicity of aromatic amines⁶⁹⁻⁷¹. This sequence consists of a GC dinucleotide repeat, G¹G²CG³CC, which has been observed to exhibit sequence dependent mutagenic properties in *Escherichia coli* (*E. coli*)⁷². Repeat sequences in general have been observed to produce frameshift mutations with much higher frequencies than non-repeat sequences⁷³⁻⁷⁵. The *NarI* sequence codes for one of two of the proteins making up the γ subunit of a nitrate reductase enzyme that allows the *E. coli* to use nitrate as an electron acceptor during anaerobic conditions. It is a hotspot for frameshift mutations, which has displayed a mutagenic frequency of 10^7 in *E. coli* over background when G³ is modified by the aryl amine adduct N-2-acetylaminofluorene (AF)⁷⁶. The frameshift mutation in *E. coli* could reduce the ability of the *NarI* enzyme to bind to the membrane and possibly reduce binding of the heme since this function is associated with the γ subunit⁷⁷.

In 1966, Streisinger had predicted that repeat sequences would be hotspots for mutations^{78,79}. He hypothesized that either the template or the daughter strand would be able to slip, resulting in a misalignment of the duplex, thus, the occurrence of in frameshift mutations (Figure 1-5)⁸⁰. The Ames tester strain TA98 contains an island of (CpG)₄ has verified the idea of his hypothesis.

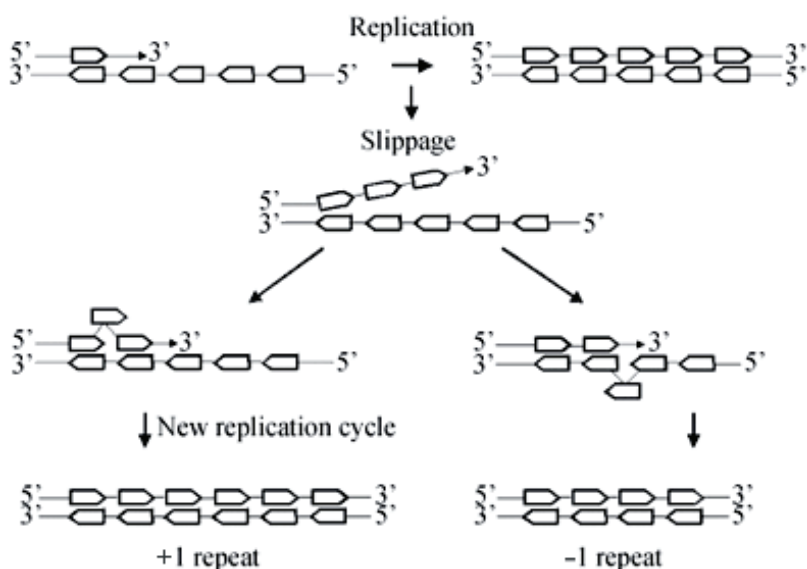


Figure 1-6. Streisinger slippage mechanism. Reprinted from reference ⁸¹.

Studies also looked at the sequence effect of the *NarI* sequence on the NER pathway in *E. coli*⁸². The incision rates of the C8-AF-dG and C8-AAF-dG by UvrABC were monitored at the G¹, G² and G³ sites in the *NarI* recognition sequence. Rates of incision appeared to be modulated by sequence effect, where the AF adduct was most efficiently cleaved at the G³ and G¹ sequence contexts. The AAF adduct, however, was incised more efficiently at the G¹ and G² sites. The incision efficiency can be correlated to the conformers present, which seems to be dictated by the sequence context.

Structural Biology Techniques for Macromolecules

Structural studies can be an important tool for understanding how biological molecules, such as proteins, DNA, lipids, etc., function. A number of tools have been developed to allow for high-resolution structures for macromolecules to be determined.

The most widely used methods are nuclear magnetic spectroscopy (NMR) and x-ray crystallography.

X-ray crystallography has long been the standard for structure determination. X-ray crystallography can be used for small molecules to macromolecules with no known size restrictions. The only requirement is that they form a stable crystal lattice. Good quality crystals can diffract with a resolution less than 1 Å. However, such a method requires electron density, and hydrogen atoms are not visible in the diffraction pattern. Flexible pieces of molecules may exhibit low density as well and be difficult to place. Also, it is not well known if crystal-packing forces could alter the native structure.

NMR has been considered an alternative to x-ray crystallography for years, but is really a complementary technique to crystallography. However, there is a size limitation to molecules that can be used in NMR. Typically molecules smaller than 40 kDa can be used for structural determination. Larger molecules may be used to obtain certain information, such as global folding; however, in order to obtain this information, a high amount of deuteration is required, meaning a loss of other important structural information as a result. Therefore, it is not likely a full structure can be determined from such large molecules. The largest structure determined by NMR is the 82 kDa *E. coli* protein malate synthase G, which also used small angle x-ray scattering (SAXS) data to improve the resolution⁸³. The benefits of NMR include being able to leave the molecules in possibly more native conditions in the solution state, if soluble; although solid state NMR is popular for nonsoluble molecules like membrane proteins. Also, hydrogen atoms are NMR active, which is often another benefit for studying biological molecules such as DNA.

X-ray Crystallography of Biological Molecules

Long considered the gold standard of structural biology, x-ray crystallography can be the simplest way to study large proteins and protein complexes in atomic or near atomic resolution. While x-ray crystallography for structure determination of small molecules has been used since 1913 after the structure of NaCl was determined⁸⁴, it was not until 1950 that it was used by Sir John Kendrew to determine the structure of the first protein, sperm whale myoglobin⁸⁵, earning him a Nobel Prize in Chemistry in 1962. Over the last 30 years, the number of structures determined by x-ray crystallography has increased exponentially, with currently more than 93,000 structures uploaded to the PDB to date⁸⁶. Unlike NMR, there are no size restrictions for crystallography. A molecule typically just has to retain a stable structure under conditions that allow for crystal formation. However, the larger the molecule, the harder it may be to resolve individual atoms.

In macromolecular x-ray crystallography, highly purified samples must be obtained in order to grow crystals. In order to induce nucleation, the sample must be concentrated, generally in a supersaturated state, and allowed to grow over time as the solubility of the sample decreases. Figure 1-7 depicts the states of the sample as a function of concentrations. The vapor diffusion method of growing crystals is based on this curve, where the precipitant should not encourage too much nucleation, but rather growth over time without reaching the precipitation stage too quickly⁸⁷.

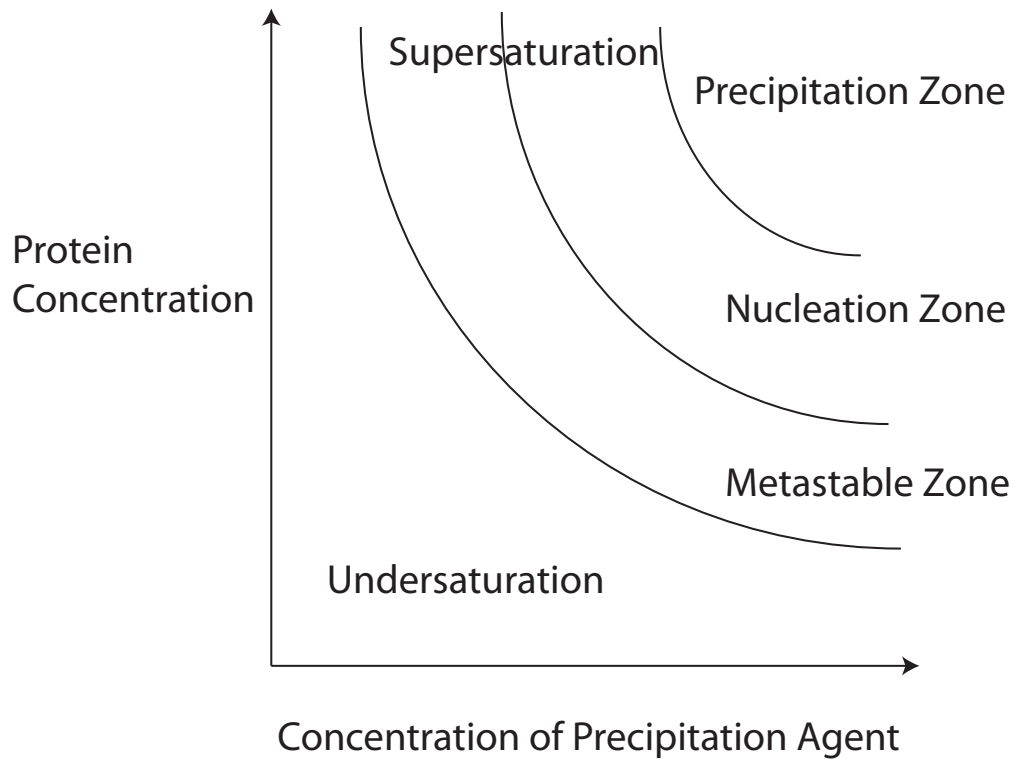


Figure 1-7. Stages of solutions in relation to the drop concentration and precipitating agent.

Figure 1-8 is an example of the hanging drop vapor diffusion method, commonly used for growing protein crystals. Other methods include sitting drop and microdialysis. Here the sample is combined with a precipitant and equilibrated against a reservoir of the precipitant. As vapor diffuses from the reservoir to the drop, the sample concentration will reach the nucleation zone and crystals begin to form. The sample concentration in the drop decreases while crystals are forming, reaching the metastable zone, allowing the crystals to grow over a period of days to months. Conditions are optimized until sizable crystals are formed.

Once the sample does crystallize, the crystals are mounted in loops, flash frozen in liquid nitrogen and ready to be studied by x-rays. X-rays are high energy electromagnetic

radiation with a small wavelength of 0.1-100 Å, with the typical wavelength for crystallography being about 1 Å. These can be generated from accelerating electrons, either from an in house source or synchrotron. When they are focused into a beam, the crystal can be subjected to the beam of x-rays. The goniostat allows the crystal to be properly aligned in the x-ray beam and kept there as the crystal is rotated. The distance between the detector and the crystal must be known and can be adjusted for desired resolution since the resolution is based on the diffraction angles. The greater the diffraction angles, the better the resolution of spots. This is based on the Bragg law defined as:

$$2d \sin \theta = n\lambda$$

where d is the spacing between the planes, θ is the diffraction angle between the incident ray and diffraction planes, n is an integer and λ is the wavelength of the x-ray beam.

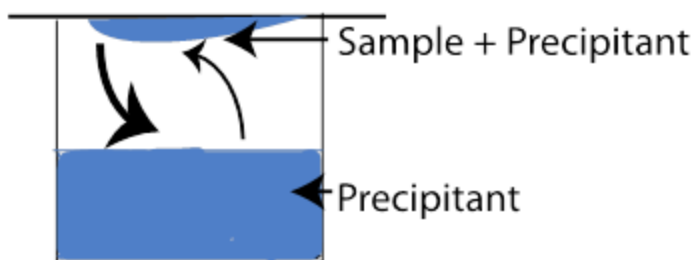


Figure 1-8. Hanging drop vapor diffusion where the precipitant in the well is more concentrated than the drop, inducing solvent from the drop to diffuse faster than from the well to the drop and promoting supersaturation of the drop.

When the crystal is exposed to the x-ray beam, the beam scatters when in proximity to electron-rich atoms, producing an observable pattern of reflections on the detector, such as in Figure A-3. The relative intensities of the reflections correspond to the arrangement of the molecules in the crystal. The spacings are dependent on the size of the molecule. The

intensities correlate to both the amplitude of the diffracted waves as well as the phase difference. The amplitudes can be calculated by the square root of the intensities⁸⁸. The phase cannot so easily be determined and, thus, is referred to as solving the phase problem. Reflections should be recorded as the crystal is rotated up to 180°, depending on symmetry, in order to understand the 3-D structure. The data can then be processed.

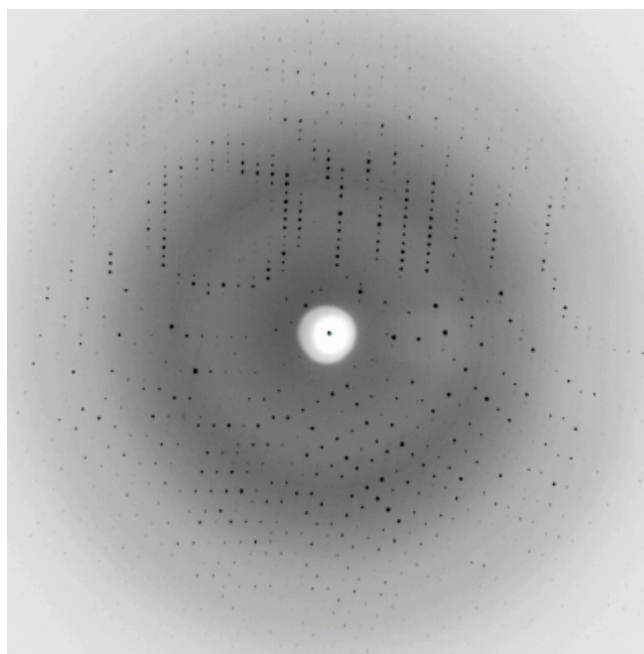


Figure 1-9. X-ray diffraction pattern.

The collected data can be analyzed to determine unit cell dimensions, crystal system and space group. The unit cell is described by lengths a , b and c and angles α , β and γ . The unit cell shape defines the crystal system. Seven crystal systems are possible and are described in Table 1-2. The space group is determined by the diffraction pattern symmetry. A total of 230 space groups exist, however, only 65 of these are possible for chiral molecules.

Table 1-2. Characteristics for each crystal system.

Crystal System	Conditions of cell geometry	# of space groups
Triclinic	$a \neq b \neq c, \alpha \neq \beta \neq \gamma$	2
Monoclinic	$a \neq b \neq c, \alpha, \gamma = 90^\circ, \beta \neq 90^\circ$	13
Orthorhombic	$a \neq b \neq c, \alpha = \beta = \gamma \neq 90^\circ$	59
Tetragonal	$a = b \neq c, \alpha = \beta = \gamma = 90^\circ$	68
Rhombohedral	$a = b = c, \alpha = \beta = \gamma \neq 90^\circ$	25
Hexagonal	$a = b \neq c, \alpha, \beta = 90^\circ, \gamma = 120^\circ$	27
Cubic	$a = b = c, \alpha, \beta, \gamma = 90^\circ$	36

There are three commonly used methods for solving the phase problem for larger proteins: Molecular replacement (MR)^{89,90}, anomalous x-ray scattering (MAD or SAD)⁹¹ and multiple isomorphous replacement (MIR)⁸⁹. MR is most commonly used if a homologous structure is available. It is the simplest method since the coordinates and phases of the previously determined structure are used to calculate the new electron density map. The map can then be used for structure determination.

MAD or SAD is usually the next option when a homologous structure is not available. The phases can be solved using a single crystal. In MAD, the crystal is subjected to the x-ray beam multiple times at different wavelengths and allow for direct solution of the phase problem by measuring the dispersive differences, if the crystal is stable enough to remain in the beam that long⁹². SAD, on the other hand, uses a single dataset at a single wavelength. Both work best if an atom in the protein can be substituted for a slightly heavier one, for instance the sulfur in methionine to a selenomethionine⁹³.

MIR requires the crystal is grown in or soaked in a solution containing heavy, electron-rich atoms that will incorporate in the crystal. The difference between scattering amplitudes caused by the presence of the heavy atom allows the phases to be solved if the

atom does not change the conformation of the protein or crystal shape⁹⁴. MIR, however, requires at least two data sets: one of the sample alone and one with the heavy atoms.

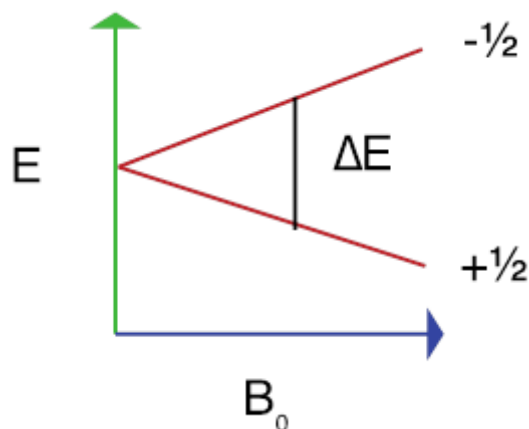
Once the phase problem has been solved, the intensities of the reflections and the phases can be converted to a density map by using the mathematical technique Fourier transform. The electron density map forms a 3-D contour map, where a model can be built in to fit the electron density. The model is used to calculate the phase. Combined with the original intensities of the spots, a new electron density map is constructed, which can be used to improve the model. The cycle continues until changes no longer improve the model. Improvements are determined by measuring R-factors, which compare the observed amplitudes with the calculated amplitudes and are typically 0.15-0.25 for the average size protein. The R_{free} is another way to evaluate model agreement with the data by randomly removing 5-10% of the collected data, known as the test set, to compare to the model. This number is often slightly higher than the R-factor but is believed to be a better representation of an accurate model⁹⁵.

Using NMR to Understand Oligonucleotides

Technological advances in NMR have made it a useful technique for examining oligonucleotides. The development of superconducting magnets able to resonate at frequencies as high as 1GHz⁹⁶ make NMR a powerful structural biology tool, improving more than thirty times the sensitivity of the original 30 MHz instrument developed in 1950. The common use of cryoprobes has further enhanced the utility of NMR towards structural biology.

NMR samples require NMR active nuclei in order to be detected. The nucleus is composed of protons and neutrons. Nuclei have an intrinsic spin (I) characteristic, determining whether it is NMR active. The spin orientations are defined as either spin up or spin down. For a nucleus to be interesting from an NMR spectroscopist's point-of-view, $I \neq 0$. This excludes atoms with an even mass and even number of neutrons. NMR active nuclei can have an even mass with odd number of neutrons or just an odd mass. The commonly used NMR active nuclei are ^1H , ^{13}C , ^{15}N , ^{19}F , and ^{31}P . Oligonucleotides are composed of elements ^1H and ^{31}P and have the potential to be ^{13}C labeled that allow for many possibilities for experiments to obtain structural information.

When a sample is placed in the spectrometer, it is subjected to the high magnetic field, which aligns the spins with or against the axis the magnetic field (Z axis) and separates the spin states so they no longer have the same energies. Scheme 1-3 Depicts the energy difference of the spin states when subjected to magnetic field B_0 , where ΔE depends on the strength of the magnetic field. Typically, a 90° RF pulse is applied to flip the spins into the perpendicular (XY) plane, creating coherence between the two spin states and allowing transitions to occur. The nuclei are then allowed to return to the equilibrium state. The transition frequency, also known as chemical shift, as they relax is detected and is dependent on the chemical environment of each atom.



Scheme 1-3. Diagram of how the energy states of spin-up and spin-down depend on the magnetic field, which is detected by NMR.

Two types of NMR interactions are commonly measured for structure determination of DNA: scalar coupling interactions and dipolar interactions. Scalar couplings, or J couplings, detect through-bond interactions. 2-D correlated spectroscopy (COSY)⁹⁷ experiments are generally used in this project to detect such interactions. Cytosine bases are the only bases that have 3J couplings and can easily be used to assess purity of the duplex by examining the aromatic portion of the spectrum. Certain phase-sensitive experiments allow for calculating J-coupling constants, which is based on the orientation of the nuclei relative to each other. 3J coupling constants are particularly useful in unambiguously assigning sugar protons on the ring. For instance, the coupling constants for protons of H2' and H2'' to H1' will differ since H2'' is on the same side of the sugar ring as H1' and will have a smaller 3J . Similarly, backbone angles can be determined using 3J between ^{31}P and nearby protons like H5' or H5''.

Dipolar interactions occur when nuclei are closer than 5 Å and occur strictly through space, allowing for distance information to be extracted. Nuclear Overhauser effect

spectroscopy (NOESY)⁹⁸ experiments are designed to detect such interactions. In a NOESY experiment, a mixing time of a certain length allows for cross magnetization to occur for protons that are in proximity to each other. The resulting crosspeak is detected between two protons during relaxation. A variety of mixing times tend to be used, ranging from 50 ms to 300 ms. Use of multiple mixing times reduces bias from spin diffusion. The intensities of the peaks are integrated and used for distance values based on Equation 1:

$$r_{ij} = r_{ref} \sqrt[6]{\frac{i_{ref}}{i_{ij}}}$$

where r_{ref} is a known distance, typically between H5 and H6 of cytosine and i being the intensity of the reference peak and the peak resulting from spins i and j .

NOESY spectra for DNA can be divided into characteristic chemical shift regions, as demonstrated in Figure 1-10 The area termed the “walking region” is where the aromatic H6/H8 protons of the bases interact with H1' of the sugar rings, where this interaction can be followed from base 1 to the end of the strand in unmodified DNA. Once this region has been assigned, the sugar protons for each base can usually be identified and assigned according to established protocols⁹⁹. The walking region can be very informative for understanding structural perturbations from adducts because the distances from these protons are well known in B-type DNA. Changes in distances or breaks in the walk are usually identifiable in this region. Chemical shift perturbations can also be informative for understanding where protons are likely located in the DNA duplex. Figure 1-11 demonstrates the typical observable interactions in the walking region, as well as some other NOEs typically observed.

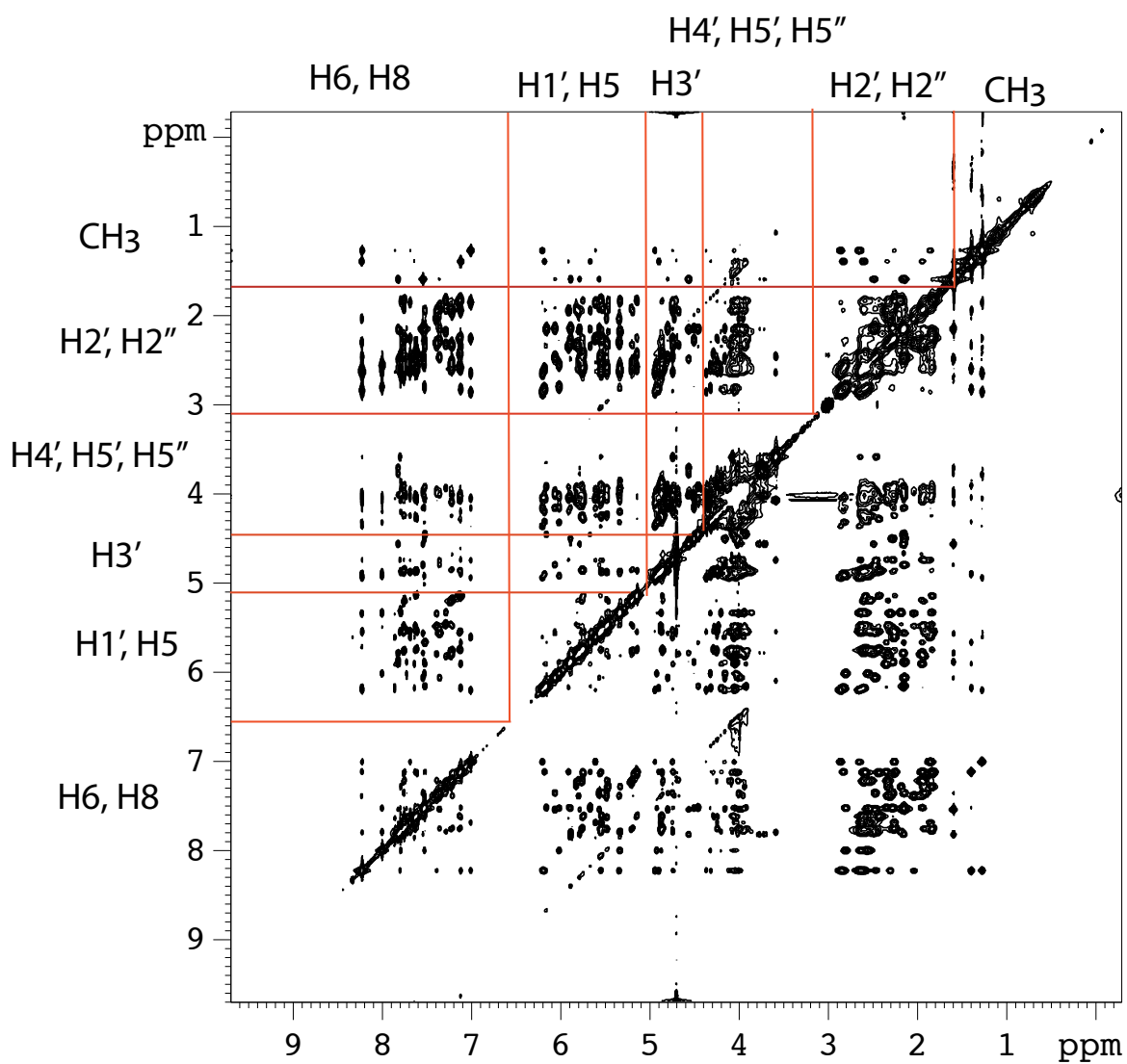


Figure 1-10. Chemical shifts for unmodified oligonucleotides are typically found in specific regions labeled on the NOESY spectrum.

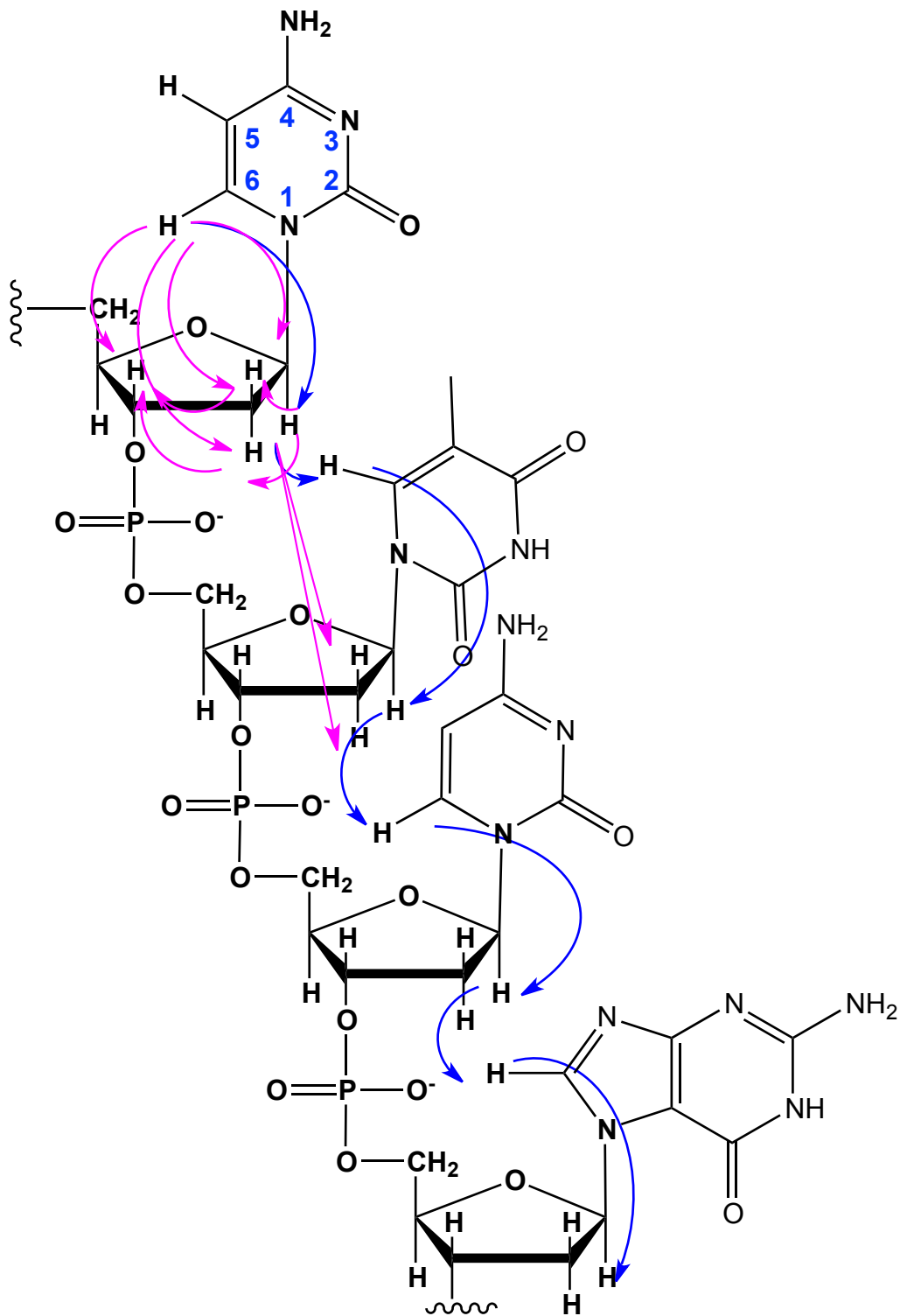


Figure 1-11. The walking region consists of the NOESY walk from aromatic base proton to H1' sugar proton, demonstrated in blue. Other NOEs, which can usually be observed, are shown in magenta.

Another important region to study for DNA involves the exchangeable imino and amino protons. The exchange rate for these protons at the nucleoside level are much faster than can typically be observed on the NMR timescale. However, since the N1H proton of guanine and the N3H of thymine are involved in hydrogen bonding when in duplex DNA, the exchange is significantly slower. Therefore, this region can be used to determine if base-stacking and Watson-Crick hydrogen bonding is maintained by being able to identify the chemical shifts of the protons involved in hydrogen bonding. Base-stacking interactions appear much like the connectivities in the walking region of the nonexchangeable region. Since parameters like the rise and twist of B-type DNA remain very characteristic to the duplex, a walk can also be observed in this region from imino to imino proton from the thymines and guanines when normal base-stacking occurs (demonstrated by red arrows in Figure 1-12). The corresponding amino group in the base pair can be identified by the NOEs to the imino proton¹⁰⁰. Disruption in hydrogen bonding may cause broadening by allowing protons to exchange with the solvent. Hoogsteen or wobble base pairs can also be identified by the chemical shifts of these protons.

Once all NMR data is collected and assigned, NOESY peak volumes can be integrated for Matrix Analysis of Relaxation for Discerning Geometry of an Aqueous Solution (MARDIGRAS)^{101,102} calculations to convert volumes to proton-proton distances. Integrating data requires resolved peaks with preferably a Gaussian shape for best accuracy. When integrating, the peaks can manually be selected, thus not accurately being able to define the bounds of overlapped peaks will lead to higher error. Likewise, the integration method assumes a Gaussian peak when integrating; therefore, broad linewidths may also contribute error. The result of the integration is a series of bounds for each

proton-proton distance based on the error value based on noise and intensity errors assigned. This yields the experimentally obtained restraints for calculations. Other restraints include canonical angles for sugars and backbone and distances for Watson-Crick hydrogen bonding. These values can also be adjusted for any deviations that are observed in the NMR data.

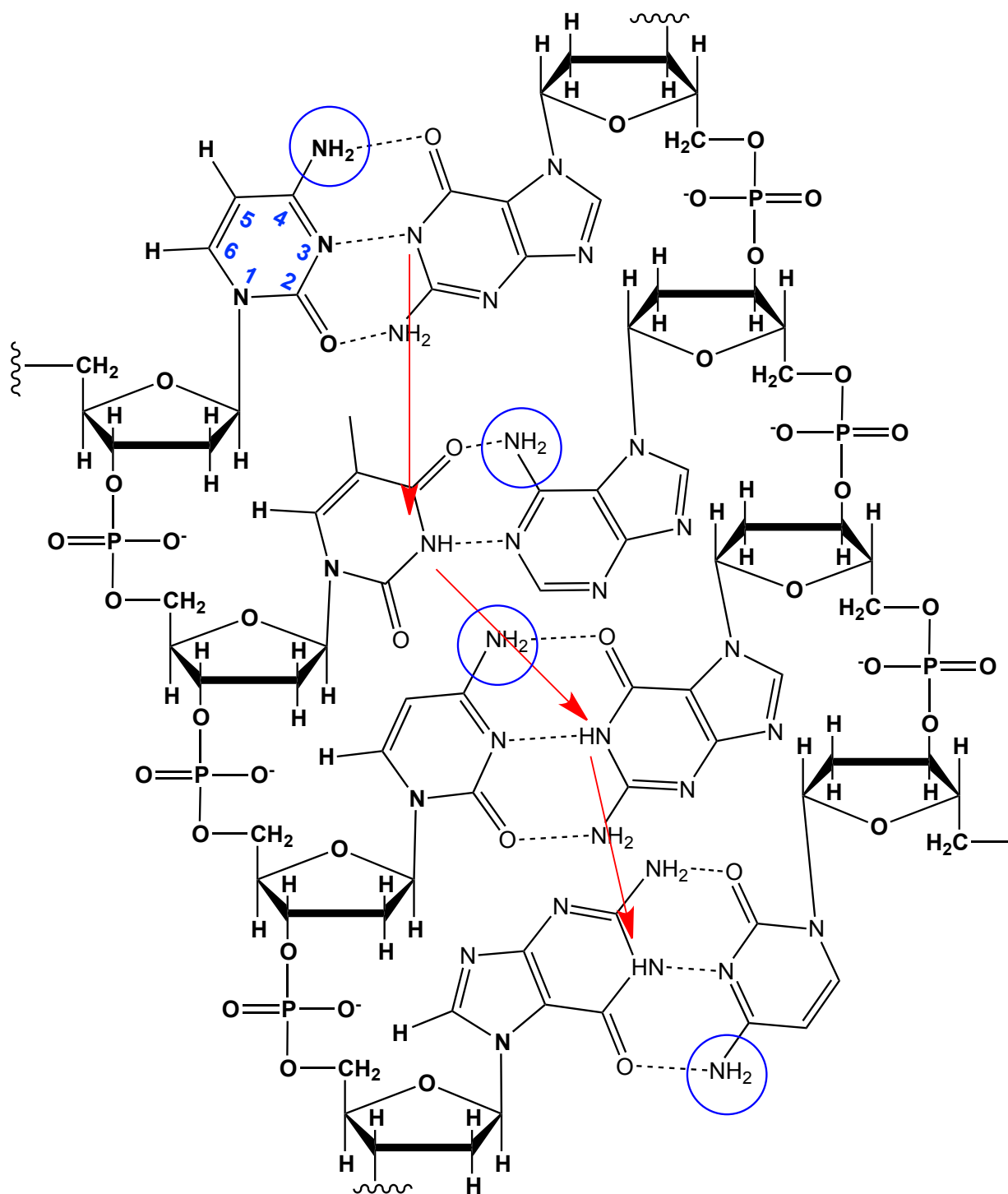
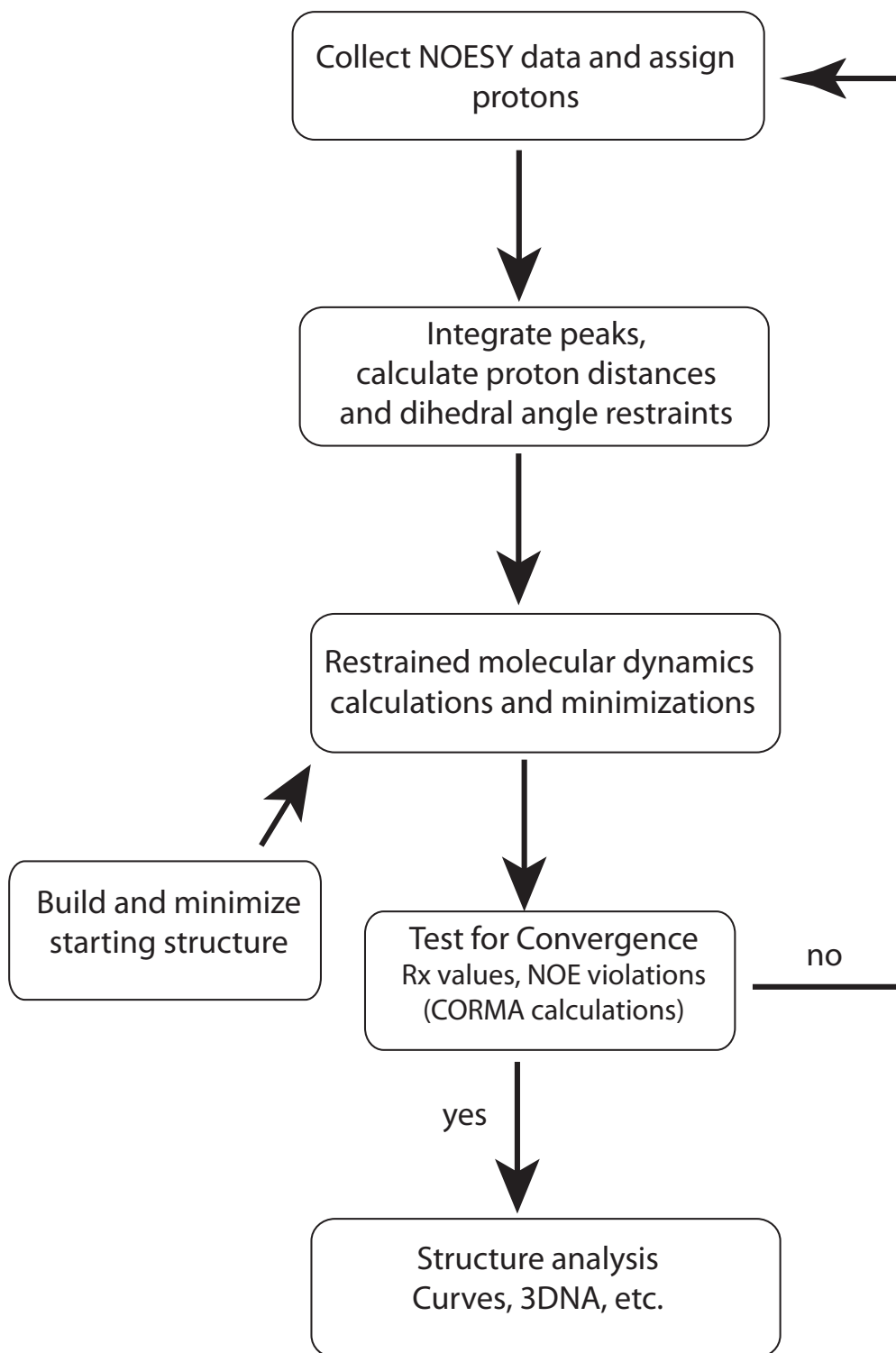


Figure 1-12. Exchangeable protons observable in NOESY experiments due to participation in hydrogen bonding.

An initial structure or series of structures can be built to obtain topology and parameter files necessary for structure calculations. Using the topology and parameter information, the structure can be minimized to reach a local energy minimum by randomly sampling a variety of conformational space to find the lowest energy structure. The experimentally obtained restraints can then be applied to the minimized structure through a series of restrained molecular dynamics (rMD) calculations¹⁰³. A simulated annealing protocol¹⁰⁴ is applied, which adds energy to the system, allowing the molecule to overcome energy barriers and increases the number of possible conformations at the higher energy. The system is cooled slowly to allow the molecule to sample probable conformational space to find the most energetically favorable conformation. Slowly cooling the system reduces the risk of becoming stuck in a local minimum. The structure is evaluated based on violations incurred to the NOE restraints, the sixth root residual R_1^x calculated by the program complete relaxation matrix analysis (CORMA)¹⁰⁵⁻¹⁰⁷, which compares calculated data to the experimental data, and root mean square deviation (rmsd) that evaluates the precision of the rMD calculations. Once these factors convey convergence of the calculated structure, helicoidal structure analysis can be performed using programs such as Curves^{62,108} or 3DNA¹⁰⁹.



Scheme 1-4. Strategy for refining oligonucleotide structures using solution NMR.

Circular Dichroism

Circular dichroism (CD) is another technique that can provide information about secondary structure of optically active chiral biological molecules. While the structural information may not be as detailed as x-ray crystallography or NMR, it is much faster and only requires a small amount of sample, approximately 0.3 OD, but is able to detect small changes in secondary structure¹¹⁰.

CD utilizes the differential absorption of circular right-handed polarized light and left-handed polarized light. When the light passes through the sample, the optically active chiral sample typically absorbs one direction preferentially. The difference in absorption between the two directions is detected. CD detects the degrees of ellipticity of the polarized light, θ . The change in polarization is a function of wavelength as well as sample conformation, which can be dependent on concentration, temperature, pH, etc. CD is typically reported in molar absorptivity:

$$[\theta] = 3298\Delta\epsilon$$

where $[\theta]$ is the molar ellipticity and $\Delta\epsilon$ is the molar absorptivity. Correlations between CD and structure have been found¹¹¹, making CD a useful tool for the field of structural biology.

Dissertation Statement

The goal of this project is to structurally characterize the N^2 -dG-IQ in the DNA duplex containing the GCGC dinucleotide repeat, where a difference in mis-coding potential has been observed with hpol η in *in vitro* assays in different sequence contexts. It is possible that the duplex structures differ between the mutagenic hotspot G^3 position where two-base deletions are observed versus the G^1 where frameshifts are rarely observed.

Structural studies could shed light why the mis-coding potential differs in the different sequence contexts by allowing the study of its structure-function relationship. It is hypothesized that the sequence context will dictate whether or not the IQ moiety will intercalate into the duplex, much like what was observed with the C8-dG-IQ adduct.

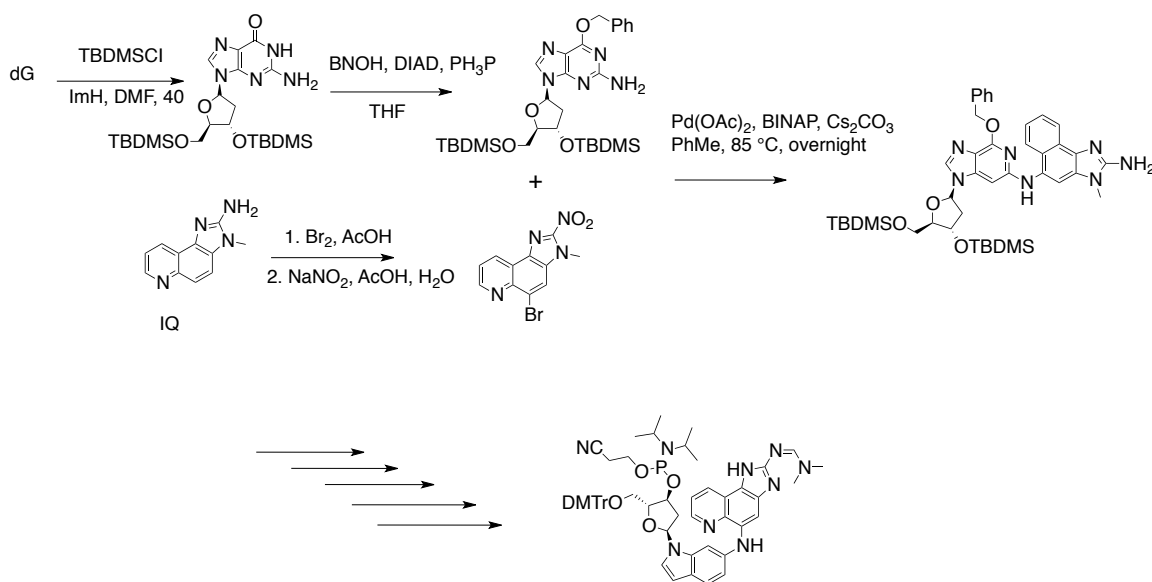
Chapter II describes the materials and methods for this project. Chapter III reveals the solution studies of N^2 -dG-IQ by NMR at the mutagenic hotspot, G^3 , in the *NarI* recognition sequence. Chapter IV details the solution studies of N^2 -dG-IQ by NMR at G^1 in the *NarI* recognition sequence. Chapter V concludes the findings for the project as well as the future directions of the work.

Chapter II

MATERIALS AND METHODS

Sample Preparation

Unmodified oligonucleotides were obtained from Midland Certified Reagent Co. (Midland, TX). The oligonucleotides were purified by reverse-phase high performance liquid chromatography (RP-HPLC) using 100 mM ammonium formate buffer at pH 7 with an acetonitrile gradient increasing at a rate of 1% every 2 minutes. The IQ-adducted strands was synthesized as previously published¹¹² and obtained from Professor Carmelo Rizzo's lab. The scheme depicting the Buchwald Hartwig palladium catalyzed reaction, which is an important step for the synthesis of the phosphoramidite is demonstrated in Scheme 2-1.



Scheme 2-1. Synthesis schematic for *N*²-dG-IQ phosphoroamidite showing the Buchwald Hartwig palladium catalyzed reaction between IQ and dG, followed by five additional reaction steps to produce the phosphoroamidite.

The identity of each oligonucleotide was confirmed by MALDI-TOF mass spectrometry Voyager-DE (PerSeptive Biosystems, Inc.) instrument in the negative ion mode using a matrix consisting of 0.5 M 3-hydroxypicolinic acid (HPA) and 0.1 M ammonium citrate. The concentration of each single strand was determined using the extinction coefficient of $1.10 \times 10^5 \text{ M}^{-1} \text{ cm}^{-1}$ at 260 nm. Each duplex was then annealed at a 1:1 ratio at room temperature in a buffer solution containing 10 mM NaH_2PO_4 buffer containing, 100 mM NaCl, and 50 μM EDTA (pH 7). Duplex purities were confirmed by RP-HPLC.

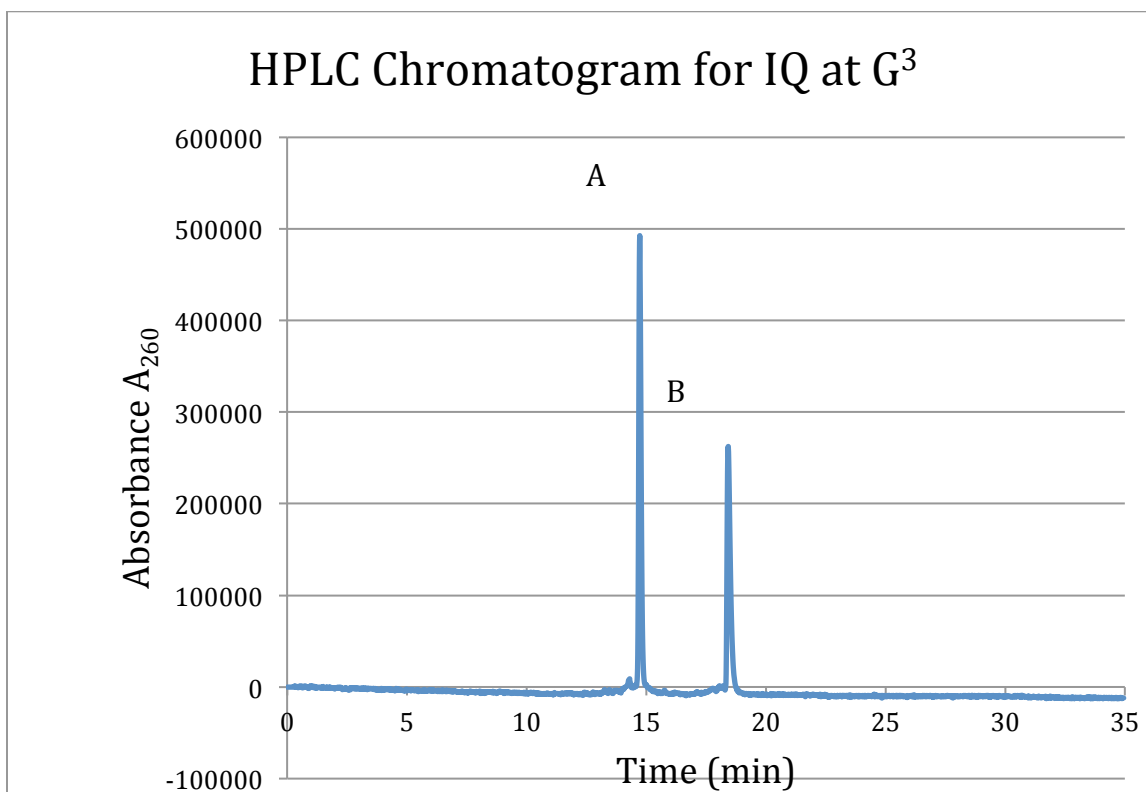


Figure 2-1. HPLC chromatogram of *NarI* modified by IQ at G³ with separation of both strands. Peak A shows the elution of the complement strand, while peak B is the IQ modified strand.

Thermal Melting Experiments

UV melting temperatures were collected on Cary 100 Bio UV (Varian, Inc. Palo Alto, CA) spectrophotometer, and data was collected in the Cary WinUV Thermal Application (v2.0). Sample in the amount of 0.5 OD (4 μ M) of duplex was suspended in 1 mL of solution containing 0.1 M NaCl, 10 mM NaH₂PO₄, and 50 μ M Na₂EDTA (pH 7.0). The temperature was increased from 25-75 °C at a rate of 1 °C per min and absorbance readings were taken every 0.5 °C. The melting temperature (T_m) was extrapolated from the first derivative of absorbance A_{260} versus temperature profiles.

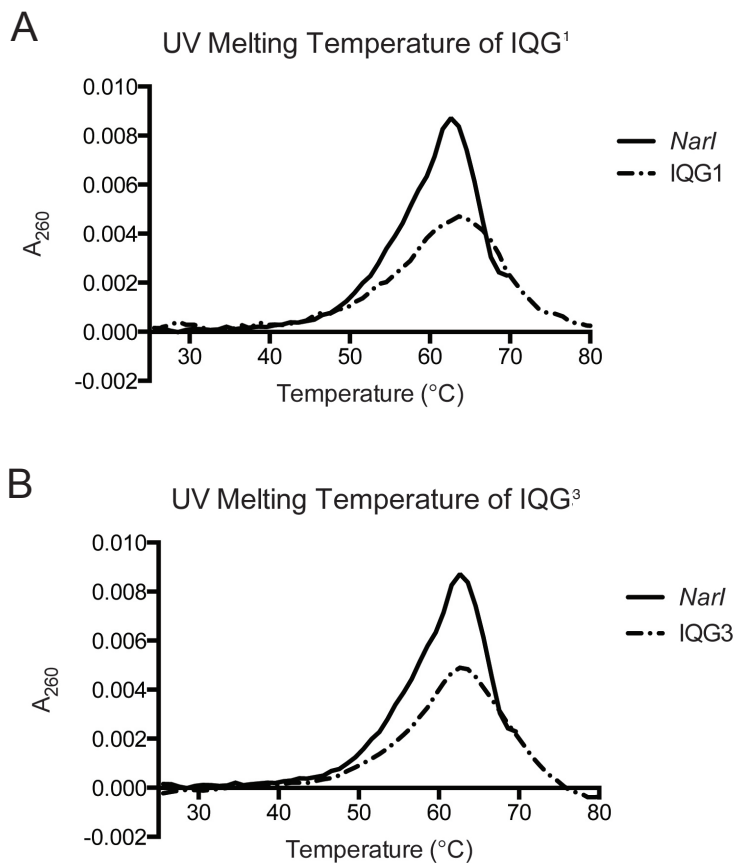


Figure 2-2. First derivative curves of UV thermal melting experiments for A) IQ at G¹ and B) IQ at G³.

Circular Dichroism

The samples contained 0.5 OD (4 μ M) of duplex in a cuvette with 1 cm pathlength in buffer conditions of 0.1 M NaCl, 10 mM sodium phosphate buffer, and 0.05 mM EDTA at pH 7.0 in 800 μ L volumes. Data was collected on Jasco 720 with a response time of 1 second, scan speed of 20 nm/min and step resolution of 1 nm across a wavelength of 400-200 nm over 10 accumulations.

NMR Spectroscopy

Duplex samples were suspended in 180 μ L buffer solution containing 10 mM NaH_2PO_4 , 100 mM NaCl, 50 μ M EDTA at pH 7. In order to observe the nonexchangeable protons, the solvent was exchanged for three rounds by drying the solvent and adding 99.9% pure D_2O , followed by an exchange with 99.996% D_2O , and finally suspended in 180 μ L 99.996% D_2O solution. Experiments to observe exchangeable protons were conducted in 9:1 H_2O : D_2O . ^1H NMR spectra were collected at 600 and 800 MHz. Nonexchangeable protons were observed at 15 $^\circ\text{C}$; exchangeable protons were monitored at 5 $^\circ\text{C}$. Chemical shifts were referenced to the water peak (4.868 ppm at 288 K). The data was processed in TOPSPIN (Bruker Biospin Inc., Billerica, MA).

NOESY data for nonexchangeable protons were collected using States-TPPI¹¹³ phase cycling with a relaxation delay of 1.8 s and mixing times of 150, 200, and 250 ms to account for spin diffusion. Spectra for exchangeable protons were collected with a relaxation delay of 1.2 s and a mixing time of 100 ms. Spectra were recorded with 512 points in the t1 dimension and 2048 points in the t2 dimension, then zero-filled to 2048 x 2048 overall matrix. Water suppression was applied through the WATERGATE sequence¹¹⁴.

Distance Restraints

Spectrum analysis and assignments were performed in SPARKY¹¹⁵. Intensities of peaks were measured by volume integration using either Gaussian method for regular peaks or box method for irregular or overlapped peaks. Bounds for overlapped peaks were manually adjusted based on typical B-DNA values, unless near the adduct. Noise was assigned half the intensity of the weakest peak and motion was assumed to be isotropic. Experimental intensities were combined with intensities obtained from complete relaxation matrix analysis of starting model to generate a hybrid intensity matrix^{116,117}. The intensities were converted to distances with the program MARDIGRAS¹⁰², which refined the hybrid intensity matrix. Calculations were performed using 150, 200, and 250 ms mixing time data and 2, 3, and 4 ns isotropic correlation times. Evaluation of the resulting distance data allowed creation of upper and lower bound distance restraints that were used in restrained molecular dynamics (rMD) calculations.

Restrained Molecular Dynamics Calculations

An unmodified B-DNA model¹¹⁸ was used as a starting structure. The guanine at position G⁷ was replaced by the *N*²-dG-IQ adduct using the program INSIGHT II (Accelrys Inc., San Diego, CA). Partial charges for the *N*²-dG-IQ adduct were calculated with the B3LYP/6-31G* basis set in GAUSSIAN¹¹⁹. The starting structure was energy minimized for 1000 cycles. Simulated annealing protocols¹²⁰ used for the rMD calculations were conducted with the parm99 force field¹²¹, using the program AMBER¹²². Force constants of 32 kcal mol⁻¹ Å⁻² were applied for distance and torsion angle restraints. The generalized

Born model¹²³ was used for solvation. The NaCl concentration was 0.1 M. The molecule was coupled to the bath temperature to control the temperature during simulated annealing. First, calculations were performed for 20 ps (20000 steps) and recording data every ps by the following protocol: During steps 0 – 1000, the system was heated from 0 to 600 K with a coupling of 0.5 ps. During steps 1001-2000, the system was kept at 600 K. The system was then cooled from 600 K to 100 K during steps 2001 – 18000 with a coupling of 4 ps. Further cooling from 100 K to 0 K occurred during steps 18001 – 20000 with a coupling of 1 ps. After initial cycles of refinement a longer 100 ps (100000 steps) calculation was performed by the following protocol: During steps 0–5000 the system was heated from 0 to 600 K with a coupling of 0.5 ps. During steps 5001-10000 the system was kept at 600 K. The system was cooled from 600 K to 100 K during steps 10001 – 90000 with a coupling of 4 ps. Additional cooling from 100 K to 0 K occurred during steps 90001 – 100000 with a coupling of 1 ps. Structure coordinates were saved after each cycle, and were subjected to potential energy minimization. Complete relaxation matrix analysis (CORMA)^{116,117} was used to compare intensities calculated from these emergent structures with the distance restraints. Helicoidal analysis was performed using the CURVES+ web server^{124,125}.

Expression and Purification of Dpo4

A glycerol stock of the vector pET22b(+) with plasmid coding for Dpo4 with a c-terminal (His)₆ tag with ampicillin resistance in *E. coli* strain BL21(DE3) competent cells (Stratagene, CA) was a gift from Professor Fred Guengerich's lab. A fresh glycerol stock was made from ~1 µL of these cells by adding to 100 mL Luria broth culture and shaking overnight at 37 °C. Seven hundred fifty µL of Luria broth was mixed with 250 µL of

glycerol, flash frozen, and stored at -80 °C. The plasmid was also isolated from remaining cells using QIAprep Spin Mini Prep Kit (Quiagen, Germany) and submitted to the DNA core for sequencing to ensure no mutations had occurred over time.

To express Dpo4, ~1 µL of the glycerol stock of cells was added to a culture flask containing a volume of 25 mL of LB per 1 L flask and shaken overnight (14-16 hrs.) at 37 °C. The overnight flask was then distributed evenly between all flasks containing 1 L LB and 1 mL of ampicillin stock solution of 100 mg/mL. The flasks shook at 37 °C until the optical density at 600 nm (OD₆₀₀) reached 0.6. The cells were then induced by adding 1 mL of 1 M IPTG to each flask. The flasks continued to shake at 37 °C for 3.5 hrs., after which the cell pellets were harvested by centrifugation at 9000 rpm at 4 °C for 45 min. (Beckman, JLA-9.100) in a Beckman Avanti-25 centrifuge and stored at -80 °C until purification.

To purify Dpo4, lysis buffer containing 50 mM Tris-HCl buffer at pH 7.5, 300 mM NaCl, 10% glycerol (v/v), 5 mM β-mercaptoethanol, 1 mg/mL lysozyme, and 1 protease inhibitor tablet (Roche Applied Science) was added to thawed cell pellet and resuspended, bringing the total volume to about 35-40 mL before cooling on ice for 30 min. The cells were lysed through 2-3 intervals of sonication (Branson Sonifier 450, Danbury, CT) (for 1 min. on and one min. off). Cell debris was removed by centrifuging at 10,000 rpm (Beckman, JA-12) at 4 °C for 45 min. The supernatant was removed and heated in water bath to 78 °C for 10 min. The denatured proteins were again spun off at 10,000 rpm (Beckman, JA-12) at 4 °C for 45 min.

The supernatant was loaded on FPLC to a 5 mL HisTrap column (GE Healthcare Life Sciences) equilibrated with Buffer A (50 mM Tris HCl (pH 7.5), 300 mM NaCl, 10% glycerol (v/v) and 5 mM β-mercaptoethanol). The column was washed with 5% Buffer B (Buffer A +

500 mM imidazole) for 5 column volumes, then changed to 100% Buffer B over 2 column volumes and held for 3 column volumes. Dpo4 elution was monitored by A_{280} .

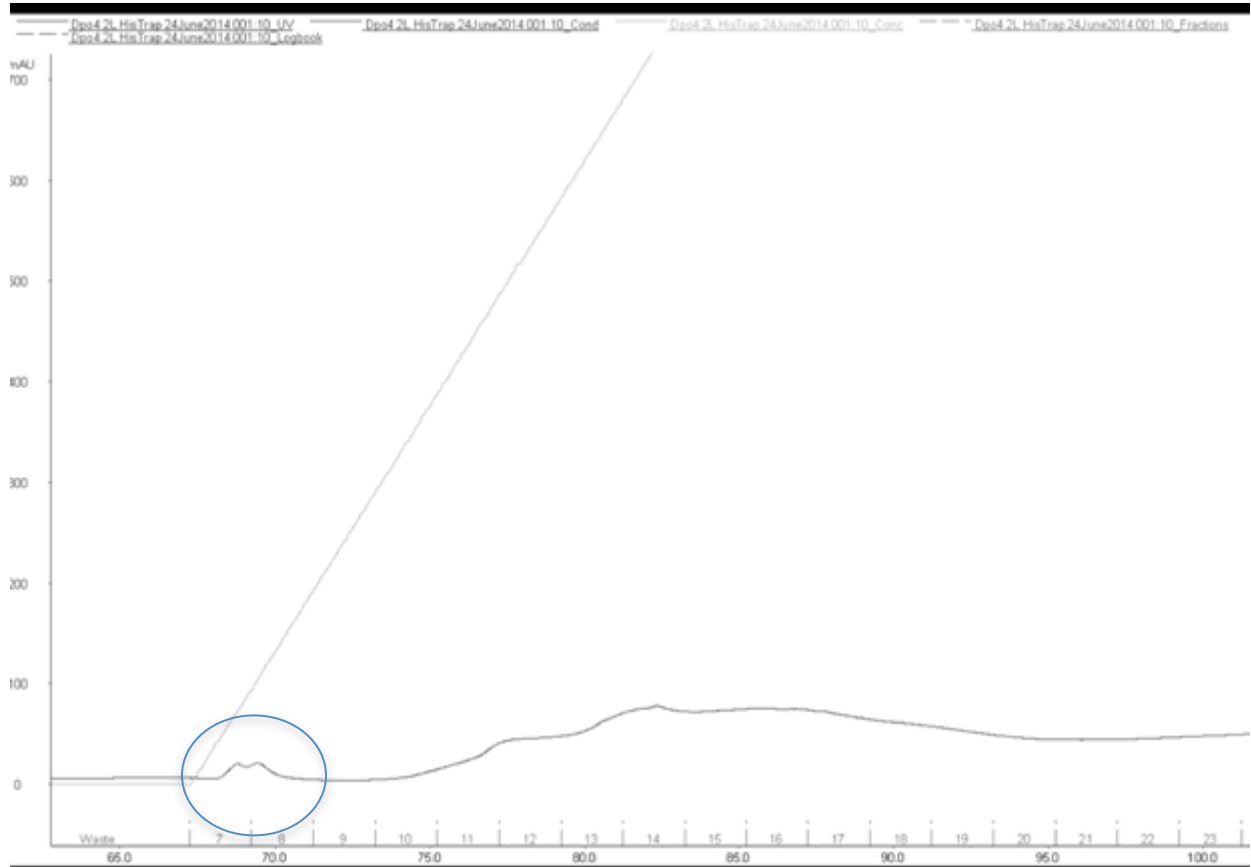


Figure 2-3. Dpo4 elution on HisTrap column.

Fractions containing Dpo4 were combined and spun down in 15 mL Millipore centrifuge filter tubes with 30kDa cut off. After the protein reached a volume of about 1-2 mL, it was diluted with Buffer A (50 mM Tris-HCl pH 7.5, 0.5 mM EDTA, 10% glycerol (v/v), and 5 mM β -mercaptoethanol) to about 20-25 mL. The protein solution was loaded onto an 8-mL MonoS column (GE Healthcare) and eluted with Buffer B (Buffer A + 500 mM NaCl) over a linear gradient for 8 column volumes, reaching 100% B. Dpo4 elution was monitored by A₂₈₀.



Figure 2-4. MonoS elution profile of Dpo4.

The purity of Dpo4 was assessed by SDS-page gel using pre-cast Nu-Page 4-12% Bis-Tris gels (Life Technologies, NY) (Figure B-3). The protein was concentrated to ~40-50 mg/mL, as determined by the A_{280} and the molar extinction coefficient of $22 \text{ mM}^{-1} \text{ cm}^{1126}$.

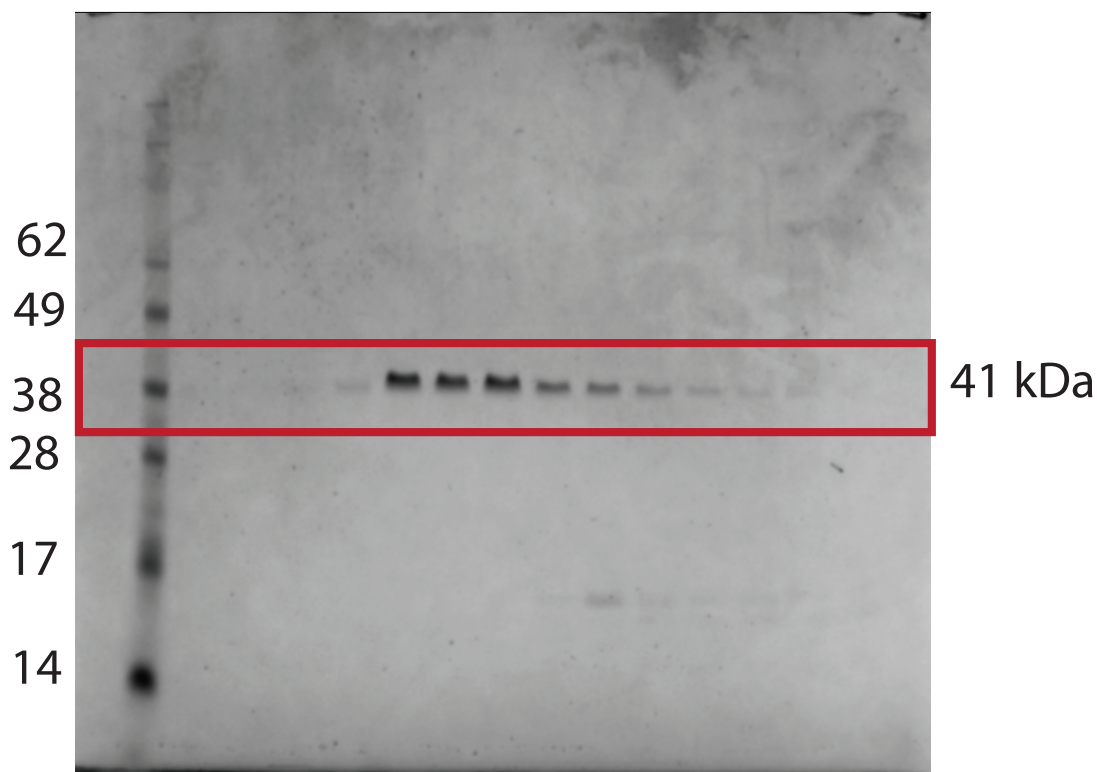


Figure 2-5. SDS-PAGE gel of Dpo4 after final purification step showing intended band at about 41 kDa.

Activity Assay

Unmodified 19mer template strand and 12mer with a 5' FAM tag were purchased from IDT (Coralville, IA) and purified by HPLC. The duplex was annealed at a 1:1 ratio by placing it in an 85 °C hot water bath for 10 minutes and allowing to cool slowly to room temperature. Dpo4/DNA reactions were run at 10 μM DNA and 100 μM Dpo4 concentrations in a buffer of 25 mM Tris-HCl (pH 7.8), 5 mM DTT, 0.1 $\text{mg}\cdot\text{mL}^{-1}$ BSA, and 5

mM MgCl₂, by incubating the mixture at 37 °C with 20 mM total dNTPs. Time points were taken at 0, 2, 5, 10, 20, 40, 60, 75, 90, 105, and 120 min. and quenched with a solution of 20 mM Na₂EDTA in 95% formamide (with bromophenol) and denatured at 90 °C for 10 min. Electrophoresis was used to separate reaction products on a denaturing gel containing 40% acrylamide solution. The gel was imaged on a UV scanner able to detect the fluorescence at 520 nm.

Crystallization of DNA:Dpo4 Complexes

The sequences 5'-TCAC(80G)GAATCCTTCCCC-3' 18mer template strand and 5'-GGGGGAAGGATTCC-3' 14mer primer strand were obtained from Midland (Midland, TX) and were based on a previously published structure^{127,128}.

Dpo4 and DNA sequences were mixed at 1:1.2 molar ratio at final 200 μM protein concentration in a buffer containing 20 mM HEPES (pH7.4), 5 mM DTT, and 100 mM NaCl and incubated on ice for 10 min. Five mM CaCl₂ was added to ternary complex solutions and incubated an additional 10 min. Individual 1 mM dNTPs were then added to the ternary complex, and they were incubation was done at 37 °C for 5 min. The complex solutions were finally spun down at 8000 rpm for 5 min. before setting up via hanging drop vapor diffusion with a 1:1 ratio of reservoir solution consisting of 20 mM HEPES (pH 7.4), 100 mM Ca(OAc)₂, and 10-20% PEG 4000 (w/v). Plates were incubated at room temperature. Crystals were looped in the mother liquor (plus an additional 25% PEG (4000) and 15% ethylene glycol) and flash frozen in liquid nitrogen.

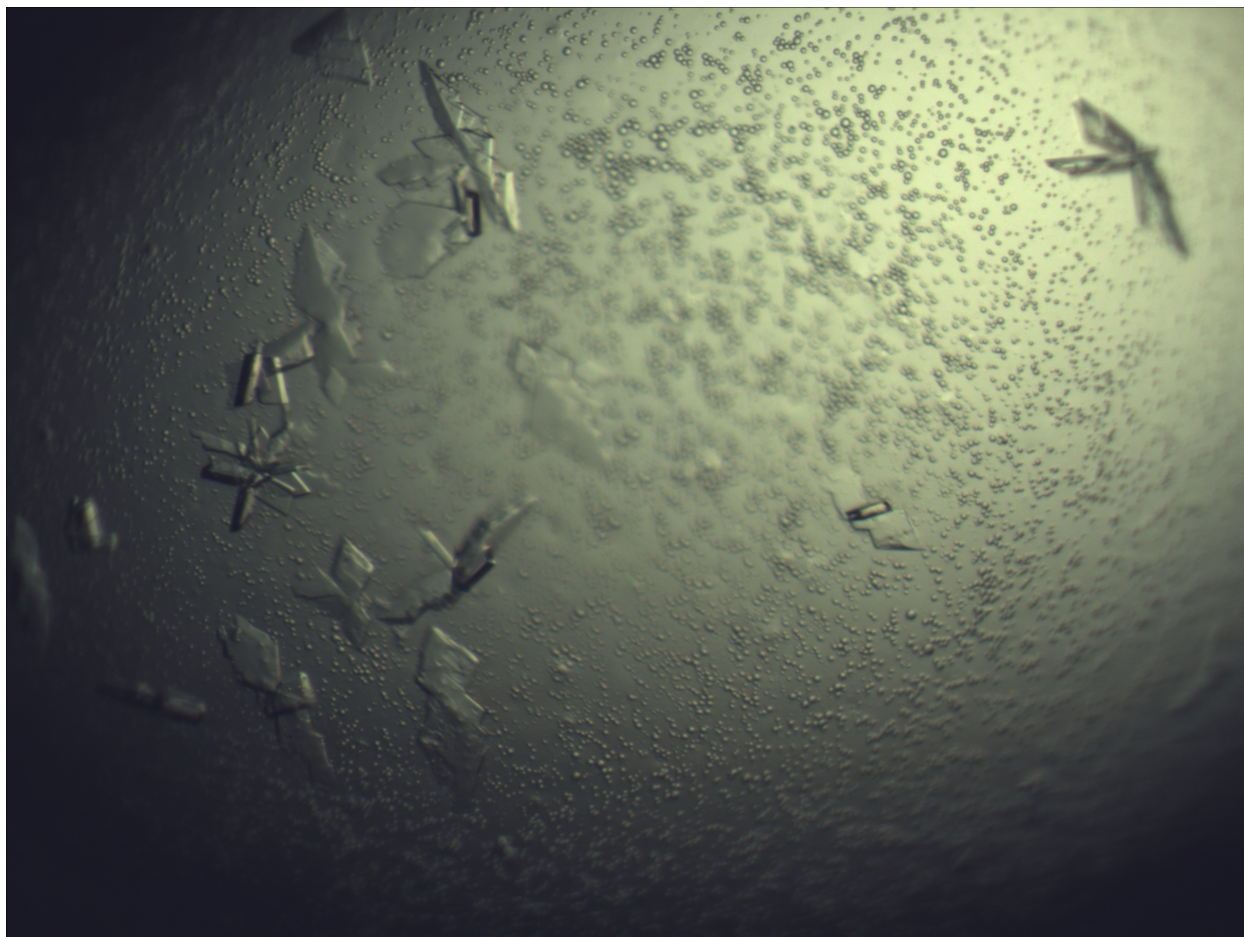


Figure 2-6. Typical crystals of Dpo4 with 8-oxoG modified oligonucleotide.

X-Ray Diffraction Data Collection and Processing

The crystals were shipped to Dr. Surajit Banerjee, who collected diffraction data at 100 K at a wavelength of 1.0 Å on beamline 24-ID-C (Northeast Collaborative Access Team NE-CAT, Advanced Photon Source, Argonne, IL). Indexing and scaling were done using HKL2000¹²⁹.

Structure Determination and Refinement

The starting model came from PDB accession code 2C22¹³⁰ without the modified 8-oxoG base (minus the waters) was also created by Dr. Surajit Banerjee. The structure was

refined using CNSsolve (v1.3)^{131,132} by rounds of minimization and individual b-factor optimization. A single waterpick was also initially run in CNS. Molecules were manually aligned with the data and water molecules were subsequently placed in positive regions of the F_o-F_c Fourier difference electron density in Coot¹³³. 10% of the reflections were excluded from the refinement for use in R_{free} calculations. Figures were prepared using Pymol¹³⁴.

Chapter III

SOLUTION STRUCTURE OF *N*²-dG-IQ AT THE MUTAGENIC HOTSPOT G³ POSITION IN THE *NarI* SEQUENCE CONTEXT*

Introduction

The IQ-dG adduct results from the metabolism of IQ upon the consumption of meat cooked at high temperatures. This chapter focuses on the NMR solution studies and characterization of the IQ adduct in the mutagenic hotspot of the 12mer based on the *NarI* recognition sequence, 5'-C¹T²C³G⁴G⁵C⁶X⁷C⁸C⁹A¹⁰T¹¹C¹²-3' paired with 5'-G¹³A¹⁴T¹⁵G¹⁶G¹⁷C¹⁸G¹⁹C²⁰C²¹G²²A²³G²⁴-3'. Thermal melting temperature experiments indicate it is a stable duplex when paired opposite the correct dC base, which does not change from the unmodified duplex. NMR data suggests this is due to intercalation into the duplex, which allows base stacking to occur with base pairs C⁶·G¹⁹ and C⁸·G¹⁷. This does, however, prevent C¹⁸ from Watson-Crick hydrogen bonding with X⁷, since it is flipped into the major groove to allow the IQ moiety to intercalate. The modified base also remains in the *anti* conformation. These results may explain why the *N*²-dG-IQ is poorly repaired when compared to the C8-dG-IQ adduct.

Results

*Oligodeoxynucleotide Containing the *N*²-dG-IQ Adduct*

The *N*²-dG-IQ adduct was incorporated into 5'-d(CTCGGCXCCATC)-3' using automated solid-phase synthesis¹³⁵. The position of the *N*²-dG-IQ adduct was located at

* Reprinted manuscript with permission from Stavros, KM; Hawkins, EK; Rizzo, CJ; Stone MP, *Nucl. Acid. Res.*, **2014**, 42(5), Copyright (2014) Oxford University Press, 1/6/15.

position X⁷, corresponding to position G³ in the *NarI* sequence. The modified oligodeoxynucleotide was purified by C18 reversed phase HPLC and characterized by MALDI-TOF mass spectrometry in the negative ion mode [m/z 3777.7, calcd for (M – H), 3776.6]. Thermal melting (T_m) profiles of 0.5 A₂₆₀ units (4 μM) of the IQ-modified duplex were monitored at 100 mM NaCl (1 mL volume) by its absorbance at 260 nm as a function of temperature. An unmodified duplex was evaluated under the same conditions to provide a basis of comparison. The T_m of the modified duplex was 63 °C and is within experimental error of the unmodified duplex (Figure S1 in the Supplementary Data). Thus, the *N*²-dG-IQ adduct did not reduce the stability of this oligodeoxynucleotide. This result differed from our previous report, which had indicated that this adduct destabilized this duplex¹³⁵. Subsequent analysis of the previous sample by mass spectrometry revealed that the complement strand was not correct, accounting for the discrepancy. Table 3-1 lists the correct T_m values of the *N*²-dG-IQ adduct at the three positions of the *NarI* sequence.

NMR

The modified duplex yielded well-resolved NMR spectra with narrow line shapes for the non-exchangeable protons at 15 °C. The best spectral quality for the exchangeable protons was obtained at 5 °C.

(a) Non-exchangeable DNA Protons. The base aromatic and deoxyribose anomeric protons were assigned using established procedures (Figure 3-1)^{136,137}. The intensity of the X⁷ H8 to X⁷ H1' NOE was not changed in the presence of the adduct, indicating minimal change in the conformation of the glycosyl torsion angle. In the complementary strand, the intensity of the NOE between C¹⁸ H1' and G¹⁹ H8 was weakened. The *N*²-dG-IQ adduct did not induce breaks in the sequential pattern of

NOEs between the aromatic base protons and the anomeric protons. With the exception of the adduct site, the internucleotide NOEs were characteristic of a B-type duplex. The adenine H2 protons were assigned based upon NOEs to the thymine imino protons of the respective A:T base pairs. With the deoxyribose H1' assignments in hand, the remainder of the deoxyribose protons were assigned from a combination of NOESY and COSY data. The assignments of the non-exchangeable DNA protons are summarized in the Appendix D.

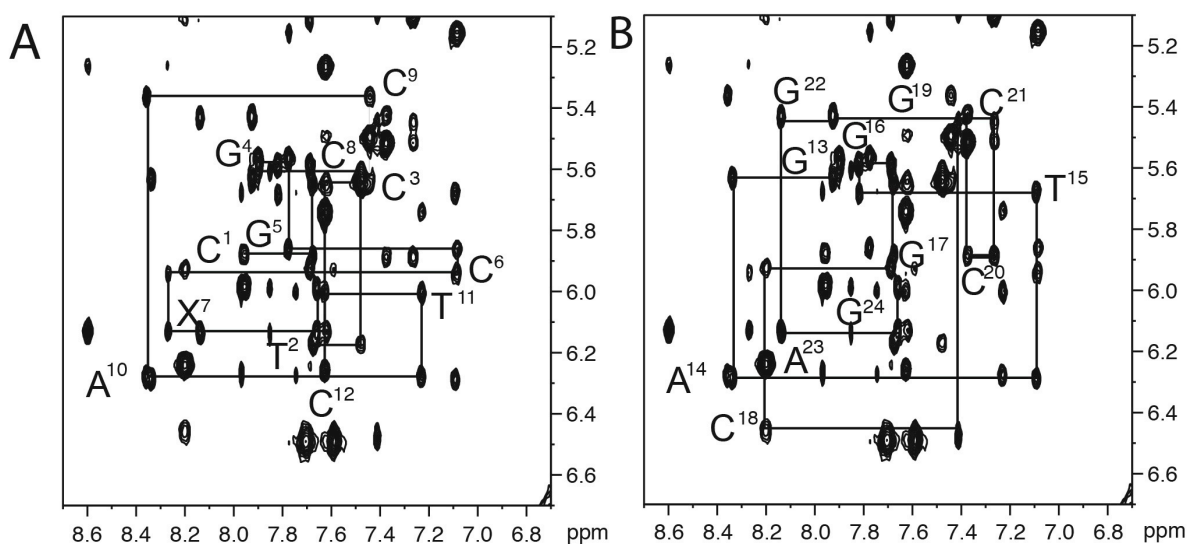


Figure 3-1. Expanded plot of the 250 ms NOESY spectrum showing NOEs between the base aromatic and deoxyribose anomeric protons of the *N*²-dG-IQ modified duplex. A. Bases C¹ to C¹² of the modified strand. B. Bases G¹³ to G²⁴ of the complementary strand. The spectrum was acquired at 800 MHz at 15 °C.

(b) Exchangeable DNA Protons. The imino and amino proton regions of the NOESY spectrum are shown in Figure 3-2. The assignments were made using established methods¹⁰⁰. The *N*²-dG-IQ adduct perturbed Watson-Crick hydrogen bonding. At the X⁷:C¹⁸ base pair, the X⁷ imino proton resonance was broadened, probably due to an enhanced rate of exchange with water. The amino protons for C¹⁸ were not

detected. No NOE was observed between the X⁷ and G¹⁹ imino protons, perhaps due to the broadening of the X⁷ imino proton. The chemical shifts of the X⁷ and G¹⁷ imino protons were almost isochronous. It was not possible to determine if a NOE between these two protons existed. Figure 3-3 shows the assigned X⁷ N1H peak visible as a shoulder to G¹⁷ N1H, which is no longer observable above 5 °C. All other base pairs were assigned, with the exception of the two terminal base pairs C¹:G²⁴ and C¹²:G¹³. The imino protons from the terminal base pairs were exchange broadened. Overall, the data suggested that the duplex maintained Watson-Crick hydrogen bonding, with the exception of the modified base pair (Figure 3-2B). The assignments of the exchangeable protons are summarized in Appendix D.

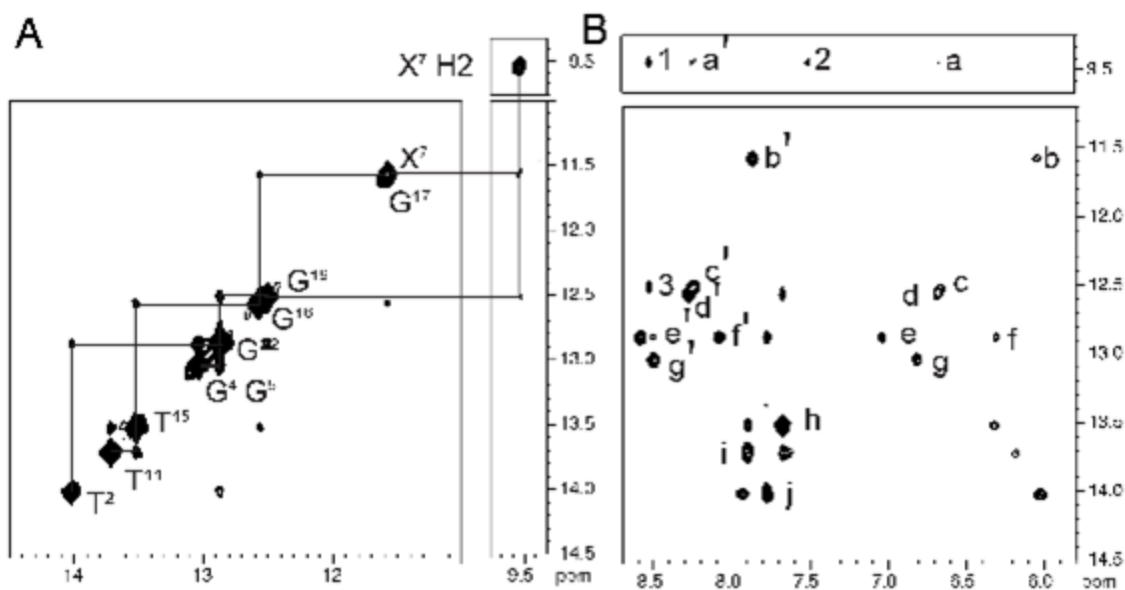


Figure 3-2. Expanded plots of the NOESY spectrum, showing the NOEs between the exchangeable imino and amino protons of the N²-dG-IQ-modified duplex. A. Sequential NOE connectivity for the imino protons of base pairs T²:A²³ to T¹¹:A¹⁴. B. NOE connectivity within Watson-Crick base pairs and between the imino protons and the amino protons. The lettered cross-peaks are assigned as follows: a', X⁷ N²H → C⁶ N⁴Hb; a, X⁷ N²H → C⁶ N⁴Ha; b', G¹⁷ N¹H → C⁸ N⁴Ha; b, G¹⁷ N¹H → C⁸ N⁴Hb; c', G¹⁹ N¹H → C⁶ N⁴Hb; c, G¹⁹ N¹H → C⁶ N⁴Ha; d', G¹⁶ N¹H → C⁹ N⁴Hb; d, G¹⁶ N¹H → C⁹ N⁴Ha; e', G²² N¹H → C³ N⁴Hb; e, G²² N¹H → C³ N⁴Ha; f', G⁵ N¹H → C²⁰ N⁴Hb; f, G⁵ N¹H → C²⁰ N⁴Ha; g', G⁴ N¹H → C²¹ N⁴Hb; g, G⁴ N¹H → C²¹ N⁴Ha; h, T¹⁵ N³H → A¹⁰ H₂; i, T¹¹ N³H → A¹⁴ H₂; j, T² N³H → A²³ H₂; 1, X⁷ N²H → IQ H₄a; 2, IQ H₇a → X⁷ N²H; 3, X¹⁹ N¹H → IQ H₄a. The spectrum was collected at 800 MHz at 5 °C.

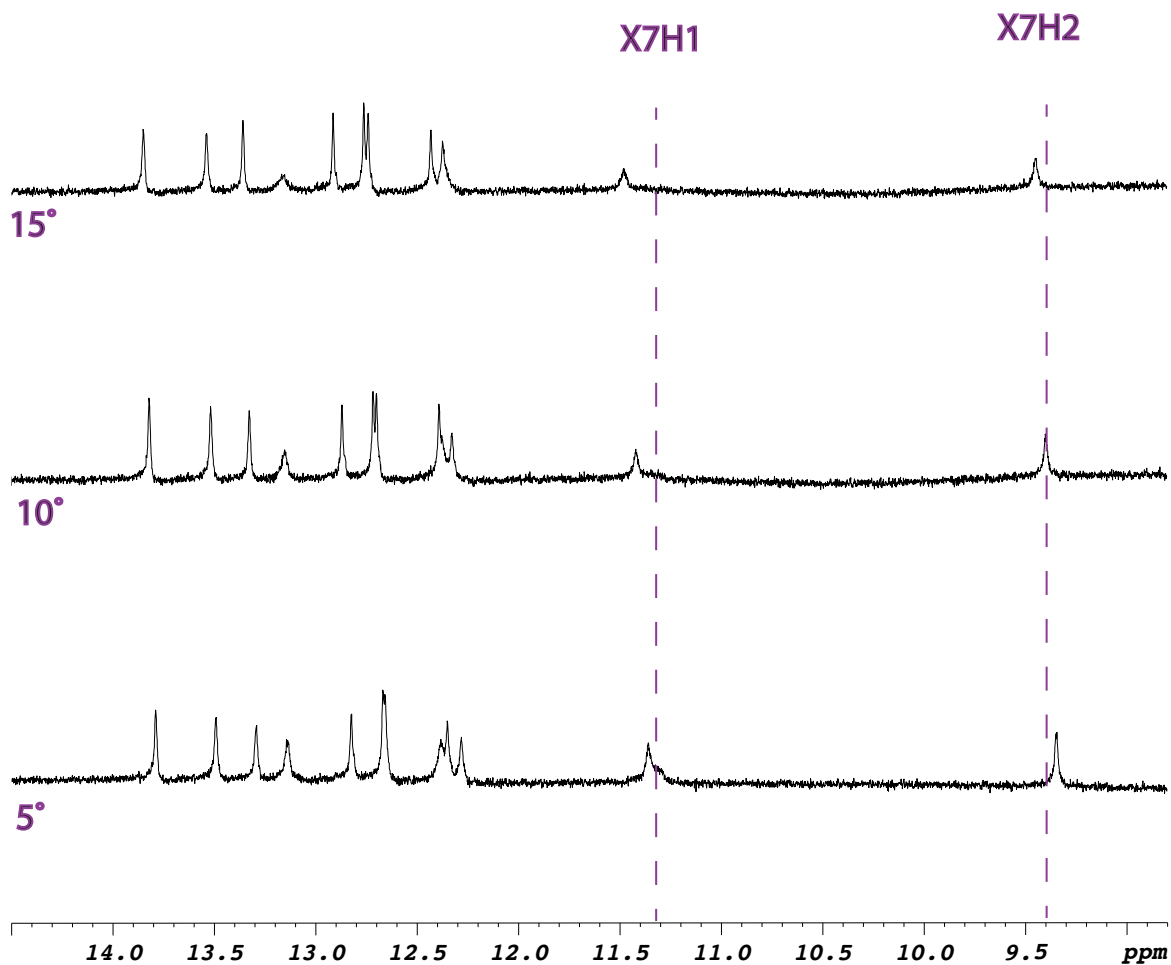


Figure 3-3. 1-D spectra of imino exchangeable region at different temperatures showing the broad peak observed at 5 °C believed to be X⁷ N1H, appearing as a shoulder to G¹⁷ and quickly disappears as the temperature increases, while the X⁷ N2H peak is much sharper.

(c) IQ Protons. The IQ protons, consisting of the CH₃ group, the H4a proton, and the H7a, H8a, and H9a spin system, were assigned from a combination of COSY and NOESY data (Figure 3-3). The CH₃ resonance was observed at 3.57 ppm. It displayed an intense NOE to the H4a proton, whose resonance was observed at 8.55 ppm. A ³J coupling between the H8a proton (δ 6.55 ppm) and the H9a proton (δ

7.65 ppm) was observed in the COSY spectrum. The H8a proton also exhibited an NOE to the H7a proton (δ 7.6 ppm). The 3J coupling between H8 and H7a exhibited weak intensity in the COSY spectrum. This was attributed to presence of the nitrogen atom in the ring, which broadened the H7a resonance. This effect was also observed for the C8-dG-IQ adduct, for which the COSY cross peak between H7a and H8a was only observed between 25-35 °C ¹³⁸. The IQ amine proton was not assigned. Assignments are shown in Figure 3-3.

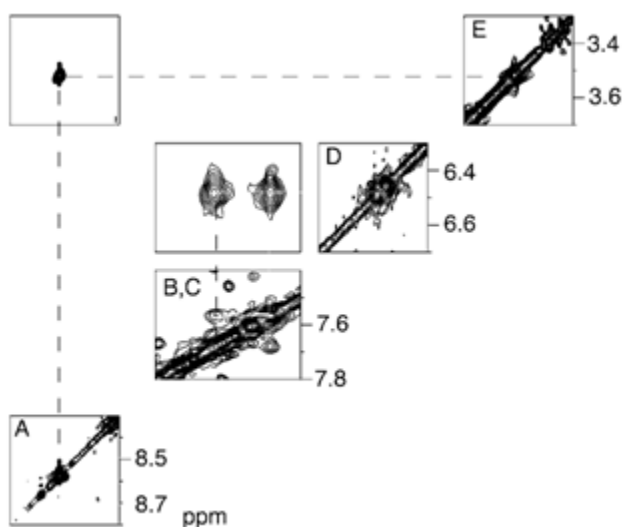


Figure 3-4. Expanded tile plot of the 250 ms NOESY spectrum showing the assignments of the IQ ring protons. A. The IQ H4a proton was observed at 8.55 ppm. B. The IQ H9a proton was observed at 7.65 ppm. C. The IQ H7a proton was observed at 7.6 ppm. D. The IQ H8a proton was observed at 6.55 ppm. E. The IQ CH3 protons were observed at 3.57 ppm. The spectrum was collected at 800 MHz at 15 °C.

(d) Chemical Shift Perturbations. The *N*²-dG-IQ adduct resulted in localized chemical shift perturbations, involving the modified base pair X⁷:C¹⁸ and the neighboring C⁶:G¹⁹ and C⁸:G¹⁷ base pairs (Figure 3-5). At the modified X⁷:C¹⁸ base pair, the X⁷ H8 resonance shifted 0.4 ppm downfield relative to the G⁷ H8 resonance in the

unmodified duplex. In contrast, the C¹⁸ H6 and C¹⁸ H1' resonances shifted 1 ppm and 0.8 ppm downfield, respectively. At the 5'-neighbor C⁶:G¹⁹ base pair, the C⁶ H6 resonance shifted upfield by 0.2 ppm, whereas the C⁶ H1' resonance shifted downfield by 0.4 ppm. The G¹⁹ H8 and H1' resonances each shifted upfield by 0.4 ppm.

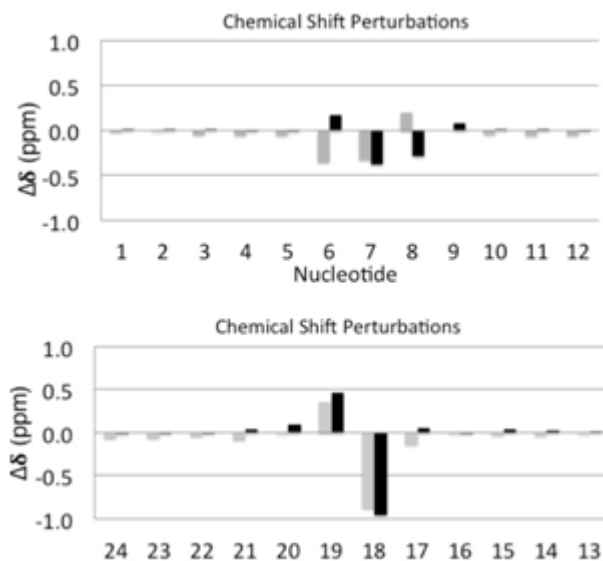


Figure 3-5. Chemical shift perturbations of the deoxyribose H1' protons (grey) and the pyrimidine H6 or purine H8 aromatic protons (black), for the N²-dG-IQ modified duplex. A. Nucleotides C¹-C¹² in the modified strand. B. Nucleotides G¹³-G²⁴ in the complementary strand. The Δδ (ppm) values were calculated as δ_{modified duplex}-δ_{unmodified duplex}. Positive Δδ values represent upfield chemical shift perturbations. Negative Δδ values represent downfield chemical shift perturbations.

At the 3'-neighbor C⁸:G¹⁷ base pair, the C⁸ H8 resonance shifted downfield by 0.3 ppm, whereas the C⁸ H1' resonance shifted upfield by 0.2 ppm. The G¹⁷ H8 resonance shifted downfield 0.1 ppm. The G¹⁷ H1' resonance showed negligible chemical shift perturbation. The resonances for the remaining base pairs in the duplex also showed negligible chemical shift perturbations. In the imino proton region of the spectrum, the X⁷ and G¹⁷ N1H imino resonances, at 11.57 and 11.59 ppm, respectively, exhibited upfield chemical shifts of greater than 1 ppm from

those of the unmodified duplex, at 13.24 and 13.16 ppm, respectively. The X⁷ N²H amine resonance was observed at 9.5 ppm.

(e) NOEs Between IQ and DNA. The CH₃, H4a, H7a, and H8a protons of IQ exhibited NOEs to the C⁸, G¹⁷, C¹⁸, and G¹⁹ bases (Table 3-1). The pattern of NOEs involving H9a was difficult to establish due to resonance overlap with G¹⁷. The CH₃ group showed medium strength NOEs to X⁷ H1' and C⁸ H6, and weak NOEs to C⁸ H1' and C⁸ H5. It also showed an NOE to the G¹⁹ N1H imino proton. The H4a proton showed a strong NOE to X⁷ H1', and medium NOEs to C⁸ H5, the X⁷ N2H amine proton, and the G¹⁹ N1H imino proton, and weak NOEs to X⁷ H2' and X⁷ H2''. The H7a proton exhibited weak NOEs to G¹⁷ H1', and the X⁷ N2H amine proton. Three NOEs from X⁷ to C¹⁸ were observed; these were of medium strength NOE between H9a and C¹⁸ H1', and H8a and medium strength between C¹⁸ H2' and H2''. The H8a proton showed a medium strength NOE to G¹⁹ H3', and weak NOEs to G¹⁷ H1' and G¹⁹ H8. Some 30% of the NOEs from the IQ ring were to protons in the complementary strand, while another 46% were to other IQ protons and protons of the modified base. The remaining 24% of the NOEs were to neighbor bases in the modified strand.

Table 3-1. Summary of NOEs observed between *N*²-dG-IQ adduct protons and oligodeoxynucleotide protons, and their intensities.

IQ proton	NOEs to Oligodeoxynucleotide Protons
CH₃	X ⁷ H1' - medium; C ⁸ H6 - medium; C ⁸ H1' - weak; C ⁸ H5 - weak
H4a	X ⁷ H1' - strong; C ⁸ H5 - medium; X ⁷ H2' - weak; X ⁷ H2'' - weak; X ⁷ N2H - medium; G ¹⁹ N1H - medium
H7a	G ¹⁷ H1' - weak, X ⁷ H2 - weak
H8a	G ¹⁹ H3' - medium; C ¹⁸ H2' - medium; C ¹⁸ H2'' - medium; G ¹⁷ H1' - weak, G ¹⁹ H8 - weak; G ¹⁷ H2'' - weak
H9a	C ¹⁸ H1' - medium

Conformational Refinement

After the unmodified duplex was constructed using B-DNA coordinates¹³⁹, the guanine at position G⁷ was replaced by the *N*²-dG-IQ adduct. The partial charges for the *N*²-dG-IQ adduct are provided in Figure S2 of the Supplementary Data. Potential energy minimization provided an energy minimized starting duplex. A total of 329 distance restraints consisting of 127 inter- and 202 intra-nucleotide distances (Table 3-2) were obtained using the program MARDIGRAS^{140,141}, from 15 °C NOESY data. Similar distance restraints were obtained if the data were collected at 150 ms, 200 ms, or 250 ms mixing times. These restraints included 16 DNA-IQ distances. A total of 49 Watson-Crick hydrogen-bonding restraints were applied for all of the base pairs except for the modified X⁷:C¹⁸ base pair. An additional 100 phosphodiester backbone and 20 deoxyribose pseudorotation restraints for base pairs not proximal to the site of modification were obtained from canonical values derived from B-DNA¹³⁹, consistent with the spectroscopic

data indicating that the duplex maintained a B-DNA like structure. A series of rMD calculations were performed using a simulated annealing protocol in which the generalized Born solvation model¹⁴² was used, with a salt concentration of 0.1 M. The emergent structures were subjected to potential energy minimization before further analysis, which involved a 100 ps rMD calculation using the protocol described above, again followed by potential energy minimization.

Table 3-2. NMR restraints used for the *N*²-dG-IQ structure calculations and refinement statistics.

NOE restraints	
Internucleotide	127
Intranucleotide	202
Total	329
Backbone Torsion Angle Restraints	100
H-bonding Restraints	49
Deoxyribose Restraints	20
Total number of restraints	498
Refinement Statistics	
Number of distance restraint violations	56
Number of torsion restraint violations	50
Total distance penalty/Maximum penalty [kcal mol ⁻¹]	2.3/0.187
Total torsion penalty/Maximum penalty [kcal mol ⁻¹]	2.8/0.177
r.m.s. distances (Å)	0.012
r.m.s. angles (°)	2.5
Distance restraint force field [kcal mol ⁻¹ Å ⁻²]	32
Torsion restraint force field [kcal mol ⁻¹ deg ⁻²]	32

The pairwise rmsd analysis of structures emergent from the rMD calculations was used to measure the precision of the structural refinement. Ten structures were chosen based on the lowest deviations from the experimental distance and dihedral restraints (Figure 3-6). These exhibited an rmsd of 0.012 Å in distances and 2.5° in torsion angles (Table 3-3). There were 56 distance violations with a maximum penalty of 0.187 kcal•mol⁻¹

and a total distance penalty of 2.3 kcal•mol⁻¹. There were 50 torsion angle violations with a maximum penalty of 0.177 kcal•mol⁻¹ and a total torsion angle penalty of 2.8 kcal•mol⁻¹. The maximum pairwise rmsd distances were 1.12 Å. These structures were averaged and subjected to potential energy minimization.

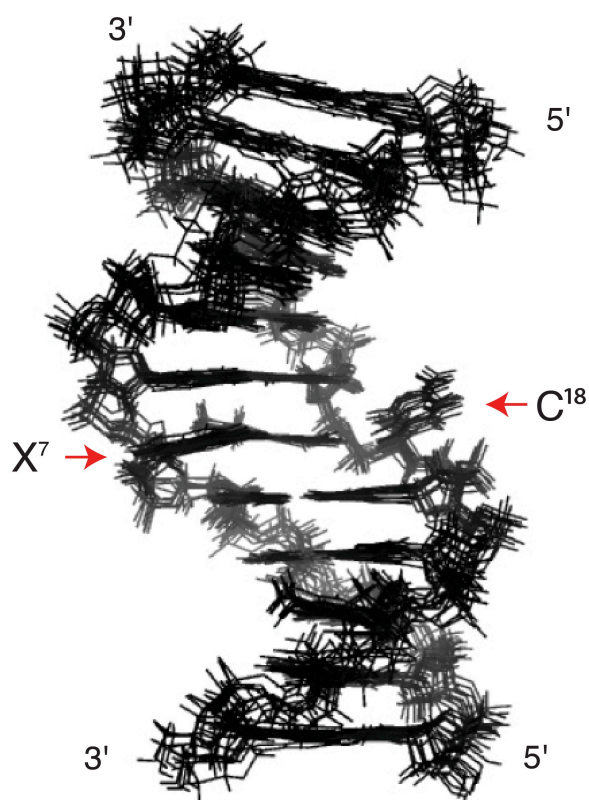


Figure 3-6. Superposition of ten potential energy minimized structures emergent from the rMD calculations of the *N*²-dG-IQ modified duplex, using distance restraints from the 250 ms NOESY data. The positions of the modified X⁷ nucleotide and the C¹⁸ nucleotide in the complementary strand are as indicated. The maximum pairwise rmsd between these ten structures was 1.12 Å.

The accuracy of the refined structures was assessed by complete relaxation matrix analyses^{140,143}, which compared intensities calculated from the refined structures with the distance restraints (Figure 3-6). The sixth root residual R^1_x value of the average structure was 8.4%, and the individual values for intra-nucleotide restraints (8.5%) and inter-nucleotide restraints (8.3%) were of similar magnitudes. This indicated agreement with

the NOE data. Nucleotide G¹⁹ exhibited a greater R_x¹ value of 17.1%, suggesting that it was not as well-refined. This was attributed to several NOEs involving G¹⁹ being overlapped with other resonances. The structural statistics are summarized in Table 3-4.

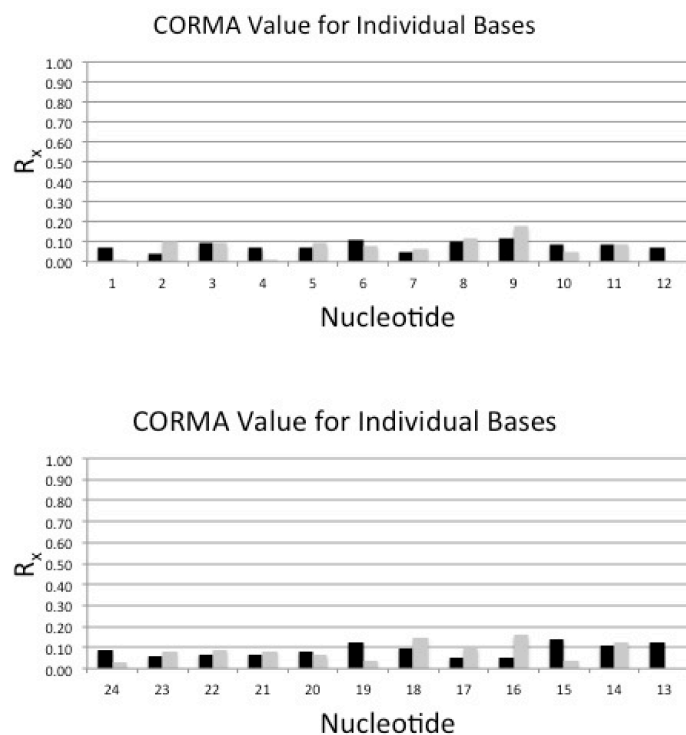


Figure 3-7. Sixth root residuals (R_1^x) calculated using complete relaxation matrix calculations from the average of ten structures emergent from the rMD calculations of the N^2 -dG-IQ modified duplex. The black bars represent intra-nucleotide sixth root residuals and the grey bars represent inter-nucleotide sixth root residuals. A. Nucleotides C¹-C¹² in the modified strand. B. Nucleotides G¹³-G²⁴ in the complementary strand.

Table 3-3. Structural statistics for the N^2 -dG-IQ modified duplex.

Average structure (obtained from 10 structures)			
RMS pairwise difference between structures		1.12	
RMS difference from average structure		0.75	
CORMA analysis for average structure ^a			
	Intranucleotide	Internucleotide	Total
R_x^1 ^b	0.085	0.083	0.084
Average error ^c			0.0037

Conformation of the *N*²-dG-IQ Adduct

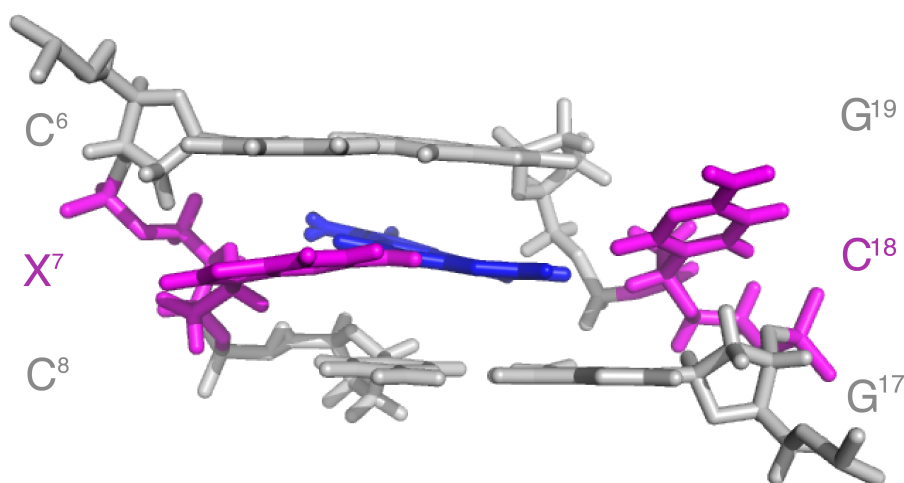


Figure 3-8. Expanded view of the average structure calculated from ten structures emergent from the rMD calculations of the *N*²-dG-IQ modified duplex, showing base pairs C⁶:G¹⁹, X⁷:C¹⁸, and C⁸:G¹⁷. The view is from the major groove. The modified base pair X⁷:C¹⁸ is shown in magenta, with the IQ moiety shown in blue.

The nucleotide X⁷ remained in the *anti* conformation about the glycosyl bond. It was displaced toward the major groove. The IQ ring was intercalated and oriented such that the H4a proton and the CH₃ group faced into the minor groove, whereas the H7a, H8a, and H9a protons faced into the major groove (Figure 3-8). The IQ ring was angled by approximately 15° with respect to the modified guanine, but otherwise remained largely in plane with the damaged base. The helix was unwound between C⁶ and X⁷, with a reduced helicoidal twist of 30°. This was partially compensated by an increased twist of 9° between X⁷ and C⁸. At base pair X⁷:C¹⁸ the roll of the X⁷ purine decreased by 24°. This was compensated at base pair C⁸:G¹⁷, where the roll decreased by 12°. Consequently, the *N*²-dG-IQ adduct induced a bend of 10° to the duplex. The IQ ring exhibited stacking with the flanking base pairs (Figure 3-9). IQ was stacked between G¹⁷ and G¹⁹ of the complementary strand of the C⁶:G¹⁹ and C⁸:G¹⁷ base pairs. The complementary nucleotide, C¹⁸, extruded

into the major groove and did not exhibit stacking with the neighboring base pairs. The base opening between X⁷ and C¹⁸ increased by 76°. This disrupted Watson-Crick hydrogen bonding. The other base pairs maintained Watson-Crick hydrogen bonding. The structural coordinates were deposited in the Protein Data Bank (www.rcsb.org): the PDB ID code for the N²-dG-IQ duplex is 2MAV.

Discussion

The N²-dG-IQ DNA adduct has been of interest following reports that it is more persistent than the C8-dG-IQ adduct in rodents and primates that were fed IQ in their diet¹⁴⁴. The synthesis of this adduct and its incorporation into oligodeoxynucleotides¹³⁵ has allowed the conformation of the N²-dG-IQ adduct at the G³-position of this sequence to be determined. This is a hot spot for two-base frameshift deletions in bacterial mutagenesis assays¹⁴⁵⁻¹⁵⁰. Additionally, human DNA polymerase (hpol) η produces two-base deletions when replicating past the N²-dG-IQ adduct at position G³ *in vitro*¹⁵¹.

Conformation of the N²-dG-IQ Adduct

The IQ ring intercalates when the N²-dG-IQ adduct is positioned at the frameshift-prone G³ position of the *NarI* sequence (Figure 3-7). The strong NOE intensities of the IQ H4a and CH₃ protons to the X⁷ and C⁸ H1' protons (Table 3-1) indicate that these protons face into the minor groove and establish the conformation about the bond between N²-dG and C5 of the IQ moiety. In contrast, NOEs involving the H8a proton of the IQ ring are primarily to bases G¹⁷, C¹⁸, and G¹⁹ of the complementary strand (Table 3-1). The chemical shifts of the IQ H7a, H8a, and H9a protons are observed between 6.5 and 8.0 ppm, which is

1.3-2.0 ppm upfield as compared to the *N*²-IQ-dG nucleoside. This is consistent with the intercalated conformation and stacking of the IQ ring below the 5'-neighboring G¹⁹ of the complementary strand and above the 3'-neighboring C⁸:G¹⁷ base pair (Figure 3-8). Chemical shift perturbations corroborate the NOE data (Figure 3-5). The IQ H4a proton resonance, observed at 9.6 ppm, is 0.4 ppm upfield from the resonance observed for the modified *N*²-dG-IQ nucleoside¹³⁵, consistent with its location below G¹⁹ and above C⁸ (Figure 3-8). The IQ moiety displaces the complementary C¹⁸ base from the duplex, and flips it into the major groove. This is supported by smaller perturbations in chemical shifts for the H4a and CH₃ protons as compared to the H7a, H8a, and H9a aromatic protons of IQ. The displacement of the modified nucleotide X⁷ toward the major groove (Figure 3-8) is supported by the downfield chemical shift change of 0.4 ppm for the X⁷ H8 and H1' protons of the modified base. The C⁸ H6 proton resonance also experiences a downfield shift of 0.3 ppm. The stacking interactions of the IQ ring with the flanking bases C⁸, G¹⁷, and G¹⁹ are reflected in the thermodynamic analysis of the adduct, in which the thermal melting temperature of 63 °C is unchanged from that of the unmodified duplex.

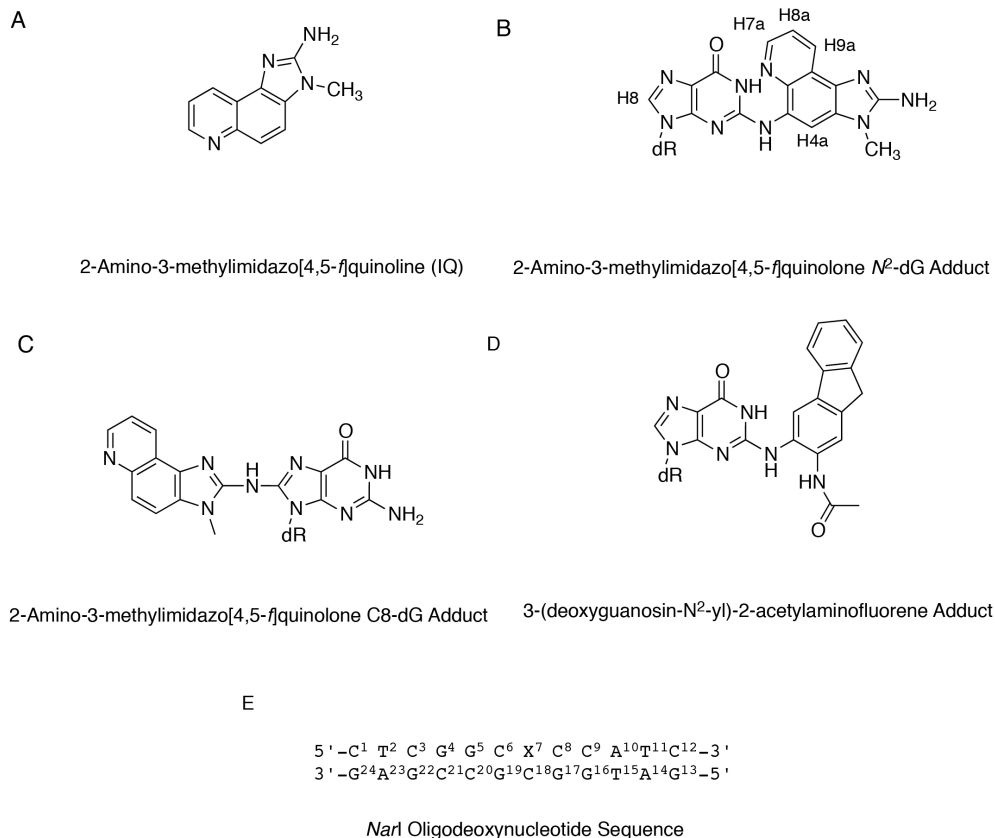


Chart 3-1. Adduct structures: A. Structure of 2-amino-3-methylimidazo[4,5-f]quinolone (IQ). B. Structure of the N^2 -dG-IQ adduct, showing the numbering of guanine base and IQ protons. C. Structure of the C8-dG-IQ adduct. D. Structure of the N^2 -dG-AAF adduct. E. The duplex containing the *NarI* sequence, showing the numbering of the nucleotides. The N^2 -dG-IQ adduct is positioned at X⁷, which corresponds to the G³ frameshift-prone position of the *NarI* sequence.

Comparison to the N^2 -Acetylaminofluorene-dG Adduct

The other N^2 -dG arylamine adduct that has been subjected to conformational analysis, although not in the *NarI* sequence of interest herein, is that arising from *N*-acetylaminofluorene (AAF; Chart 3-1)¹⁵². The N^2 -dG-AAF adduct conformation has also been examined using computational approaches¹⁵³. Zaliznyak et al.¹⁵² have shown that the AAF moiety resides in the minor groove with its long axis directed toward the 5'-end of the modified strand. This shields the hydrophobic AAF ring from water. Similar to the N^2 -dG-IQ adduct, the modified nucleotide maintains the *anti* conformation about the glycosyl

bond. Notably, the *N*²-dG-AAF adduct increases the stability of the DNA by 6 °C, which has been attributed to a favorable entropic effect¹⁵². The present data reveal that the base-displaced intercalated conformation of the *N*²-dG-IQ adduct at position G³ of the *NarI* sequence differs from that of the *N*²-dG-AAF adduct, suggesting that the conformations of *N*²-dG arylamine adducts vary rather than following a common motif. At the molecular level, the factors governing whether planar aromatic molecules such as AAF or IQ favor DNA groove binding vs. intercalation are not well established, but may be influenced both by their electronic structures and their respective geometries¹⁵⁴. Replication bypass studies have revealed that the *N*²-dG-AAF adduct largely blocked DNA synthesis but when bypassed, mis-incorporation of dATP opposite the lesion was observed¹⁵⁵.

Comparison to the C8-dG-IQ Adduct

When the C8-dG-IQ adduct was placed into the *NarI* sequence at the frameshift-prone G³ position, the IQ ring also intercalated into the duplex and the complementary C¹⁸ base was extruded into the major groove. The conformation of the C8-dG-IQ adduct also was characterized as base-displaced intercalated¹⁵⁶. Thus, at the G³ position within the *NarI* sequence, both the C8-dG-IQ and *N*²-dG-IQ adducts share a motif in which the IQ ring intercalates and C¹⁸ extrudes into the major groove. However, the two conformations are distinctive. Apart from the difference in the regiochemistry of alkylation (C8 vs. *N*², Scheme 1-1), a major difference between the C8-dG-IQ and *N*²-dG-IQ adducts is that the C8-dG-IQ-modified guanine adopts a *syn* conformation about the glycosyl bond, whereas the *N*²-dG-IQ-modified guanine maintains the *anti* conformation about the glycosyl bond (Figures 3-8 and 3-9). In addition, for the C8-dG-IQ adduct, rotation of the glycosyl bond into the *syn*

conformation places the Watson–Crick hydrogen bonding edge of the modified dG into the major groove. The X⁷ imino and amino protons are exposed to solvent. The orientation of the IQ ring of the C8-dG-IQ adduct about the linkage between the C8-dG and the N²-IQ atoms also differs, such that the IQ CH₃ group and H4a and H5a protons face the major groove rather than the minor groove¹⁵⁶. The orientation of the C8-dG-IQ adduct in the duplex rotates the bulk of the IQ aromatic ring away from the flanking bases, resulting in a loss of base-stacking interactions, as shown in Figure 3-9. In comparison, the N²-dG-IQ adduct appears to have more favorable stacking interactions with G¹⁹. These differences may lead to differential processing during both DNA repair and DNA replication.

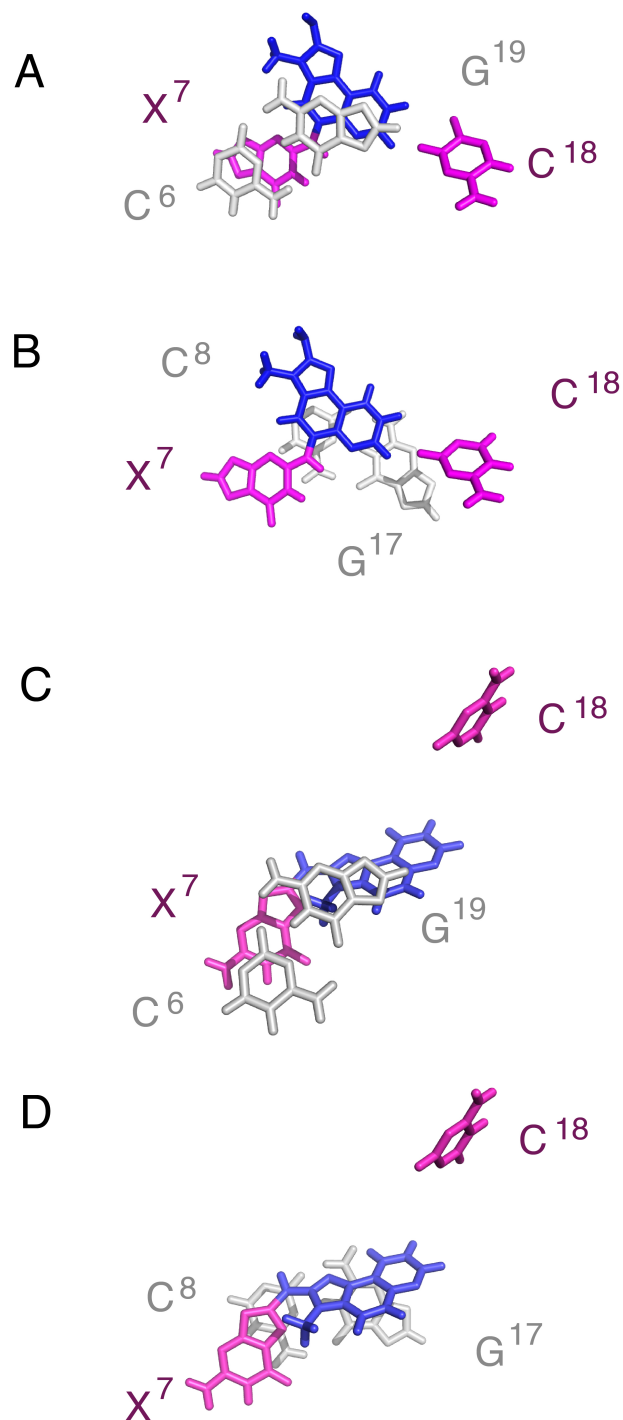


Figure 3-9. Expanded views of the average structure calculated from ten structures emergent from the rMD calculations of the *N*²-dG-IQ modified duplex. Base-stacking of the modified X⁷:C¹⁸ base pair with the 5'-neighbor and 3'-neighbor base pairs. A. Stacking of C⁶:G¹⁹ above X⁷:C¹⁸. B. Stacking of X⁷:C¹⁸ above C⁸:G¹⁷. Expanded views of the average structure of the corresponding C8-dG-IQ adduct at X⁷.⁷⁵ C. Stacking of C⁶:G¹⁹ above X⁷:C¹⁸. D. Stacking of X⁷:C¹⁸ above C⁸:G¹⁷. In each instance the modified base pair X⁷:C¹⁸ is shown in magenta, with the IQ moiety shown in blue.

Structure-Activity Relationships

The N^2 -dG-IQ adduct is less efficiently removed from genomic DNA by nucleotide excision repair^{144,157}. The NER machinery is thought to recognize bulky DNA damage that is destabilizing and distortive to the duplex¹⁵⁸⁻¹⁶¹. It has been proposed that the thermal stabilization of the N^2 -dG-AAF adduct hinders NER¹⁵². We observe that the T_m of the N^2 -dG-IQ adduct at position G³ within the *NarI* sequence does not destabilize the duplex (Table 3-4), correcting our original report¹³⁵. The T_m of the N^2 -dG-IQ modified duplex is 63° C and does not differ significantly from the unmodified duplex. This is remarkable, given that the intercalated IQ moiety disrupts Watson-Crick hydrogen bonding and that the complementary C¹⁸ base is displaced into the major groove. The stability of the N^2 -dG-IQ modified duplex likely arises from favorable stacking between the IQ moiety and the neighboring base pairs (Figure 3-9). It is also interesting to note that unlike the N^2 -dG-IQ adduct, the C8-dG-IQ adduct (which does not stack with the neighboring bases as well at this position (Figure 3-9)) thermally destabilizes the duplex, reducing the T_m by 4°C. Yeo et al.¹⁶² examined acetylaminofluorene (AAF) and aminofluorene (AF) C8-dG adducts within the *NarI* sequence and observed a correlation between the degree of destabilization induced by the lesions, binding affinities to the damage recognition protein XPC-RAD23B, and overall NER efficiencies. Likewise, Zaliznyak et al. attributed the increased stability of the N^2 -dG-AAF adduct to its orientation within the minor groove and the entropy-favored release of waters from the duplex¹⁵². Similar conclusions were reached by Cai et. al.¹⁶³ who correlated thermodynamic stabilities and van der Waals interaction energies with repair efficiencies for stereoisomeric intercalated N^6 -dA PAH adducts. Their studies showed that intercalated adducts with fewer DNA structural distortions and increased van der Waals

interactions with neighboring bases correlated with reduced repair efficiencies. The heterocyclic amine PhIP adduct has been compared with the *cis*-B[a]P-*N*²-dG adduct in duplex DNA and in a nucleotide deletion duplex and it was concluded that local stabilization induced by these adducts governs the ability of the β -hairpins of NER proteins to recognize the damage¹⁶⁴. In summary, it seems plausible that the thermal stability of the *N*²-dG-IQ adduct may, in part, explain the persistence of the *N*²-dG-IQ adduct in rats and primates.

Table 3-4. Thermal melting temperatures (T_m measurements) of *NarI* duplexes containing the *N*²-dG-IQ adducts.

<i>NarI</i> <i>N</i> ² -dG-IQ Modified Duplex	T_m °C	ΔT_m^* °C
5' -CTC <u>X</u> GCGCCATC-3' 3' -GAGCCGCGGTAG-5'	62	-1
5' -CTCG <u>X</u> CGCCATC-3' 3' -GAGCCGCGGTAG-5'	64	+1
5' -CTCGGC <u>X</u> CCATC-3' 3' -GAGCCGCGGTAG-5'	63	0

If not repaired, the *N*²-dG-IQ adduct is anticipated to be genotoxic. Indeed, IQ is an order of magnitude more mutagenic than is aflatoxin B₁ in Ames assays. The mutations occur primarily at G:C base pairs^{165,166}. The replication of the *N*²-dG-IQ-adducts within the *NarI* sequence is influenced by the identity of the DNA polymerase. Because the damaged guanine remains in the *anti* conformation about the glycosyl bond (Figures 3-7 and 3-8), one might anticipate that the *N*²-dG-IQ lesion should block Watson-Crick base pairing with incoming dNTPs during lesion bypass. Stover et al.¹⁶⁷ incorporated the *N*²-dG-IQ-adduct into the G¹- and G³-positions of the *NarI* sequence and examined replication of the oligodeoxynucleotides with Klenow fragment of *E. coli* polymerases (pol) I (exonuclease

deficient), exonuclease deficient pol II, and the *Solfolobus solfataricus* P2 DNA polymerase IV (Dpo4), *in vitro*. At the G³ position the N²-dG-IQ adduct blocked the *E. coli* polymerases. Pol II *exo*⁻ favored correct incorporation of dCTP over dGTP but was unable to extend either of these initial insertion products. In contrast, the Dpo4 polymerase bypassed the N²-dG-IQ adduct and produced an error-free product. The present studies do not necessarily predict the structure of the N²-dG-IQ adduct during trans-lesion bypass. Consequently, it will be of interest to prepare complexes of bypass polymerases with N²-dG-IQ modified template: primers in an effort to determine how the N²-dG-IQ adduct is accommodated during lesion bypass and how polymerases, e.g., the Dpo4 polymerase¹⁶⁸ allow bypass of this lesion.

Bypass of the N²-dG-IQ adduct has been reported to be dependent upon its position in the *NarI* sequence. Choi et al.¹⁵¹ have demonstrated that the human DNA polymerase (hpol) η can extend primers beyond template N²-dG-IQ adducts. Pol η correctly inserts dCTP and incorrectly inserts dATP. Analyses of hpol η extension products reveal that a -2 bp deletion occurs with the G³ N²-dG-IQ adduct. In contrast, at the G¹ position replication past the N²-dG-IQ adduct results in error-free incorporation of dCTP, but further extension is inhibited and the polymerase stalls. In contrast, hpol η does not yield -2 bp deletions with the C8-dG-IQ adduct located at position G³. While further studies will be necessary to probe the basis for these observations, it is of interest to note that the stability of the N²-dG-IQ adduct placed opposite a 2-bp deletion increases as compared to the fully complementary duplex, suggesting that the adduct may stabilize a 2-bp strand slippage intermediate¹³⁵. At the G¹ position, the N²-dG-IQ adduct is bypassed and extended by the *E. coli* polymerases and the Dpo4 polymerase and error-free product is observed. Thus, it will also be of

interest to examine the structure of the *N*²-dG-IQ adduct when positioned at position G¹ of the *NarI* sequence.

Summary

Analysis of the *N*²-dG-IQ adduct placed at position G³ of the *NarI* sequence¹⁴⁵⁻¹⁵⁰, where it has been observed to cause -2 bp deletions when bypassed by hpol η¹⁵¹, reveals that it adopts a base-displaced intercalated conformation in which the H4a and CH₃ protons of the IQ ring face the minor groove and the H7a, H8a, and H9a protons face the major groove. The IQ ring is shielded from water and stacks with the 5'- and 3'-neighbor base pairs. Remarkably, despite this conformational perturbation, the *N*²-dG-IQ adduct does not destabilize the duplex, which may correlate with the observation that it is refractory to repair by NER^{144,157}. Additionally, the IQ moiety disrupts the potential for Watson-Crick hydrogen bonding with incoming dNTPs, which perhaps explains why this lesion blocks DNA synthesis by many polymerases.

Chapter IV

SOLUTION STRUCTURE OF N^2 -dG-IQ AT THE MUTAGENIC HOTSPOT G^1 POSITION IN THE *NAR*I SEQUENCE CONTEXT

Introduction

This chapter examines the effect of IQ attached at the N^2 position of dG when located at the G^1 position in the *NarI* sequence. *In vitro* replication data for this adduct results in error-free bypass for both human and prokaryotic polymerases^{169,170}. This result contrasts to IQ at the G^3 location, which was observed to be a hotspot for -2 bp deletions. Structural comparisons of the G^1 adduct to the G^3 adduct could provide suggest possible explanations for the replication data. However, NMR data for the G^1 duplex support a similar base-displaced intercalated type structure, providing limited insight to replication results. Cell culture experiments conducted by Basu's lab at the University of Connecticut support similar duplex structures, since his lab has observed bypass to be more polymerase dependent rather than sequence context dependent (communicated by Dr. Basu). These structures do allow the N^2 adducts to be differentiated to the C8 adduct and provide a better understanding of the discrepancy in repair efficiencies.

Results

Circular Dichroism

When IQ is located at the G^1 and G^3 position in the *NarI* sequence, there are distinct shifts for each sequence relative to the unmodified sequence, indicating that both sequences have been perturbed. The adducts at G^1 and G^3 had a maximum UV absorption at 270 and 269 nm, respectively. These display blue shifts of 4 and 5 nm relative to the

unmodified duplex. They crossed 0 at 260 and 257 nm for G¹ and G³ IQ modified sequences and had a minimum at 249 and 248 nm compared to the unmodified at 260 and 249 nm. The intensities of the modified spectra are also reduced with respect to the *NarI* sequence. The absorbance of the IQ moiety would be predicted to be visible between 300-360 nm, according to the results of the C8-IQ-dG single strand¹⁷¹, although the signal was broad. In all sequences for *N*²-IQ-dG, there was negligible signal detected in this range as well as in the UV absorption spectrum. The CD spectrum of the *N*²-AF-dG adduct had a negative ellipticity in the 300-360 nm range at the G², which was characterized as a groove-bound conformation but positive ellipticity was observed at the G¹ or G³⁷¹. Since all sequences agree in this range, this could support the hypothesis that all three adducts adopt similar conformations, although the linkage for *N*²-IQ-dG could broaden the signal, making it difficult to detect and hard to interpret.

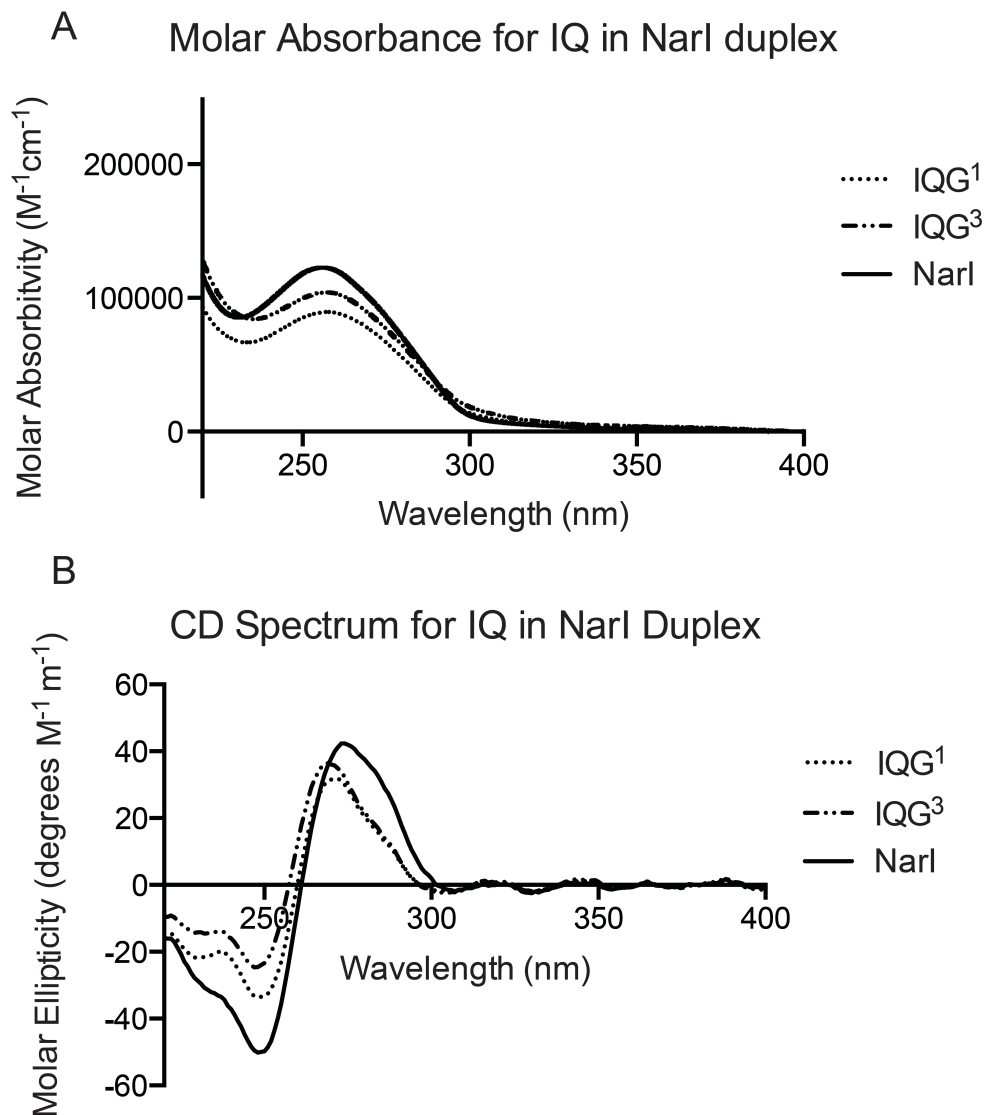


Figure 4-1. A) UV and B) CD spectra for *N*²-dG-IQ at G¹ and G³ as well as the unmodified *NarI* sequence.

NMR

The IQ-modified duplex yielded sharp, well resolved peaks at 15 °C for nonexchangeable proton spectra that were able to be unambiguously assigned, with the exception of many of the H4', H5' H5'' protons, which were overlapped and the majority were not included in structure calculations, with the exception of T² and C²¹. Data was

collected at 5 °C for exchangeable protons, which provided optimal resolution and sharpest peaks.

Magnitude COSY experiments helped to identify cytosine shifts as well as the aromatic protons of the IQ adduct with 3J coupling. However, crosspeaks between H7a and H8a were broadened due to the presence of the nitrogen atom. This effect was also observed in NMR experiments of the nucleoside¹³⁸.

The guanine proton X⁴ H8 was shifted downfield 0.47 ppm relative to the unmodified oligonucleotide and the H1' shifted downfield by 0.74 ppm. The opposite base C²¹H6 and H1' was shifted downfield by 0.81 and 1.26 ppm indicating a deshielding effect for this base. The intensity of the NOE for C²¹ H1' and G²² H8 was very weak, indicating the most significant impact on the base opposite the adduct. C³H1' and H6 were shifted 0.51 and 0.46 ppm downfield, while its partner, G²², was shifted 0.17 and 0.34 ppm downfield. G⁵ H8 was shifted 0.28 downfield, while C²⁰ H6 was shifted 0.19 ppm upfield. These shifts were likely due to a shift in base stacking by the presence of the IQ. The remaining peaks were relatively unaffected by the presence of IQ, shifting less than 0.1 ppm from the unmodified duplex. The relative pattern of chemical shift perturbations closely resembled that of the IQ at G³ as well. The base opposite the adduct had the greatest downfield shifts, while the perturbations to the bases to either side of the opposite bases were less than half the magnitude of the base directly opposite, either C¹⁸ or C²¹ for G³ and G¹. The modified base itself was shifted downfield as well by 0.4 ppm, and the bases flanking it were also perturbed by a similar magnitude.

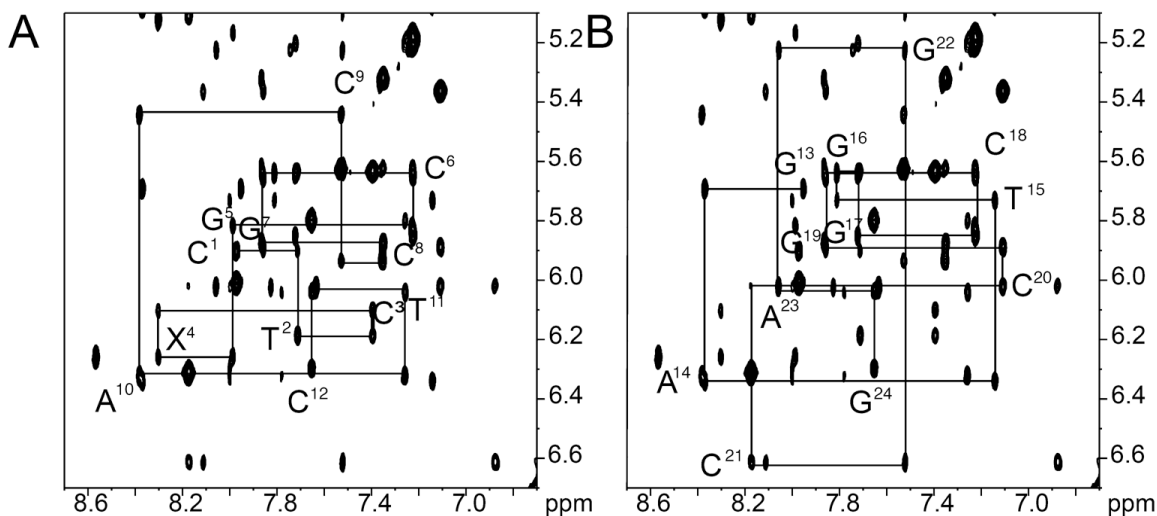


Figure 4-2. Plot of NOESY spectrum with 150 ms mixing time showing connectivities between base aromatic protons to deoxyribose anomeric protons for adduct *N*²-dG-IQ located at G¹ position. A) Bases C¹ to C¹² for modified strand. B) bases G¹³ to G²⁴ for complementary strand. Spectrum was acquired at 900 MHz at 15 °C.

IQ Proton Assignments

All chemical shifts for adduct protons have been identified and are shown in Figure 4-2. The IQ CH₃ group and H4a had NOEs with protons X⁴H1' and X⁵H1' in the minor groove of the duplex indicating the imidazole ring of IQ is oriented into the minor groove. The IQ H8a and H9a protons were identified by the ³J coupling in the aromatic region of the COSY spectrum. The IQ H7a to H8a crosspeak is observed in the NOESY spectrum and was easily assigned. These protons had many NOEs to bases from the complementary strand, mostly to C²⁰ and C²¹ and a single NOE to G²² that was identified. Figure 4-3 depicts the assignments of the IQ ring, while Table 4-1 describes the observed NOEs to the DNA.

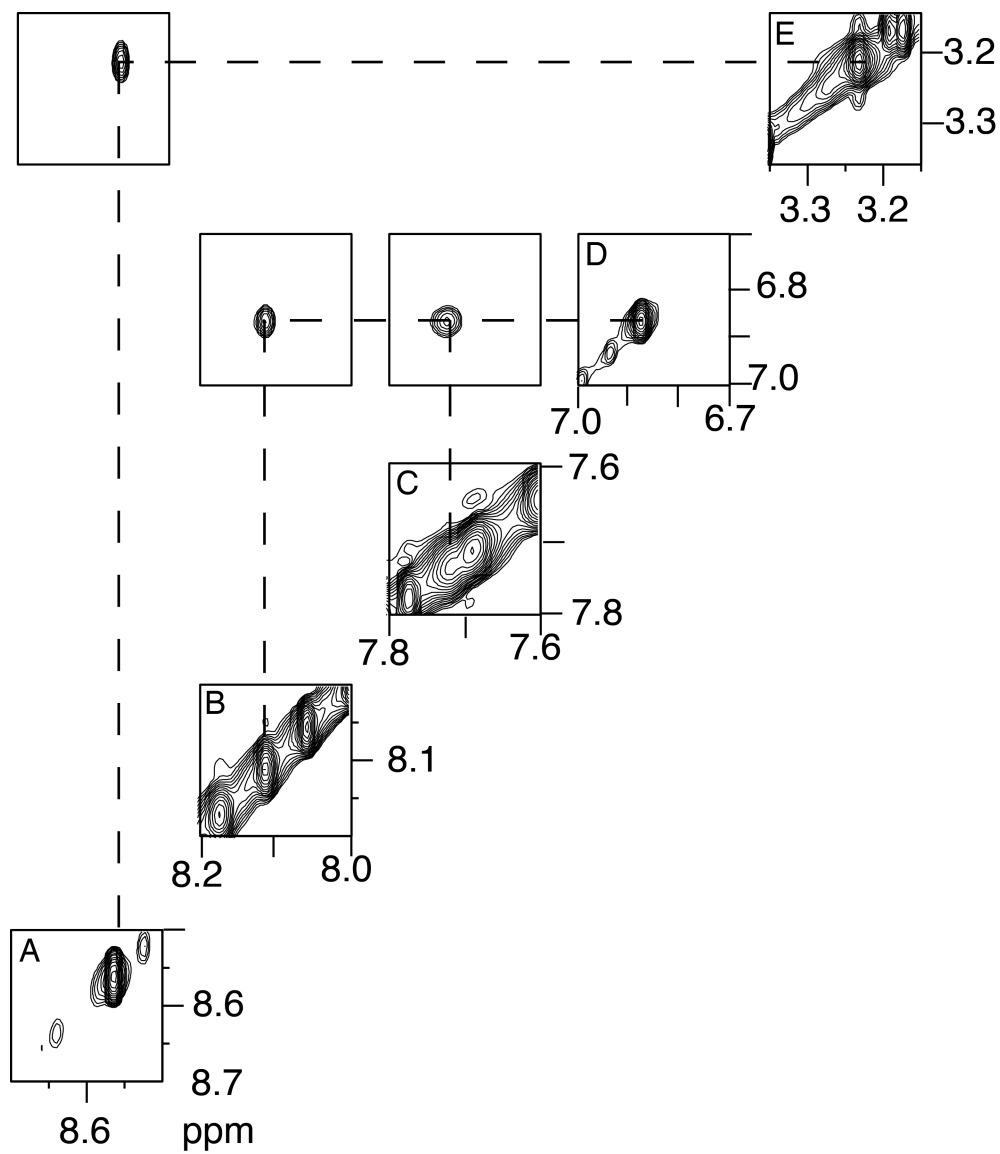


Figure 4-3. Plot of NOESY spectrum showing IQ ring proton assignments. A. IQ H4a proton was observed at 8.56 ppm. B. H7a was observed at 8.11 ppm. C. IQ H9a was observed at 7.74 ppm. D. IQ H8a was observed at 6.87 ppm. E. IQ CH₃ was observed at 3.23 ppm.

Table 4-1. Summary of observed NOEs from IQ to DNA and their intensities.

IQ proton	NOEs to oligonucleotide protons:
CH ₃	X ⁴ H1' – strong; G ⁵ H8 – medium; X ⁴ H2''; X ⁴ H2'; G ⁵ H1' – weak
H4a	X ⁴ H1' – strong; X ⁴ H2'' –weak; X ⁴ H2' – weak
H7a	G ²² H1' – medium
H8a	C ²¹ H1' – medium; C ²⁰ H1' – medium; C ²¹ H4' – medium; C ²⁰ H2'' – medium; G ²² H8 – weak; C ²⁰ H6 – weak; C ²¹ H2' – weak; C ²¹ H2'' – weak; C ²¹ H5' – weak; C ²¹ H5'' – weak
H9a	C ²¹ H1' – medium; C ²⁰ H5 – medium; C ²⁰ H2'' – weak

Exchangeable Protons

The 1D ¹H spectrum of the imino region of the duplex supported the assignments of the 2D NOESY spectrum. Here we could observe the broadened imino proton peak for the modified base at low temperatures that was too broad to be observed in the NOESY spectrum at 11.8 ppm. The peak quickly broadened in the 1D with increased temperature as shown in Figure 4-4. The sharp upfield peak at 9.5 ppm was assigned as X⁴N2H, which is typically not observed. However, the peak was very sharp and persistent and was visible up to a temperature of ~55 °C, when most of the duplex had melted, suggesting a stabilizing effect comes from an intrastrand interaction. This peak also had NOEs to the amino protons of C³ and C²¹ as well as IQ protons H4a and H9a.

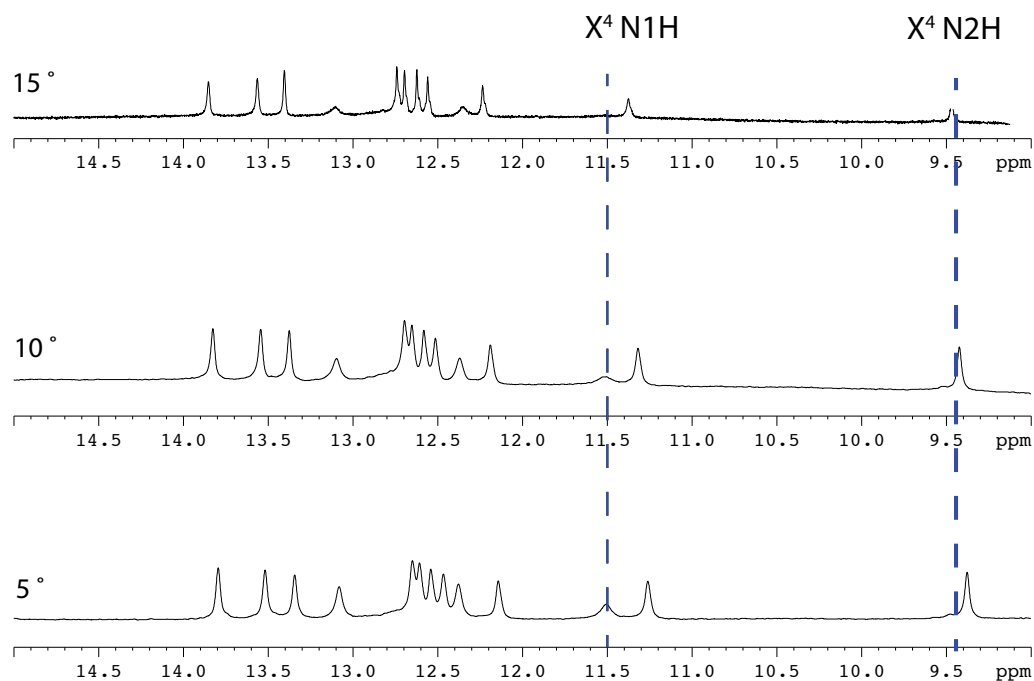


Figure 4-4. 1-D spectrum of imino region from 5 °C – 15 °C showing the assignment of X⁴ N1H proton, which quickly broadens as temperature increases.

The imino/amino proton region of the NOESY spectrum indicated a loss of hydrogen bonding between X⁴ and C²¹ (Figure 4-5). The imino proton of X⁴ was visible at 11.8 ppm in the 1D spectrum at 5 °C, but was nearly completely broadened out of the spectrum at 10 °C. X⁴ N1H does not have crosspeaks to the flanking base-pair imino protons, suggesting a shift in the base stacking at the modified base pair. X⁴ N1H did have a weak crosspeak to X⁴ N2H; however, the X⁴ N1H has broadened, likely due to solvent exchange and was not visible in the NOESY spectrum. All protons involved in hydrogen bonding were observed except for C²¹ amino protons. No other Watson-Crick hydrogen bonding for other base pairs appeared to be affected by the presence of the IQ ring.

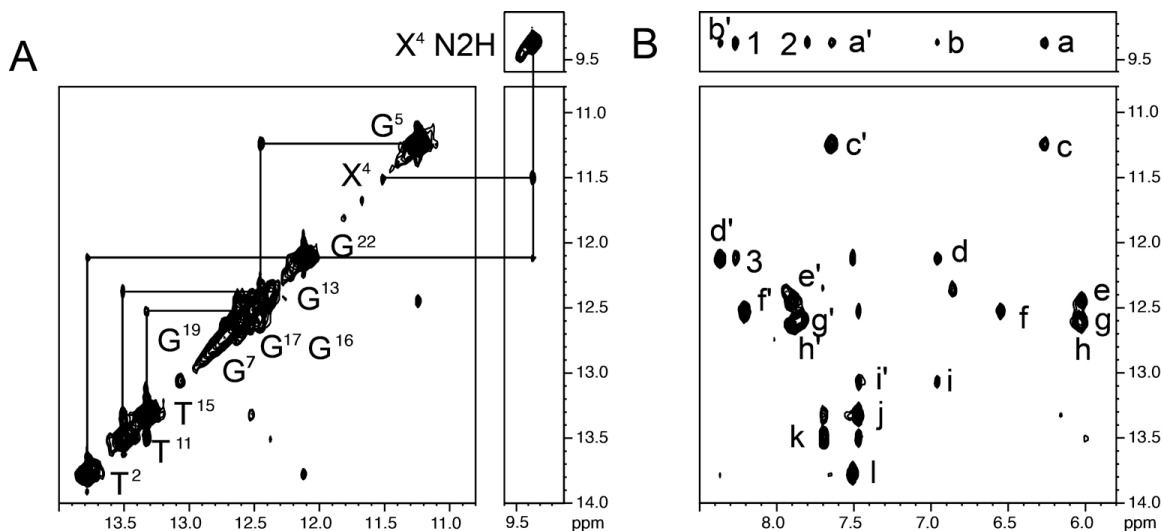


Figure 4-5. NOESY plot with exchangeable proton assignments for N^2 -dG-IQ modified duplex at position G1. A. Sequential connectivity of imino protons from T² to T¹¹. B. NOE connectivity from imino protons to amino protons involved in Watson-Crick hydrogen bonding: a', X⁴N2H→C²⁰H4b; a, X⁴N2H→C²⁰H4a; b', X⁴N2H→C³H4b; b, X⁴N2H→C³H4a; c', G⁵N1H→C²⁰H4b; c, G⁵N1H→C²⁰H4a; d', G²²N1H→C³H4b; e', G¹⁹N1H→C⁶N4b; e, G¹⁹N1H→C⁶N4a; f', G¹⁶N1H→C⁹H4b; f, G¹⁶N1H→C⁹H4a; g', G¹⁷N1H→C⁸N4b; g, G¹⁷→C⁸N4a; h', G⁷N1H→C¹⁸N4b; h, G⁷N1H→C¹⁸H4a; i', G²⁴N1H→C¹N4b; i, G²⁴N1H→C¹N4a; j, T¹⁵N3H→A¹⁰H2; k, T¹¹N3H→A¹⁴H2; l, T²N3H→A²³H2; 1, X⁴N2H→IQ H4a; 2, X⁴N2H→IQ H9a; 3, G²²N2H→IQ H4a.

Structure Refinement

A total of 283 NOEs were obtained for structure calculations using NOESY data collected with a mixing time of 150 ms at 15 °C. Twenty-three NOEs were from IQ to DNA. Forty-nine restraints for Watson-Crick hydrogen bonding were applied, omitting restraints for the X⁴:C²¹ base pair. Another 100 restraints for the phosphodiester backbone and 20 deoxyribose pseudorotation based on canonical values for B-DNA¹¹⁸ were applied to bases not immediately surrounding the modification. NOEs from bases G⁷ and G¹⁹ were not included in structure calculations due to high amount of overlap between peaks. Similar chemical environments resulted in chemical shifts within 0.02 ppm for all protons of these bases and were unable to be resolved. However, the chemical shifts are ±0.05 ppm of the

unmodified bases and were presumed to be unaffected by the presence of the adduct. Table 4-2 summarizes the total restraints used and refinement statistics.

Table 4-2. Refinement statistics for *N*²-dG-IQ at G¹ position in the *NarI* sequence.

NOE restraints	
Internucleotide	155
Intranucleotide	128
Total	283
Backbone Torsion Angle Restraints	100
H-bonding Restraints	49
Deoxyribose Restraints	20
Total number of restraints	442
Refinement Statistics	
Number of distance restraint violations	70
Number of torsion restraint violations	46
Total distance penalty/Maximum penalty [kcal mol ⁻¹]	3.0/0.24
Total torsion penalty/Maximum penalty [kcal mol ⁻¹]	1.7/0.16
r.m.s. distances (Å)	0.012
r.m.s. angles (°)	2.5
Distance restraint force field [kcal mol ⁻¹ Å ⁻²]	32
Torsion restraint force field [kcal mol ⁻¹ deg ⁻²]	32

Ten emergent structures based on the lowest deviation from experimental and dihedral restraints were selected to best represent the structure. The end of the duplex near the adduct appears as if there is poor agreement, presumably because of the unwinding induced by the IQ so close to the end of the duplex. The total distance penalty was 3.0 kcal • mol⁻¹, with a single maximum penalty of 0.245 kcal • mol⁻¹. The total torsion penalty was 1.7 kcal • mol⁻¹, with a single maximum penalty of 0.161 kcal • mol⁻¹.

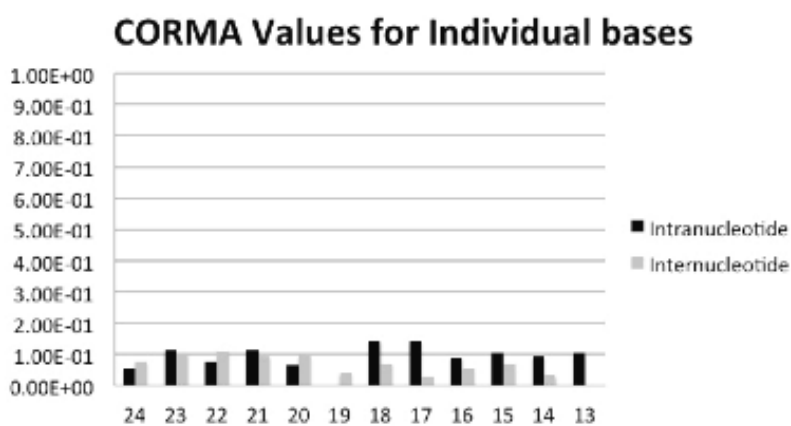
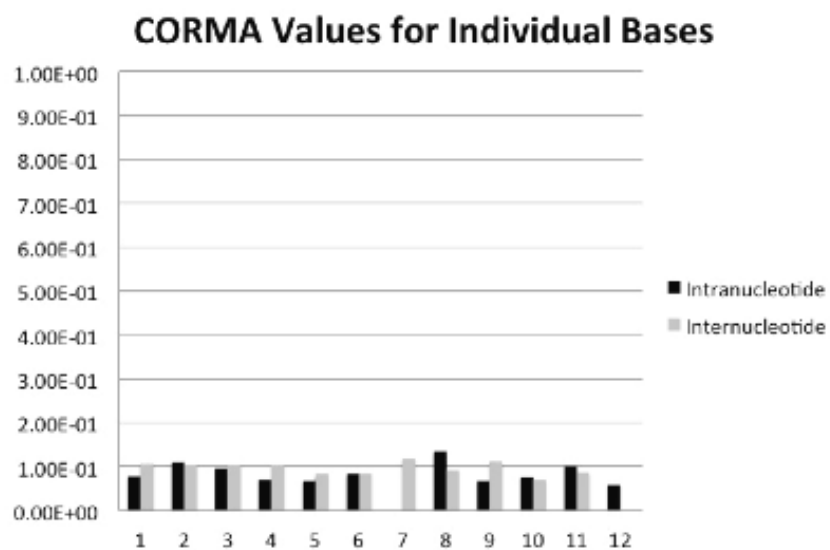


Figure 4-6. Sixth root residuals (R_1^x) calculated using complete relaxation matrix calculations from the average of ten structures emergent from the rMD calculations of the N^2 -dG-IQ modified duplex. The black bars represent intra-nucleotide sixth root residuals and the grey bars represent inter-nucleotide sixth root residuals. A. Nucleotides C¹-C¹² in the modified strand. B. Nucleotides G¹³-G²⁴ in the complementary strand.

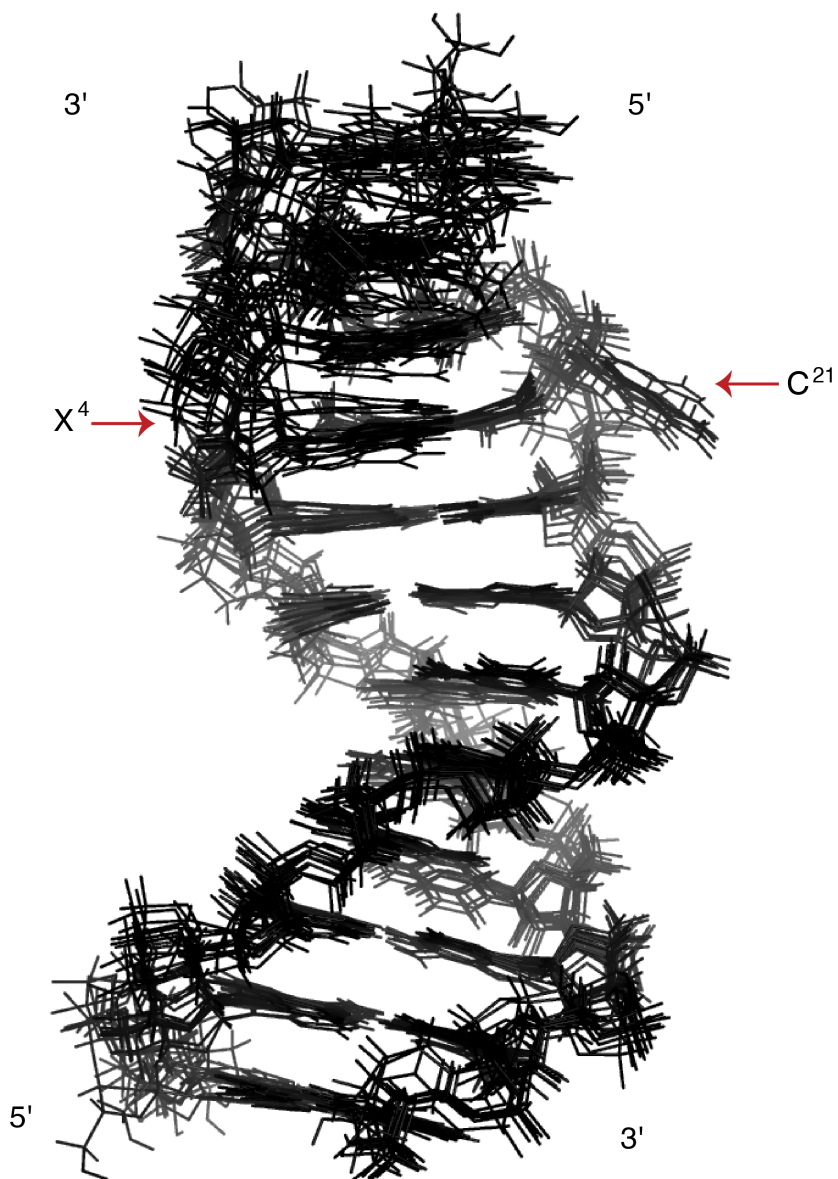


Figure 4-7. Ten best fitting structures calculated from NOESY data with 150 ms mixing time superimposed. The modified X⁴ base and complementary C²¹ are indicated.

Conformation of N²-dG-IQ at G¹

The imidazole portion containing the methyl group of the IQ ring faced the minor groove of the duplex and is oriented towards the modified strand of the duplex. The quinolone ring intercalates between bases of the complementary strand since all NOEs

came from C²⁰, C²¹, and G²². The aromatic protons on the quinolone ring, H7a, H8a, and H9a, are oriented towards the major groove. The IQ remained in plane with X⁴, with a dihedral angle of 178°. It did increase the tilt of C³:G²² by 20°. The tilt between C³ and X⁴ as well as X⁴ to G⁵ was decreased by 13° and increased by 23°, respectively. Likewise, the roll between the three bases was altered by -24° and 21°, respectively. The opposite base C²¹ rotated into the major groove and had a base opening that was 98° greater than the unmodified base pair. The modified guanine maintained its *anti* conformation. The adduct induced a bend of 10° into the duplex compared to the unmodified duplex and a localized unwinding effect, increasing the helical twist by 15° at the adduction site.

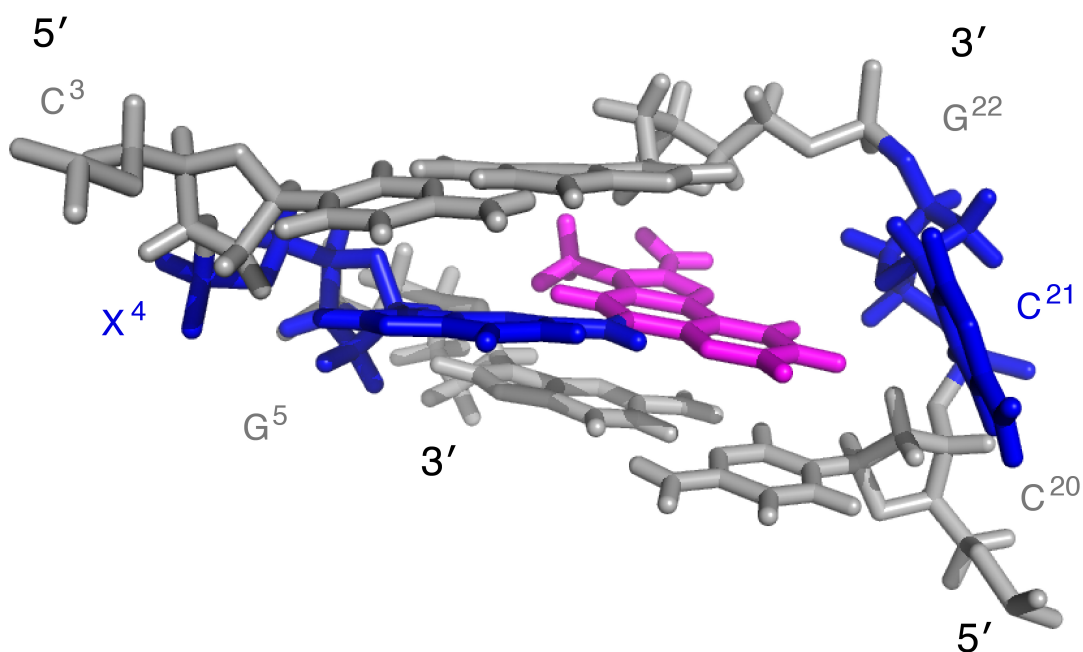


Figure 4-8. Expanded view of calculated structure from major groove, showing base pairs C³:G²², X⁴:C²¹, G⁵:C²⁰. The IQ moiety is shown in magenta.

Discussion

Structural characterization of the N^2 -dG-IQ adduct is of interest since IQ appears to be one of the most genotoxic substances tested in the Ames assay, being approximately fifteen times more mutagenic than aflatoxin B₁, a known human carcinogen¹⁷². The N^2 -dG-IQ adduct has been shown to be the more persistent than the C8-dG-IQ adduct and could possibly contribute more towards the carcinogenic properties of the IQ, considering persistence is a factor when assessing human risk¹⁷³. The N^2 -dG-IQ adduct also induces frameshift mutations when replicated by hpol η as demonstrated in *in vitro* extension assays¹⁷⁴. Site-specific synthesis of the oligonucleotide containing this adduct has allowed for high resolution structural studies by NMR to understand more of the structure-function relationship of the N^2 HCA adducts¹¹².

The T_m for the N^2 -dG-IQ adduct at the G¹ position did not change the thermal stability of the duplex. The modified duplex has a melting temperature of 62 °C compared to the unmodified duplex, which has a melting temperature of 63 °C, meaning that the adduct has little effect on the overall stability of the duplex¹⁷⁵. The N^2 -dG-IQ adduct is able to disrupt the Watson-Crick hydrogen bonding of the modified base pair and maintain thermal stability, likely due to the strong base-stacking interactions which make up for the loss of hydrogen bonding.

The assignments of the N1H and N2H protons of X⁴ in the water data are based on the observed stabilities of the peaks at different temperatures. X⁴ N2H is within proximity of the nitrogen atom in the IQ ring allowing for hydrogen bonding interactions, which are able to slow solvent exchange so we can observe this peak on the NMR timescale and

remains sharp until the temperature nearly reaches the T_m of the duplex. The N2H proton has a crosspeak to the broadened peak corresponding to N1H. The N1H proton is visible at 5 °C and quickly broadens as the temperature increases. The N1H proton does not have crosspeaks to C²¹ amino protons, indicating a loss of hydrogen bonding at that base pair. No crosspeaks corresponding to the C²¹ amino groups are visible in the spectrum, indicating that they are likely solvent exposed.

The N²-dG-IQ modified base adopts a base-displaced intercalated structure, where the IQ moiety takes the place of the opposite base, C²¹, disrupting base pairing and rotates into the major groove to accommodate the adduct. This is supported by the chemical shift change of 1.3 ppm of the H6 proton downfield relative the unmodified guanine. The IQ ring is accommodated into the duplex and stacks well with the flanking base pairs, as shown in Figure 4-9. NOEs from the IQ adduct to other DNA bases show it is oriented in a specific orientation across the duplex. The protons of the quinolone moiety have NOEs to the opposite strand, while the protons attached to the imidazole ring have NOEs to the same strand. The planarity of the IQ ring may be facilitated by the possible hydrogen bonding interactions between X⁴ N2H and the nitrogen atom in the IQ ring, which allows the N2H proton to be observed in the NOESY spectrum. The visible N2H proton chemical shift is also observed for the adduct at the G³ position¹⁷⁵.

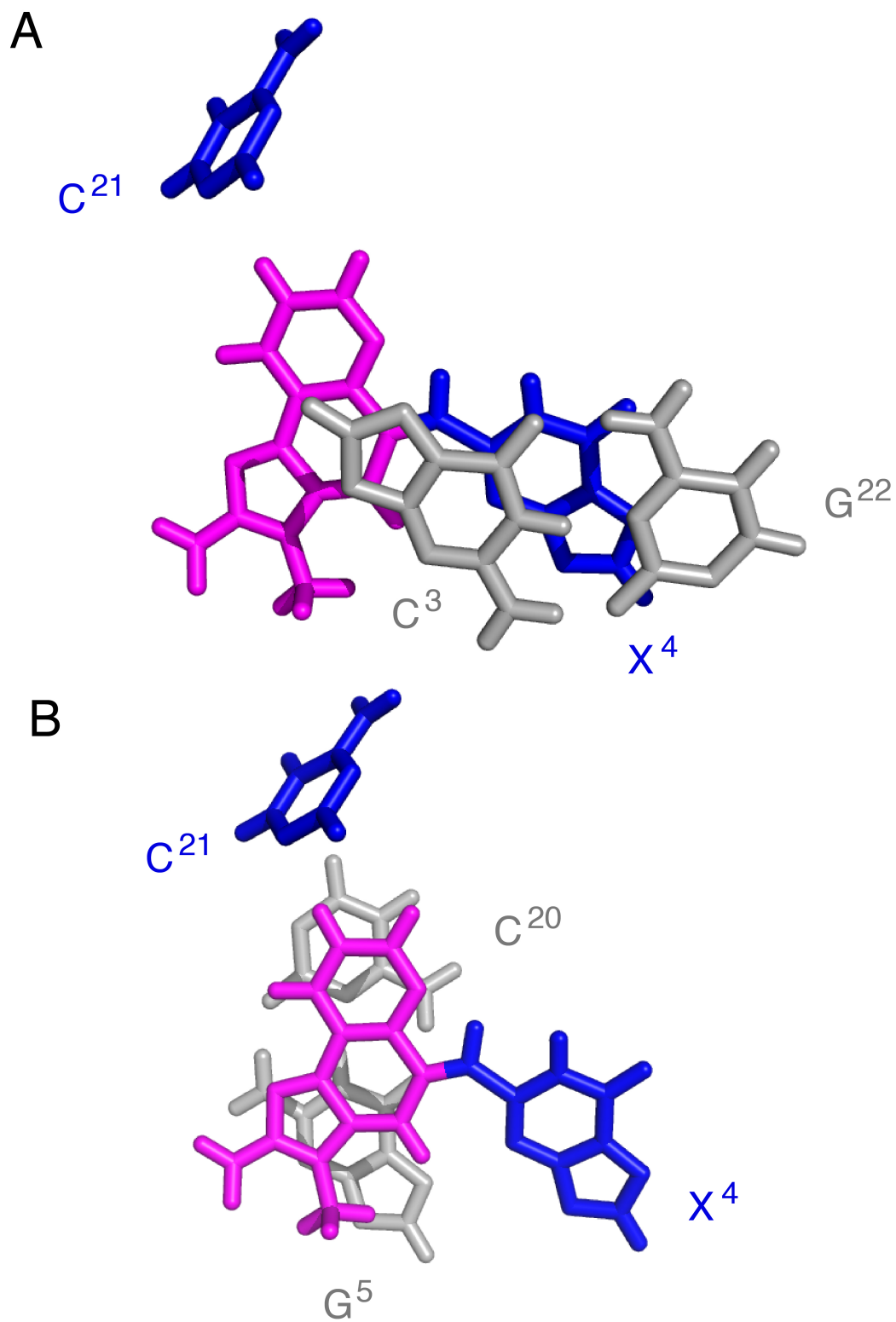


Figure 4-9. View from top of duplex looking at base-stacking interactions. A. base pairs C³:G²² and X⁴:C²¹, with IQ shown in magenta. B. Base pairs X⁴:C²¹ and G⁵:C²⁰.

The aromaticity of the IQ ring allows for strong base-stacking interactions between the other bases in the duplex, and these interactions are reflected in the melting temperature of 62 °C, compared to the unmodified sequence with a melting temperature of 63 °C. Within experimental error, the presence of the adduct does not change the thermal stability of the duplex. The base-stacking interactions are able to overcome the instability introduced by the loss of hydrogen bonding between the modified base pair. Primarily, IQ appears to be stacking with bases C²⁰ and G²², as shown in Figure 4-9. Similar effects can be observed by other aromatic adducts, demonstrating the importance of base stacking to duplex stability¹⁷⁶.

The chemical shifts of the aromatic IQ protons (H4a, H7a, H8a, H9a) range from 6.87 - 8.56 ppm. These chemical shifts are 0.5 – 0.9 ppm upfield from the nucleoside, indicating a shielding effect from the duplex and supporting intercalation of the IQ ring exhibited by the structure. Likewise, the CH₃ proton resonance on the imidazole ring shifts upfield 0.4 ppm, suggesting it might be slightly less shielded and more groove bound than the aromatic protons. This is supported by the refined structure, in which this group is located in the minor groove of the duplex and not in the base stack. C²¹H6 and H1' had the largest downfield shifts. In the structure, this base is extruded into the major groove and is no longer base stacking with neighbor bases, explaining the large chemical perturbations for this base. The bases neighboring X⁴, namely C³, G⁵, G²² and C²⁰, are only shifted several tenths of a ppm from the change in base stacking induced by the presence of the IQ ring that has replaced C²¹ in the duplex. This structure resembles other C8 HCA adducts as well as some polyaromatic hydrocarbon adducts (PAH), such as benzo(a)pyrene, whose anti-*N*²-dG *cis* adduct favors a similar base displaced intercalated conformation¹⁷⁷. In this solution

structure, the adduct displaces the modified guanine into the major groove and flips the opposite cytosine into the major groove as well. The modified guanine is displaced to a greater extent than with IQ, in order to accommodate the much larger ring system of B[a]P. The B[a]P ring spans the duplex, with the majority of the ring oriented into the major groove.

Sequence Dependence of N²-dG-IQ in NarI

The structure at the mutagenic hotspot, G³, in the *NarI* recognition sequence has previously been determined¹⁷⁵. The conformations of IQ at all three positions adopt similar structures with subtle differences between the positions. The CD spectra indicate each sequence maintains B DNA structure but is perturbed by the presence of the adduct. A lack of a visible signal for all three sequences between 300 and 360 nm, where the IQ-induced signal should occur, could support that the conformation of the modified base adopts a similar conformation in all sequences. However, the lack of signal could also be due to a perturbation of in the IQ chromophore from the linkage at dGuo N² to the IQ ring.

At the G¹ position, the IQ ring intercalates between the C³:G²² and G⁵:C²⁰ base pair. C²¹ flips out into the major groove to allow for the intercalation of the IQ ring. Comparable observations were made for C¹⁸ opposite IQ attached to X⁷, where the H6 proton resonance of both bases is shifted downfield more than 1 ppm¹⁷⁵. According to the calculated structures, C²¹ was rotated 20° further out of the duplex than C¹⁸. A similar effect on the helical twist between the 5' neighbor base to the modified was observed, which was reduced by 30°. However, G¹ had a greater unwinding effect from the modified base to the

3' neighbor, with an increase of 15° compared to the 9° increase for G³. The blue shifts in the CD data correspond to adduct-induced twisting and/or bending for both duplexes. The 10° bend observed at G³ likely contributes to the increased differences in shifts by 1-3 at the maximum, 0 and minimum wavelengths.

The chemical shifts of the IQ proton H7a and H9a between G¹ and G³ differ by 0.45 and 0.3 ppm further downfield for G¹, while all other protons on the IQ ring differed by less than 0.1 ppm, which could indicate this portion of the IQ ring is oriented more towards the major groove than the G³ adduct. One difference in the orientation of IQ is at G¹, it maintained planarity with X⁴. At the G³ position, however, IQ was inserted at a 15° angle relative to X⁷.

N² vs. C8-dG-IQ

While the C8 and N²-dG-IQ adducts at G³ both intercalate within the duplex, the N² at the G¹ and G² positions adopt much more contrasting conformations from that of the C8-dG-IQ adduct. The structures of the C8-dG-IQ adduct at G¹ and G² were groove-bound, where the IQ ring was located in the minor groove of the duplex.

The N²-dG-IQ adduct has demonstrated different biological processing from the C8-dG-IQ adduct. Both adducts at the G¹ position were able to be bypassed *in vitro* by both prokaryotic^{169,174} as well as human polymerases²⁰, with few instances of frameshift mutations at the G¹ position in the *NarI* sequence. Structurally, however, these adopt different conformations in the duplex DNA. The N² adduct maintains the *anti* configuration, unlike the C8-dG-IQ adduct which is flipped in the *syn* conformation¹⁷⁸. The IQ ring of C8-

dG-IQ is located in the minor groove of the duplex. In contrast, the N^2 -IQ-dG adduct remains intercalated in the duplex at the G^1 position, very similar to the G^3 position. The conformational differences result in adducts which induce various amounts of stabilities to the duplex. C8-dG-IQ decreases the thermal stability by 4-7 °C¹⁷¹, while N^2 does not significantly change the thermal stability of the duplex at any position¹⁷⁵. These differences between the two adducts could contribute to the observed discrepancy in repair efficiency since local instabilities induced by the adduct lead to recognition of DNA damage by NER proteins. The structural data provides less insight as to why N^2 -dG-IQ results in frameshift mutations when bypassed by pol η , yet can bypass C8-dG-IQ. It does, however, provide evidence that the point of attachment for these DNA adducts is important for structure-function relationships.

Summary

As a result, this data would suggest that N^2 -dG-HCA adducts could have a unique mechanism of biological processing compared to the C8-dG adducts. The structures demonstrate a sequence dependence dictating the whether the C8-dG-IQ adduct is intercalated or groove bound but has little effect on the conformation of the N^2 -dG-IQ adduct at the various positions. Yet, bypass by pol η suggests the sequence plays a role in extension beyond the adduct. Therefore, it is likely that the sequence dependence plays a larger role in determining the results of bypass via polymerase interactions for the N^2 -dG-IQ than perhaps the structure of the duplex itself. Further experiments looking at the

adduct in a polymerase active site at the ss-ds junction will determine how these interactions differ and lead to sequence dependence mutagenesis.

CHAPTER V

CONCLUSIONS AND FUTURE DIRECTIONS

Conclusions

Structures of IQ have been determined at both the mutagenic hotspot, G³ position, in the *NarI* sequence and the less potent mutagenic G¹ position of the *NarI* sequence (G¹G²CX³CC) by solution NMR. The different sequence contexts are interesting due to exhibited differences in mutagenic results from *in vitro* assays. Based on the different biological processing, it was believed that the duplex structure of the G³ sequence inducing frameshift mutations would differ significantly from the duplex structure when IQ is attached to G¹, which is more likely to induce point mutations. Perhaps these differences would suggest possible reasons why hpol η could induce frameshift mutations in one context but not the other.

However, results from solution NMR data collected on both samples indicated a much smaller difference in structure than what was predicted. Both IQ moieties intercalate into the duplex, taking the place of the opposite base, which was relocated to the major groove. The modified base is also displaced to some extent to the major groove to accommodate the IQ in the duplex in such a fashion that does not seem to disrupt the surrounding bases. The thermal stabilities of these duplexes do not change with the presence of the adduct and the CD spectrum for each sequence are comparable, thus supporting the idea that these duplex structures are likely very similar. The placement of the IQ within the duplex is different to some extent, with IQ at G³ at about a 15° angle relative to the modified dG base. This could change its base-stacking ability or position it in

such a way that it interacts with the polymerase active site differently. It is clear, however, that further experiments are necessary to understand the bypass of these adducts.

These structures are interesting in the context of comparing with the C8-dG-IQ adducts, nevertheless. Because the C8-dG-IQ is preferentially repaired and its ability to be bypassed by hpol η but not Dpo4, these adducts would also be predicted to be very different. This work provides a better understanding of the persistence of N^2 -dG-IQ relative to C8-dG-IQ, since the N^2 adduct modifies the duplex with much smaller perturbations to the overall duplex. The IQ has strong base-stacking interactions with flanking bases that allow the duplex to maintain its thermal stability, whereas the C8 adduct is destabilizing and creates far more perturbations to the duplex. The C8 adduct must flip the modified base into the *syn* conformation in order to intercalate, meanwhile bending the backbone as well. These perturbations likely increase the likelihood for the adduct to be recognized by the NER pathway for repair. Determining the Crystal Structure of 8-oxoguanine with Y-family Polymerase Dpo4

Introduction

Understanding the replication of DNA adducts requires direct observation of structural features of polymerase and DNA at a ss-ds junction. Observing the interactions between the adduct/modified base through x-ray crystallography can be the best way to identify these interactions, which can dictate how likely an adduct is to be mutagenic. Dpo4 is a Y-family polymerase originating from the archaeal bacteria *Sulfolobus solfataricus* that has mechanistic similarities to hpol η . In order to study bypass of IQ, Dpo4 was initially crystallized with the adduct 8-oxoG, which has been published previously^{128,179}, as a way to develop skills and methods for designing crystal trials using IQ. Results from diffraction of

crystals of the binary complex of correctly paired 8-oxoG:C diffracted with a resolution of 2.7 Å, for which molecular replacement was used to solve the phasing problem. Results reflected those previously published, showing that when 8-oxoG pairs with dC, 8-oxoG maintains the anti configuration in the active site. The quality of data collected is also comparable to published results and ensures the methods are suitable for obtaining useful crystal data.

Results

Activity Assay

Dpo4 is a robust polymerase that is stable both at high temperatures and can be stored at low temperatures for long periods of time and maintain activity. The extension assay was used to test for polymerase activity before setting up crystals to ensure the polymerase maintained its activity and could form active complexes with DNA after purification. Figure 5-1 shows the results of incubating Dpo4 with unmodified DNA in excess dNTPs to allow for full-length extension within a 2 hr. time frame. The starting material is rapidly begun to be extended in the first 5 min. After an hour, more fully extended product, or nearly fully extended, product is visible than initial substrate. At 2 hrs., it still appears as though extension is occurring, although full-length product is clearly the major product at this point, along with a small percent of blunt end extension.

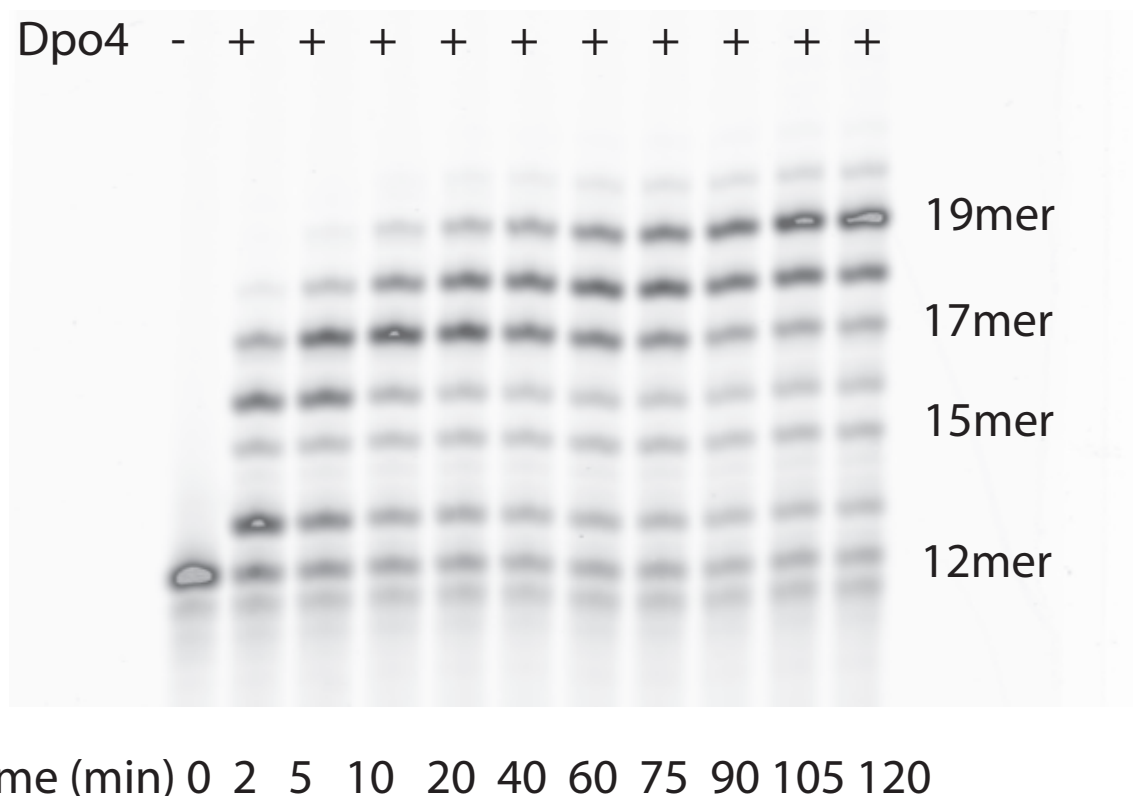


Figure 5-1. Extension of unmodified oligonucleotide by Dpo4.

Crystal Structures of Dpo4:8-oxoG

Only binary crystal complexes with correct dC opposite the 8-oxoG diffracted with enough data and enough resolution for useful structure determination. The best data set had a resolution of 2.1 Å to a space group of P_1 . The crystal contained a mosaicity of 0.75. The unit cell contained two molecules and had dimensions of 53.05, 53.12, and 98.85 Å with angles of 80.00°, 77.50°, and 70.33°. The overall completeness was 98.1 and a redundancy of 1.8. A total of 205 images were collected over 205°. The R_{free} for the final structure was 0.30 and the R-value was 0.23.

The crystal structure contains the correctly paired 8-oxoG:C in the active site of Dpo4. The modified 8-oxoG base remains in the *anti* conformation. Because the oxygen modification is located opposite the Watson-Crick hydrogen bonding face of the guanine, the modification does not affect base-pairing. R332 was located 3.8 Å away from the oxygen at C8 of the modified base.

Discussion

The crystal structure yielded similar results to the previously published structures^{128,130,179}. The space groups for the published structures were P2₁2₁2 but were still able to use molecular replacement to phase the data. The R values for the refined structure are also comparable to previously published structures^{128,130,179}.

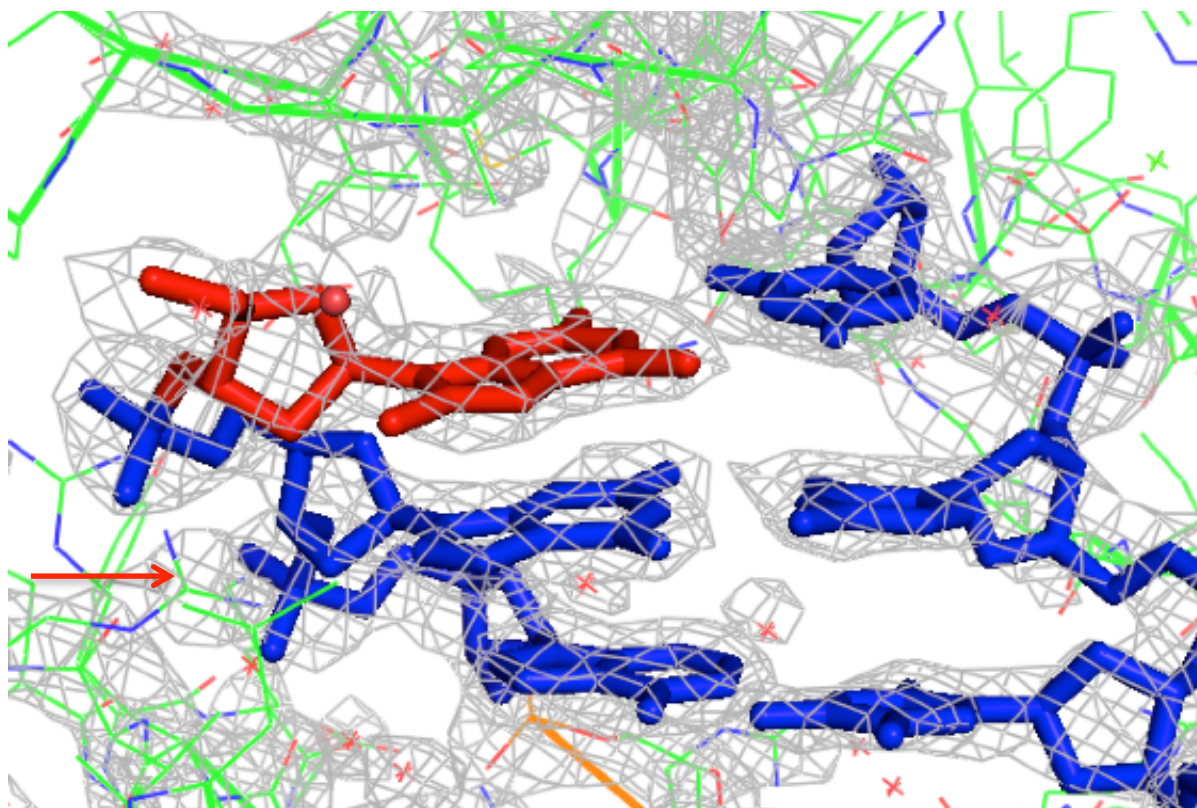


Figure 5-2. The active site of Dpo4 containing an 8-oxoG modified DNA sequence (modified base shown in red) paired opposite dC. The arrow highlights residue R332.

Dpo4 has been shown to incorporate dCTP opposite 8-oxoG more than 95% over the mutagenic dATP and can extend the correct pair 4-fold more efficiently¹³⁰. R332 in the active site has been shown to play a role in correct bypass of 8-oxoG through hydrogen bonding with the oxygen of the modified base, which stabilizes the guanine in the *anti* conformation¹²⁸. In this crystal structure, the nitrogen of one of the amine groups of R332 is 3.8 Å from the oxygen, meaning the hydrogen atoms could potentially interact with the oxygen during insertion of dCTP.

While the structure provides no unique information about bypass of 8-oxoG by Dpo4, it does confirm that the purification procedures produce clean, active polymerase, and the crystal setup and buffers are able to yield crystals that diffract with high enough resolution to discern what is happening in the active site. The results are able to confirm that good technique is being used for protein expression and crystallography, as similar techniques are necessary to further investigate the bypass of IQ. Observing the crystal structure of C8-dG-IQ adduct in the active site of Dpo4 would likely involve a similar protocol, despite modifying the DNA sequence to incorporate a GC repeat. The general technique would also be applicable for studying polη complexes with *N*²-dG-IQ, while more specific protocol details, such as purification and buffers, would be modified. Crystal structures can provide valuable insight into interactions between DNA and polymerase, which can be useful for understanding the miscoding by DNA adducts.

Future Directions

There are still questions in the field about if duplex structures can directly be related to ss-ds junctions in the polymerase complex. Because the duplex structures of IQ at the G¹ and G³ position in the *NarI* DNA recognition sequence appear very similar according to the NMR data, it is especially difficult to predict why the G³ adduct is prone to frameshifts over G¹. The only way to answer these questions is to directly examine the DNA•polymerase complex. Crystal structures of IQ in the active site of hpol η would better be able to address why the mutagenesis of these adducts differ because it allows the active site to be visualized and provides a snapshot of what is occurring. This could be a viable experiment since crystals of hpolη have already successfully been obtained and were able to demonstrate the specificity of hpolη to cyclobutane pyrimidine dimers through interactions of the crosslink with hydrophobic residues¹⁸⁰.

However, *in vitro* experiments testing single polymerases may not provide an accurate idea of how the adducts are actually bypassed. Many pathways in human cells involve multiple proteins. Thus, a single polymerase may not be responsible for bypassing IQ. More detailed experiments into the bypass mechanics would, therefore, be needed to understand how relevant the frameshift mutations are in human cells.

APPENDIX A

RMD INPUT FILES

20 ps Simulated Annealing Protocol

simulated annealing protocol, 18A cut off, 20ps

```
&cntrl
  imin=0, ntr=0, ntc=2, ntf=2,
  cut=18.0, igb=1, saltcon=0.1, gbsa=0, offset=0.13,
  ntrp=1000, ntwx=1000, nstlim=20000, dt=0.001,
  ntt=1, ntx=1, irest=0, ntb=0, vlimit=20,
  pencut=-0.001, nmropt=1,
&end

#
#Simple simulated annealing algorithm:
#
#from steps 0 to 1000: heat the system to 600K with short tautp
#from steps 1001 to 2000: keep the temperature at 600K
#from steps 2001 to 18000: cool down the system to 100K with long tautp
#from steps 18001 to 20000: cool down the system to 0K with short tautp
#

&wt type='TEMP0', istep1=0,istep2=1000,value1=0.0,
  value2=600.0, &end

&wt type='TEMP0', istep1=1000,istep2=2000,value1=600.0,
  value2=600.0, &end

&wt type='TEMP0', istep1=2001, istep2=18000, value1=600.0,
  value2=100.0, &end

&wt type='TEMP0', istep1=18001, istep2=20000, value1=100.0,
  value2=0.0, &end

&wt type='TAUTP', istep1=0,istep2=2000,value1=0.5,
  value2=0.5, &end

&wt type='TAUTP', istep1=2001,istep2=18000,value1=4.0,
```

```

value2=4.0, &end

&wt type='TAUTP', istep1=18001,istep2=20000,value1=1.0,
value2=1.0, &end

&wt type='REST', istep1=0,istep2=2000,value1=0.1,
value2=1.0, &end

&wt type='REST', istep1=2001,istep2=20000,value1=1.0,
value2=1.0, &end

&wt type='END' &end
LISTOUT=POUT
DISANG=IQG3.rst

```

100 ps Simulated Annealing Protocol

simulated annealing protocol, 18A cut off, 100ps

```

&cntrl
imin=0, ntr=0, ntc=2, ntf=2,
cut=18.0, igb=1, saltcon=0.1, gbsa=0, offset=0.13,
ntpr=1000, ntwx=1000, nstlim=100000, dt=0.001,
ntt=1, ntx=1, irect=0, ntb=0, vlimit=20,
pencut=-0.001, nmropt=1,
&end

#
#Simple simulated annealing algorithm:
#
#from steps 0 to 5000: heat the system to 600K with short tautp
#from steps 5000 to 10000: keep the temperature at 600K
#from steps 10001 to 90000: cool down the system to 100K with long tautp
#from steps 90001 to 100000: cool down the system to 0K with short tautp
#
&wt type='TEMP0', istep1=0,istep2=5000,value1=0.0,
value2=600.0, &end

&wt type='TEMP0', istep1=5000,istep2=10000,value1=600.0,
value2=600.0, &end

&wt type='TEMP0', istep1=10001, istep2=90000, value1=600.0,

```

```
value2=100.0, &end

&wt type='TEMP0', istep1=90001, istep2=100000, value1=100.0,
value2=0.0, &end

&wt type='TAUTP', istep1=0,istep2=10000,value1=0.5,
value2=0.5, &end

&wt type='TAUTP', istep1=10001,istep2=90000,value1=4.0,
value2=4.0, &end

&wt type='TAUTP', istep1=90001,istep2=100000,value1=1.0,
value2=1.0, &end

&wt type='REST', istep1=0,istep2=20000,value1=0.1,
value2=1.0, &end

&wt type='REST', istep1=20001,istep2=100000,value1=1.0,
value2=1.0, &end

&wt type='END' &end
LISTOUT=POUT
DISANG=IQG3.rst
```

APPENDIX B

PDB OUTPUT FILES

N²-dG-IQ at G³

REMARK

ATOM	1	H5T	DC5	1	-17.117	7.764	23.225
ATOM	2	O5*	DC5	1	-16.783	7.198	23.924
ATOM	3	C5*	DC5	1	-17.522	7.419	25.116
ATOM	4	1H5*	DC5	1	-18.579	7.206	24.958
ATOM	5	2H5*	DC5	1	-17.422	8.464	25.409
ATOM	6	C4*	DC5	1	-17.049	6.550	26.295
ATOM	7	H4*	DC5	1	-17.448	6.981	27.213
ATOM	8	O4*	DC5	1	-17.559	5.227	26.215
ATOM	9	C1*	DC5	1	-16.492	4.303	26.126
ATOM	10	H1*	DC5	1	-16.422	3.774	27.076
ATOM	11	N1	DC5	1	-16.716	3.318	25.016
ATOM	12	C6	DC5	1	-17.050	3.756	23.759
ATOM	13	H6	DC5	1	-17.148	4.817	23.579
ATOM	14	C5	DC5	1	-17.222	2.859	22.760
ATOM	15	H5	DC5	1	-17.451	3.216	21.767
ATOM	16	C4	DC5	1	-17.073	1.473	23.083
ATOM	17	N4	DC5	1	-17.294	0.554	22.198
ATOM	18	H41	DC5	1	-17.519	0.873	21.266
ATOM	19	H42	DC5	1	-17.246	-0.413	22.488
ATOM	20	N3	DC5	1	-16.817	1.033	24.304
ATOM	21	C2	DC5	1	-16.622	1.938	25.288
ATOM	22	O2	DC5	1	-16.363	1.481	26.405
ATOM	23	C3*	DC5	1	-15.513	6.467	26.466
ATOM	24	H3*	DC5	1	-14.990	7.222	25.880
ATOM	25	C2*	DC5	1	-15.194	5.086	25.901
ATOM	26	1H2*	DC5	1	-14.349	4.603	26.391
ATOM	27	2H2*	DC5	1	-14.980	5.175	24.835
ATOM	28	O3*	DC5	1	-15.165	6.597	27.859
ATOM	29	P	DT	2	-13.647	6.762	28.365
ATOM	30	O1P	DT	2	-13.706	7.326	29.738

ATOM	31	O2P	DT	2	-12.862	7.493	27.330
ATOM	32	O5*	DT	2	-13.083	5.266	28.471
ATOM	33	C5*	DT	2	-13.591	4.373	29.451
ATOM	34	1H5*	DT	2	-14.680	4.355	29.394
ATOM	35	2H5*	DT	2	-13.299	4.773	30.422
ATOM	36	C4*	DT	2	-13.096	2.924	29.302
ATOM	37	H4*	DT	2	-13.460	2.338	30.146
ATOM	38	O4*	DT	2	-13.590	2.321	28.098
ATOM	39	C1*	DT	2	-12.583	1.473	27.582
ATOM	40	H1*	DT	2	-12.625	0.532	28.131
ATOM	41	N1	DT	2	-12.772	1.246	26.119
ATOM	42	C6	DT	2	-12.874	2.314	25.250
ATOM	43	H6	DT	2	-12.692	3.307	25.633
ATOM	44	C5	DT	2	-13.197	2.140	23.934
ATOM	45	C7	DT	2	-13.263	3.350	23.000
ATOM	46	1H7	DT	2	-14.239	3.417	22.519
ATOM	47	2H7	DT	2	-13.055	4.274	23.540
ATOM	48	3H7	DT	2	-12.521	3.239	22.209
ATOM	49	C4	DT	2	-13.461	0.787	23.414
ATOM	50	O4	DT	2	-13.775	0.468	22.265
ATOM	51	N3	DT	2	-13.324	-0.203	24.349
ATOM	52	H3	DT	2	-13.416	-1.144	23.993
ATOM	53	C2	DT	2	-12.988	-0.051	25.670
ATOM	54	O2	DT	2	-12.870	-1.035	26.390
ATOM	55	C3*	DT	2	-11.552	2.805	29.290
ATOM	56	H3*	DT	2	-11.075	3.783	29.345
ATOM	57	C2*	DT	2	-11.278	2.167	27.919
ATOM	58	1H2*	DT	2	-10.454	1.454	27.947
ATOM	59	2H2*	DT	2	-11.053	2.953	27.197
ATOM	60	O3*	DT	2	-11.117	1.974	30.373
ATOM	61	P	DC	3	-9.538	1.680	30.689
ATOM	62	O1P	DC	3	-9.347	1.531	32.156
ATOM	63	O2P	DC	3	-8.714	2.697	29.970
ATOM	64	O5*	DC	3	-9.344	0.241	29.959
ATOM	65	C5*	DC	3	-10.078	-0.898	30.431
ATOM	66	1H5*	DC	3	-11.142	-0.683	30.335

ATOM	67	2H5*	DC	3	-9.818	-1.030	31.481
ATOM	68	C4*	DC	3	-9.764	-2.204	29.668
ATOM	69	H4*	DC	3	-10.267	-3.017	30.191
ATOM	70	O4*	DC	3	-10.248	-2.112	28.330
ATOM	71	C1*	DC	3	-9.232	-2.489	27.416
ATOM	72	H1*	DC	3	-9.286	-3.563	27.237
ATOM	73	N1	DC	3	-9.405	-1.771	26.121
ATOM	74	C6	DC	3	-9.214	-0.409	26.058
ATOM	75	H6	DC	3	-8.895	0.117	26.945
ATOM	76	C5	DC	3	-9.486	0.266	24.915
ATOM	77	H5	DC	3	-9.356	1.336	24.853
ATOM	78	C4	DC	3	-9.955	-0.492	23.817
ATOM	79	N4	DC	3	-10.227	0.117	22.702
ATOM	80	H41	DC	3	-10.014	1.100	22.606
ATOM	81	H42	DC	3	-10.578	-0.434	21.932
ATOM	82	N3	DC	3	-10.128	-1.800	23.838
ATOM	83	C2	DC	3	-9.862	-2.449	24.993
ATOM	84	O2	DC	3	-10.042	-3.668	24.972
ATOM	85	C3*	DC	3	-8.253	-2.495	29.599
ATOM	86	H3*	DC	3	-7.717	-1.748	30.184
ATOM	87	C2*	DC	3	-7.902	-2.272	28.136
ATOM	88	1H2*	DC	3	-7.135	-2.950	27.762
ATOM	89	2H2*	DC	3	-7.539	-1.254	27.997
ATOM	90	O3*	DC	3	-7.818	-3.760	30.134
ATOM	91	P	DG	4	-8.357	-5.242	29.732
ATOM	92	O1P	DG	4	-9.830	-5.274	29.659
ATOM	93	O2P	DG	4	-7.692	-6.215	30.667
ATOM	94	O5*	DG	4	-7.806	-5.522	28.244
ATOM	95	C5*	DG	4	-6.435	-5.650	27.977
ATOM	96	1H5*	DG	4	-6.039	-6.529	28.485
ATOM	97	2H5*	DG	4	-5.886	-4.783	28.344
ATOM	98	C4*	DG	4	-6.203	-5.819	26.454
ATOM	99	H4*	DG	4	-6.597	-6.787	26.143
ATOM	100	O4*	DG	4	-6.829	-4.759	25.735
ATOM	101	C1*	DG	4	-5.928	-4.352	24.727
ATOM	102	H1*	DG	4	-5.958	-5.086	23.922

ATOM	103	N9	DG	4	-6.239	-3.031	24.153
ATOM	104	C8	DG	4	-6.041	-1.776	24.673
ATOM	105	H8	DG	4	-5.658	-1.635	25.673
ATOM	106	N7	DG	4	-6.331	-0.800	23.839
ATOM	107	C5	DG	4	-6.769	-1.472	22.680
ATOM	108	C6	DG	4	-7.226	-0.986	21.400
ATOM	109	O6	DG	4	-7.348	0.185	21.013
ATOM	110	N1	DG	4	-7.640	-1.989	20.544
ATOM	111	1H	DG	4	-7.949	-1.694	19.629
ATOM	112	C2	DG	4	-7.578	-3.314	20.841
ATOM	113	N2	DG	4	-7.977	-4.172	19.920
ATOM	114	H21	DG	4	-7.937	-5.154	20.152
ATOM	115	H22	DG	4	-8.326	-3.854	19.028
ATOM	116	N3	DG	4	-7.103	-3.789	21.983
ATOM	117	C4	DG	4	-6.723	-2.831	22.872
ATOM	118	C3*	DG	4	-4.685	-5.756	26.133
ATOM	119	H3*	DG	4	-4.065	-5.787	27.029
ATOM	120	C2*	DG	4	-4.561	-4.416	25.421
ATOM	121	1H2*	DG	4	-3.765	-4.418	24.676
ATOM	122	2H2*	DG	4	-4.443	-3.611	26.145
ATOM	123	O3*	DG	4	-4.295	-6.756	25.209
ATOM	124	P	DG	5	-3.784	-8.217	25.682
ATOM	125	O1P	DG	5	-4.738	-8.812	26.665
ATOM	126	O2P	DG	5	-2.345	-8.095	26.047
ATOM	127	O5*	DG	5	-3.901	-8.988	24.293
ATOM	128	C5*	DG	5	-5.126	-9.535	23.807
ATOM	129	1H5*	DG	5	-5.949	-8.858	24.036
ATOM	130	2H5*	DG	5	-5.329	-10.475	24.320
ATOM	131	C4*	DG	5	-5.136	-9.816	22.297
ATOM	132	H4*	DG	5	-5.892	-10.584	22.136
ATOM	133	O4*	DG	5	-5.455	-8.636	21.573
ATOM	134	C1*	DG	5	-4.338	-8.238	20.794
ATOM	135	H1*	DG	5	-4.546	-8.491	19.754
ATOM	136	N9	DG	5	-4.112	-6.776	20.917
ATOM	137	C8	DG	5	-3.641	-6.069	21.992
ATOM	138	H8	DG	5	-3.306	-6.524	22.912

ATOM	139	N7	DG	5	-3.601	-4.780	21.817
ATOM	140	C5	DG	5	-4.147	-4.613	20.529
ATOM	141	C6	DG	5	-4.432	-3.433	19.746
ATOM	142	O6	DG	5	-4.317	-2.246	20.044
ATOM	143	N1	DG	5	-4.886	-3.703	18.468
ATOM	144	1H	DG	5	-5.061	-2.916	17.860
ATOM	145	C2	DG	5	-5.118	-4.957	18.005
ATOM	146	N2	DG	5	-5.532	-5.071	16.775
ATOM	147	H21	DG	5	-5.648	-5.990	16.373
ATOM	148	H22	DG	5	-5.673	-4.236	16.223
ATOM	149	N3	DG	5	-4.887	-6.065	18.695
ATOM	150	C4	DG	5	-4.412	-5.840	19.956
ATOM	151	C3*	DG	5	-3.805	-10.353	21.769
ATOM	152	H3*	DG	5	-3.233	-10.814	22.574
ATOM	153	C2*	DG	5	-3.142	-9.087	21.245
ATOM	154	1H2*	DG	5	-2.463	-9.299	20.419
ATOM	155	2H2*	DG	5	-2.575	-8.590	22.032
ATOM	156	O3*	DG	5	-4.032	-11.350	20.775
ATOM	157	P	DC	6	-2.842	-12.095	19.966
ATOM	158	O1P	DC	6	-3.416	-13.342	19.417
ATOM	159	O2P	DC	6	-1.627	-12.201	20.834
ATOM	160	O5*	DC	6	-2.501	-11.109	18.733
ATOM	161	C5*	DC	6	-3.402	-10.960	17.633
ATOM	162	1H5*	DC	6	-4.379	-10.665	18.015
ATOM	163	2H5*	DC	6	-3.515	-11.919	17.129
ATOM	164	C4*	DC	6	-2.913	-9.907	16.628
ATOM	165	H4*	DC	6	-3.608	-9.903	15.789
ATOM	166	O4*	DC	6	-2.897	-8.597	17.197
ATOM	167	C1*	DC	6	-1.772	-7.927	16.712
ATOM	168	H1*	DC	6	-1.962	-7.566	15.702
ATOM	169	N1	DC	6	-1.458	-6.775	17.594
ATOM	170	C6	DC	6	-1.018	-6.966	18.884
ATOM	171	H6	DC	6	-0.857	-7.968	19.255
ATOM	172	C5	DC	6	-0.879	-5.909	19.725
ATOM	173	H5	DC	6	-0.571	-6.093	20.744
ATOM	174	C4	DC	6	-1.178	-4.618	19.189

ATOM	175	N4	DC	6	-1.142	-3.543	19.922
ATOM	176	H41	DC	6	-0.986	-3.621	20.917
ATOM	177	H42	DC	6	-1.393	-2.677	19.468
ATOM	178	N3	DC	6	-1.514	-4.408	17.947
ATOM	179	C2	DC	6	-1.631	-5.462	17.106
ATOM	180	O2	DC	6	-1.966	-5.220	15.948
ATOM	181	C3*	DC	6	-1.498	-10.212	16.103
ATOM	182	H3*	DC	6	-1.129	-11.141	16.537
ATOM	183	C2*	DC	6	-0.692	-9.007	16.605
ATOM	184	1H2*	DC	6	0.082	-8.707	15.899
ATOM	185	2H2*	DC	6	-0.258	-9.259	17.572
ATOM	186	O3*	DC	6	-1.555	-10.303	14.683
ATOM	187	P	DKA	7	-0.358	-10.863	13.750
ATOM	188	O1P	DKA	7	-0.930	-11.231	12.419
ATOM	189	O2P	DKA	7	0.453	-11.874	14.489
ATOM	190	O5*	DKA	7	0.562	-9.568	13.562
ATOM	191	C5*	DKA	7	0.143	-8.446	12.784
ATOM	192	1H5*	DKA	7	-0.866	-8.145	13.062
ATOM	193	2H5*	DKA	7	0.148	-8.754	11.738
ATOM	194	C4*	DKA	7	1.103	-7.248	12.931
ATOM	195	H4*	DKA	7	0.807	-6.507	12.188
ATOM	196	O4*	DKA	7	0.973	-6.702	14.231
ATOM	197	C1*	DKA	7	2.282	-6.455	14.720
ATOM	198	H1*	DKA	7	2.682	-5.548	14.266
ATOM	199	N9	DKA	7	2.277	-6.337	16.200
ATOM	200	C8	DKA	7	2.655	-7.211	17.190
ATOM	201	H8	DKA	7	2.941	-8.228	16.968
ATOM	202	N7	DKA	7	2.684	-6.678	18.394
ATOM	203	C5	DKA	7	2.278	-5.339	18.165
ATOM	204	C6	DKA	7	2.127	-4.195	19.016
ATOM	205	O6	DKA	7	2.267	-4.119	20.227
ATOM	206	N1	DKA	7	1.754	-3.036	18.353
ATOM	207	1H	DKA	7	1.560	-2.228	18.927
ATOM	208	C2	DKA	7	1.524	-2.964	17.013
ATOM	209	N2	DKA	7	1.228	-1.745	16.552
ATOM	210	2H	DKA	7	1.293	-1.012	17.244

ATOM	211	C23	DKA	7	0.963	-1.287	15.300
ATOM	212	C22	DKA	7	0.959	0.136	15.063
ATOM	213	N21	DKA	7	1.182	0.982	16.121
ATOM	214	C20	DKA	7	1.047	2.370	15.897
ATOM	215	H20	DKA	7	1.046	3.053	16.734
ATOM	216	C19	DKA	7	0.912	2.851	14.582
ATOM	217	H19	DKA	7	0.852	3.913	14.394
ATOM	218	C18	DKA	7	0.892	1.978	13.492
ATOM	219	H18	DKA	7	0.883	2.352	12.479
ATOM	220	C17	DKA	7	0.750	0.612	13.738
ATOM	221	C16	DKA	7	0.442	-0.251	12.689
ATOM	222	N15	DKA	7	0.228	-0.002	11.362
ATOM	223	C14	DKA	7	-0.092	-1.242	10.847
ATOM	224	N14	DKA	7	-0.416	-1.473	9.511
ATOM	225	1H14	DKA	7	-1.376	-1.760	9.386
ATOM	226	2H14	DKA	7	0.325	-1.949	9.019
ATOM	227	N13	DKA	7	-0.035	-2.279	11.755
ATOM	228	C13	DKA	7	-0.169	-3.714	11.414
ATOM	229	1H13	DKA	7	0.784	-4.121	11.076
ATOM	230	2H13	DKA	7	-0.475	-4.285	12.290
ATOM	231	3H13	DKA	7	-0.946	-3.884	10.668
ATOM	232	C12	DKA	7	0.369	-1.658	12.916
ATOM	233	C11	DKA	7	0.634	-2.134	14.217
ATOM	234	H11	DKA	7	0.562	-3.207	14.318
ATOM	235	N3	DKA	7	1.700	-3.999	16.198
ATOM	236	C4	DKA	7	2.070	-5.142	16.828
ATOM	237	C3*	DKA	7	2.568	-7.680	12.726
ATOM	238	H3*	DKA	7	2.656	-8.687	12.318
ATOM	239	C2*	DKA	7	3.107	-7.605	14.151
ATOM	240	1H2*	DKA	7	4.180	-7.417	14.178
ATOM	241	2H2*	DKA	7	2.872	-8.533	14.673
ATOM	242	O3*	DKA	7	3.280	-6.776	11.897
ATOM	243	P	DC	8	3.086	-6.777	10.303
ATOM	244	O1P	DC	8	1.806	-7.420	9.944
ATOM	245	O2P	DC	8	4.336	-7.288	9.676
ATOM	246	O5*	DC	8	2.920	-5.216	9.959

ATOM	247	C5*	DC	8	4.031	-4.323	9.868
ATOM	248	1H5*	DC	8	4.644	-4.603	9.011
ATOM	249	2H5*	DC	8	4.641	-4.373	10.771
ATOM	250	C4*	DC	8	3.550	-2.876	9.636
ATOM	251	H4*	DC	8	2.762	-2.881	8.884
ATOM	252	O4*	DC	8	3.044	-2.355	10.863
ATOM	253	C1*	DC	8	3.849	-1.265	11.284
ATOM	254	H1*	DC	8	3.352	-0.325	11.045
ATOM	255	N1	DC	8	4.109	-1.319	12.761
ATOM	256	C6	DC	8	4.256	-2.520	13.416
ATOM	257	H6	DC	8	4.218	-3.454	12.874
ATOM	258	C5	DC	8	4.471	-2.529	14.759
ATOM	259	H5	DC	8	4.621	-3.466	15.274
ATOM	260	C4	DC	8	4.550	-1.272	15.418
ATOM	261	N4	DC	8	4.762	-1.224	16.714
ATOM	262	H41	DC	8	4.909	-2.068	17.250
ATOM	263	H42	DC	8	4.812	-0.309	17.139
ATOM	264	N3	DC	8	4.381	-0.127	14.826
ATOM	265	C2	DC	8	4.163	-0.107	13.492
ATOM	266	O2	DC	8	3.984	1.004	12.960
ATOM	267	C3*	DC	8	4.701	-1.968	9.179
ATOM	268	H3*	DC	8	5.500	-2.574	8.751
ATOM	269	C2*	DC	8	5.158	-1.336	10.495
ATOM	270	1H2*	DC	8	5.595	-0.350	10.340
ATOM	271	2H2*	DC	8	5.875	-1.986	10.998
ATOM	272	O3*	DC	8	4.222	-1.001	8.259
ATOM	273	P	DC	9	5.182	-0.228	7.196
ATOM	274	O1P	DC	9	4.327	0.369	6.140
ATOM	275	O2P	DC	9	6.262	-1.162	6.787
ATOM	276	O5*	DC	9	5.822	0.950	8.065
ATOM	277	C5*	DC	9	5.069	2.068	8.506
ATOM	278	1H5*	DC	9	4.226	1.711	9.097
ATOM	279	2H5*	DC	9	4.667	2.614	7.653
ATOM	280	C4*	DC	9	5.886	3.072	9.348
ATOM	281	H4*	DC	9	5.359	4.026	9.308
ATOM	282	O4*	DC	9	5.900	2.667	10.696

ATOM	283	C1*	DC	9	7.218	2.795	11.182
ATOM	284	H1*	DC	9	7.388	3.844	11.426
ATOM	285	N1	DC	9	7.439	1.970	12.415
ATOM	286	C6	DC	9	7.659	0.618	12.381
ATOM	287	H6	DC	9	7.694	0.118	11.425
ATOM	288	C5	DC	9	7.823	-0.092	13.538
ATOM	289	H5	DC	9	7.994	-1.158	13.494
ATOM	290	C4	DC	9	7.844	0.645	14.752
ATOM	291	N4	DC	9	7.990	0.051	15.896
ATOM	292	H41	DC	9	8.143	-0.945	15.953
ATOM	293	H42	DC	9	7.948	0.612	16.735
ATOM	294	N3	DC	9	7.645	1.946	14.817
ATOM	295	C2	DC	9	7.417	2.617	13.659
ATOM	296	O2	DC	9	7.231	3.819	13.758
ATOM	297	C3*	DC	9	7.355	3.252	8.908
ATOM	298	H3*	DC	9	7.519	2.845	7.910
ATOM	299	C2*	DC	9	8.115	2.506	9.987
ATOM	300	1H2*	DC	9	9.133	2.867	10.139
ATOM	301	2H2*	DC	9	8.128	1.444	9.744
ATOM	302	O3*	DC	9	7.673	4.634	8.945
ATOM	303	P	DA	10	8.942	5.233	8.151
ATOM	304	O1P	DA	10	8.430	5.933	6.933
ATOM	305	O2P	DA	10	9.974	4.192	8.007
ATOM	306	O5*	DA	10	9.475	6.332	9.190
ATOM	307	C5*	DA	10	8.712	7.485	9.556
ATOM	308	1H5*	DA	10	7.710	7.191	9.871
ATOM	309	2H5*	DA	10	8.593	8.146	8.697
ATOM	310	C4*	DA	10	9.325	8.269	10.723
ATOM	311	H4*	DA	10	8.736	9.179	10.834
ATOM	312	O4*	DA	10	9.196	7.526	11.927
ATOM	313	C1*	DA	10	10.489	7.289	12.471
ATOM	314	H1*	DA	10	10.653	7.907	13.353
ATOM	315	N9	DA	10	10.580	5.878	12.884
ATOM	316	C8	DA	10	10.544	4.769	12.071
ATOM	317	H8	DA	10	10.412	4.884	11.005
ATOM	318	N7	DA	10	10.588	3.620	12.687

ATOM	319	C5	DA	10	10.726	4.018	14.036
ATOM	320	C6	DA	10	10.852	3.342	15.291
ATOM	321	N6	DA	10	10.892	2.030	15.428
ATOM	322	1H6	DA	10	10.956	1.655	16.363
ATOM	323	2H6	DA	10	10.785	1.416	14.634
ATOM	324	N1	DA	10	10.958	4.007	16.432
ATOM	325	C2	DA	10	10.954	5.324	16.387
ATOM	326	H2	DA	10	11.022	5.805	17.351
ATOM	327	N3	DA	10	10.862	6.102	15.306
ATOM	328	C4	DA	10	10.728	5.378	14.157
ATOM	329	C3*	DA	10	10.790	8.670	10.537
ATOM	330	H3*	DA	10	11.088	8.578	9.493
ATOM	331	C2*	DA	10	11.518	7.641	11.395
ATOM	332	1H2*	DA	10	12.442	8.026	11.826
ATOM	333	2H2*	DA	10	11.745	6.773	10.777
ATOM	334	O3*	DA	10	10.935	10.008	10.971
ATOM	335	P	DT	11	12.312	10.841	10.796
ATOM	336	O1P	DT	11	11.980	12.279	10.957
ATOM	337	O2P	DT	11	13.003	10.360	9.574
ATOM	338	O5*	DT	11	13.190	10.413	12.087
ATOM	339	C5*	DT	11	12.792	10.815	13.396
ATOM	340	1H5*	DT	11	11.752	10.546	13.580
ATOM	341	2H5*	DT	11	12.869	11.898	13.497
ATOM	342	C4*	DT	11	13.658	10.153	14.449
ATOM	343	H4*	DT	11	13.453	10.590	15.426
ATOM	344	O4*	DT	11	13.346	8.751	14.534
ATOM	345	C1*	DT	11	14.560	8.057	14.777
ATOM	346	H1*	DT	11	14.856	8.161	15.821
ATOM	347	N1	DT	11	14.406	6.600	14.464
ATOM	348	C6	DT	11	14.406	6.125	13.171
ATOM	349	H6	DT	11	14.469	6.820	12.347
ATOM	350	C5	DT	11	14.239	4.807	12.888
ATOM	351	C7	DT	11	14.209	4.347	11.442
ATOM	352	1H7	DT	11	14.321	5.189	10.760
ATOM	353	2H7	DT	11	15.002	3.620	11.261
ATOM	354	3H7	DT	11	13.259	3.856	11.231

ATOM	355	C4	DT	11	14.096	3.843	13.976
ATOM	356	O4	DT	11	13.936	2.639	13.860
ATOM	357	N3	DT	11	14.134	4.389	15.245
ATOM	358	H3	DT	11	14.112	3.750	16.028
ATOM	359	C2	DT	11	14.274	5.721	15.537
ATOM	360	O2	DT	11	14.288	6.058	16.719
ATOM	361	C3*	DT	11	15.175	10.278	14.157
ATOM	362	H3*	DT	11	15.372	10.882	13.271
ATOM	363	C2*	DT	11	15.594	8.822	13.951
ATOM	364	1H2*	DT	11	16.605	8.628	14.309
ATOM	365	2H2*	DT	11	15.505	8.592	12.889
ATOM	366	O3*	DT	11	15.828	10.897	15.268
ATOM	367	P	DC3	12	17.392	11.312	15.281
ATOM	368	O1P	DC3	12	17.512	12.682	15.838
ATOM	369	O2P	DC3	12	18.010	10.993	13.969
ATOM	370	O5*	DC3	12	17.960	10.242	16.347
ATOM	371	C5*	DC3	12	17.734	10.420	17.740
ATOM	372	1H5*	DC3	12	16.682	10.617	17.946
ATOM	373	2H5*	DC3	12	18.296	11.296	18.064
ATOM	374	C4*	DC3	12	18.188	9.236	18.567
ATOM	375	H4*	DC3	12	18.142	9.519	19.618
ATOM	376	O4*	DC3	12	17.312	8.150	18.363
ATOM	377	C1*	DC3	12	18.002	6.934	18.622
ATOM	378	H1*	DC3	12	17.712	6.559	19.604
ATOM	379	N1	DC3	12	17.769	5.929	17.547
ATOM	380	C6	DC3	12	17.649	6.306	16.231
ATOM	381	H6	DC3	12	17.701	7.352	15.967
ATOM	382	C5	DC3	12	17.522	5.363	15.266
ATOM	383	H5	DC3	12	17.463	5.666	14.230
ATOM	384	C4	DC3	12	17.499	3.997	15.672
ATOM	385	N4	DC3	12	17.413	3.036	14.782
ATOM	386	H41	DC3	12	17.360	3.283	13.804
ATOM	387	H42	DC3	12	17.342	2.088	15.121
ATOM	388	N3	DC3	12	17.565	3.626	16.940
ATOM	389	C2	DC3	12	17.708	4.583	17.892
ATOM	390	O2	DC3	12	17.746	4.214	19.067

ATOM	391	C3*	DC3	12	19.594	8.733	18.241
ATOM	392	H3*	DC3	12	19.789	8.734	17.168
ATOM	393	C2*	DC3	12	19.490	7.298	18.726
ATOM	394	1H2*	DC3	12	19.776	7.241	19.776
ATOM	395	2H2*	DC3	12	20.150	6.662	18.136
ATOM	396	O3*	DC3	12	20.609	9.422	18.945
ATOM	397	H3T	DC3	12	20.765	10.262	18.507
TER							
ATOM	398	H5T	DG5	13	20.344	-6.206	19.658
ATOM	399	O5*	DG5	13	20.094	-6.974	20.177
ATOM	400	C5*	DG5	13	18.750	-6.818	20.633
ATOM	401	1H5*	DG5	13	18.485	-7.636	21.303
ATOM	402	2H5*	DG5	13	18.068	-6.790	19.783
ATOM	403	C4*	DG5	13	18.595	-5.520	21.438
ATOM	404	H4*	DG5	13	19.315	-5.512	22.256
ATOM	405	O4*	DG5	13	18.833	-4.409	20.579
ATOM	406	C1*	DG5	13	17.698	-3.571	20.558
ATOM	407	H1*	DG5	13	17.784	-2.787	21.310
ATOM	408	N9	DG5	13	17.538	-2.932	19.209
ATOM	409	C8	DG5	13	17.362	-3.529	17.982
ATOM	410	H8	DG5	13	17.283	-4.603	17.897
ATOM	411	N7	DG5	13	17.292	-2.672	16.997
ATOM	412	C5	DG5	13	17.453	-1.403	17.614
ATOM	413	C6	DG5	13	17.513	-0.065	17.081
ATOM	414	O6	DG5	13	17.456	0.311	15.913
ATOM	415	N1	DG5	13	17.653	0.896	18.076
ATOM	416	1H	DG5	13	17.664	1.869	17.806
ATOM	417	C2	DG5	13	17.787	0.619	19.387
ATOM	418	N2	DG5	13	17.897	1.624	20.207
ATOM	419	H21	DG5	13	17.953	1.398	21.190
ATOM	420	H22	DG5	13	17.885	2.575	19.868
ATOM	421	N3	DG5	13	17.777	-0.601	19.911
ATOM	422	C4	DG5	13	17.603	-1.581	18.971
ATOM	423	C3*	DG5	13	17.179	-5.361	22.008
ATOM	424	H3*	DG5	13	16.671	-6.321	22.095
ATOM	425	C2*	DG5	13	16.522	-4.474	20.946

ATOM	426	1H2*	DG5	13	15.695	-3.903	21.368
ATOM	427	2H2*	DG5	13	16.207	-5.051	20.077
ATOM	428	O3*	DG5	13	17.260	-4.713	23.267
ATOM	429	P	DA	14	15.981	-4.444	24.199
ATOM	430	O1P	DA	14	16.417	-4.489	25.615
ATOM	431	O2P	DA	14	14.855	-5.297	23.791
ATOM	432	O5*	DA	14	15.612	-2.919	23.869
ATOM	433	C5*	DA	14	16.434	-1.816	24.263
ATOM	434	1H5*	DA	14	17.387	-1.920	23.744
ATOM	435	2H5*	DA	14	16.586	-1.875	25.341
ATOM	436	C4*	DA	14	15.840	-0.438	23.924
ATOM	437	H4*	DA	14	16.393	0.334	24.459
ATOM	438	O4*	DA	14	15.926	-0.181	22.510
ATOM	439	C1*	DA	14	14.637	0.253	22.067
ATOM	440	H1*	DA	14	14.527	1.319	22.267
ATOM	441	N9	DA	14	14.446	-0.016	20.639
ATOM	442	C8	DA	14	14.299	-1.220	20.005
ATOM	443	H8	DA	14	14.330	-2.146	20.560
ATOM	444	N7	DA	14	14.188	-1.127	18.695
ATOM	445	C5	DA	14	14.210	0.258	18.456
ATOM	446	C6	DA	14	14.144	1.103	17.318
ATOM	447	N6	DA	14	13.999	0.676	16.081
ATOM	448	1H6	DA	14	13.976	1.353	15.332
ATOM	449	2H6	DA	14	13.885	-0.311	15.899
ATOM	450	N1	DA	14	14.230	2.426	17.437
ATOM	451	C2	DA	14	14.400	2.944	18.642
ATOM	452	H2	DA	14	14.450	4.021	18.697
ATOM	453	N3	DA	14	14.457	2.290	19.791
ATOM	454	C4	DA	14	14.363	0.937	19.635
ATOM	455	C3*	DA	14	14.354	-0.373	24.323
ATOM	456	H3*	DA	14	14.072	-1.201	24.973
ATOM	457	C2*	DA	14	13.668	-0.504	22.988
ATOM	458	1H2*	DA	14	12.675	-0.055	22.979
ATOM	459	2H2*	DA	14	13.600	-1.554	22.702
ATOM	460	O3*	DA	14	13.978	0.895	24.858
ATOM	461	P	DT	15	14.145	1.283	26.424

ATOM	462	O1P	DT	15	15.593	1.331	26.718
ATOM	463	O2P	DT	15	13.264	0.401	27.233
ATOM	464	O5*	DT	15	13.599	2.793	26.459
ATOM	465	C5*	DT	15	12.237	3.084	26.139
ATOM	466	1H5*	DT	15	11.825	3.655	26.971
ATOM	467	2H5*	DT	15	11.643	2.176	26.037
ATOM	468	C4*	DT	15	12.090	3.912	24.850
ATOM	469	H4*	DT	15	12.805	4.735	24.855
ATOM	470	O4*	DT	15	12.263	3.122	23.687
ATOM	471	C1*	DT	15	11.607	3.823	22.644
ATOM	472	H1*	DT	15	12.205	4.693	22.371
ATOM	473	N1	DT	15	11.328	2.991	21.441
ATOM	474	C6	DT	15	10.964	1.672	21.564
ATOM	475	H6	DT	15	10.862	1.269	22.561
ATOM	476	C5	DT	15	10.749	0.882	20.476
ATOM	477	C7	DT	15	10.370	-0.574	20.683
ATOM	478	1H7	DT	15	10.243	-0.799	21.742
ATOM	479	2H7	DT	15	9.432	-0.761	20.160
ATOM	480	3H7	DT	15	11.150	-1.217	20.274
ATOM	481	C4	DT	15	10.919	1.450	19.127
ATOM	482	O4	DT	15	10.792	0.861	18.052
ATOM	483	N3	DT	15	11.234	2.784	19.091
ATOM	484	H3	DT	15	11.330	3.218	18.184
ATOM	485	C2	DT	15	11.433	3.591	20.182
ATOM	486	O2	DT	15	11.697	4.784	20.039
ATOM	487	C3*	DT	15	10.677	4.502	24.772
ATOM	488	H3*	DT	15	9.975	3.938	25.386
ATOM	489	C2*	DT	15	10.321	4.321	23.298
ATOM	490	1H2*	DT	15	9.988	5.239	22.815
ATOM	491	2H2*	DT	15	9.537	3.569	23.209
ATOM	492	O3*	DT	15	10.712	5.881	25.160
ATOM	493	P	DG	16	9.380	6.745	25.487
ATOM	494	O1P	DG	16	9.798	7.909	26.291
ATOM	495	O2P	DG	16	8.359	5.819	26.045
ATOM	496	O5*	DG	16	8.882	7.265	24.025
ATOM	497	C5*	DG	16	9.614	8.244	23.312

ATOM	498	1H5*	DG	16	10.574	7.818	23.021
ATOM	499	2H5*	DG	16	9.823	9.101	23.953
ATOM	500	C4*	DG	16	8.905	8.759	22.040
ATOM	501	H4*	DG	16	9.469	9.618	21.676
ATOM	502	O4*	DG	16	8.903	7.759	21.022
ATOM	503	C1*	DG	16	7.551	7.411	20.713
ATOM	504	H1*	DG	16	7.217	7.905	19.800
ATOM	505	N9	DG	16	7.504	5.944	20.523
ATOM	506	C8	DG	16	7.498	4.903	21.427
ATOM	507	H8	DG	16	7.506	5.103	22.488
ATOM	508	N7	DG	16	7.576	3.711	20.891
ATOM	509	C5	DG	16	7.577	3.986	19.513
ATOM	510	C6	DG	16	7.616	3.129	18.354
ATOM	511	O6	DG	16	7.685	1.886	18.290
ATOM	512	N1	DG	16	7.574	3.806	17.154
ATOM	513	1H	DG	16	7.663	3.236	16.324
ATOM	514	C2	DG	16	7.507	5.142	17.043
ATOM	515	N2	DG	16	7.409	5.658	15.843
ATOM	516	H21	DG	16	7.238	6.651	15.775
ATOM	517	H22	DG	16	7.339	5.059	15.033
ATOM	518	N3	DG	16	7.485	5.975	18.085
ATOM	519	C4	DG	16	7.528	5.338	19.295
ATOM	520	C3*	DG	16	7.468	9.199	22.272
ATOM	521	H3*	DG	16	7.273	9.427	23.320
ATOM	522	C2*	DG	16	6.707	7.947	21.847
ATOM	523	1H2*	DG	16	5.683	8.145	21.532
ATOM	524	2H2*	DG	16	6.696	7.253	22.687
ATOM	525	O3*	DG	16	7.214	10.322	21.450
ATOM	526	P	DG	17	5.784	11.028	21.298
ATOM	527	O1P	DG	17	5.995	12.440	20.858
ATOM	528	O2P	DG	17	4.971	10.788	22.519
ATOM	529	O5*	DG	17	5.140	10.187	20.089
ATOM	530	C5*	DG	17	5.521	10.363	18.724
ATOM	531	1H5*	DG	17	6.567	10.082	18.600
ATOM	532	2H5*	DG	17	5.383	11.405	18.434
ATOM	533	C4*	DG	17	4.626	9.542	17.764

ATOM	534	H4*	DG	17	4.788	9.913	16.751
ATOM	535	O4*	DG	17	4.968	8.153	17.807
ATOM	536	C1*	DG	17	3.758	7.437	17.820
ATOM	537	H1*	DG	17	3.278	7.458	16.842
ATOM	538	N9	DG	17	3.987	6.015	18.174
ATOM	539	C8	DG	17	4.084	5.472	19.423
ATOM	540	H8	DG	17	4.092	6.097	20.304
ATOM	541	N7	DG	17	4.217	4.173	19.444
ATOM	542	C5	DG	17	4.183	3.824	18.081
ATOM	543	C6	DG	17	4.330	2.550	17.440
ATOM	544	O6	DG	17	4.505	1.441	17.952
ATOM	545	N1	DG	17	4.288	2.628	16.061
ATOM	546	1H	DG	17	4.321	1.755	15.554
ATOM	547	C2	DG	17	4.116	3.778	15.373
ATOM	548	N2	DG	17	3.973	3.666	14.088
ATOM	549	H21	DG	17	3.727	4.478	13.539
ATOM	550	H22	DG	17	4.002	2.740	13.687
ATOM	551	N3	DG	17	3.988	4.997	15.920
ATOM	552	C4	DG	17	4.051	4.950	17.289
ATOM	553	C3*	DG	17	3.124	9.630	18.145
ATOM	554	H3*	DG	17	2.959	10.413	18.885
ATOM	555	C2*	DG	17	2.887	8.250	18.770
ATOM	556	1H2*	DG	17	1.846	7.928	18.755
ATOM	557	2H2*	DG	17	3.279	8.250	19.787
ATOM	558	O3*	DG	17	2.208	9.783	17.064
ATOM	559	P	DC	18	2.260	10.984	15.994
ATOM	560	O1P	DC	18	3.320	11.948	16.406
ATOM	561	O2P	DC	18	0.868	11.486	15.811
ATOM	562	O5*	DC	18	2.727	10.275	14.621
ATOM	563	C5*	DC	18	1.830	9.552	13.801
ATOM	564	1H5*	DC	18	2.150	9.747	12.777
ATOM	565	2H5*	DC	18	0.803	9.902	13.900
ATOM	566	C4*	DC	18	1.905	8.024	13.984
ATOM	567	H4*	DC	18	2.909	7.693	13.719
ATOM	568	O4*	DC	18	1.598	7.670	15.325
ATOM	569	C1*	DC	18	0.475	6.804	15.358

ATOM	570	H1*	DC	18	0.856	5.784	15.409
ATOM	571	N1	DC	18	-0.363	7.126	16.547
ATOM	572	C6	DC	18	-0.637	8.428	16.901
ATOM	573	H6	DC	18	-0.274	9.221	16.264
ATOM	574	C5	DC	18	-1.319	8.694	18.039
ATOM	575	H5	DC	18	-1.495	9.723	18.316
ATOM	576	C4	DC	18	-1.755	7.581	18.815
ATOM	577	N4	DC	18	-2.438	7.752	19.910
ATOM	578	H41	DC	18	-2.682	8.684	20.214
ATOM	579	H42	DC	18	-2.714	6.924	20.418
ATOM	580	N3	DC	18	-1.519	6.328	18.513
ATOM	581	C2	DC	18	-0.808	6.078	17.386
ATOM	582	O2	DC	18	-0.618	4.908	17.065
ATOM	583	C3*	DC	18	0.873	7.304	13.076
ATOM	584	H3*	DC	18	0.578	7.986	12.278
ATOM	585	C2*	DC	18	-0.268	7.018	14.053
ATOM	586	1H2*	DC	18	-0.854	6.141	13.779
ATOM	587	2H2*	DC	18	-0.931	7.883	14.078
ATOM	588	O3*	DC	18	1.443	6.111	12.508
ATOM	589	P	DG	19	0.840	5.400	11.186
ATOM	590	O1P	DG	19	1.811	4.402	10.700
ATOM	591	O2P	DG	19	0.391	6.466	10.251
ATOM	592	O5*	DG	19	-0.464	4.648	11.771
ATOM	593	C5*	DG	19	-1.249	3.820	10.935
ATOM	594	1H5*	DG	19	-0.658	2.983	10.566
ATOM	595	2H5*	DG	19	-1.637	4.396	10.095
ATOM	596	C4*	DG	19	-2.462	3.241	11.682
ATOM	597	H4*	DG	19	-2.990	2.593	10.982
ATOM	598	O4*	DG	19	-2.037	2.432	12.775
ATOM	599	C1*	DG	19	-3.161	2.207	13.604
ATOM	600	H1*	DG	19	-3.785	1.434	13.157
ATOM	601	N9	DG	19	-2.737	1.760	14.956
ATOM	602	C8	DG	19	-2.521	2.478	16.116
ATOM	603	H8	DG	19	-2.601	3.554	16.158
ATOM	604	N7	DG	19	-2.198	1.758	17.161
ATOM	605	C5	DG	19	-2.241	0.447	16.666

ATOM	606	C6	DG	19	-2.003	-0.806	17.315
ATOM	607	O6	DG	19	-1.650	-1.040	18.478
ATOM	608	N1	DG	19	-2.168	-1.891	16.477
ATOM	609	1H	DG	19	-1.915	-2.803	16.831
ATOM	610	C2	DG	19	-2.513	-1.794	15.162
ATOM	611	N2	DG	19	-2.545	-2.889	14.477
ATOM	612	H21	DG	19	-2.699	-2.822	13.481
ATOM	613	H22	DG	19	-2.367	-3.759	14.959
ATOM	614	N3	DG	19	-2.740	-0.643	14.540
ATOM	615	C4	DG	19	-2.574	0.447	15.328
ATOM	616	C3*	DG	19	-3.469	4.252	12.297
ATOM	617	H3*	DG	19	-2.887	5.115	12.621
ATOM	618	C2*	DG	19	-3.923	3.535	13.567
ATOM	619	1H2*	DG	19	-4.995	3.340	13.559
ATOM	620	2H2*	DG	19	-3.644	4.173	14.405
ATOM	621	O3*	DG	19	-4.597	4.694	11.524
ATOM	622	P	DC	20	-5.369	3.845	10.389
ATOM	623	O1P	DC	20	-4.426	3.611	9.272
ATOM	624	O2P	DC	20	-6.627	4.582	10.122
ATOM	625	O5*	DC	20	-5.769	2.433	11.070
ATOM	626	C5*	DC	20	-5.483	1.217	10.406
ATOM	627	1H5*	DC	20	-4.408	1.088	10.280
ATOM	628	2H5*	DC	20	-5.924	1.246	9.409
ATOM	629	C4*	DC	20	-6.077	-0.017	11.126
ATOM	630	H4*	DC	20	-5.853	-0.887	10.509
ATOM	631	O4*	DC	20	-5.493	-0.168	12.416
ATOM	632	C1*	DC	20	-6.477	-0.762	13.242
ATOM	633	H1*	DC	20	-6.495	-1.839	13.075
ATOM	634	N1	DC	20	-6.156	-0.479	14.671
ATOM	635	C6	DC	20	-6.096	0.810	15.132
ATOM	636	H6	DC	20	-6.311	1.618	14.449
ATOM	637	C5	DC	20	-5.787	1.041	16.420
ATOM	638	H5	DC	20	-5.738	2.057	16.785
ATOM	639	C4	DC	20	-5.523	-0.082	17.261
ATOM	640	N4	DC	20	-5.197	0.083	18.490
ATOM	641	H41	DC	20	-5.124	1.011	18.883

ATOM	642	H42	DC	20	-4.969	-0.728	19.047
ATOM	643	N3	DC	20	-5.566	-1.317	16.833
ATOM	644	C2	DC	20	-5.915	-1.542	15.540
ATOM	645	O2	DC	20	-6.004	-2.706	15.182
ATOM	646	C3*	DC	20	-7.604	0.056	11.293
ATOM	647	H3*	DC	20	-7.955	1.041	10.987
ATOM	648	C2*	DC	20	-7.796	-0.145	12.793
ATOM	649	1H2*	DC	20	-8.624	-0.812	13.033
ATOM	650	2H2*	DC	20	-7.968	0.830	13.249
ATOM	651	O3*	DC	20	-8.245	-0.943	10.506
ATOM	652	P	DC	21	-9.856	-1.012	10.288
ATOM	653	O1P	DC	21	-10.097	-1.825	9.060
ATOM	654	O2P	DC	21	-10.410	0.357	10.360
ATOM	655	O5*	DC	21	-10.403	-1.829	11.569
ATOM	656	C5*	DC	21	-10.018	-3.181	11.810
ATOM	657	1H5*	DC	21	-8.941	-3.277	11.679
ATOM	658	2H5*	DC	21	-10.524	-3.835	11.100
ATOM	659	C4*	DC	21	-10.415	-3.646	13.212
ATOM	660	H4*	DC	21	-10.194	-4.712	13.278
ATOM	661	O4*	DC	21	-9.612	-2.954	14.171
ATOM	662	C1*	DC	21	-10.456	-2.614	15.261
ATOM	663	H1*	DC	21	-10.596	-3.497	15.884
ATOM	664	N1	DC	21	-9.861	-1.528	16.044
ATOM	665	C6	DC	21	-9.921	-0.227	15.636
ATOM	666	H6	DC	21	-10.317	0.028	14.664
ATOM	667	C5	DC	21	-9.443	0.763	16.433
ATOM	668	H5	DC	21	-9.525	1.786	16.098
ATOM	669	C4	DC	21	-8.914	0.373	17.689
ATOM	670	N4	DC	21	-8.484	1.264	18.538
ATOM	671	H41	DC	21	-8.531	2.244	18.298
ATOM	672	H42	DC	21	-8.074	0.917	19.393
ATOM	673	N3	DC	21	-8.817	-0.880	18.090
ATOM	674	C2	DC	21	-9.255	-1.847	17.261
ATOM	675	O2	DC	21	-9.122	-3.021	17.621
ATOM	676	C3*	DC	21	-11.901	-3.407	13.580
ATOM	677	H3*	DC	21	-12.511	-3.089	12.734

ATOM	678	C2*	DC	21	-11.796	-2.304	14.609
ATOM	679	1H2*	DC	21	-12.597	-2.319	15.348
ATOM	680	2H2*	DC	21	-11.800	-1.335	14.109
ATOM	681	O3*	DC	21	-12.479	-4.537	14.219
ATOM	682	P	DG	22	-13.074	-5.763	13.389
ATOM	683	O1P	DG	22	-12.192	-6.104	12.246
ATOM	684	O2P	DG	22	-14.505	-5.486	13.093
ATOM	685	O5*	DG	22	-13.019	-6.943	14.493
ATOM	686	C5*	DG	22	-11.864	-7.718	14.725
ATOM	687	1H5*	DG	22	-10.965	-7.140	14.509
ATOM	688	2H5*	DG	22	-11.896	-8.576	14.053
ATOM	689	C4*	DG	22	-11.745	-8.229	16.170
ATOM	690	H4*	DG	22	-11.045	-9.064	16.146
ATOM	691	O4*	DG	22	-11.241	-7.209	17.007
ATOM	692	C1*	DG	22	-12.142	-6.953	18.064
ATOM	693	H1*	DG	22	-11.862	-7.549	18.933
ATOM	694	N9	DG	22	-12.137	-5.500	18.382
ATOM	695	C8	DG	22	-12.570	-4.427	17.649
ATOM	696	H8	DG	22	-13.024	-4.560	16.679
ATOM	697	N7	DG	22	-12.369	-3.259	18.185
ATOM	698	C5	DG	22	-11.748	-3.584	19.409
ATOM	699	C6	DG	22	-11.259	-2.762	20.496
ATOM	700	O6	DG	22	-11.196	-1.545	20.609
ATOM	701	N1	DG	22	-10.832	-3.480	21.586
ATOM	702	1H	DG	22	-10.578	-2.956	22.410
ATOM	703	C2	DG	22	-10.744	-4.850	21.614
ATOM	704	N2	DG	22	-10.294	-5.413	22.698
ATOM	705	H21	DG	22	-10.318	-6.422	22.741
ATOM	706	H22	DG	22	-10.043	-4.851	23.499
ATOM	707	N3	DG	22	-11.125	-5.636	20.609
ATOM	708	C4	DG	22	-11.640	-4.957	19.539
ATOM	709	C3*	DG	22	-13.077	-8.714	16.778
ATOM	710	H3*	DG	22	-13.830	-8.930	16.020
ATOM	711	C2*	DG	22	-13.494	-7.487	17.576
ATOM	712	1H2*	DG	22	-14.163	-7.762	18.392
ATOM	713	2H2*	DG	22	-14.000	-6.750	16.952

ATOM	714	O3*	DG	22	-12.817	-9.848	17.609
ATOM	715	P	DA	23	-13.975	-10.661	18.389
ATOM	716	O1P	DA	23	-13.617	-12.108	18.318
ATOM	717	O2P	DA	23	-15.315	-10.218	17.915
ATOM	718	O5*	DA	23	-13.830	-10.139	19.913
ATOM	719	C5*	DA	23	-12.710	-10.502	20.719
ATOM	720	1H5*	DA	23	-11.790	-10.127	20.271
ATOM	721	2H5*	DA	23	-12.628	-11.589	20.722
ATOM	722	C4*	DA	23	-12.751	-10.025	22.173
ATOM	723	H4*	DA	23	-11.889	-10.440	22.694
ATOM	724	O4*	DA	23	-12.654	-8.602	22.261
ATOM	725	C1*	DA	23	-13.761	-8.067	22.970
ATOM	726	H1*	DA	23	-13.501	-7.922	24.019
ATOM	727	N9	DA	23	-14.107	-6.785	22.316
ATOM	728	C8	DA	23	-14.635	-6.581	21.067
ATOM	729	H8	DA	23	-14.892	-7.394	20.403
ATOM	730	N7	DA	23	-14.802	-5.320	20.739
ATOM	731	C5	DA	23	-14.335	-4.653	21.887
ATOM	732	C6	DA	23	-14.192	-3.285	22.250
ATOM	733	N6	DA	23	-14.478	-2.258	21.477
ATOM	734	1H6	DA	23	-14.299	-1.329	21.831
ATOM	735	2H6	DA	23	-14.820	-2.394	20.536
ATOM	736	N1	DA	23	-13.678	-2.933	23.426
ATOM	737	C2	DA	23	-13.278	-3.906	24.238
ATOM	738	H2	DA	23	-12.857	-3.603	25.185
ATOM	739	N3	DA	23	-13.355	-5.221	24.058
ATOM	740	C4	DA	23	-13.884	-5.530	22.834
ATOM	741	C3*	DA	23	-14.044	-10.446	22.908
ATOM	742	H3*	DA	23	-14.590	-11.226	22.377
ATOM	743	C2*	DA	23	-14.833	-9.150	22.907
ATOM	744	1H2*	DA	23	-15.506	-9.086	23.762
ATOM	745	2H2*	DA	23	-15.391	-9.076	21.973
ATOM	746	O3*	DA	23	-13.685	-10.932	24.201
ATOM	747	P	DG3	24	-14.770	-11.471	25.263
ATOM	748	O1P	DG3	24	-14.095	-12.467	26.121
ATOM	749	O2P	DG3	24	-15.996	-11.887	24.537

ATOM	750	O5*	DG3	24	-15.105	-10.154	26.157
ATOM	751	C5*	DG3	24	-14.094	-9.576	26.989
ATOM	752	1H5*	DG3	24	-13.211	-9.328	26.401
ATOM	753	2H5*	DG3	24	-13.765	-10.311	27.724
ATOM	754	C4*	DG3	24	-14.594	-8.317	27.710
ATOM	755	H4*	DG3	24	-13.866	-8.082	28.487
ATOM	756	O4*	DG3	24	-14.678	-7.237	26.804
ATOM	757	C1*	DG3	24	-15.860	-6.506	27.095
ATOM	758	H1*	DG3	24	-15.670	-5.822	27.922
ATOM	759	N9	DG3	24	-16.336	-5.733	25.909
ATOM	760	C8	DG3	24	-16.733	-6.194	24.674
ATOM	761	H8	DG3	24	-16.719	-7.250	24.445
ATOM	762	N7	DG3	24	-17.090	-5.264	23.833
ATOM	763	C5	DG3	24	-16.899	-4.070	24.566
ATOM	764	C6	DG3	24	-17.041	-2.686	24.186
ATOM	765	O6	DG3	24	-17.416	-2.215	23.107
ATOM	766	N1	DG3	24	-16.679	-1.794	25.170
ATOM	767	1H	DG3	24	-16.732	-0.810	24.949
ATOM	768	C2	DG3	24	-16.261	-2.188	26.406
ATOM	769	N2	DG3	24	-15.967	-1.226	27.245
ATOM	770	H21	DG3	24	-15.624	-1.469	28.163
ATOM	771	H22	DG3	24	-16.041	-0.252	26.987
ATOM	772	N3	DG3	24	-16.095	-3.447	26.810
ATOM	773	C4	DG3	24	-16.415	-4.360	25.820
ATOM	774	C3*	DG3	24	-15.980	-8.455	28.394
ATOM	775	H3*	DG3	24	-16.353	-9.478	28.339
ATOM	776	C2*	DG3	24	-16.877	-7.535	27.576
ATOM	777	1H2*	DG3	24	-17.646	-7.088	28.207
ATOM	778	2H2*	DG3	24	-17.326	-8.090	26.752
ATOM	779	O3*	DG3	24	-15.930	-8.019	29.747
ATOM	780	H3T	DG3	24	-16.765	-8.213	30.180
TER							
END							

N²-dG-IQ at G¹

REMARK 99

REMARK 99 MOE v2012.10 (Chemical Computing Group Inc.) Fri Feb 14
14:14:16 2014

LINK		O3*	DC5	1		P	DT	2	1555
1555	1.63								
LINK		O3'	DC	3		P	DKA	4	1555
1555	1.63								
LINK		O3*	DKA	4		P	DG	5	1555
1555	1.64								
LINK		O3'	DT	11		P	DC3	12	1555
1555	1.64								
LINK		O3*	DG5	13		P	DA	14	1555
1555	1.63								
LINK		O3'	DA	23		P	DG3	24	1555
1555	1.63								

CRYST1	10.000	10.000	10.000	90.00	90.00	90.00	P1		
HETATM	1	O5*	DC5	1	-13.629	18.420	22.409	0.00	0.00
HETATM	2	C5*	DC5	1	-14.816	17.820	22.920	0.00	0.00
HETATM	3	C4*	DC5	1	-14.931	16.355	22.496	0.00	0.00
HETATM	4	O4*	DC5	1	-15.211	16.291	21.072	0.00	0.00
HETATM	5	C1*	DC5	1	-14.336	15.294	20.510	0.00	0.00
HETATM	6	N1	DC5	1	-14.106	15.543	19.086	0.00	0.00
HETATM	7	C6	DC5	1	-13.808	16.816	18.651	0.00	0.00
HETATM	8	C5	DC5	1	-13.585	17.076	17.364	0.00	0.00
HETATM	9	C4	DC5	1	-13.668	15.925	16.439	0.00	0.00
HETATM	10	N4	DC5	1	-13.443	16.123	15.107	0.00	0.00
HETATM	11	N3	DC5	1	-13.950	14.719	16.840	0.00	0.00
HETATM	12	C2	DC5	1	-14.188	14.476	18.181	0.00	0.00
HETATM	13	O2	DC5	1	-14.478	13.331	18.532	0.00	0.00
HETATM	14	C3*	DC5	1	-13.655	15.545	22.745	0.00	0.00
HETATM	15	C2*	DC5	1	-13.076	15.365	21.360	0.00	0.00
HETATM	16	O3*	DC5	1	-14.019	14.254	23.223	0.00	0.00
HETATM	17	'HO5	DC5	1	-13.567	19.306	22.809	0.00	0.00
HETATM	18	H5*	DC5	1	-15.668	18.395	22.545	0.00	0.00
HETATM	19	'H5*	DC5	1	-14.786	17.891	24.012	0.00	0.00
HETATM	20	H4*	DC5	1	-15.793	15.908	23.006	0.00	0.00

HETATM	21	H1*	DC5	1	-14.829	14.323	20.643	0.00	0.00
HETATM	22	H6	DC5	1	-13.768	17.599	19.401	0.00	0.00
HETATM	23	H5	DC5	1	-13.353	18.062	16.989	0.00	0.00
HETATM	24	H41	DC5	1	-13.236	17.026	14.704	0.00	0.00
HETATM	25	H42	DC5	1	-13.479	15.317	14.468	0.00	0.00
HETATM	26	H3*	DC5	1	-12.968	16.024	23.449	0.00	0.00
HETATM	27	H2*	DC5	1	-12.468	14.466	21.251	0.00	0.00
HETATM	28	'H2*	DC5	1	-12.466	16.236	21.097	0.00	0.00
ATOM	29	P	DT	2	-13.148	13.620	24.450	0.00	0.00
ATOM	30	OP1	DT	2	-13.712	14.145	25.752	0.00	0.00
ATOM	31	OP2	DT	2	-11.685	13.775	24.096	0.00	0.00
ATOM	32	O5'	DT	2	-13.527	12.045	24.237	0.00	0.00
ATOM	33	C5'	DT	2	-14.885	11.635	24.293	0.00	0.00
ATOM	34	C4'	DT	2	-15.156	10.424	23.380	0.00	0.00
ATOM	35	O4'	DT	2	-14.862	10.789	22.002	0.00	0.00
ATOM	36	C1'	DT	2	-14.038	9.745	21.456	0.00	0.00
ATOM	37	N1	DT	2	-13.188	10.244	20.378	0.00	0.00
ATOM	38	C6	DT	2	-12.334	11.307	20.610	0.00	0.00
ATOM	39	C5	DT	2	-11.475	11.764	19.691	0.00	0.00
ATOM	40	C7	DT	2	-10.516	12.887	19.911	0.00	0.00
ATOM	41	C4	DT	2	-11.446	11.090	18.374	0.00	0.00
ATOM	42	O4	DT	2	-10.681	11.446	17.479	0.00	0.00
ATOM	43	N3	DT	2	-12.323	10.054	18.208	0.00	0.00
ATOM	44	C2	DT	2	-13.247	9.612	19.132	0.00	0.00
ATOM	45	O2	DT	2	-14.065	8.754	18.796	0.00	0.00
ATOM	46	C3'	DT	2	-14.328	9.166	23.700	0.00	0.00
ATOM	47	C2'	DT	2	-13.258	9.193	22.639	0.00	0.00
ATOM	48	O3'	DT	2	-15.150	8.008	23.499	0.00	0.00
ATOM	49	H5'	DT	2	-15.533	12.462	23.983	0.00	0.00
ATOM	50	'H5'	DT	2	-15.124	11.385	25.331	0.00	0.00
ATOM	51	H4'	DT	2	-16.227	10.196	23.425	0.00	0.00
ATOM	52	H1'	DT	2	-14.716	8.977	21.065	0.00	0.00
ATOM	53	H6	DT	2	-12.391	11.764	21.597	0.00	0.00
ATOM	54	1H7	DT	2	-9.496	12.583	19.656	0.00	0.00
ATOM	55	2H7	DT	2	-10.787	13.747	19.291	0.00	0.00
ATOM	56	3H7	DT	2	-10.503	13.210	20.957	0.00	0.00

ATOM	57	H3	DT	2	-12.311	9.571	17.314	0.00	0.00
ATOM	58	H3'	DT	2	-13.944	9.176	24.723	0.00	0.00
ATOM	59	H2'	DT	2	-12.815	8.225	22.409	0.00	0.00
ATOM	60	'H2'	DT	2	-12.453	9.867	22.950	0.00	0.00
ATOM	61	P	DC	3	-14.675	6.563	24.105	0.00	0.00
ATOM	62	OP1	DC	3	-15.891	5.662	24.177	0.00	0.00
ATOM	63	OP2	DC	3	-13.848	6.827	25.343	0.00	0.00
ATOM	64	O5'	DC	3	-13.715	6.013	22.888	0.00	0.00
ATOM	65	C5'	DC	3	-14.395	5.541	21.725	0.00	0.00
ATOM	66	C4'	DC	3	-13.477	5.211	20.537	0.00	0.00
ATOM	67	O4'	DC	3	-12.749	6.408	20.150	0.00	0.00
ATOM	68	C1'	DC	3	-11.416	5.968	19.860	0.00	0.00
ATOM	69	N1	DC	3	-10.512	7.096	19.804	0.00	0.00
ATOM	70	C6	DC	3	-10.181	7.816	20.927	0.00	0.00
ATOM	71	C5	DC	3	-9.321	8.833	20.864	0.00	0.00
ATOM	72	C4	DC	3	-8.750	9.110	19.532	0.00	0.00
ATOM	73	N4	DC	3	-7.819	10.086	19.364	0.00	0.00
ATOM	74	N3	DC	3	-9.090	8.458	18.462	0.00	0.00
ATOM	75	C2	DC	3	-9.994	7.428	18.554	0.00	0.00
ATOM	76	O2	DC	3	-10.294	6.828	17.521	0.00	0.00
ATOM	77	C3'	DC	3	-12.427	4.097	20.753	0.00	0.00
ATOM	78	C2'	DC	3	-11.147	4.896	20.901	0.00	0.00
ATOM	79	O3'	DC	3	-12.328	3.332	19.534	0.00	0.00
ATOM	80	H5'	DC	3	-15.100	6.320	21.411	0.00	0.00
ATOM	81	'H5'	DC	3	-14.964	4.644	21.992	0.00	0.00
ATOM	82	H4'	DC	3	-14.119	4.950	19.686	0.00	0.00
ATOM	83	H1'	DC	3	-11.455	5.498	18.870	0.00	0.00
ATOM	84	H6	DC	3	-10.647	7.530	21.863	0.00	0.00
ATOM	85	H5	DC	3	-9.040	9.431	21.718	0.00	0.00
ATOM	86	H41	DC	3	-7.507	10.680	20.118	0.00	0.00
ATOM	87	H42	DC	3	-7.412	10.216	18.432	0.00	0.00
ATOM	88	H3'	DC	3	-12.664	3.433	21.589	0.00	0.00
ATOM	89	H2'	DC	3	-10.235	4.339	20.685	0.00	0.00
ATOM	90	'H2'	DC	3	-11.082	5.306	21.914	0.00	0.00
HETATM	91	P	DKA	4	-11.571	1.884	19.536	0.00	0.00
HETATM	92	O1P	DKA	4	-12.564	0.831	19.109	0.00	0.00

HETATM	93	O2P	DKA	4	-10.785	1.750	20.819	0.00	0.00
HETATM	94	O5*	DKA	4	-10.510	2.120	18.311	0.00	0.00
HETATM	95	C5*	DKA	4	-10.979	2.102	16.969	0.00	0.00
HETATM	96	C4*	DKA	4	-9.809	1.942	15.980	0.00	0.00
HETATM	97	O4*	DKA	4	-9.020	3.157	15.976	0.00	0.00
HETATM	98	C1*	DKA	4	-7.718	2.872	16.516	0.00	0.00
HETATM	99	N9	DKA	4	-7.408	3.929	17.465	0.00	0.00
HETATM	100	C8	DKA	4	-8.013	4.118	18.688	0.00	0.00
HETATM	101	N7	DKA	4	-7.554	5.169	19.333	0.00	0.00
HETATM	102	C5	DKA	4	-6.609	5.667	18.495	0.00	0.00
HETATM	103	C6	DKA	4	-5.760	6.807	18.694	0.00	0.00
HETATM	104	O6	DKA	4	-5.708	7.503	19.703	0.00	0.00
HETATM	105	N1	DKA	4	-4.936	7.023	17.604	0.00	0.00
HETATM	106	C2	DKA	4	-4.881	6.202	16.471	0.00	0.00
HETATM	107	N2	DKA	4	-3.794	6.632	15.440	0.00	0.00
HETATM	108	C23	DKA	4	-3.524	6.261	14.240	0.00	0.00
HETATM	109	C22	DKA	4	-2.318	6.924	13.670	0.00	0.00
HETATM	110	N21	DKA	4	-1.734	7.793	14.541	0.00	0.00
HETATM	111	C20	DKA	4	-0.638	8.431	14.074	0.00	0.00
HETATM	112	C19	DKA	4	-0.104	8.218	12.811	0.00	0.00
HETATM	113	C18	DKA	4	-0.736	7.327	11.946	0.00	0.00
HETATM	114	C17	DKA	4	-1.868	6.667	12.391	0.00	0.00
HETATM	115	C16	DKA	4	-2.612	5.742	11.580	0.00	0.00
HETATM	116	N15	DKA	4	-2.404	5.370	10.349	0.00	0.00
HETATM	117	C14	DKA	4	-3.457	4.550	10.040	0.00	0.00
HETATM	118	N14	DKA	4	-3.602	4.100	8.822	0.00	0.00
HETATM	119	N13	DKA	4	-4.272	4.306	11.092	0.00	0.00
HETATM	120	C13	DKA	4	-5.454	3.452	11.107	0.00	0.00
HETATM	121	C12	DKA	4	-3.812	5.085	12.138	0.00	0.00
HETATM	122	C11	DKA	4	-4.265	5.292	13.382	0.00	0.00
HETATM	123	N3	DKA	4	-5.641	5.160	16.283	0.00	0.00
HETATM	124	C4	DKA	4	-6.488	4.937	17.327	0.00	0.00
HETATM	125	C3*	DKA	4	-8.858	0.783	16.316	0.00	0.00
HETATM	126	C2*	DKA	4	-7.752	1.461	17.101	0.00	0.00
HETATM	127	O3*	DKA	4	-8.246	0.227	15.149	0.00	0.00
HETATM	128	1H5*	DKA	4	-11.505	3.044	16.784	0.00	0.00

HETATM	129	2H5*	DKA	4	-11.674	1.269	16.831	0.00	0.00
HETATM	130	H4*	DKA	4	-10.226	1.868	14.976	0.00	0.00
HETATM	131	H1*	DKA	4	-7.001	2.928	15.689	0.00	0.00
HETATM	132	H8	DKA	4	-8.784	3.462	19.067	0.00	0.00
HETATM	133	1H	DKA	4	-4.361	7.850	17.699	0.00	0.00
HETATM	134	2H	DKA	4	-3.127	7.352	15.767	0.00	0.00
HETATM	135	H20	DKA	4	-0.176	9.138	14.754	0.00	0.00
HETATM	136	H19	DKA	4	0.795	8.742	12.505	0.00	0.00
HETATM	137	H18	DKA	4	-0.346	7.161	10.946	0.00	0.00
HETATM	138	H141	DKA	4	-2.942	4.370	8.111	1.00	0.00
HETATM	139	H142	DKA	4	-4.573	3.765	8.511	1.00	0.00
HETATM	140	1H13	DKA	4	-5.650	3.087	12.118	0.00	0.00
HETATM	141	2H13	DKA	4	-6.325	4.026	10.785	0.00	0.00
HETATM	142	3H13	DKA	4	-5.305	2.591	10.451	0.00	0.00
HETATM	143	H11	DKA	4	-5.151	4.795	13.759	0.00	0.00
HETATM	144	H3*	DKA	4	-9.335	-0.023	16.882	0.00	0.00
HETATM	145	1H2*	DKA	4	-6.777	0.972	16.999	0.00	0.00
HETATM	146	2H2*	DKA	4	-8.001	1.462	18.167	0.00	0.00
ATOM	147	P	DG	5	-9.120	-0.865	14.292	0.00	0.00
ATOM	148	OP1	DG	5	-10.218	-0.064	13.635	0.00	0.00
ATOM	149	OP2	DG	5	-9.423	-2.057	15.170	0.00	0.00
ATOM	150	O5'	DG	5	-7.967	-1.254	13.191	0.00	0.00
ATOM	151	C5'	DG	5	-8.329	-1.172	11.817	0.00	0.00
ATOM	152	C4'	DG	5	-7.115	-1.274	10.885	0.00	0.00
ATOM	153	O4'	DG	5	-6.270	-0.114	11.096	0.00	0.00
ATOM	154	C1'	DG	5	-4.962	-0.570	11.483	0.00	0.00
ATOM	155	N9	DG	5	-4.448	0.352	12.482	0.00	0.00
ATOM	156	C8	DG	5	-5.023	0.620	13.706	0.00	0.00
ATOM	157	N7	DG	5	-4.337	1.504	14.407	0.00	0.00
ATOM	158	C5	DG	5	-3.273	1.805	13.602	0.00	0.00
ATOM	159	C6	DG	5	-2.182	2.720	13.827	0.00	0.00
ATOM	160	O6	DG	5	-2.044	3.457	14.806	0.00	0.00
ATOM	161	N1	DG	5	-1.311	2.761	12.751	0.00	0.00
ATOM	162	C2	DG	5	-1.482	2.075	11.558	0.00	0.00
ATOM	163	N2	DG	5	-0.542	2.347	10.618	0.00	0.00
ATOM	164	N3	DG	5	-2.479	1.255	11.343	0.00	0.00

ATOM	165	C4	DG	5	-3.326	1.136	12.397	0.00	0.00
ATOM	166	C3'	DG	5	-6.251	-2.520	11.099	0.00	0.00
ATOM	167	C2'	DG	5	-5.119	-2.006	11.959	0.00	0.00
ATOM	168	O3'	DG	5	-5.759	-2.962	9.829	0.00	0.00
ATOM	169	H5'	DG	5	-8.811	-0.205	11.637	0.00	0.00
ATOM	170	'H5'	DG	5	-9.042	-1.973	11.599	0.00	0.00
ATOM	171	H4'	DG	5	-7.471	-1.219	9.850	0.00	0.00
ATOM	172	H1'	DG	5	-4.320	-0.520	10.597	0.00	0.00
ATOM	173	H8	DG	5	-5.943	0.146	14.024	0.00	0.00
ATOM	174	1H	DG	5	-0.491	3.359	12.857	0.00	0.00
ATOM	175	H21	DG	5	-0.547	1.803	9.762	0.00	0.00
ATOM	176	H22	DG	5	0.173	3.078	10.745	0.00	0.00
ATOM	177	H3'	DG	5	-6.821	-3.327	11.568	0.00	0.00
ATOM	178	H2'	DG	5	-4.189	-2.562	11.851	0.00	0.00
ATOM	179	'H2'	DG	5	-5.412	-2.050	13.013	0.00	0.00
ATOM	180	P	DC	6	-5.154	-4.478	9.691	0.00	0.00
ATOM	181	OP1	DC	6	-5.212	-4.909	8.238	0.00	0.00
ATOM	182	OP2	DC	6	-5.780	-5.339	10.764	0.00	0.00
ATOM	183	O5'	DC	6	-3.593	-4.173	10.079	0.00	0.00
ATOM	184	C5'	DC	6	-2.828	-3.482	9.098	0.00	0.00
ATOM	185	C4'	DC	6	-1.401	-3.215	9.568	0.00	0.00
ATOM	186	O4'	DC	6	-1.408	-2.142	10.554	0.00	0.00
ATOM	187	C1'	DC	6	-0.448	-2.529	11.565	0.00	0.00
ATOM	188	N1	DC	6	-0.629	-1.738	12.782	0.00	0.00
ATOM	189	C6	DC	6	-1.733	-1.930	13.581	0.00	0.00
ATOM	190	C5	DC	6	-1.924	-1.227	14.695	0.00	0.00
ATOM	191	C4	DC	6	-0.899	-0.217	15.008	0.00	0.00
ATOM	192	N4	DC	6	-1.038	0.558	16.124	0.00	0.00
ATOM	193	N3	DC	6	0.145	-0.009	14.260	0.00	0.00
ATOM	194	C2	DC	6	0.338	-0.774	13.120	0.00	0.00
ATOM	195	O2	DC	6	1.366	-0.577	12.467	0.00	0.00
ATOM	196	C3'	DC	6	-0.717	-4.428	10.218	0.00	0.00
ATOM	197	C2'	DC	6	-0.661	-4.037	11.682	0.00	0.00
ATOM	198	O3'	DC	6	0.628	-4.505	9.748	0.00	0.00
ATOM	199	H5'	DC	6	-3.327	-2.536	8.863	0.00	0.00
ATOM	200	'H5'	DC	6	-2.789	-4.098	8.193	0.00	0.00

ATOM	201	H4'	DC	6	-0.818	-2.843	8.717	0.00	0.00
ATOM	202	H1'	DC	6	0.546	-2.324	11.150	0.00	0.00
ATOM	203	H6	DC	6	-2.456	-2.675	13.275	0.00	0.00
ATOM	204	H5	DC	6	-2.787	-1.346	15.333	0.00	0.00
ATOM	205	H41	DC	6	-1.873	0.537	16.699	0.00	0.00
ATOM	206	H42	DC	6	-0.271	1.190	16.403	0.00	0.00
ATOM	207	H3'	DC	6	-1.232	-5.375	10.030	0.00	0.00
ATOM	208	H2'	DC	6	0.132	-4.528	12.248	0.00	0.00
ATOM	209	'H2'	DC	6	-1.621	-4.285	12.146	0.00	0.00
ATOM	210	P	DG	7	1.278	-5.980	9.491	0.00	0.00
ATOM	211	OP1	DG	7	0.893	-6.426	8.099	0.00	0.00
ATOM	212	OP2	DG	7	0.967	-6.839	10.694	0.00	0.00
ATOM	213	O5'	DG	7	2.867	-5.569	9.532	0.00	0.00
ATOM	214	C5'	DG	7	3.354	-4.736	8.484	0.00	0.00
ATOM	215	C4'	DG	7	4.517	-3.841	8.947	0.00	0.00
ATOM	216	O4'	DG	7	4.033	-2.990	10.015	0.00	0.00
ATOM	217	C1'	DG	7	4.867	-3.194	11.174	0.00	0.00
ATOM	218	N9	DG	7	4.042	-3.152	12.368	0.00	0.00
ATOM	219	C8	DG	7	2.888	-3.873	12.565	0.00	0.00
ATOM	220	N7	DG	7	2.326	-3.620	13.731	0.00	0.00
ATOM	221	C5	DG	7	3.157	-2.700	14.306	0.00	0.00
ATOM	222	C6	DG	7	3.052	-2.044	15.588	0.00	0.00
ATOM	223	O6	DG	7	2.146	-2.186	16.409	0.00	0.00
ATOM	224	N1	DG	7	4.142	-1.216	15.826	0.00	0.00
ATOM	225	C2	DG	7	5.212	-1.025	14.959	0.00	0.00
ATOM	226	N2	DG	7	6.194	-0.198	15.406	0.00	0.00
ATOM	227	N3	DG	7	5.294	-1.603	13.786	0.00	0.00
ATOM	228	C4	DG	7	4.244	-2.416	13.506	0.00	0.00
ATOM	229	C3'	DG	7	5.744	-4.596	9.472	0.00	0.00
ATOM	230	C2'	DG	7	5.583	-4.520	10.971	0.00	0.00
ATOM	231	O3'	DG	7	6.939	-3.903	9.077	0.00	0.00
ATOM	232	H5'	DG	7	2.542	-4.096	8.122	0.00	0.00
ATOM	233	'H5'	DG	7	3.677	-5.380	7.660	0.00	0.00
ATOM	234	H4'	DG	7	4.797	-3.185	8.115	0.00	0.00
ATOM	235	H1'	DG	7	5.579	-2.362	11.213	0.00	0.00
ATOM	236	H8	DG	7	2.506	-4.562	11.823	0.00	0.00

ATOM	237	1H	DG	7	4.132	-0.728	16.723	0.00	0.00
ATOM	238	H21	DG	7	7.021	-0.086	14.831	0.00	0.00
ATOM	239	H22	DG	7	6.143	0.327	16.297	0.00	0.00
ATOM	240	H3'	DG	7	5.773	-5.621	9.094	0.00	0.00
ATOM	241	H2'	DG	7	6.527	-4.546	11.515	0.00	0.00
ATOM	242	'H2'	DG	7	4.970	-5.360	11.317	0.00	0.00
ATOM	243	P	DC	8	8.363	-4.720	8.999	0.00	0.00
ATOM	244	OP1	DC	8	9.288	-4.002	8.036	0.00	0.00
ATOM	245	OP2	DC	8	8.056	-6.188	8.801	0.00	0.00
ATOM	246	O5'	DC	8	8.918	-4.472	10.529	0.00	0.00
ATOM	247	C5'	DC	8	9.487	-3.188	10.790	0.00	0.00
ATOM	248	C4'	DC	8	10.045	-3.024	12.211	0.00	0.00
ATOM	249	O4'	DC	8	8.954	-2.870	13.150	0.00	0.00
ATOM	250	C1'	DC	8	9.302	-3.602	14.343	0.00	0.00
ATOM	251	N1	DC	8	8.063	-3.938	15.061	0.00	0.00
ATOM	252	C6	DC	8	7.132	-4.753	14.459	0.00	0.00
ATOM	253	C5	DC	8	5.978	-5.050	15.047	0.00	0.00
ATOM	254	C4	DC	8	5.743	-4.450	16.374	0.00	0.00
ATOM	255	N4	DC	8	4.544	-4.707	16.979	0.00	0.00
ATOM	256	N3	DC	8	6.612	-3.693	16.980	0.00	0.00
ATOM	257	C2	DC	8	7.810	-3.399	16.338	0.00	0.00
ATOM	258	O2	DC	8	8.593	-2.636	16.909	0.00	0.00
ATOM	259	C3'	DC	8	10.945	-4.166	12.718	0.00	0.00
ATOM	260	C2'	DC	8	10.120	-4.784	13.832	0.00	0.00
ATOM	261	O3'	DC	8	12.156	-3.599	13.230	0.00	0.00
ATOM	262	H5'	DC	8	8.716	-2.432	10.608	0.00	0.00
ATOM	263	'H5'	DC	8	10.311	-3.030	10.087	0.00	0.00
ATOM	264	H4'	DC	8	10.592	-2.073	12.237	0.00	0.00
ATOM	265	H1'	DC	8	9.928	-2.944	14.957	0.00	0.00
ATOM	266	H6	DC	8	7.362	-5.131	13.471	0.00	0.00
ATOM	267	H5	DC	8	5.219	-5.665	14.586	0.00	0.00
ATOM	268	H41	DC	8	3.815	-5.251	16.532	0.00	0.00
ATOM	269	H42	DC	8	4.332	-4.344	17.919	0.00	0.00
ATOM	270	H3'	DC	8	11.200	-4.875	11.924	0.00	0.00
ATOM	271	H2'	DC	8	10.698	-5.246	14.630	0.00	0.00
ATOM	272	'H2'	DC	8	9.484	-5.560	13.395	0.00	0.00

ATOM	273	P	DC	9	13.402	-4.573	13.664	0.00	0.00
ATOM	274	OP1	DC	9	14.684	-3.767	13.615	0.00	0.00
ATOM	275	OP2	DC	9	13.286	-5.877	12.909	0.00	0.00
ATOM	276	O5'	DC	9	13.015	-4.808	15.236	0.00	0.00
ATOM	277	C5'	DC	9	13.097	-3.656	16.067	0.00	0.00
ATOM	278	C4'	DC	9	12.528	-3.916	17.456	0.00	0.00
ATOM	279	O4'	DC	9	11.105	-4.197	17.355	0.00	0.00
ATOM	280	C1'	DC	9	10.849	-5.191	18.360	0.00	0.00
ATOM	281	N1	DC	9	9.560	-5.824	18.170	0.00	0.00
ATOM	282	C6	DC	9	9.339	-6.646	17.090	0.00	0.00
ATOM	283	C5	DC	9	8.213	-7.340	16.968	0.00	0.00
ATOM	284	C4	DC	9	7.234	-7.167	18.055	0.00	0.00
ATOM	285	N4	DC	9	6.103	-7.919	18.042	0.00	0.00
ATOM	286	N3	DC	9	7.388	-6.318	19.027	0.00	0.00
ATOM	287	C2	DC	9	8.555	-5.583	19.119	0.00	0.00
ATOM	288	O2	DC	9	8.658	-4.753	20.026	0.00	0.00
ATOM	289	C3'	DC	9	13.158	-5.103	18.194	0.00	0.00
ATOM	290	C2'	DC	9	12.046	-6.122	18.234	0.00	0.00
ATOM	291	O3'	DC	9	13.395	-4.719	19.547	0.00	0.00
ATOM	292	H5'	DC	9	12.537	-2.839	15.599	0.00	0.00
ATOM	293	'H5'	DC	9	14.148	-3.359	16.153	0.00	0.00
ATOM	294	H4'	DC	9	12.625	-2.996	18.046	0.00	0.00
ATOM	295	H1'	DC	9	10.865	-4.681	19.330	0.00	0.00
ATOM	296	H6	DC	9	10.114	-6.711	16.334	0.00	0.00
ATOM	297	H5	DC	9	8.002	-7.986	16.131	0.00	0.00
ATOM	298	H41	DC	9	5.909	-8.621	17.345	0.00	0.00
ATOM	299	H42	DC	9	5.387	-7.780	18.769	0.00	0.00
ATOM	300	H3'	DC	9	14.084	-5.466	17.735	0.00	0.00
ATOM	301	H2'	DC	9	12.090	-6.832	19.063	0.00	0.00
ATOM	302	'H2'	DC	9	12.049	-6.682	17.293	0.00	0.00
ATOM	303	P	DA	10	14.613	-5.484	20.310	0.00	0.00
ATOM	304	OP1	DA	10	15.898	-4.855	19.827	0.00	0.00
ATOM	305	OP2	DA	10	14.378	-6.971	20.198	0.00	0.00
ATOM	306	O5'	DA	10	14.309	-5.034	21.851	0.00	0.00
ATOM	307	C5'	DA	10	14.395	-3.654	22.183	0.00	0.00
ATOM	308	C4'	DA	10	13.444	-3.306	23.341	0.00	0.00

ATOM	309	O4'	DA	10	12.092	-3.616	22.911	0.00	0.00
ATOM	310	C1'	DA	10	11.543	-4.579	23.830	0.00	0.00
ATOM	311	N9	DA	10	10.714	-5.534	23.123	0.00	0.00
ATOM	312	C8	DA	10	11.033	-6.208	21.974	0.00	0.00
ATOM	313	N7	DA	10	10.102	-7.073	21.626	0.00	0.00
ATOM	314	C5	DA	10	9.130	-6.943	22.600	0.00	0.00
ATOM	315	C6	DA	10	7.899	-7.596	22.791	0.00	0.00
ATOM	316	N6	DA	10	7.445	-8.543	21.900	0.00	0.00
ATOM	317	N1	DA	10	7.141	-7.249	23.869	0.00	0.00
ATOM	318	C2	DA	10	7.586	-6.230	24.657	0.00	0.00
ATOM	319	N3	DA	10	8.735	-5.529	24.547	0.00	0.00
ATOM	320	C4	DA	10	9.471	-5.958	23.510	0.00	0.00
ATOM	321	C3'	DA	10	13.705	-4.092	24.632	0.00	0.00
ATOM	322	C2'	DA	10	12.720	-5.230	24.534	0.00	0.00
ATOM	323	O3'	DA	10	13.393	-3.273	25.769	0.00	0.00
ATOM	324	H5'	DA	10	14.126	-3.051	21.310	0.00	0.00
ATOM	325	'H5'	DA	10	15.430	-3.427	22.457	0.00	0.00
ATOM	326	H4'	DA	10	13.488	-2.226	23.523	0.00	0.00
ATOM	327	H1'	DA	10	10.914	-4.027	24.538	0.00	0.00
ATOM	328	H8	DA	10	11.957	-6.038	21.439	0.00	0.00
ATOM	329	1H6	DA	10	6.532	-8.999	21.983	0.00	0.00
ATOM	330	2H6	DA	10	8.049	-8.804	21.132	0.00	0.00
ATOM	331	H2	DA	10	6.930	-5.943	25.474	0.00	0.00
ATOM	332	H3'	DA	10	14.748	-4.412	24.708	0.00	0.00
ATOM	333	H2'	DA	10	12.425	-5.647	25.495	0.00	0.00
ATOM	334	'H2'	DA	10	13.147	-6.041	23.935	0.00	0.00
ATOM	335	P	DT	11	13.776	-3.818	27.270	0.00	0.00
ATOM	336	OP1	DT	11	14.167	-2.643	28.142	0.00	0.00
ATOM	337	OP2	DT	11	14.695	-5.010	27.120	0.00	0.00
ATOM	338	O5'	DT	11	12.310	-4.348	27.763	0.00	0.00
ATOM	339	C5'	DT	11	11.287	-3.378	27.954	0.00	0.00
ATOM	340	C4'	DT	11	10.039	-3.981	28.613	0.00	0.00
ATOM	341	O4'	DT	11	9.476	-4.964	27.708	0.00	0.00
ATOM	342	C1'	DT	11	9.405	-6.209	28.420	0.00	0.00
ATOM	343	N1	DT	11	9.534	-7.324	27.492	0.00	0.00
ATOM	344	C6	DT	11	10.734	-7.581	26.860	0.00	0.00

ATOM	345	C5	DT	11	10.900	-8.591	25.998	0.00	0.00
ATOM	346	C7	DT	11	12.173	-8.893	25.280	0.00	0.00
ATOM	347	C4	DT	11	9.740	-9.470	25.738	0.00	0.00
ATOM	348	O4	DT	11	9.811	-10.427	24.971	0.00	0.00
ATOM	349	N3	DT	11	8.582	-9.159	26.389	0.00	0.00
ATOM	350	C2	DT	11	8.402	-8.097	27.240	0.00	0.00
ATOM	351	O2	DT	11	7.282	-7.871	27.695	0.00	0.00
ATOM	352	C3'	DT	11	10.297	-4.694	29.949	0.00	0.00
ATOM	353	C2'	DT	11	10.454	-6.133	29.517	0.00	0.00
ATOM	354	O3'	DT	11	9.132	-4.565	30.781	0.00	0.00
ATOM	355	H5'	DT	11	11.021	-2.973	26.972	0.00	0.00
ATOM	356	'H5'	DT	11	11.666	-2.565	28.581	0.00	0.00
ATOM	357	H4'	DT	11	9.288	-3.191	28.732	0.00	0.00
ATOM	358	H1'	DT	11	8.412	-6.237	28.882	0.00	0.00
ATOM	359	H6	DT	11	11.552	-6.903	27.083	0.00	0.00
ATOM	360	1H7	DT	11	12.037	-8.788	24.199	0.00	0.00
ATOM	361	2H7	DT	11	12.981	-8.219	25.583	0.00	0.00
ATOM	362	3H7	DT	11	12.502	-9.916	25.492	0.00	0.00
ATOM	363	H3	DT	11	7.765	-9.741	26.227	0.00	0.00
ATOM	364	H3'	DT	11	11.159	-4.285	30.483	0.00	0.00
ATOM	365	H2'	DT	11	10.272	-6.866	30.300	0.00	0.00
ATOM	366	'H2'	DT	11	11.470	-6.296	29.149	0.00	0.00
HETATM	367	P	DC3	12	9.166	-5.212	32.284	0.00	0.00
HETATM	368	OP1	DC3	12	8.351	-4.358	33.231	0.00	0.00
HETATM	369	OP2	DC3	12	10.586	-5.605	32.617	0.00	0.00
HETATM	370	O5*	DC3	12	8.338	-6.586	31.993	0.00	0.00
HETATM	371	C5*	DC3	12	6.960	-6.473	31.671	0.00	0.00
HETATM	372	C4*	DC3	12	6.274	-7.839	31.701	0.00	0.00
HETATM	373	O4*	DC3	12	6.794	-8.661	30.633	0.00	0.00
HETATM	374	C1*	DC3	12	7.189	-9.927	31.188	0.00	0.00
HETATM	375	N1	DC3	12	8.269	-10.486	30.384	0.00	0.00
HETATM	376	C6	DC3	12	9.437	-9.777	30.232	0.00	0.00
HETATM	377	C5	DC3	12	10.422	-10.215	29.454	0.00	0.00
HETATM	378	C4	DC3	12	10.166	-11.481	28.740	0.00	0.00
HETATM	379	N4	DC3	12	11.098	-11.919	27.845	0.00	0.00
HETATM	380	N3	DC3	12	9.086	-12.188	28.913	0.00	0.00

HETATM	381	C2	DC3	12	8.097	-11.723	29.758	0.00	0.00
HETATM	382	O2	DC3	12	7.092	-12.418	29.918	0.00	0.00
HETATM	383	C3*	DC3	12	6.485	-8.620	32.996	0.00	0.00
HETATM	384	C2*	DC3	12	7.535	-9.648	32.644	0.00	0.00
HETATM	385	O3*	DC3	12	5.278	-9.326	33.304	0.00	0.00
HETATM	386	H5*	DC3	12	6.874	-6.034	30.672	0.00	0.00
HETATM	387	'H5*	DC3	12	6.468	-5.810	32.390	0.00	0.00
HETATM	388	H4*	DC3	12	5.206	-7.694	31.496	0.00	0.00
HETATM	389	H1*	DC3	12	6.308	-10.578	31.136	0.00	0.00
HETATM	390	H6	DC3	12	9.516	-8.834	30.760	0.00	0.00
HETATM	391	H5	DC3	12	11.346	-9.676	29.306	0.00	0.00
HETATM	392	H41	DC3	12	11.916	-11.380	27.590	0.00	0.00
HETATM	393	H42	DC3	12	10.972	-12.833	27.387	0.00	0.00
HETATM	394	H3*	DC3	12	6.738	-7.994	33.856	0.00	0.00
HETATM	395	H2*	DC3	12	7.493	-10.561	33.247	0.00	0.00
HETATM	396	'H2*	DC3	12	8.531	-9.208	32.757	0.00	0.00
HETATM	397	'HO3	DC3	12	5.407	-9.737	34.178	0.00	0.00
TER	398		DC3	12					
HETATM	399	O5*	DG5	13	6.757	-20.608	21.392	0.00	0.00
HETATM	400	C5*	DG5	13	5.810	-21.001	22.380	0.00	0.00
HETATM	401	C4*	DG5	13	5.540	-19.876	23.372	0.00	0.00
HETATM	402	O4*	DG5	13	6.769	-19.445	23.992	0.00	0.00
HETATM	403	C1*	DG5	13	6.422	-18.195	24.635	0.00	0.00
HETATM	404	N9	DG5	13	7.604	-17.398	24.902	0.00	0.00
HETATM	405	C8	DG5	13	8.848	-17.518	24.333	0.00	0.00
HETATM	406	N7	DG5	13	9.712	-16.647	24.824	0.00	0.00
HETATM	407	C5	DG5	13	8.987	-15.928	25.739	0.00	0.00
HETATM	408	C6	DG5	13	9.390	-14.838	26.603	0.00	0.00
HETATM	409	O6	DG5	13	10.520	-14.355	26.693	0.00	0.00
HETATM	410	N1	DG5	13	8.324	-14.376	27.365	0.00	0.00
HETATM	411	C2	DG5	13	7.038	-14.904	27.346	0.00	0.00
HETATM	412	N2	DG5	13	6.159	-14.288	28.174	0.00	0.00
HETATM	413	N3	DG5	13	6.675	-15.905	26.584	0.00	0.00
HETATM	414	C4	DG5	13	7.682	-16.369	25.804	0.00	0.00
HETATM	415	C3*	DG5	13	4.956	-18.611	22.758	0.00	0.00
HETATM	416	C2*	DG5	13	5.383	-17.530	23.737	0.00	0.00

HETATM	417	O3*	DG5	13	3.550	-18.741	22.655	0.00	0.00
HETATM	418	'HO5	DG5	13	7.531	-20.271	21.880	0.00	0.00
HETATM	419	H5*	DG5	13	6.228	-21.870	22.898	0.00	0.00
HETATM	420	'H5*	DG5	13	4.890	-21.308	21.873	0.00	0.00
HETATM	421	H4*	DG5	13	4.877	-20.267	24.157	0.00	0.00
HETATM	422	H1*	DG5	13	5.983	-18.450	25.608	0.00	0.00
HETATM	423	H8	DG5	13	9.068	-18.261	23.576	0.00	0.00
HETATM	424	1H	DG5	13	8.535	-13.582	27.973	0.00	0.00
HETATM	425	H21	DG5	13	5.176	-14.525	28.112	0.00	0.00
HETATM	426	H22	DG5	13	6.448	-13.575	28.855	0.00	0.00
HETATM	427	H3*	DG5	13	5.396	-18.423	21.772	0.00	0.00
HETATM	428	H2*	DG5	13	4.552	-17.143	24.335	0.00	0.00
HETATM	429	'H2*	DG5	13	5.812	-16.686	23.186	0.00	0.00
ATOM	430	P	DA	14	2.695	-17.678	21.755	0.00	0.00
ATOM	431	OP1	DA	14	1.520	-18.414	21.162	0.00	0.00
ATOM	432	OP2	DA	14	3.649	-16.871	20.905	0.00	0.00
ATOM	433	O5'	DA	14	2.149	-16.690	22.932	0.00	0.00
ATOM	434	C5'	DA	14	1.292	-17.218	23.930	0.00	0.00
ATOM	435	C4'	DA	14	0.901	-16.135	24.948	0.00	0.00
ATOM	436	O4'	DA	14	2.111	-15.556	25.499	0.00	0.00
ATOM	437	C1'	DA	14	2.171	-14.165	25.118	0.00	0.00
ATOM	438	N9	DA	14	3.532	-13.821	24.740	0.00	0.00
ATOM	439	C8	DA	14	4.234	-14.305	23.666	0.00	0.00
ATOM	440	N7	DA	14	5.454	-13.813	23.593	0.00	0.00
ATOM	441	C5	DA	14	5.530	-12.927	24.644	0.00	0.00
ATOM	442	C6	DA	14	6.553	-12.052	25.058	0.00	0.00
ATOM	443	N6	DA	14	7.754	-11.983	24.388	0.00	0.00
ATOM	444	N1	DA	14	6.319	-11.237	26.121	0.00	0.00
ATOM	445	C2	DA	14	5.120	-11.356	26.749	0.00	0.00
ATOM	446	N3	DA	14	4.098	-12.193	26.471	0.00	0.00
ATOM	447	C4	DA	14	4.357	-12.931	25.381	0.00	0.00
ATOM	448	C3'	DA	14	0.078	-14.978	24.370	0.00	0.00
ATOM	449	C2'	DA	14	1.137	-13.958	24.020	0.00	0.00
ATOM	450	O3'	DA	14	-0.784	-14.497	25.407	0.00	0.00
ATOM	451	H5'	DA	14	1.829	-18.017	24.452	0.00	0.00
ATOM	452	'H5'	DA	14	0.396	-17.641	23.465	0.00	0.00

ATOM	453	H4'	DA	14	0.366	-16.615	25.775	0.00	0.00
ATOM	454	H1'	DA	14	1.908	-13.581	26.006	0.00	0.00
ATOM	455	H8	DA	14	3.817	-15.009	22.960	0.00	0.00
ATOM	456	1H6	DA	14	8.528	-11.373	24.673	0.00	0.00
ATOM	457	2H6	DA	14	7.870	-12.566	23.569	0.00	0.00
ATOM	458	H2	DA	14	4.962	-10.681	27.587	0.00	0.00
ATOM	459	H3'	DA	14	-0.536	-15.288	23.519	0.00	0.00
ATOM	460	H2'	DA	14	0.782	-12.928	23.995	0.00	0.00
ATOM	461	'H2'	DA	14	1.545	-14.179	23.029	0.00	0.00
ATOM	462	P	DT	15	-1.848	-13.296	25.093	0.00	0.00
ATOM	463	OP1	DT	15	-3.016	-13.433	26.048	0.00	0.00
ATOM	464	OP2	DT	15	-2.064	-13.231	23.598	0.00	0.00
ATOM	465	O5'	DT	15	-0.955	-11.999	25.561	0.00	0.00
ATOM	466	C5'	DT	15	-0.627	-11.919	26.945	0.00	0.00
ATOM	467	C4'	DT	15	0.166	-10.659	27.318	0.00	0.00
ATOM	468	O4'	DT	15	1.446	-10.659	26.643	0.00	0.00
ATOM	469	C1'	DT	15	1.631	-9.354	26.063	0.00	0.00
ATOM	470	N1	DT	15	2.525	-9.467	24.919	0.00	0.00
ATOM	471	C6	DT	15	2.151	-10.209	23.817	0.00	0.00
ATOM	472	C5	DT	15	2.938	-10.379	22.750	0.00	0.00
ATOM	473	C7	DT	15	2.570	-11.174	21.542	0.00	0.00
ATOM	474	C4	DT	15	4.264	-9.730	22.779	0.00	0.00
ATOM	475	O4	DT	15	5.060	-9.827	21.847	0.00	0.00
ATOM	476	N3	DT	15	4.573	-9.008	23.896	0.00	0.00
ATOM	477	C2	DT	15	3.764	-8.834	24.990	0.00	0.00
ATOM	478	O2	DT	15	4.193	-8.190	25.946	0.00	0.00
ATOM	479	C3'	DT	15	-0.517	-9.326	26.990	0.00	0.00
ATOM	480	C2'	DT	15	0.227	-8.851	25.763	0.00	0.00
ATOM	481	O3'	DT	15	-0.261	-8.435	28.084	0.00	0.00
ATOM	482	H5'	DT	15	-0.032	-12.801	27.205	0.00	0.00
ATOM	483	'H5'	DT	15	-1.551	-11.941	27.532	0.00	0.00
ATOM	484	H4'	DT	15	0.386	-10.717	28.392	0.00	0.00
ATOM	485	H1'	DT	15	2.090	-8.728	26.837	0.00	0.00
ATOM	486	H6	DT	15	1.169	-10.670	23.855	0.00	0.00
ATOM	487	1H7	DT	15	1.566	-11.603	21.628	0.00	0.00
ATOM	488	2H7	DT	15	2.586	-10.542	20.648	0.00	0.00

ATOM	489	3H7	DT	15	3.274	-12.000	21.397	0.00	0.00
ATOM	490	H3	DT	15	5.477	-8.547	23.951	0.00	0.00
ATOM	491	H3'	DT	15	-1.595	-9.435	26.849	0.00	0.00
ATOM	492	H2'	DT	15	0.211	-7.772	25.603	0.00	0.00
ATOM	493	'H2'	DT	15	-0.207	-9.328	24.879	0.00	0.00
ATOM	494	P	DG	16	-1.085	-7.030	28.189	0.00	0.00
ATOM	495	OP1	DG	16	-1.101	-6.605	29.642	0.00	0.00
ATOM	496	OP2	DG	16	-2.353	-7.168	27.384	0.00	0.00
ATOM	497	O5'	DG	16	-0.048	-6.059	27.379	0.00	0.00
ATOM	498	C5'	DG	16	1.166	-5.726	28.036	0.00	0.00
ATOM	499	C4'	DG	16	2.068	-4.865	27.156	0.00	0.00
ATOM	500	O4'	DG	16	2.591	-5.658	26.056	0.00	0.00
ATOM	501	C1'	DG	16	2.591	-4.788	24.909	0.00	0.00
ATOM	502	N9	DG	16	2.748	-5.548	23.691	0.00	0.00
ATOM	503	C8	DG	16	1.844	-6.411	23.123	0.00	0.00
ATOM	504	N7	DG	16	2.273	-6.907	21.977	0.00	0.00
ATOM	505	C5	DG	16	3.515	-6.357	21.822	0.00	0.00
ATOM	506	C6	DG	16	4.485	-6.556	20.775	0.00	0.00
ATOM	507	O6	DG	16	4.345	-7.312	19.814	0.00	0.00
ATOM	508	N1	DG	16	5.634	-5.809	20.994	0.00	0.00
ATOM	509	C2	DG	16	5.848	-4.969	22.080	0.00	0.00
ATOM	510	N2	DG	16	7.027	-4.295	22.078	0.00	0.00
ATOM	511	N3	DG	16	4.978	-4.806	23.042	0.00	0.00
ATOM	512	C4	DG	16	3.840	-5.522	22.866	0.00	0.00
ATOM	513	C3'	DG	16	1.380	-3.653	26.523	0.00	0.00
ATOM	514	C2'	DG	16	1.290	-4.024	25.056	0.00	0.00
ATOM	515	O3'	DG	16	2.273	-2.543	26.618	0.00	0.00
ATOM	516	H5'	DG	16	1.687	-6.651	28.306	0.00	0.00
ATOM	517	'H5'	DG	16	0.928	-5.173	28.951	0.00	0.00
ATOM	518	H4'	DG	16	2.936	-4.557	27.753	0.00	0.00
ATOM	519	H1'	DG	16	3.455	-4.118	24.997	0.00	0.00
ATOM	520	H8	DG	16	0.891	-6.637	23.583	0.00	0.00
ATOM	521	1H	DG	16	6.360	-5.922	20.284	0.00	0.00
ATOM	522	H21	DG	16	7.264	-3.676	22.849	0.00	0.00
ATOM	523	H22	DG	16	7.713	-4.384	21.312	0.00	0.00
ATOM	524	H3'	DG	16	0.419	-3.402	26.982	0.00	0.00

ATOM	525	H2 '	DG	16	1.240	-3.177	24.368	0.00	0.00
ATOM	526	'H2 '	DG	16	0.419	-4.668	24.892	0.00	0.00
ATOM	527	P	DG	17	1.594	-1.069	26.685	0.00	0.00
ATOM	528	OP1	DG	17	1.157	-0.819	28.108	0.00	0.00
ATOM	529	OP2	DG	17	0.628	-0.954	25.528	0.00	0.00
ATOM	530	O5 '	DG	17	2.885	-0.151	26.291	0.00	0.00
ATOM	531	C5 '	DG	17	4.036	-0.131	27.113	0.00	0.00
ATOM	532	C4 '	DG	17	5.278	0.318	26.315	0.00	0.00
ATOM	533	O4 '	DG	17	5.567	-0.685	25.303	0.00	0.00
ATOM	534	C1 '	DG	17	5.532	-0.052	24.003	0.00	0.00
ATOM	535	N9	DG	17	4.918	-0.944	23.027	0.00	0.00
ATOM	536	C8	DG	17	3.668	-1.515	23.154	0.00	0.00
ATOM	537	N7	DG	17	3.324	-2.234	22.103	0.00	0.00
ATOM	538	C5	DG	17	4.421	-2.155	21.284	0.00	0.00
ATOM	539	C6	DG	17	4.650	-2.778	20.001	0.00	0.00
ATOM	540	O6	DG	17	3.900	-3.560	19.415	0.00	0.00
ATOM	541	N1	DG	17	5.870	-2.409	19.454	0.00	0.00
ATOM	542	C2	DG	17	6.798	-1.574	20.056	0.00	0.00
ATOM	543	N2	DG	17	7.909	-1.335	19.306	0.00	0.00
ATOM	544	N3	DG	17	6.622	-1.046	21.245	0.00	0.00
ATOM	545	C4	DG	17	5.421	-1.359	21.814	0.00	0.00
ATOM	546	C3 '	DG	17	5.130	1.664	25.591	0.00	0.00
ATOM	547	C2 '	DG	17	4.772	1.255	24.183	0.00	0.00
ATOM	548	O3 '	DG	17	6.392	2.340	25.594	0.00	0.00
ATOM	549	H5 '	DG	17	4.210	-1.133	27.518	0.00	0.00
ATOM	550	'H5 '	DG	17	3.854	0.557	27.945	0.00	0.00
ATOM	551	H4 '	DG	17	6.137	0.334	26.996	0.00	0.00
ATOM	552	H1 '	DG	17	6.569	0.130	23.699	0.00	0.00
ATOM	553	H8	DG	17	3.050	-1.357	24.029	0.00	0.00
ATOM	554	1H	DG	17	6.082	-2.795	18.536	0.00	0.00
ATOM	555	H21	DG	17	8.575	-0.652	19.646	0.00	0.00
ATOM	556	H22	DG	17	8.129	-1.821	18.423	0.00	0.00
ATOM	557	H3 '	DG	17	4.373	2.294	26.065	0.00	0.00
ATOM	558	H2 '	DG	17	5.048	1.983	23.423	0.00	0.00
ATOM	559	'H2 '	DG	17	3.689	1.102	24.111	0.00	0.00
ATOM	560	P	DC	18	6.439	3.962	25.374	0.00	0.00

ATOM	561	OP1	DC	18	7.784	4.474	25.852	0.00	0.00
ATOM	562	OP2	DC	18	5.160	4.554	25.916	0.00	0.00
ATOM	563	O5'	DC	18	6.414	4.020	23.745	0.00	0.00
ATOM	564	C5'	DC	18	7.640	3.718	23.091	0.00	0.00
ATOM	565	C4'	DC	18	7.436	3.522	21.599	0.00	0.00
ATOM	566	O4'	DC	18	6.667	2.329	21.347	0.00	0.00
ATOM	567	C1'	DC	18	6.254	2.446	19.974	0.00	0.00
ATOM	568	N1	DC	18	5.064	1.658	19.697	0.00	0.00
ATOM	569	C6	DC	18	3.980	1.681	20.543	0.00	0.00
ATOM	570	C5	DC	18	2.916	0.910	20.321	0.00	0.00
ATOM	571	C4	DC	18	2.996	0.017	19.145	0.00	0.00
ATOM	572	N4	DC	18	1.994	-0.871	18.889	0.00	0.00
ATOM	573	N3	DC	18	3.999	0.023	18.316	0.00	0.00
ATOM	574	C2	DC	18	5.043	0.900	18.528	0.00	0.00
ATOM	575	O2	DC	18	5.923	0.987	17.669	0.00	0.00
ATOM	576	C3'	DC	18	6.675	4.638	20.893	0.00	0.00
ATOM	577	C2'	DC	18	6.077	3.928	19.699	0.00	0.00
ATOM	578	O3'	DC	18	7.543	5.694	20.519	0.00	0.00
ATOM	579	H5'	DC	18	8.059	2.804	23.526	0.00	0.00
ATOM	580	'H5'	DC	18	8.335	4.547	23.262	0.00	0.00
ATOM	581	H4'	DC	18	8.425	3.382	21.140	0.00	0.00
ATOM	582	H1'	DC	18	7.093	2.069	19.375	0.00	0.00
ATOM	583	H6	DC	18	4.025	2.357	21.390	0.00	0.00
ATOM	584	H5	DC	18	2.049	0.887	20.964	0.00	0.00
ATOM	585	H41	DC	18	1.222	-1.012	19.526	0.00	0.00
ATOM	586	H42	DC	18	2.024	-1.427	18.024	0.00	0.00
ATOM	587	H3'	DC	18	5.875	5.033	21.530	0.00	0.00
ATOM	588	H2'	DC	18	6.562	4.178	18.756	0.00	0.00
ATOM	589	'H2'	DC	18	5.021	4.203	19.617	0.00	0.00
ATOM	590	P	DG	19	6.934	7.006	19.755	0.00	0.00
ATOM	591	OP1	DG	19	7.872	8.166	19.983	0.00	0.00
ATOM	592	OP2	DG	19	5.455	7.127	20.044	0.00	0.00
ATOM	593	O5'	DG	19	7.075	6.546	18.194	0.00	0.00
ATOM	594	C5'	DG	19	8.361	6.222	17.683	0.00	0.00
ATOM	595	C4'	DG	19	8.270	5.718	16.230	0.00	0.00
ATOM	596	O4'	DG	19	7.370	4.579	16.206	0.00	0.00

ATOM	597	C1'	DG	19	6.272	4.895	15.326	0.00	0.00
ATOM	598	N9	DG	19	5.044	4.358	15.889	0.00	0.00
ATOM	599	C8	DG	19	4.429	4.784	17.044	0.00	0.00
ATOM	600	N7	DG	19	3.331	4.106	17.322	0.00	0.00
ATOM	601	C5	DG	19	3.231	3.213	16.291	0.00	0.00
ATOM	602	C6	DG	19	2.181	2.264	16.003	0.00	0.00
ATOM	603	O6	DG	19	1.170	2.075	16.681	0.00	0.00
ATOM	604	N1	DG	19	2.397	1.613	14.799	0.00	0.00
ATOM	605	C2	DG	19	3.479	1.827	13.956	0.00	0.00
ATOM	606	N2	DG	19	3.475	1.080	12.823	0.00	0.00
ATOM	607	N3	DG	19	4.433	2.685	14.215	0.00	0.00
ATOM	608	C4	DG	19	4.261	3.351	15.384	0.00	0.00
ATOM	609	C3'	DG	19	7.737	6.754	15.229	0.00	0.00
ATOM	610	C2'	DG	19	6.274	6.403	15.124	0.00	0.00
ATOM	611	O3'	DG	19	8.372	6.571	13.953	0.00	0.00
ATOM	612	H5'	DG	19	8.790	5.431	18.306	0.00	0.00
ATOM	613	'H5'	DG	19	9.009	7.103	17.739	0.00	0.00
ATOM	614	H4'	DG	19	9.259	5.357	15.923	0.00	0.00
ATOM	615	H1'	DG	19	6.465	4.384	14.375	0.00	0.00
ATOM	616	H8	DG	19	4.826	5.593	17.647	0.00	0.00
ATOM	617	1H	DG	19	1.679	0.939	14.533	0.00	0.00
ATOM	618	H21	DG	19	4.234	1.174	12.159	0.00	0.00
ATOM	619	H22	DG	19	2.741	0.391	12.601	0.00	0.00
ATOM	620	H3'	DG	19	7.914	7.772	15.582	0.00	0.00
ATOM	621	H2'	DG	19	5.824	6.671	14.169	0.00	0.00
ATOM	622	'H2'	DG	19	5.717	6.922	15.911	0.00	0.00
ATOM	623	P	DC	20	8.368	7.809	12.873	0.00	0.00
ATOM	624	OP1	DC	20	9.494	7.597	11.883	0.00	0.00
ATOM	625	OP2	DC	20	8.255	9.104	13.646	0.00	0.00
ATOM	626	O5'	DC	20	6.930	7.536	12.126	0.00	0.00
ATOM	627	C5'	DC	20	6.917	6.601	11.052	0.00	0.00
ATOM	628	C4'	DC	20	5.511	6.313	10.495	0.00	0.00
ATOM	629	O4'	DC	20	4.745	5.585	11.502	0.00	0.00
ATOM	630	C1'	DC	20	3.402	6.073	11.367	0.00	0.00
ATOM	631	N1	DC	20	2.577	5.740	12.515	0.00	0.00
ATOM	632	C6	DC	20	2.831	6.313	13.737	0.00	0.00

ATOM	633	C5	DC	20	2.059	6.070	14.789	0.00	0.00
ATOM	634	C4	DC	20	0.956	5.123	14.566	0.00	0.00
ATOM	635	N4	DC	20	0.150	4.802	15.611	0.00	0.00
ATOM	636	N3	DC	20	0.703	4.553	13.427	0.00	0.00
ATOM	637	C2	DC	20	1.513	4.842	12.345	0.00	0.00
ATOM	638	O2	DC	20	1.228	4.322	11.263	0.00	0.00
ATOM	639	C3'	DC	20	4.652	7.534	10.072	0.00	0.00
ATOM	640	C2'	DC	20	3.587	7.567	11.137	0.00	0.00
ATOM	641	O3'	DC	20	3.946	7.241	8.857	0.00	0.00
ATOM	642	H5'	DC	20	7.359	5.666	11.413	0.00	0.00
ATOM	643	'H5'	DC	20	7.539	6.999	10.244	0.00	0.00
ATOM	644	H4'	DC	20	5.624	5.629	9.644	0.00	0.00
ATOM	645	H1'	DC	20	2.977	5.601	10.473	0.00	0.00
ATOM	646	H6	DC	20	3.674	6.986	13.815	0.00	0.00
ATOM	647	H5	DC	20	2.226	6.505	15.764	0.00	0.00
ATOM	648	H41	DC	20	0.351	5.088	16.564	0.00	0.00
ATOM	649	H42	DC	20	-0.676	4.209	15.439	0.00	0.00
ATOM	650	H3'	DC	20	5.227	8.458	9.981	0.00	0.00
ATOM	651	H2'	DC	20	2.649	8.037	10.839	0.00	0.00
ATOM	652	'H2'	DC	20	3.982	8.087	12.015	0.00	0.00
ATOM	653	P	DC	21	3.588	8.428	7.790	0.00	0.00
ATOM	654	OP1	DC	21	3.056	7.772	6.532	0.00	0.00
ATOM	655	OP2	DC	21	4.776	9.361	7.754	0.00	0.00
ATOM	656	O5'	DC	21	2.360	9.206	8.552	0.00	0.00
ATOM	657	C5'	DC	21	1.031	8.715	8.396	0.00	0.00
ATOM	658	C4'	DC	21	-0.051	9.660	8.978	0.00	0.00
ATOM	659	O4'	DC	21	0.265	9.956	10.366	0.00	0.00
ATOM	660	C1'	DC	21	0.304	11.391	10.517	0.00	0.00
ATOM	661	N1	DC	21	1.260	11.777	11.559	0.00	0.00
ATOM	662	C6	DC	21	2.492	11.164	11.606	0.00	0.00
ATOM	663	C5	DC	21	3.386	11.462	12.544	0.00	0.00
ATOM	664	C4	DC	21	2.979	12.492	13.520	0.00	0.00
ATOM	665	N4	DC	21	3.852	12.827	14.517	0.00	0.00
ATOM	666	N3	DC	21	1.835	13.109	13.470	0.00	0.00
ATOM	667	C2	DC	21	0.918	12.787	12.481	0.00	0.00
ATOM	668	O2	DC	21	-0.171	13.363	12.433	0.00	0.00

ATOM	669	C3'	DC	21	-0.203	11.012	8.266	0.00	0.00
ATOM	670	C2'	DC	21	0.641	11.928	9.132	0.00	0.00
ATOM	671	O3'	DC	21	-1.531	11.546	8.364	0.00	0.00
ATOM	672	H5'	DC	21	0.983	7.753	8.917	0.00	0.00
ATOM	673	'H5'	DC	21	0.818	8.547	7.336	0.00	0.00
ATOM	674	H4'	DC	21	-0.998	9.114	8.982	0.00	0.00
ATOM	675	H1'	DC	21	-0.703	11.704	10.816	0.00	0.00
ATOM	676	H6	DC	21	2.714	10.427	10.841	0.00	0.00
ATOM	677	H5	DC	21	4.367	11.009	12.598	0.00	0.00
ATOM	678	H41	DC	21	4.720	12.325	14.665	0.00	0.00
ATOM	679	H42	DC	21	3.627	13.603	15.129	0.00	0.00
ATOM	680	H3'	DC	21	0.102	11.007	7.216	0.00	0.00
ATOM	681	H2'	DC	21	0.389	12.989	9.040	0.00	0.00
ATOM	682	'H2'	DC	21	1.703	11.800	8.897	0.00	0.00
ATOM	683	P	DG	22	-2.790	10.873	7.574	0.00	0.00
ATOM	684	OP1	DG	22	-2.259	9.893	6.555	0.00	0.00
ATOM	685	OP2	DG	22	-3.771	11.969	7.216	0.00	0.00
ATOM	686	O5'	DG	22	-3.409	10.010	8.815	0.00	0.00
ATOM	687	C5'	DG	22	-4.744	9.535	8.683	0.00	0.00
ATOM	688	C4'	DG	22	-4.842	8.095	9.203	0.00	0.00
ATOM	689	O4'	DG	22	-4.610	8.063	10.644	0.00	0.00
ATOM	690	C1'	DG	22	-5.871	7.781	11.305	0.00	0.00
ATOM	691	N9	DG	22	-5.953	8.540	12.535	0.00	0.00
ATOM	692	C8	DG	22	-5.208	9.654	12.850	0.00	0.00
ATOM	693	N7	DG	22	-5.409	10.060	14.088	0.00	0.00
ATOM	694	C5	DG	22	-6.389	9.233	14.555	0.00	0.00
ATOM	695	C6	DG	22	-7.025	9.220	15.851	0.00	0.00
ATOM	696	O6	DG	22	-6.694	9.910	16.812	0.00	0.00
ATOM	697	N1	DG	22	-8.001	8.238	15.921	0.00	0.00
ATOM	698	C2	DG	22	-8.266	7.291	14.932	0.00	0.00
ATOM	699	N2	DG	22	-9.245	6.404	15.233	0.00	0.00
ATOM	700	N3	DG	22	-7.625	7.251	13.787	0.00	0.00
ATOM	701	C4	DG	22	-6.732	8.265	13.634	0.00	0.00
ATOM	702	C3'	DG	22	-6.236	7.495	9.005	0.00	0.00
ATOM	703	C2'	DG	22	-6.952	7.973	10.258	0.00	0.00
ATOM	704	O3'	DG	22	-6.089	6.081	9.088	0.00	0.00

ATOM	705	H5'	DG	22	-5.051	9.571	7.633	0.00	0.00
ATOM	706	'H5'	DG	22	-5.380	10.211	9.261	0.00	0.00
ATOM	707	H4'	DG	22	-4.058	7.480	8.747	0.00	0.00
ATOM	708	H1'	DG	22	-5.849	6.729	11.601	0.00	0.00
ATOM	709	H8	DG	22	-4.515	10.103	12.147	0.00	0.00
ATOM	710	1H	DG	22	-8.545	8.226	16.788	0.00	0.00
ATOM	711	H21	DG	22	-9.505	5.683	14.568	0.00	0.00
ATOM	712	H22	DG	22	-9.763	6.444	16.127	0.00	0.00
ATOM	713	H3'	DG	22	-6.727	7.792	8.075	0.00	0.00
ATOM	714	H2'	DG	22	-7.837	7.383	10.500	0.00	0.00
ATOM	715	'H2'	DG	22	-7.236	9.027	10.170	0.00	0.00
ATOM	716	P	DA	23	-6.592	5.041	7.941	0.00	0.00
ATOM	717	OP1	DA	23	-5.725	3.800	8.175	0.00	0.00
ATOM	718	OP2	DA	23	-6.618	5.724	6.599	0.00	0.00
ATOM	719	O5'	DA	23	-8.095	4.754	8.505	0.00	0.00
ATOM	720	C5'	DA	23	-9.199	5.570	8.092	0.00	0.00
ATOM	721	C4'	DA	23	-10.378	5.347	9.062	0.00	0.00
ATOM	722	O4'	DA	23	-10.117	6.105	10.279	0.00	0.00
ATOM	723	C1'	DA	23	-11.327	6.804	10.645	0.00	0.00
ATOM	724	N9	DA	23	-10.978	7.955	11.462	0.00	0.00
ATOM	725	C8	DA	23	-10.203	9.020	11.075	0.00	0.00
ATOM	726	N7	DA	23	-9.990	9.875	12.055	0.00	0.00
ATOM	727	C5	DA	23	-10.710	9.373	13.121	0.00	0.00
ATOM	728	C6	DA	23	-10.891	9.840	14.442	0.00	0.00
ATOM	729	N6	DA	23	-10.259	10.965	14.932	0.00	0.00
ATOM	730	N1	DA	23	-11.701	9.130	15.270	0.00	0.00
ATOM	731	C2	DA	23	-12.260	7.993	14.789	0.00	0.00
ATOM	732	N3	DA	23	-12.123	7.437	13.566	0.00	0.00
ATOM	733	C4	DA	23	-11.342	8.187	12.769	0.00	0.00
ATOM	734	C3'	DA	23	-11.761	5.809	8.545	0.00	0.00
ATOM	735	C2'	DA	23	-12.001	7.098	9.313	0.00	0.00
ATOM	736	O3'	DA	23	-12.716	4.812	8.924	0.00	0.00
ATOM	737	H5'	DA	23	-9.471	5.261	7.079	0.00	0.00
ATOM	738	'H5'	DA	23	-8.893	6.620	8.088	0.00	0.00
ATOM	739	H4'	DA	23	-10.405	4.291	9.357	0.00	0.00
ATOM	740	H1'	DA	23	-11.931	6.123	11.255	0.00	0.00

ATOM	741	H8	DA	23	-9.809	9.114	10.071	0.00	0.00
ATOM	742	1H6	DA	23	-10.410	11.233	15.915	0.00	0.00
ATOM	743	2H6	DA	23	-9.658	11.503	14.324	0.00	0.00
ATOM	744	H2	DA	23	-12.905	7.456	15.476	0.00	0.00
ATOM	745	H3'	DA	23	-11.782	5.932	7.459	0.00	0.00
ATOM	746	H2'	DA	23	-13.051	7.369	9.436	0.00	0.00
ATOM	747	'H2'	DA	23	-11.496	7.920	8.791	0.00	0.00
HETATM	748	P	DG3	24	-14.230	4.794	8.312	0.00	0.00
HETATM	749	OP1	DG3	24	-14.772	3.383	8.419	0.00	0.00
HETATM	750	OP2	DG3	24	-14.262	5.555	7.007	0.00	0.00
HETATM	751	O5*	DG3	24	-14.986	5.707	9.432	0.00	0.00
HETATM	752	C5*	DG3	24	-15.051	5.173	10.746	0.00	0.00
HETATM	753	C4*	DG3	24	-15.515	6.223	11.735	0.00	0.00
HETATM	754	O4*	DG3	24	-14.654	7.383	11.752	0.00	0.00
HETATM	755	C1*	DG3	24	-15.401	8.312	12.563	0.00	0.00
HETATM	756	N9	DG3	24	-14.842	9.644	12.500	0.00	0.00
HETATM	757	C8	DG3	24	-14.351	10.297	11.398	0.00	0.00
HETATM	758	N7	DG3	24	-13.951	11.525	11.683	0.00	0.00
HETATM	759	C5	DG3	24	-14.176	11.650	13.032	0.00	0.00
HETATM	760	C6	DG3	24	-13.963	12.770	13.925	0.00	0.00
HETATM	761	O6	DG3	24	-13.574	13.892	13.598	0.00	0.00
HETATM	762	N1	DG3	24	-14.324	12.470	15.233	0.00	0.00
HETATM	763	C2	DG3	24	-14.853	11.256	15.653	0.00	0.00
HETATM	764	N2	DG3	24	-15.123	11.173	16.979	0.00	0.00
HETATM	765	N3	DG3	24	-15.085	10.256	14.841	0.00	0.00
HETATM	766	C4	DG3	24	-14.725	10.503	13.559	0.00	0.00
HETATM	767	C3*	DG3	24	-16.900	6.798	11.461	0.00	0.00
HETATM	768	C2*	DG3	24	-16.840	8.195	12.068	0.00	0.00
HETATM	769	O3*	DG3	24	-17.908	6.012	12.081	0.00	0.00
HETATM	770	H5*	DG3	24	-14.057	4.822	11.039	0.00	0.00
HETATM	771	'H5*	DG3	24	-15.739	4.321	10.749	0.00	0.00
HETATM	772	H4*	DG3	24	-15.485	5.764	12.734	0.00	0.00
HETATM	773	H1*	DG3	24	-15.325	7.968	13.603	0.00	0.00
HETATM	774	H8	DG3	24	-14.324	9.835	10.418	0.00	0.00
HETATM	775	1H	DG3	24	-14.187	13.225	15.906	0.00	0.00
HETATM	776	H21	DG3	24	-15.473	10.310	17.380	0.00	0.00

HETATM	777	H22	DG3	24	-14.966	11.949	17.635	0.00	0.00
HETATM	778	H3*	DG3	24	-17.115	6.860	10.388	0.00	0.00
HETATM	779	H2*	DG3	24	-17.559	8.360	12.877	0.00	0.00
HETATM	780	'H2*	DG3	24	-17.049	8.937	11.288	0.00	0.00
HETATM	781	'HO3	DG3	24	-18.768	6.331	11.757	0.00	0.00
TER	782		DG3	24					
CONNECT	1	17	2						
CONNECT	2	1	18	19	3				
CONNECT	3	2	20	4	14				
CONNECT	4	3	5						
CONNECT	5	4	21	6	15				
CONNECT	6	5	7	12					
CONNECT	7	6	22	8	8				
CONNECT	8	7	7	23	9				
CONNECT	9	8	10	11	11				
CONNECT	10	9	24	25					
CONNECT	11	9	9	12					
CONNECT	12	6	11	13	13				
CONNECT	13	12	12						
CONNECT	14	3	26	15	16				
CONNECT	15	5	14	27	28				
CONNECT	16	14	29						
CONNECT	17	1							
CONNECT	18	2							
CONNECT	19	2							
CONNECT	20	3							
CONNECT	21	5							
CONNECT	22	7							
CONNECT	23	8							
CONNECT	24	10							
CONNECT	25	10							
CONNECT	26	14							
CONNECT	27	15							
CONNECT	28	15							
CONNECT	29	16	30	31	32				
CONNECT	30	29							

CONNECT	31	29			
CONNECT	32	29	33		
CONNECT	33	32	49	50	34
CONNECT	34	33	51	35	46
CONNECT	35	34	36		
CONNECT	36	35	52	37	47
CONNECT	37	36	38	44	
CONNECT	38	37	53	39	39
CONNECT	39	38	38	40	41
CONNECT	40	39	54	55	56
CONNECT	41	39	42	42	43
CONNECT	42	41	41		
CONNECT	43	41	57	44	
CONNECT	44	37	43	45	45
CONNECT	45	44	44		
CONNECT	46	34	58	47	48
CONNECT	47	36	46	59	60
CONNECT	48	46			
CONNECT	49	33			
CONNECT	50	33			
CONNECT	51	34			
CONNECT	52	36			
CONNECT	53	38			
CONNECT	54	40			
CONNECT	55	40			
CONNECT	56	40			
CONNECT	57	43			
CONNECT	58	46			
CONNECT	59	47			
CONNECT	60	47			
CONNECT	61	62	63	64	
CONNECT	62	61			
CONNECT	63	61			
CONNECT	64	61	65		
CONNECT	65	64	80	81	66
CONNECT	66	65	82	67	77

CONNECT	67	66	68		
CONNECT	68	67	83	69	78
CONNECT	69	68	70	75	
CONNECT	70	69	84	71	71
CONNECT	71	70	70	85	72
CONNECT	72	71	73	74	74
CONNECT	73	72	86	87	
CONNECT	74	72	72	75	
CONNECT	75	69	74	76	76
CONNECT	76	75	75		
CONNECT	77	66	88	78	79
CONNECT	78	68	77	89	90
CONNECT	79	77	91		
CONNECT	80	65			
CONNECT	81	65			
CONNECT	82	66			
CONNECT	83	68			
CONNECT	84	70			
CONNECT	85	71			
CONNECT	86	73			
CONNECT	87	73			
CONNECT	88	77			
CONNECT	89	78			
CONNECT	90	78			
CONNECT	91	79	92	93	94
CONNECT	92	91			
CONNECT	93	91			
CONNECT	94	91	95		
CONNECT	95	94	128	129	96
CONNECT	96	95	130	97	125
CONNECT	97	96	98		
CONNECT	98	97	131	99	126
CONNECT	99	98	100	124	
CONNECT	100	99	132	101	101
CONNECT	101	100	100	102	
CONNECT	102	101	103	124	124

CONNECT	103	102	104	104	105
CONNECT	104	103	103		
CONNECT	105	103	133	106	
CONNECT	106	105	107	123	123
CONNECT	107	106	134	108	108
CONNECT	108	107	107	109	122
CONNECT	109	108	110	114	114
CONNECT	110	109	111	111	
CONNECT	111	110	110	135	112
CONNECT	112	111	136	113	113
CONNECT	113	112	112	137	114
CONNECT	114	109	109	113	115
CONNECT	115	114	116	116	121
CONNECT	116	115	115	117	
CONNECT	117	116	118	118	119
CONNECT	118	117	117	138	139
CONNECT	119	117	120	121	
CONNECT	120	119	140	141	142
CONNECT	121	115	119	122	122
CONNECT	122	108	121	121	143
CONNECT	123	106	106	124	
CONNECT	124	99	102	102	123
CONNECT	125	96	144	126	127
CONNECT	126	98	125	145	146
CONNECT	127	125	147		
CONNECT	128	95			
CONNECT	129	95			
CONNECT	130	96			
CONNECT	131	98			
CONNECT	132	100			
CONNECT	133	105			
CONNECT	134	107			
CONNECT	135	111			
CONNECT	136	112			
CONNECT	137	113			
CONNECT	138	118			

CONNECT	139	118			
CONNECT	140	120			
CONNECT	141	120			
CONNECT	142	120			
CONNECT	143	122			
CONNECT	144	125			
CONNECT	145	126			
CONNECT	146	126			
CONNECT	147	127	148	149	150
CONNECT	148	147			
CONNECT	149	147			
CONNECT	150	147	151		
CONNECT	151	150	169	170	152
CONNECT	152	151	171	153	166
CONNECT	153	152	154		
CONNECT	154	153	172	155	167
CONNECT	155	154	156	165	
CONNECT	156	155	173	157	157
CONNECT	157	156	156	158	
CONNECT	158	157	159	165	165
CONNECT	159	158	160	160	161
CONNECT	160	159	159		
CONNECT	161	159	174	162	
CONNECT	162	161	163	164	164
CONNECT	163	162	175	176	
CONNECT	164	162	162	165	
CONNECT	165	155	158	158	164
CONNECT	166	152	177	167	168
CONNECT	167	154	166	178	179
CONNECT	168	166			
CONNECT	169	151			
CONNECT	170	151			
CONNECT	171	152			
CONNECT	172	154			
CONNECT	173	156			
CONNECT	174	161			

CONNECT	175	163			
CONNECT	176	163			
CONNECT	177	166			
CONNECT	178	167			
CONNECT	179	167			
CONNECT	180	181	182	183	
CONNECT	181	180			
CONNECT	182	180			
CONNECT	183	180	184		
CONNECT	184	183	199	200	185
CONNECT	185	184	201	186	196
CONNECT	186	185	187		
CONNECT	187	186	202	188	197
CONNECT	188	187	189	194	
CONNECT	189	188	203	190	190
CONNECT	190	189	189	204	191
CONNECT	191	190	192	193	193
CONNECT	192	191	205	206	
CONNECT	193	191	191	194	
CONNECT	194	188	193	195	195
CONNECT	195	194	194		
CONNECT	196	185	207	197	198
CONNECT	197	187	196	208	209
CONNECT	198	196			
CONNECT	199	184			
CONNECT	200	184			
CONNECT	201	185			
CONNECT	202	187			
CONNECT	203	189			
CONNECT	204	190			
CONNECT	205	192			
CONNECT	206	192			
CONNECT	207	196			
CONNECT	208	197			
CONNECT	209	197			
CONNECT	210	211	212	213	

CONNECT	211	210			
CONNECT	212	210			
CONNECT	213	210	214		
CONNECT	214	213	232	233	215
CONNECT	215	214	234	216	229
CONNECT	216	215	217		
CONNECT	217	216	235	218	230
CONNECT	218	217	219	228	
CONNECT	219	218	236	220	220
CONNECT	220	219	219	221	
CONNECT	221	220	222	228	228
CONNECT	222	221	223	223	224
CONNECT	223	222	222		
CONNECT	224	222	237	225	
CONNECT	225	224	226	227	227
CONNECT	226	225	238	239	
CONNECT	227	225	225	228	
CONNECT	228	218	221	221	227
CONNECT	229	215	240	230	231
CONNECT	230	217	229	241	242
CONNECT	231	229			
CONNECT	232	214			
CONNECT	233	214			
CONNECT	234	215			
CONNECT	235	217			
CONNECT	236	219			
CONNECT	237	224			
CONNECT	238	226			
CONNECT	239	226			
CONNECT	240	229			
CONNECT	241	230			
CONNECT	242	230			
CONNECT	243	244	245	246	
CONNECT	244	243			
CONNECT	245	243			
CONNECT	246	243	247		

CONNECT	247	246	262	263	248
CONNECT	248	247	264	249	259
CONNECT	249	248	250		
CONNECT	250	249	265	251	260
CONNECT	251	250	252	257	
CONNECT	252	251	266	253	253
CONNECT	253	252	252	267	254
CONNECT	254	253	255	256	256
CONNECT	255	254	268	269	
CONNECT	256	254	254	257	
CONNECT	257	251	256	258	258
CONNECT	258	257	257		
CONNECT	259	248	270	260	261
CONNECT	260	250	259	271	272
CONNECT	261	259			
CONNECT	262	247			
CONNECT	263	247			
CONNECT	264	248			
CONNECT	265	250			
CONNECT	266	252			
CONNECT	267	253			
CONNECT	268	255			
CONNECT	269	255			
CONNECT	270	259			
CONNECT	271	260			
CONNECT	272	260			
CONNECT	273	274	275	276	
CONNECT	274	273			
CONNECT	275	273			
CONNECT	276	273	277		
CONNECT	277	276	292	293	278
CONNECT	278	277	294	279	289
CONNECT	279	278	280		
CONNECT	280	279	295	281	290
CONNECT	281	280	282	287	
CONNECT	282	281	296	283	283

CONNECT	283	282	282	297	284
CONNECT	284	283	285	286	286
CONNECT	285	284	298	299	
CONNECT	286	284	284	287	
CONNECT	287	281	286	288	288
CONNECT	288	287	287		
CONNECT	289	278	300	290	291
CONNECT	290	280	289	301	302
CONNECT	291	289			
CONNECT	292	277			
CONNECT	293	277			
CONNECT	294	278			
CONNECT	295	280			
CONNECT	296	282			
CONNECT	297	283			
CONNECT	298	285			
CONNECT	299	285			
CONNECT	300	289			
CONNECT	301	290			
CONNECT	302	290			
CONNECT	303	304	305	306	
CONNECT	304	303			
CONNECT	305	303			
CONNECT	306	303	307		
CONNECT	307	306	324	325	308
CONNECT	308	307	326	309	321
CONNECT	309	308	310		
CONNECT	310	309	327	311	322
CONNECT	311	310	312	320	
CONNECT	312	311	328	313	313
CONNECT	313	312	312	314	
CONNECT	314	313	315	320	320
CONNECT	315	314	316	317	317
CONNECT	316	315	329	330	
CONNECT	317	315	315	318	
CONNECT	318	317	331	319	319

CONNECT	319	318	318	320	
CONNECT	320	311	314	314	319
CONNECT	321	308	332	322	323
CONNECT	322	310	321	333	334
CONNECT	323	321			
CONNECT	324	307			
CONNECT	325	307			
CONNECT	326	308			
CONNECT	327	310			
CONNECT	328	312			
CONNECT	329	316			
CONNECT	330	316			
CONNECT	331	318			
CONNECT	332	321			
CONNECT	333	322			
CONNECT	334	322			
CONNECT	335	336	337	338	
CONNECT	336	335			
CONNECT	337	335			
CONNECT	338	335	339		
CONNECT	339	338	355	356	340
CONNECT	340	339	357	341	352
CONNECT	341	340	342		
CONNECT	342	341	358	343	353
CONNECT	343	342	344	350	
CONNECT	344	343	359	345	345
CONNECT	345	344	344	346	347
CONNECT	346	345	360	361	362
CONNECT	347	345	348	348	349
CONNECT	348	347	347		
CONNECT	349	347	363	350	
CONNECT	350	343	349	351	351
CONNECT	351	350	350		
CONNECT	352	340	364	353	354
CONNECT	353	342	352	365	366
CONNECT	354	352	367		

CONNECT	355	339			
CONNECT	356	339			
CONNECT	357	340			
CONNECT	358	342			
CONNECT	359	344			
CONNECT	360	346			
CONNECT	361	346			
CONNECT	362	346			
CONNECT	363	349			
CONNECT	364	352			
CONNECT	365	353			
CONNECT	366	353			
CONNECT	367	354	368	369	370
CONNECT	368	367			
CONNECT	369	367			
CONNECT	370	367	371		
CONNECT	371	370	386	387	372
CONNECT	372	371	388	373	383
CONNECT	373	372	374		
CONNECT	374	373	389	375	384
CONNECT	375	374	376	381	
CONNECT	376	375	390	377	377
CONNECT	377	376	376	391	378
CONNECT	378	377	379	380	380
CONNECT	379	378	392	393	
CONNECT	380	378	378	381	
CONNECT	381	375	380	382	382
CONNECT	382	381	381		
CONNECT	383	372	394	384	385
CONNECT	384	374	383	395	396
CONNECT	385	383	397		
CONNECT	386	371			
CONNECT	387	371			
CONNECT	388	372			
CONNECT	389	374			
CONNECT	390	376			

CONNECT	391	377			
CONNECT	392	379			
CONNECT	393	379			
CONNECT	394	383			
CONNECT	395	384			
CONNECT	396	384			
CONNECT	397	385			
CONNECT	399	418	400		
CONNECT	400	399	419	420	401
CONNECT	401	400	421	402	415
CONNECT	402	401	403		
CONNECT	403	402	422	404	416
CONNECT	404	403	405	414	
CONNECT	405	404	423	406	406
CONNECT	406	405	405	407	
CONNECT	407	406	408	414	414
CONNECT	408	407	409	409	410
CONNECT	409	408	408		
CONNECT	410	408	424	411	
CONNECT	411	410	412	413	413
CONNECT	412	411	425	426	
CONNECT	413	411	411	414	
CONNECT	414	404	407	407	413
CONNECT	415	401	427	416	417
CONNECT	416	403	415	428	429
CONNECT	417	415	430		
CONNECT	418	399			
CONNECT	419	400			
CONNECT	420	400			
CONNECT	421	401			
CONNECT	422	403			
CONNECT	423	405			
CONNECT	424	410			
CONNECT	425	412			
CONNECT	426	412			
CONNECT	427	415			

CONNECT	428	416			
CONNECT	429	416			
CONNECT	430	417	431	432	433
CONNECT	431	430			
CONNECT	432	430			
CONNECT	433	430	434		
CONNECT	434	433	451	452	435
CONNECT	435	434	453	436	448
CONNECT	436	435	437		
CONNECT	437	436	454	438	449
CONNECT	438	437	439	447	
CONNECT	439	438	455	440	440
CONNECT	440	439	439	441	
CONNECT	441	440	442	447	447
CONNECT	442	441	443	444	444
CONNECT	443	442	456	457	
CONNECT	444	442	442	445	
CONNECT	445	444	458	446	446
CONNECT	446	445	445	447	
CONNECT	447	438	441	441	446
CONNECT	448	435	459	449	450
CONNECT	449	437	448	460	461
CONNECT	450	448			
CONNECT	451	434			
CONNECT	452	434			
CONNECT	453	435			
CONNECT	454	437			
CONNECT	455	439			
CONNECT	456	443			
CONNECT	457	443			
CONNECT	458	445			
CONNECT	459	448			
CONNECT	460	449			
CONNECT	461	449			
CONNECT	462	463	464	465	
CONNECT	463	462			

CONNECT	464	462			
CONNECT	465	462	466		
CONNECT	466	465	482	483	467
CONNECT	467	466	484	468	479
CONNECT	468	467	469		
CONNECT	469	468	485	470	480
CONNECT	470	469	471	477	
CONNECT	471	470	486	472	472
CONNECT	472	471	471	473	474
CONNECT	473	472	487	488	489
CONNECT	474	472	475	475	476
CONNECT	475	474	474		
CONNECT	476	474	490	477	
CONNECT	477	470	476	478	478
CONNECT	478	477	477		
CONNECT	479	467	491	480	481
CONNECT	480	469	479	492	493
CONNECT	481	479			
CONNECT	482	466			
CONNECT	483	466			
CONNECT	484	467			
CONNECT	485	469			
CONNECT	486	471			
CONNECT	487	473			
CONNECT	488	473			
CONNECT	489	473			
CONNECT	490	476			
CONNECT	491	479			
CONNECT	492	480			
CONNECT	493	480			
CONNECT	494	495	496	497	
CONNECT	495	494			
CONNECT	496	494			
CONNECT	497	494	498		
CONNECT	498	497	516	517	499
CONNECT	499	498	518	500	513

CONECT	500	499	501		
CONECT	501	500	519	502	514
CONECT	502	501	503	512	
CONECT	503	502	520	504	504
CONECT	504	503	503	505	
CONECT	505	504	506	512	512
CONECT	506	505	507	507	508
CONECT	507	506	506		
CONECT	508	506	521	509	
CONECT	509	508	510	511	511
CONECT	510	509	522	523	
CONECT	511	509	509	512	
CONECT	512	502	505	505	511
CONECT	513	499	524	514	515
CONECT	514	501	513	525	526
CONECT	515	513			
CONECT	516	498			
CONECT	517	498			
CONECT	518	499			
CONECT	519	501			
CONECT	520	503			
CONECT	521	508			
CONECT	522	510			
CONECT	523	510			
CONECT	524	513			
CONECT	525	514			
CONECT	526	514			
CONECT	527	528	529	530	
CONECT	528	527			
CONECT	529	527			
CONECT	530	527	531		
CONECT	531	530	549	550	532
CONECT	532	531	551	533	546
CONECT	533	532	534		
CONECT	534	533	552	535	547
CONECT	535	534	536	545	

CONNECT	536	535	553	537	537
CONNECT	537	536	536	538	
CONNECT	538	537	539	545	545
CONNECT	539	538	540	540	541
CONNECT	540	539	539		
CONNECT	541	539	554	542	
CONNECT	542	541	543	544	544
CONNECT	543	542	555	556	
CONNECT	544	542	542	545	
CONNECT	545	535	538	538	544
CONNECT	546	532	557	547	548
CONNECT	547	534	546	558	559
CONNECT	548	546			
CONNECT	549	531			
CONNECT	550	531			
CONNECT	551	532			
CONNECT	552	534			
CONNECT	553	536			
CONNECT	554	541			
CONNECT	555	543			
CONNECT	556	543			
CONNECT	557	546			
CONNECT	558	547			
CONNECT	559	547			
CONNECT	560	561	562	563	
CONNECT	561	560			
CONNECT	562	560			
CONNECT	563	560	564		
CONNECT	564	563	579	580	565
CONNECT	565	564	581	566	576
CONNECT	566	565	567		
CONNECT	567	566	582	568	577
CONNECT	568	567	569	574	
CONNECT	569	568	583	570	570
CONNECT	570	569	569	584	571
CONNECT	571	570	572	573	573

CONNECT	572	571	585	586	
CONNECT	573	571	571	574	
CONNECT	574	568	573	575	575
CONNECT	575	574	574		
CONNECT	576	565	587	577	578
CONNECT	577	567	576	588	589
CONNECT	578	576			
CONNECT	579	564			
CONNECT	580	564			
CONNECT	581	565			
CONNECT	582	567			
CONNECT	583	569			
CONNECT	584	570			
CONNECT	585	572			
CONNECT	586	572			
CONNECT	587	576			
CONNECT	588	577			
CONNECT	589	577			
CONNECT	590	591	592	593	
CONNECT	591	590			
CONNECT	592	590			
CONNECT	593	590	594		
CONNECT	594	593	612	613	595
CONNECT	595	594	614	596	609
CONNECT	596	595	597		
CONNECT	597	596	615	598	610
CONNECT	598	597	599	608	
CONNECT	599	598	616	600	600
CONNECT	600	599	599	601	
CONNECT	601	600	602	608	608
CONNECT	602	601	603	603	604
CONNECT	603	602	602		
CONNECT	604	602	617	605	
CONNECT	605	604	606	607	607
CONNECT	606	605	618	619	
CONNECT	607	605	605	608	

CONECT	608	598	601	601	607
CONECT	609	595	620	610	611
CONECT	610	597	609	621	622
CONECT	611	609			
CONECT	612	594			
CONECT	613	594			
CONECT	614	595			
CONECT	615	597			
CONECT	616	599			
CONECT	617	604			
CONECT	618	606			
CONECT	619	606			
CONECT	620	609			
CONECT	621	610			
CONECT	622	610			
CONECT	623	624	625	626	
CONECT	624	623			
CONECT	625	623			
CONECT	626	623	627		
CONECT	627	626	642	643	628
CONECT	628	627	644	629	639
CONECT	629	628	630		
CONECT	630	629	645	631	640
CONECT	631	630	632	637	
CONECT	632	631	646	633	633
CONECT	633	632	632	647	634
CONECT	634	633	635	636	636
CONECT	635	634	648	649	
CONECT	636	634	634	637	
CONECT	637	631	636	638	638
CONECT	638	637	637		
CONECT	639	628	650	640	641
CONECT	640	630	639	651	652
CONECT	641	639			
CONECT	642	627			
CONECT	643	627			

CONNECT	644	628			
CONNECT	645	630			
CONNECT	646	632			
CONNECT	647	633			
CONNECT	648	635			
CONNECT	649	635			
CONNECT	650	639			
CONNECT	651	640			
CONNECT	652	640			
CONNECT	653	654	655	656	
CONNECT	654	653			
CONNECT	655	653			
CONNECT	656	653	657		
CONNECT	657	656	672	673	658
CONNECT	658	657	674	659	669
CONNECT	659	658	660		
CONNECT	660	659	675	661	670
CONNECT	661	660	662	667	
CONNECT	662	661	676	663	663
CONNECT	663	662	662	677	664
CONNECT	664	663	665	666	666
CONNECT	665	664	678	679	
CONNECT	666	664	664	667	
CONNECT	667	661	666	668	668
CONNECT	668	667	667		
CONNECT	669	658	680	670	671
CONNECT	670	660	669	681	682
CONNECT	671	669			
CONNECT	672	657			
CONNECT	673	657			
CONNECT	674	658			
CONNECT	675	660			
CONNECT	676	662			
CONNECT	677	663			
CONNECT	678	665			
CONNECT	679	665			

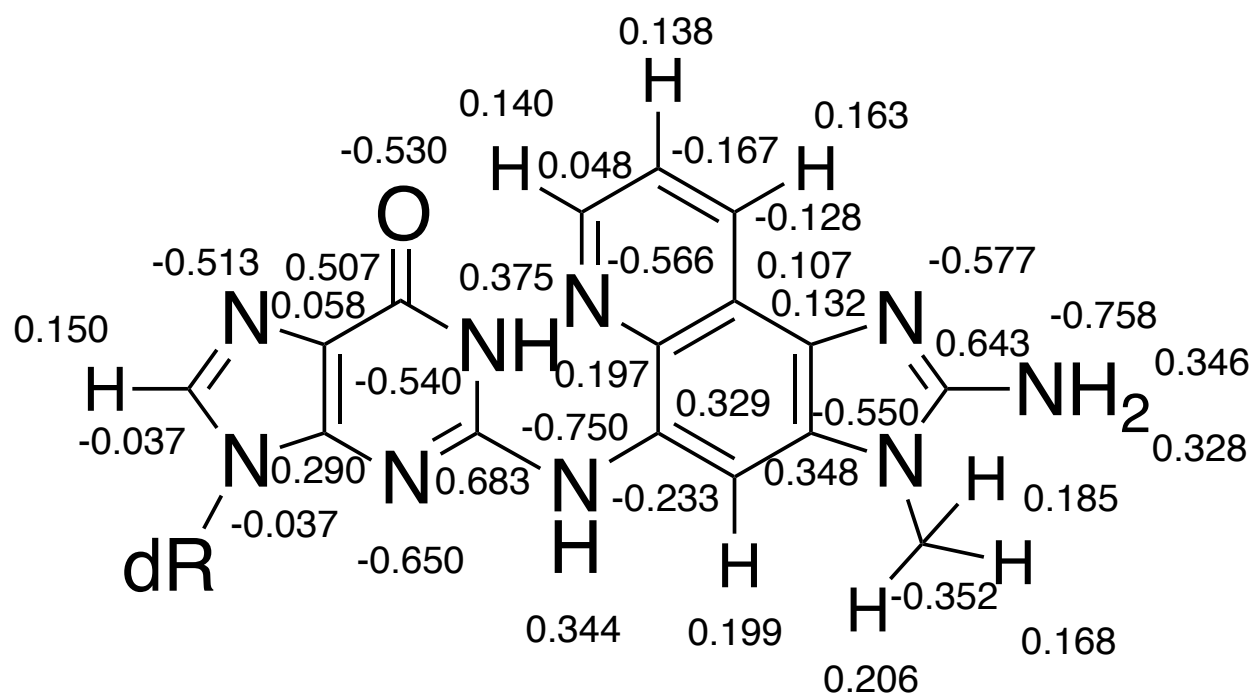
CONNECT	680	669			
CONNECT	681	670			
CONNECT	682	670			
CONNECT	683	684	685	686	
CONNECT	684	683			
CONNECT	685	683			
CONNECT	686	683	687		
CONNECT	687	686	705	706	688
CONNECT	688	687	707	689	702
CONNECT	689	688	690		
CONNECT	690	689	708	691	703
CONNECT	691	690	692	701	
CONNECT	692	691	709	693	693
CONNECT	693	692	692	694	
CONNECT	694	693	695	701	701
CONNECT	695	694	696	696	697
CONNECT	696	695	695		
CONNECT	697	695	710	698	
CONNECT	698	697	699	700	700
CONNECT	699	698	711	712	
CONNECT	700	698	698	701	
CONNECT	701	691	694	694	700
CONNECT	702	688	713	703	704
CONNECT	703	690	702	714	715
CONNECT	704	702			
CONNECT	705	687			
CONNECT	706	687			
CONNECT	707	688			
CONNECT	708	690			
CONNECT	709	692			
CONNECT	710	697			
CONNECT	711	699			
CONNECT	712	699			
CONNECT	713	702			
CONNECT	714	703			
CONNECT	715	703			

CONECT	716	717	718	719	
CONECT	717	716			
CONECT	718	716			
CONECT	719	716	720		
CONECT	720	719	737	738	721
CONECT	721	720	739	722	734
CONECT	722	721	723		
CONECT	723	722	740	724	735
CONECT	724	723	725	733	
CONECT	725	724	741	726	726
CONECT	726	725	725	727	
CONECT	727	726	728	733	733
CONECT	728	727	729	730	730
CONECT	729	728	742	743	
CONECT	730	728	728	731	
CONECT	731	730	744	732	732
CONECT	732	731	731	733	
CONECT	733	724	727	727	732
CONECT	734	721	745	735	736
CONECT	735	723	734	746	747
CONECT	736	734	748		
CONECT	737	720			
CONECT	738	720			
CONECT	739	721			
CONECT	740	723			
CONECT	741	725			
CONECT	742	729			
CONECT	743	729			
CONECT	744	731			
CONECT	745	734			
CONECT	746	735			
CONECT	747	735			
CONECT	748	736	749	750	751
CONECT	749	748			
CONECT	750	748			
CONECT	751	748	752		

CONNECT 752 751 770 771 753
CONNECT 753 752 772 754 767
CONNECT 754 753 755
CONNECT 755 754 773 756 768
CONNECT 756 755 757 766
CONNECT 757 756 774 758 758
CONNECT 758 757 757 759
CONNECT 759 758 760 766 766
CONNECT 760 759 761 761 762
CONNECT 761 760 760
CONNECT 762 760 775 763
CONNECT 763 762 764 765 765
CONNECT 764 763 776 777
CONNECT 765 763 763 766
CONNECT 766 756 759 759 765
CONNECT 767 753 778 768 769
CONNECT 768 755 767 779 780
CONNECT 769 767 781
CONNECT 770 752
CONNECT 771 752
CONNECT 772 753
CONNECT 773 755
CONNECT 774 757
CONNECT 775 762
CONNECT 776 764
CONNECT 777 764
CONNECT 778 767
CONNECT 779 768
CONNECT 780 768
CONNECT 781 769
END

APPENDIX C

PARTIAL CHARGES FOR MODIFIED BASE



APPENDIX D

CHEMICAL SHIFTS

Nonexchangeable protons for IQ modified duplex at G³

	H1'	H2'	H2''	H3'	H8/H6	H5/H2
C ¹	5.72	2.10	2.43	4.49	7.73	5.78
T ²	5.96	2.39	2.05	4.49	7.45	1.51
C ³	5.45	2.21	1.86	4.64	7.25	5.44
G ⁴	5.40	2.56	2.52	4.85	7.67	
G ⁵	5.70	2.35	2.51	4.82	7.55	
C ⁶	5.78	1.48	2.21	4.64	6.85	4.98
X ⁷	5.96	2.65	2.45	4.88	8.04	
C ⁸	5.48	2.23	1.76	4.41	7.40	5.05
C ⁹	5.20	2.23	1.95	4.66	7.21	5.31
A ¹⁰	6.11	2.56	2.77	4.87	8.13	7.52
T ¹¹	5.84	2.29	1.87	4.88	7.00	1.32
C ¹²	6.09	2.06	2.09	4.41	7.40	5.58
G ¹³	5.47	2.56	2.41	4.67	7.70	
A ¹⁴	6.12	2.77	2.57	4.88	8.11	7.74
T ¹⁵	5.52	2.17	1.75	4.64	6.87	1.14
G ¹⁶	5.42	2.50	2.55	4.85	7.59	
G ¹⁷	5.76	2.37	2.45	4.94	7.46	
C ¹⁸	6.29	2.61	2.11	4.88	7.98	6.08
G ¹⁹	5.28	2.05	2.42	4.42	7.18	
C ²⁰	5.72	2.23	1.87	4.64	7.04	4.93
C ²¹	5.26	2.11	1.76	4.63	7.15	5.35
G ²²	5.27	2.58	2.53	4.83	7.70	
A ²³	5.97	2.76	2.51	4.87	7.91	7.62
G ²⁴	5.83	2.08	2.22	4.45	7.44	

Exchangeable protons for IQ modified duplex at G³

	N1H/N3H	H4a	H4b
C ¹ •G ²⁴	13.37	7.21	7.79
T ² •A ²³	14.02		
C ³ •G ²²	12.90	7.04	8.61
G ⁴ •C ²¹	13.05	6.81	8.53
G ⁵ •C ²⁰	12.89	6.29	8.14
C ⁶ •G ¹⁹	12.52	6.66	8.30
X ⁷ •C ¹⁸	11.56		
C ⁸ •G ¹⁷	11.59	6.05	7.89
C ⁹ •G ¹⁶	12.58	6.68	8.30
A ¹⁰ •T ¹⁵	13.52		
T ¹¹ •A ¹⁴	13.72		
C ¹² •G ¹³	12.61	7.11	8.19

Chemical Shifts for IQ ring for G³ modified base

IQ Proton	δ (ppm)
H4a	8.37
H7a	7.48
H8a	6.33
H9a	7.36
CH3	3.35

Nonexchangeable Protons for IQ modified duplex at G¹

	H1'	H2'	H2''	H3'	H6/H8	H2/H5
C ¹	5.90	2.32	2.63	4.70	7.93	6.01
T ²	6.18	2.28	2.61	4.94	7.71	1.76
C ³	6.10	1.76	2.39	4.94	7.39	5.63
G ⁴	6.26	2.91	2.77	5.12	8.30	
G ⁵	5.81	2.562	2.72	5.03	7.98	
C ⁶	5.62	2.01	2.38	4.98	7.22	5.17
G ⁷	5.87	2.64	2.72	5.00	7.86	
C ⁸	5.93	2.08	2.46	4.82	7.35	5.32
C ⁹	5.44	2.17	2.43	4.94	7.52	5.62
A ¹⁰	6.32	2.74	2.97	5.05	8.38	7.78
T ¹¹	6.04	2.07	2.48	5.04	7.25	1.53
C ¹²	6.30	2.28	2.29	4.60	7.65	5.80
G ¹³	5.69	2.61	2.78		7.95	
A ¹⁴	6.34	2.78	2.99	5.08	8.37	8.00
T ¹⁵	5.73	1.97	2.36	5.08	7.14	1.39
G ¹⁶	5.64	2.65	2.73	5.00	7.81	
G ¹⁷	5.85	2.68	2.68	2.54	7.72	
C ¹⁸	5.65	1.95	2.37	4.83	7.22	5.20
G ¹⁹	5.89	2.63	2.74	5.02	7.86	
C ²⁰	6.02	2.17	2.50	5.00	7.10	5.36
C ²¹	6.61	2.43	2.71	5.11	8.17	6.31
G ²²	5.22	2.05	2.44	4.93	7.52	
A ²³	6.02	2.65	2.89	5.01	8.05	7.82
G ²⁴	6.01	2.27	2.40	4.63	7.63	

Exchangeable protons for IQ modified duplex at G¹

	N1H/N3H	H4a	H4b
C ¹ •G ²⁴	13.35	7.24	7.76
T ² •A ²³	14.06		
C ³ •G ²²	12.41	7.23	8.65
X ⁴ •C ²¹	11.79		
G ⁵ •C ²⁰	11.53	6.55	7.93
C ⁶ •G ¹⁹	12.74	6.32	8.18
G ⁷ •C ¹⁸	11.56	6.31	7.71
C ⁸ •G ¹⁷	12.88	6.32	8.14
C ⁹ •G ¹⁶	12.81	6.83	8.50
A ¹⁰ •T ¹⁵	13.61		
T ¹¹ •A ¹⁴	13.79		
C ¹² •G ¹³	12.65	7.14	8.22

Chemical Shifts for IQ modified G¹

IQ Proton	δ (ppm)
H4a	8.568
H7a	8.114
H8a	6.877
H9a	7.744
CH ₃	3.233

APPENDIX E

DISTANCE RESTRAINTS FILES

IQ at G³

```
#
# 7 DKA H2  6 DC H42  3.930  4.780
&rst
ixpk= 0, nxpk= 0, iat= 210, 177, r1= 3.43, r2= 3.93, r3= 4.78, r4= 5.28,
rk2=20.0, rk3=20.0, ir6=1, ialtd=0,
&end
#
# 7 DKA H2  6 DC H41  4.520  6.300
&rst
ixpk= 0, nxpk= 0, iat= 210, 176, r1= 4.02, r2= 4.52, r3= 6.30, r4= 6.80, &end
#
# 7 DKA H20  7 DKA H2          4.160  5.270 (#165 4.660  6.270 )
&rst
ixpk= 4, nxpk= 0, iat= 215, 210, r1= 3.66, r2= 4.16, r3= 5.27, r4= 5.77, &end
#
# 7 DKA H11  7 DKA H2          3.710  5.770 (#4.310  5.770 )
&rst
ixpk= 5, nxpk= 0, iat= 234, 210, r1= 3.21, r2= 3.71, r3= 5.77, r4= 6.27, &end
#
# 1 DC5 H2'2  1 DC5 H1'  1.780  3.050  (#op 6,13,17,54  1.680  2.250)
&rst
ixpk= 6, nxpk= 0, iat= 27, 10, r1= 1.28, r2= 1.78, r3= 3.05, r4= 3.55, &end
#
# 1 DC5 H2'1  1 DC5 H1'  2.030  2.530
&rst
ixpk= 6, nxpk= 0, iat= 26, 10, r1= 1.53, r2= 2.03, r3= 2.53, r4= 3.03, &end
#
# 1 DC5 H3'  1 DC5 H2'2  2.340  4.640  (#59 2.440  4.640 )
&rst
ixpk= 2, nxpk= 0, iat= 24, 27, r1= 1.84, r2= 2.34, r3= 4.64, r4= 5.14, &end
#
# 1 DC5 H3'  1 DC5 H2'1  2.130  2.750  (#42,74  2.130  2.550 )
&rst
ixpk= 2, nxpk= 0, iat= 24, 26, r1= 1.63, r2= 2.13, r3= 2.75, r4= 3.25, &end
#
# 1 DC5 H5'1  1 DC5 H1'  3.170  5.720
&rst
ixpk= 2, nxpk= 0, iat= 4, 10, r1= 2.67, r2= 3.17, r3= 5.72, r4= 6.22, &end
#
# 1 DC5 H5'2  1 DC5 H1'  3.680  5.700
&rst
ixpk= 2, nxpk= 0, iat= 5, 10, r1= 3.18, r2= 3.68, r3= 5.70, r4= 6.20, &end
#
# 1 DC5 H6  1 DC5 H1'  2.340  3.880
&rst
ixpk= 2, nxpk= 0, iat= 13, 10, r1= 1.84, r2= 2.34, r3= 3.88, r4= 4.38, &end
#
# 1 DC5 H6  1 DC5 H2'2  1.850  2.910
```

```

&rst
ixpk= 2, nxpk= 0, iat= 13, 27, r1= 1.35, r2= 1.85, r3= 2.91, r4= 3.41, &end
#
# 1 DC5 H6 1 DC5 H2'1 2.120 4.030 (#61,85,105 2.120 3.730 )
&rst
ixpk= 2, nxpk= 0, iat= 13, 26, r1= 1.62, r2= 2.12, r3= 4.03, r4= 4.53, &end
#
# 1 DC5 H6 1 DC5 H3' 3.260 5.610
&rst
ixpk= 2, nxpk= 0, iat= 13, 24, r1= 2.76, r2= 3.26, r3= 5.61, r4= 6.11, &end
#
# 1 DC5 H6 1 DC5 H5'1 2.460 3.110 (#132 2.460 3.010 )
&rst
ixpk= 2, nxpk= 0, iat= 13, 4, r1= 1.96, r2= 2.46, r3= 3.11, r4= 3.61, &end
#
# 1 DC5 H6 1 DC5 H5'2 2.830 4.320
&rst
ixpk= 2, nxpk= 0, iat= 13, 5, r1= 2.33, r2= 2.83, r3= 4.32, r4= 4.82, &end
#
# 1 DC5 H5 1 DC5 H3' 3.450 6.380 (#90,94,112 3.450 6.080 )
&rst
ixpk= 3, nxpk= 0, iat= 15, 24, r1= 2.95, r2= 3.45, r3= 6.38, r4= 6.88, &end
#
# 1 DC5 H5 1 DC5 H5'2 3.670 6.470 (#63,72,91,126,141 3.670 5.970 )
&rst
ixpk= 3, nxpk= 0, iat= 15, 5, r1= 3.17, r2= 3.67, r3= 6.47, r4= 6.97, &end
#
# 2 DT H2'2 2 DT H1' 2.840 4.760
&rst
ixpk= 3, nxpk= 0, iat= 59, 40, r1= 2.34, r2= 2.84, r3= 4.76, r4= 5.26, &end
#
# 2 DT H2'1 2 DT H1' 2.130 2.940
&rst
ixpk= 3, nxpk= 0, iat= 58, 40, r1= 1.63, r2= 2.13, r3= 2.94, r4= 3.44, &end
#
# 2 DT H6 1 DC5 H1' 3.580 4.670
&rst
ixpk= 3, nxpk= 0, iat= 43, 10, r1= 3.08, r2= 3.58, r3= 4.67, r4= 5.17, &end
#
# 2 DT H6 2 DT H3' 3.080 4.550 (#op 58,76,83,100 3.080 3.850 )
&rst
ixpk= 58, nxpk= 0, iat= 43, 56, r1= 2.58, r2= 3.08, r3= 4.55, r4= 5.05, &end
#
# 2 DT H6 2 DT H1' 2.030 3.680 (#21,71,92 2.030 2.580 (*3.780))
&rst
ixpk= 2, nxpk= 0, iat= 43, 40, r1= 1.53, r2= 2.03, r3= 3.68, r4= 4.18, &end
#
# 2 DT Q5 1 DC5 H1' 2.690 5.260
&rst
ixpk= 2, nxpk= 0, iat= -1, 10, r1= 2.19, r2= 2.69, r3= 6.32, r4= 6.82,
igr1= 46, 47, 48,
&end
#
# 2 DT Q5 1 DC5 H2'2 2.680 4.410 (#64,68,82,88,97 3.280 4.410 )
&rst

```



```

ixpk= 3, nxpk= 0, iat= -1, 27, r1= 2.18, r2= 2.68, r3= 5.30, r4= 5.80,
igr1= 46, 47, 48,
&end
#
# 2 DT Q5 1 DC5 H3' 3.050 3.970 (#104,114,123 3.050 3.770(*4.770) )
&rst
ixpk= 3, nxpk= 0, iat= -1, 24, r1= 2.55, r2= 3.05, r3= 4.77, r4= 5.27,
igr1= 46, 47, 48,
&end
#
# 2 DT Q5 1 DC5 H6 2.420 4.020
&rst
ixpk= 3, nxpk= 0, iat= -1, 13, r1= 1.92, r2= 2.42, r3= 4.83, r4= 5.33,
igr1= 46, 47, 48,
&end
#
# 2 DT Q5 1 DC5 H5 2.610 5.980
&rst
ixpk= 3, nxpk= 0, iat= -1, 15, r1= 2.11, r2= 2.61, r3= 7.18, r4= 7.68,
igr1= 46, 47, 48,
&end
#
# 2 DT Q5 2 DT H2'2 2.280 4.060 (#78,86,91,105 2.280 3.660 )
&rst
ixpk= 2, nxpk= 0, iat= -1, 59, r1= 1.78, r2= 2.28, r3= 4.88, r4= 5.38,
igr1= 46, 47, 48,
&end
#
# 2 DT Q5 2 DT H6 2.700 5.690 (#18,26,52,79 3.200 5.690 )
&rst
ixpk= 3, nxpk= 0, iat= -1, 43, r1= 2.20, r2= 2.70, r3= 6.83, r4= 7.33,
igr1= 46, 47, 48,
&end
#
# 3 DC H2'2 3 DC H1' 1.740 3.080 (#op 7,15,23,28,55,117 1.740 2.380)
&rst
ixpk= 7, nxpk= 0, iat= 89, 72, r1= 1.24, r2= 1.74, r3= 3.08, r4= 3.58, &end
#
# 3 DC H2'1 3 DC H1' 1.980 2.580
(#3 DC H2'1 2 DT H2'2 1.950 2.540 near diagonal)
&rst
ixpk= 7, nxpk= 0, iat= 88, 72, r1= 1.48, r2= 1.98, r3= 2.58, r4= 3.08, &end
#
# 3 DC H6 2 DT H1' 3.070 5.200
&rst
ixpk= 7, nxpk= 0, iat= 75, 40, r1= 2.57, r2= 3.07, r3= 5.20, r4= 5.70, &end
#
# 3 DC H6 2 DT H2'2 2.150 3.780
&rst
ixpk= 7, nxpk= 0, iat= 75, 59, r1= 1.65, r2= 2.15, r3= 3.78, r4= 4.28, &end
#
# 3 DC H6 2 DT H2'1 2.250 5.520 (#87,121 2.450 5.520 )
&rst
ixpk= 2, nxpk= 0, iat= 75, 58, r1= 1.75, r2= 2.25, r3= 5.52, r4= 6.02, &end
#

```

```

# 3 DC H6  2 DT H6  3.240  5.300  (#60,69 3.240  5.100  )
&rst
ixpk= 3, nxpk= 0, iat= 75, 43, r1= 2.74, r2= 3.24, r3= 5.30, r4= 5.80, &end
#
# 3 DC H6  3 DC H1'  2.980  3.780  (#op 1,2,10,13,54,92  1.780  2.680 ci)
&rst
ixpk= 1, nxpk= 0, iat= 75, 72, r1= 2.48, r2= 2.98, r3= 3.78, r4= 4.28, &end
#
# 3 DC H6  3 DC H2'2  2.170  3.180  (#op 56 2.270  3.180  )
&rst
ixpk= 56, nxpk= 0, iat= 75, 89, r1= 1.67, r2= 2.17, r3= 3.18, r4= 3.68, &end
#
# 3 DC H6  3 DC H2'1  2.290  3.730  (#45,53,98,129  2.290  3.330  )
&rst
ixpk= 2, nxpk= 0, iat= 75, 88, r1= 1.79, r2= 2.29, r3= 3.73, r4= 4.23, &end
#
# 3 DC H5  2 DT H1'  3.910  5.690
&rst
ixpk= 2, nxpk= 0, iat= 77, 40, r1= 3.41, r2= 3.91, r3= 5.69, r4= 6.19, &end
#
# 3 DC H5  2 DT H2'1  2.910  4.380
&rst
ixpk= 2, nxpk= 0, iat= 77, 58, r1= 2.41, r2= 2.91, r3= 4.38, r4= 4.88, &end
#
# 3 DC H5  2 DT H6  3.720  5.960
&rst
ixpk= 2, nxpk= 0, iat= 77, 43, r1= 3.22, r2= 3.72, r3= 5.96, r4= 6.46, &end
#
# 3 DC H5  2 DT Q5  3.220  4.540
&rst
ixpk= 2, nxpk= 0, iat= 77, -1, r1= 2.72, r2= 3.22, r3= 5.45, r4= 5.95,
igr2= 46, 47, 48,
&end
#
# 8 DC H1'  8 DC H2'1  2.330  2.960  (#op)
&rst
ixpk= 2, nxpk= 0, iat= 254, 270, r1= 1.83, r2= 2.33, r3= 2.96, r4= 3.46, &end
#
# 4 DG H3'  3 DC H2'1  3.280  4.230  (#65,100 3.280  4.030  )
&rst
ixpk= 3, nxpk= 0, iat= 119, 88, r1= 2.78, r2= 3.28, r3= 4.23, r4= 4.73, &end
#
# 4 DG H3'  4 DG H1'  2.780  4.400
&rst
ixpk= 3, nxpk= 0, iat= 119, 102, r1= 2.28, r2= 2.78, r3= 4.40, r4= 4.90, &end
#
# 4 DG H8  3 DC H1'  2.820  4.380  (#op 57,73,75,76,82,103  2.520  3.780 )
&rst
ixpk= 57, nxpk= 0, iat= 105, 72, r1= 2.32, r2= 2.82, r3= 4.38, r4= 4.88, &end
#
# 4 DG H8  3 DC H2'2  2.810  3.450
&rst
ixpk= 57, nxpk= 0, iat= 105, 89, r1= 2.31, r2= 2.81, r3= 3.45, r4= 3.95, &end
#
# 4 DG H8  3 DC H2'1  2.820  4.160  (#93,126,138 3.120  4.160  )

```

```

&rst
ixpk= 3, nxpk= 0, iat= 105, 88, r1= 2.32, r2= 2.82, r3= 4.16, r4= 4.66, &end
#
# 4 DG H8 4 DG H1' 2.760 4.050
&rst
ixpk= 3, nxpk= 0, iat= 105, 102, r1= 2.26, r2= 2.76, r3= 4.05, r4= 4.55, &end
#
# 4 DG H8 4 DG H3' 3.000 5.740
&rst
ixpk= 3, nxpk= 0, iat= 105, 119, r1= 2.50, r2= 3.00, r3= 5.74, r4= 6.24, &end
#
# 4 DG H8 4 DG H4' 4.510 5.450 (#14,19,58,62,74 3.310 4.350 ci)
&rst
ixpk= 3, nxpk= 0, iat= 105, 99, r1= 4.01, r2= 4.51, r3= 5.45, r4= 5.95, &end
#
# 4 DG H8 4 DG H5'1 4.080 6.300
&rst
ixpk= 3, nxpk= 0, iat= 105, 96, r1= 3.58, r2= 4.08, r3= 6.30, r4= 6.80, &end
#
# 4 DG H8 4 DG H5'2 3.370 4.220
&rst
ixpk= 3, nxpk= 0, iat= 105, 97, r1= 2.87, r2= 3.37, r3= 4.22, r4= 4.72, &end
#
# 5 DG H2'2 5 DC H1' 2.080 3.070 (#op 52,81,117 2.080 2.770 )
&rst
ixpk= 52, nxpk= 0, iat= 155, 135, r1= 1.58, r2= 2.08, r3= 3.07, r4= 3.57, &end
#
# 5 DG H2'1 5 DC H1' 2.180 3.410
&rst
ixpk= 52, nxpk= 0, iat= 154, 135, r1= 1.68, r2= 2.18, r3= 3.41, r4= 3.91, &end
#
# 5 DG H3' 5 DC H1' 3.320 5.460
&rst
ixpk= 52, nxpk= 0, iat= 152, 135, r1= 2.82, r2= 3.32, r3= 5.46, r4= 5.96, &end
#
# 5 DG H3' 5 DG H2'1 2.440 3.140
&rst
ixpk= 52, nxpk= 0, iat= 152, 154, r1= 1.94, r2= 2.44, r3= 3.14, r4= 3.64, &end
#
# 5 DG H8 4 DG H1' 2.590 3.560 (#66,133 2.590 3.360 )
&rst
ixpk= 2, nxpk= 0, iat= 138, 102, r1= 2.09, r2= 2.59, r3= 3.56, r4= 4.06, &end
#
# 5 DG H8 4 DG H3' 3.680 6.720
&rst
ixpk= 2, nxpk= 0, iat= 138, 119, r1= 3.18, r2= 3.68, r3= 6.72, r4= 7.22, &end
#
# 5 DG H8 5 DG H1' 2.870 4.060
&rst
ixpk= 2, nxpk= 0, iat= 138, 135, r1= 2.37, r2= 2.87, r3= 4.06, r4= 4.56, &end
#
# 5 DG H8 5 DG H2'1 2.110 3.870 (#1,13,18,27,34,49,61,90 2.110 2.570 )
&rst
ixpk= 2, nxpk= 0, iat= 138, 154, r1= 1.61, r2= 2.11, r3= 3.87, r4= 4.37, &end
#

```

```

# 5 DG H8 5 DG H3' 3.430 5.560
&rst
ixpk= 2, nxpk= 0, iat= 138, 152, r1= 2.93, r2= 3.43, r3= 5.56, r4= 6.06, &end
#
# 6 DC H2'2 6 DC H1' 2.140 3.010 (#16,69 2.140 2.610 )
&rst
ixpk= 2, nxpk= 0, iat= 185, 168, r1= 1.64, r2= 2.14, r3= 3.01, r4= 3.51, &end
#
# 6 DC H2'1 6 DC H1' 2.360 3.820 (#30,52,57 2.660 3.820 )
&rst
ixpk= 2, nxpk= 0, iat= 184, 168, r1= 1.86, r2= 2.36, r3= 3.82, r4= 4.32, &end
#
# 6 DC H3' 6 DC H2'1 2.780 4.000
(#21 DC H3' 20 DC H2'1 1.830 2.860 #wa,op? 166,167 1.830 2.560 )
&rst
ixpk= 2, nxpk= 0, iat= 182, 184, r1= 2.28, r2= 2.78, r3= 4.00, r4= 4.50, &end
#
# 6 DC H6 5 DG H1' 2.820 4.160 (#17,31,40,48,139 2.820 3.560 )
&rst
ixpk= 2, nxpk= 0, iat= 171, 135, r1= 2.32, r2= 2.82, r3= 4.16, r4= 4.66, &end
#
# 6 DC H6 5 DG H2'2 2.300 3.350 (#op 53,83 2.300 3.050 )
&rst
ixpk= 53, nxpk= 0, iat= 171, 155, r1= 1.80, r2= 2.30, r3= 3.35, r4= 3.85, &end
#
# 6 DC H6 5 DG H2'1 2.350 4.300 (#op 2,6,9,11,15,26,78,97 3.350 4.900)
&rst
ixpk= 2, nxpk= 0, iat= 171, 154, r1= 1.85, r2= 2.35, r3= 4.30, r4= 4.80, &end
#
# 6 DC H6 5 DG H3' 4.870 6.720
&rst
ixpk= 2, nxpk= 0, iat= 171, 152, r1= 4.37, r2= 4.87, r3= 6.72, r4= 7.22, &end
#
# 6 DC H6 5 DG H8 3.640 4.600 (#62,119 3.640 4.400 )
&rst
ixpk= 3, nxpk= 0, iat= 171, 138, r1= 3.14, r2= 3.64, r3= 4.60, r4= 5.10, &end
#
# 6 DC H6 6 DC H1' 2.930 3.720 (#28,54,63,72 2.930 3.320 )
&rst
ixpk= 2, nxpk= 0, iat= 171, 168, r1= 2.43, r2= 2.93, r3= 3.72, r4= 4.22, &end
#
# 6 DC H6 6 DC H2'2 2.050 3.460 (#op 29,32,60 2.350 3.460 )
&rst
ixpk= 29, nxpk= 0, iat= 171, 185, r1= 1.55, r2= 2.05, r3= 3.46, r4= 3.96, &end
#
# 6 DC H6 6 DC H2'1 2.330 3.750 (#51,55,64,77,81,93 2.330 2.850)
&rst
ixpk= 2, nxpk= 0, iat= 171, 184, r1= 1.83, r2= 2.33, r3= 3.75, r4= 4.25, &end
#
# 6 DC H6 6 DC H3' 3.680 6.060
&rst
ixpk= 2, nxpk= 0, iat= 171, 182, r1= 3.18, r2= 3.68, r3= 6.06, r4= 6.56, &end
#
# 6 DC H5 5 DG H1' 3.690 5.010
&rst

```

```

ixpk= 2, nxpk= 0, iat= 173, 135, r1= 3.19, r2= 3.69, r3= 5.01, r4= 5.51, &end
#
# 6 DC H5 5 DG H2'2 2.890 3.940
&rst
ixpk= 2, nxpk= 0, iat= 173, 155, r1= 2.39, r2= 2.89, r3= 3.94, r4= 4.44, &end
#
# 6 DC H5 5 DG H2'1 2.840 3.750 (#OP 96 2.840 3.750 )
&rst
ixpk= 96, nxpk= 0, iat= 173, 154, r1= 2.34, r2= 2.84, r3= 3.75, r4= 4.25, &end
#
# 6 DC H5 5 DG H8 3.370 4.000
&rst
ixpk= 96, nxpk= 0, iat= 173, 138, r1= 2.87, r2= 3.37, r3= 4.00, r4= 4.50, &end
#
# 6 DC H5 6 DC H2'2 3.350 4.500
&rst
ixpk= 96, nxpk= 0, iat= 173, 185, r1= 2.85, r2= 3.35, r3= 4.50, r4= 5.00, &end
#
# 7 DKA H1' 6 DC H2'2 4.870 5.870 (#wp 33,34 4.870 5.670 )
&rst
ixpk= 33, nxpk= 0, iat= 198, 185, r1= 4.37, r2= 4.87, r3= 5.87, r4= 6.37, &end
#
# 7 DKA H2'2 7 DKA H1' 3.060 3.900 (#op 37 3.160 3.900 )
&rst
ixpk= 37, nxpk= 0, iat= 241, 198, r1= 2.56, r2= 3.06, r3= 3.90, r4= 4.40, &end
#
# 7 DKA H2'1 7 DKA H1' 2.300 4.020 (#6,12,13,27,38,57,70 3.300 4.120)
&rst
ixpk= 3, nxpk= 0, iat= 240, 198, r1= 1.80, r2= 2.30, r3= 4.02, r4= 4.52, &end
#
# 7 DKA H3' 7 DKA H1' 3.310 3.990
(#7 DKA H2'1 7 DKA H2'2 2.240 2.680 near diagonal)
&rst
ixpk= 3, nxpk= 0, iat= 238, 198, r1= 2.81, r2= 3.31, r3= 3.99, r4= 4.49, &end
#
# 7 DKA H8 6 DC H1' 3.430 5.120 (#19,45,56,59,68,73,76 3.330 3.720 )
&rst
ixpk= 3, nxpk= 0, iat= 201, 168, r1= 2.93, r2= 3.43, r3= 5.12, r4= 5.62, &end
#
# 7 DKA H8 6 DC H2'2 2.730 3.810 (#1,10,35 2.730 3.210 )
&rst
ixpk= 2, nxpk= 0, iat= 201, 185, r1= 2.23, r2= 2.73, r3= 3.81, r4= 4.31, &end
#
# 7 DKA H8 6 DC H2'1 2.670 3.800 (#7,17,18 3.070 3.800 )
&rst
ixpk= 3, nxpk= 0, iat= 201, 184, r1= 2.17, r2= 2.67, r3= 3.80, r4= 4.30, &end
#
# 7 DKA H8 6 DC H3' 4.040 6.290
&rst
ixpk= 3, nxpk= 0, iat= 201, 182, r1= 3.54, r2= 4.04, r3= 6.29, r4= 6.79, &end
#
# 7 DKA H8 6 DC H6 3.900 4.770
&rst
ixpk= 3, nxpk= 0, iat= 201, 171, r1= 3.40, r2= 3.90, r3= 4.77, r4= 5.27, &end
#

```

```

# 7 DKA H8 7 DKA H1' 3.690 4.190
&rst
ixpk= 3, nxpk= 0, iat= 201, 198, r1= 3.19, r2= 3.69, r3= 4.19, r4= 4.69, &end
#
# 7 DKA H8 7 DKA H2'2 2.290 3.630 (#2,66,79,93,106 2.690 3.430)
&rst
ixpk= 2, nxpk= 0, iat= 201, 241, r1= 1.79, r2= 2.29, r3= 3.63, r4= 4.13, &end
#
# 7 DKA H8 7 DKA H3' 3.260 6.180
&rst
ixpk= 2, nxpk= 0, iat= 201, 238, r1= 2.76, r2= 3.26, r3= 6.18, r4= 6.68, &end
#
# 7 DKA H8 7 DKA H4' 4.100 6.350
&rst
ixpk= 2, nxpk= 0, iat= 201, 195, r1= 3.60, r2= 4.10, r3= 6.35, r4= 6.85, &end
#
# 7 DKA H19 7 DKA H18 2.170 2.730
&rst
ixpk= 2, nxpk= 0, iat= 217, 219, r1= 1.67, r2= 2.17, r3= 2.73, r4= 3.23, &end
#
# 7 DKA H20 7 DKA H19 2.210 2.510
&rst
ixpk= 2, nxpk= 0, iat= 215, 217, r1= 1.71, r2= 2.21, r3= 2.51, r4= 3.01, &end
#
# 7 DKA Q13 7 DKA H1' 3.720 4.190
&rst
ixpk= 2, nxpk= 0, iat= -1, 198, r1= 3.22, r2= 3.72, r3= 5.03, r4= 5.53,
igr1= 229, 230, 231,
&end
#
# 7 DKA H11 7 DKA H1' 2.960 4.110 (#2,8,21,45,61 3.660 4.110 )
&rst
ixpk= 3, nxpk= 0, iat= 234, 198, r1= 2.46, r2= 2.96, r3= 4.11, r4= 4.61, &end
#
# 7 DKA H11 7 DKA H2'1 4.130 6.740
&rst
ixpk= 3, nxpk= 0, iat= 234, 240, r1= 3.63, r2= 4.13, r3= 6.74, r4= 7.24, &end
#
# 7 DKA H11 7 DKA H2'2 3.860 5.740 (#85,97,103,122 3.860 5.240 )
&rst
ixpk= 3, nxpk= 0, iat= 234, 241, r1= 3.36, r2= 3.86, r3= 5.74, r4= 6.24, &end
#
# 7 DKA H11 7 DKA H5'1 4.820 6.540
&rst
ixpk= 3, nxpk= 0, iat= 234, 192, r1= 4.32, r2= 4.82, r3= 6.54, r4= 7.04, &end
#
# 7 DKA H11 7 DKA H4' 3.580 4.450 (#25,28,31,35,41 3.580 4.250 )
&rst
ixpk= 3, nxpk= 0, iat= 234, 195, r1= 3.08, r2= 3.58, r3= 4.45, r4= 4.95, &end
#
# 7 DKA H11 7 DKA Q13 2.290 3.020
&rst
ixpk= 3, nxpk= 0, iat= 234, -1, r1= 1.79, r2= 2.29, r3= 3.63, r4= 4.13,
igr2= 229, 230, 231,
&end

```

```

#
# 8 DC H1' 7 DKA Q13 2.810 4.360
&rst
ixpk= 3, nxpk= 0, iat= 254, -1, r1= 2.31, r2= 2.81, r3= 5.24, r4= 5.74,
igr2= 229, 230, 231,
&end
#
# 8 DC H2'1 8 DC H1' 2.280 3.720 (#op 54 2.380 3.720 )
&rst
ixpk= 54, nxpk= 0, iat= 270, 254, r1= 1.78, r2= 2.28, r3= 3.72, r4= 4.22, &end
#
# 8 DC H6 7 DKA H1' 2.090 2.930 (#op 88,114,120 2.090 2.530 )
&rst
ixpk= 88, nxpk= 0, iat= 257, 198, r1= 1.59, r2= 2.09, r3= 2.93, r4= 3.43, &end
#
# 8 DC H6 7 DKA H2'1 2.700 4.120 (#4,22,26,29,50,166 3.100 3.720 )
&rst
ixpk= 3, nxpk= 0, iat= 257, 240, r1= 2.20, r2= 2.70, r3= 4.12, r4= 4.62, &end
#
# 8 DC H6 7 DKA Q13 3.950 4.570
&rst
ixpk= 3, nxpk= 0, iat= 257, -1, r1= 3.45, r2= 3.95, r3= 5.49, r4= 5.99,
igr2= 229, 230, 231,
&end
#
# 8 DC H6 8 DC H1' 3.680 6.420
&rst
ixpk= 3, nxpk= 0, iat= 257, 254, r1= 3.18, r2= 3.68, r3= 6.42, r4= 6.92, &end
#
# 8 DC H6 8 DC H2'2 2.670 4.070 (#op 98,118,123,128 3.270 4.270 )
&rst
ixpk= 98, nxpk= 0, iat= 257, 271, r1= 2.17, r2= 2.67, r3= 4.07, r4= 4.57, &end
#
# 8 DC H6 8 DC H2'1 3.210 5.620
&rst
ixpk= 98, nxpk= 0, iat= 257, 270, r1= 2.71, r2= 3.21, r3= 5.62, r4= 6.12, &end
#
# 8 DC H5 7 DKA H1' 2.900 3.310
&rst
ixpk= 98, nxpk= 0, iat= 259, 198, r1= 2.40, r2= 2.90, r3= 3.31, r4= 3.81, &end
#
# 8 DC H5 7 DKA H2'1 3.550 4.300 (#111,137 3.550 4.100 )
&rst
ixpk= 3, nxpk= 0, iat= 259, 240, r1= 3.05, r2= 3.55, r3= 4.30, r4= 4.80, &end
#
# 8 DC H5 7 DKA H8 3.970 6.610
&rst
ixpk= 3, nxpk= 0, iat= 259, 201, r1= 3.47, r2= 3.97, r3= 6.61, r4= 7.11, &end
#
# 8 DC H5 7 DKA Q13 4.520 6.150
&rst
ixpk= 3, nxpk= 0, iat= 259, -1, r1= 4.02, r2= 4.52, r3= 7.39, r4= 7.89,
igr2= 229, 230, 231,
&end
#

```

```

# 8 DC H5 7 DKA H11 3.320 4.610 (#167 3.320 4.510 )
&rst
ixpk= 3, nxpk= 0, iat= 259, 234, r1= 2.82, r2= 3.32, r3= 4.61, r4= 5.11, &end
#
# 9 DC H2'2 9 DC H1' 2.100 2.970 (#23,32,48,66,93 2.100 2.370 )
&rst
ixpk= 2, nxpk= 0, iat= 301, 284, r1= 1.60, r2= 2.10, r3= 2.97, r4= 3.47, &end
#
# 9 DC H2'1 9 DC H1' 2.210 3.660 (#28,33,37 2.510 3.660 )
&rst
ixpk= 2, nxpk= 0, iat= 300, 284, r1= 1.71, r2= 2.21, r3= 3.66, r4= 4.16, &end
#
# 9 DC H3' 9 DC H1' 3.140 5.370
&rst
ixpk= 2, nxpk= 0, iat= 298, 284, r1= 2.64, r2= 3.14, r3= 5.37, r4= 5.87, &end
#
# 9 DC H3' 9 DC H2'1 2.780 3.680
&rst
ixpk= 2, nxpk= 0, iat= 298, 300, r1= 2.28, r2= 2.78, r3= 3.68, r4= 4.18, &end
#
# 19 DG H8 7 DKA H20 3.070 4.000 (#1,10,13,26,31,36,44 3.070 3.400 )
&rst
ixpk= 3, nxpk= 0, iat= 603, 215, r1= 2.57, r2= 3.07, r3= 4.00, r4= 4.50, &end
#
# 9 DC H6 8 DC H1' 3.300 4.350 (#76,78 3.100 4.250 )
&rst
ixpk= 3, nxpk= 0, iat= 287, 254, r1= 2.80, r2= 3.30, r3= 4.35, r4= 4.85, &end
#
# 9 DC H6 8 DC H2'1 2.240 4.410 (#41,46,55,57,59,61,65 3.240 4.410 )
&rst
ixpk= 3, nxpk= 0, iat= 287, 270, r1= 1.74, r2= 2.24, r3= 4.41, r4= 4.91, &end
#
# 9 DC H6 8 DC H6 3.890 5.790
&rst
ixpk= 3, nxpk= 0, iat= 287, 257, r1= 3.39, r2= 3.89, r3= 5.79, r4= 6.29, &end
#
# 9 DC H6 9 DC H1' 2.790 3.750 (#18,104 2.790 3.350 )
&rst
ixpk= 2, nxpk= 0, iat= 287, 284, r1= 2.29, r2= 2.79, r3= 3.75, r4= 4.25, &end
#
# 9 DC H6 9 DC H3' 2.750 5.530 (#42,49,57,62,70,73,74 3.450 5.530 )
&rst
ixpk= 3, nxpk= 0, iat= 287, 298, r1= 2.25, r2= 2.75, r3= 5.53, r4= 6.03, &end
#
# 9 DC H5 8 DC H2'1 2.640 4.170 (#op 102,140 2.640 3.870 )
&rst
ixpk= 102, nxpk= 0, iat= 289, 270, r1= 2.14, r2= 2.64, r3= 4.17, r4= 4.67, &end
#
# 9 DC H5 8 DC H6 3.900 4.800 (#3.900 4.700 )
&rst
ixpk= 4, nxpk= 0, iat= 289, 257, r1= 3.40, r2= 3.90, r3= 4.80, r4= 5.30, &end
#
# 9 DC H5 8 DC H5 3.880 4.970
&rst
ixpk= 4, nxpk= 0, iat= 289, 259, r1= 3.38, r2= 3.88, r3= 4.97, r4= 5.47, &end

```



```

#
# 9 DC H5 9 DC H2'2 2.450 4.570 (#op 48,68,77,80,83,92 2.450 3.470 )
&rst
ixpk= 48, nxpk= 0, iat= 289, 301, r1= 1.95, r2= 2.45, r3= 4.57, r4= 5.07, &end
#
# 9 DC H5 9 DC H2'1 3.030 6.050
&rst
ixpk= 48, nxpk= 0, iat= 289, 300, r1= 2.53, r2= 3.03, r3= 6.05, r4= 6.55, &end
#
# 21 DC H5 20 DC H3' 3.940 5.760 (#broad 46,60,64,67,69,72 3.640 4.260)
&rst
ixpk= 46, nxpk= 0, iat= 668, 647, r1= 3.44, r2= 3.94, r3= 5.76, r4= 6.26, &end
#
# 10 DA H2'2 10 DA H1' 1.690 3.960
&rst
ixpk= 46, nxpk= 0, iat= 333, 314, r1= 1.19, r2= 1.69, r3= 3.96, r4= 4.46, &end
#
# 10 DA H3' 10 DA H2'2 1.680 2.380 (#71,93,135 1.680 2.080 )
&rst
ixpk= 1, nxpk= 0, iat= 330, 333, r1= 1.18, r2= 1.68, r3= 2.38, r4= 2.88, &end
#
# 10 DA H4' 10 DA H1' 2.980 5.570 (#119 3.080 5.570 )
&rst
ixpk= 3, nxpk= 0, iat= 311, 314, r1= 2.48, r2= 2.98, r3= 5.57, r4= 6.07, &end
#
# 10 DA H8 9 DC H1' 2.980 4.560 (#26,29,30,33,36,40,43 2.580 3.460 )
&rst
ixpk= 2, nxpk= 0, iat= 317, 284, r1= 2.48, r2= 2.98, r3= 4.56, r4= 5.06, &end
#
# 10 DA H8 9 DC H2'2 2.560 5.540
&rst
ixpk= 2, nxpk= 0, iat= 317, 301, r1= 2.06, r2= 2.56, r3= 5.54, r4= 6.04, &end
#
# 10 DA H8 9 DC H2'1 2.570 5.870 (#35,38,45,47* 2.970 5.270 )
&rst
ixpk= 2, nxpk= 0, iat= 317, 300, r1= 2.07, r2= 2.57, r3= 5.87, r4= 6.37, &end
#
# 10 DA H8 10 DA H3' 2.600 4.220
(#10 DA H8 10 DA H1' 1.790 2.760 #op)
&rst
ixpk= 2, nxpk= 0, iat= 317, 330, r1= 2.10, r2= 2.60, r3= 4.22, r4= 4.72, &end
#
# 10 DA H8 10 DA H4' 3.730 6.150
&rst
ixpk= 2, nxpk= 0, iat= 317, 311, r1= 3.23, r2= 3.73, r3= 6.15, r4= 6.65, &end
#
# 10 DA H8 10 DA H5'2 3.380 5.400
&rst
ixpk= 2, nxpk= 0, iat= 317, 309, r1= 2.88, r2= 3.38, r3= 5.40, r4= 5.90, &end
#
# 11 DT H2'2 11 DT H1' 2.420 3.020
&rst
ixpk= 2, nxpk= 0, iat= 365, 346, r1= 1.92, r2= 2.42, r3= 3.02, r4= 3.52, &end
#
# 11 DT H2'1 11 DT H1' 2.310 3.130 (#52,102 2.610 3.130 )

```

```

&rst
ixpk= 2, nxpk= 0, iat= 364, 346, r1= 1.81, r2= 2.31, r3= 3.13, r4= 3.63, &end
#
# 11 DT H3' 11 DT H2'1 2.730 3.250
&rst
ixpk= 2, nxpk= 0, iat= 362, 364, r1= 2.23, r2= 2.73, r3= 3.25, r4= 3.75, &end
#
# 20 DC H5 20 DC H2'2 2.840 4.290 (#11,15,17,51,63,77 3.140 3.990 )
&rst
ixpk= 3, nxpk= 0, iat= 638, 650, r1= 2.34, r2= 2.84, r3= 4.29, r4= 4.79, &end
#
# 11 DT H6 10 DA H1' 2.970 4.430 (#19,38,41,42,46,62,65 2.370 3.130 )
&rst
ixpk= 2, nxpk= 0, iat= 349, 314, r1= 2.47, r2= 2.97, r3= 4.43, r4= 4.93, &end
#
# 11 DT H6 10 DA H2'2 2.250 3.400 (#50,57,75,101,110 2.250 2.800 )
&rst
ixpk= 2, nxpk= 0, iat= 349, 333, r1= 1.75, r2= 2.25, r3= 3.40, r4= 3.90, &end
#
# 11 DT H6 10 DA H2'1 2.440 5.090 (#14,37,42,126,129 3.040 5.190 )
&rst
ixpk= 3, nxpk= 0, iat= 349, 332, r1= 1.94, r2= 2.44, r3= 5.09, r4= 5.59, &end
#
# 11 DT H6 10 DA H8 3.360 6.460
&rst
ixpk= 3, nxpk= 0, iat= 349, 317, r1= 2.86, r2= 3.36, r3= 6.46, r4= 6.96, &end
#
# 11 DT H6 11 DT H1' 3.090 3.800
&rst
ixpk= 3, nxpk= 0, iat= 349, 346, r1= 2.59, r2= 3.09, r3= 3.80, r4= 4.30, &end
#
# 11 DT H6 11 DT H2'2 1.980 3.120 (#op 39,66,103,105 2.380 3.120 )
&rst
ixpk= 39, nxpk= 0, iat= 349, 365, r1= 1.48, r2= 1.98, r3= 3.12, r4= 3.62, &end
#
# 11 DT H6 11 DT H2'1 2.090 3.380 (#op 78,80,113,121 2.090 2.880 )
&rst
ixpk= 78, nxpk= 0, iat= 349, 364, r1= 1.59, r2= 2.09, r3= 3.38, r4= 3.88, &end
#
# 11 DT H6 11 DT H3' 3.930 6.050
&rst
ixpk= 78, nxpk= 0, iat= 349, 362, r1= 3.43, r2= 3.93, r3= 6.05, r4= 6.55, &end
#
# 11 DT Q5 10 DA H2'2 3.120 4.710
&rst
ixpk= 78, nxpk= 0, iat= -1, 333, r1= 2.62, r2= 3.12, r3= 5.66, r4= 6.16,
igr1= 352, 353, 354,
&end
#
# 11 DT Q5 10 DA H2'1 2.770 3.970
&rst
ixpk= 78, nxpk= 0, iat= -1, 332, r1= 2.27, r2= 2.77, r3= 4.77, r4= 5.27,
igr1= 352, 353, 354,
&end
#

```

```

# 11 DT Q5 10 DA H8 2.480 3.320 (#170 2.480 3.220 )
&rst
ixpk= 2, nxpk= 0, iat= -1, 317, r1= 1.98, r2= 2.48, r3= 3.99, r4= 4.49,
igr1= 352, 353, 354,
&end
#
# 11 DT Q5 11 DT H1' 4.410 5.560
&rst
ixpk= 2, nxpk= 0, iat= -1, 346, r1= 3.91, r2= 4.41, r3= 6.68, r4= 7.18,
igr1= 352, 353, 354,
&end
#
# 11 DT Q5 11 DT H2'2 2.880 4.320
&rst
ixpk= 2, nxpk= 0, iat= -1, 365, r1= 2.38, r2= 2.88, r3= 5.19, r4= 5.69,
igr1= 352, 353, 354,
&end
#
# 11 DT Q5 11 DT H6 2.440 3.100
(#11 DT Q5 11 DT H3' 3.600 5.370 #2,3,4,9,23,27,28,31 3.600 4.170 )
&rst
ixpk= 2, nxpk= 0, iat= -1, 349, r1= 1.94, r2= 2.44, r3= 3.72, r4= 4.22,
igr1= 352, 353, 354,
&end
#
# 12 DC3 H3' 12 DC3 H1' 3.240 5.470
(#12 DC3 H1' 11 DT Q5 3.250 4.250 #33,34,40,42,45 3.250 3.750 )
&rst
ixpk= 2, nxpk= 0, iat= 392, 378, r1= 2.74, r2= 3.24, r3= 5.47, r4= 5.97, &end
#
# 12 DC3 H3' 12 DC3 H2'2 1.560 2.360 (#op, 1,2,3 1.560 2.060 )
&rst
ixpk= 1, nxpk= 0, iat= 392, 395, r1= 1.06, r2= 1.56, r3= 2.36, r4= 2.86, &end
#
# 12 DC3 H6 11 DT H1' 2.030 2.920 (#op 99,124,141 2.030 2.520 )
&rst
ixpk= 99, nxpk= 0, iat= 381, 346, r1= 1.53, r2= 2.03, r3= 2.92, r4= 3.42, &end
#
# 12 DC3 H6 11 DT H2'1 2.390 4.560 (#18,67,84,116,127 2.890 4.560)
&rst
ixpk= 2, nxpk= 0, iat= 381, 364, r1= 1.89, r2= 2.39, r3= 4.56, r4= 5.06, &end
#
# 12 DC3 H6 11 DT H6 3.250 4.960 (#48,73,92,114,117,130 3.250 4.260 )
&rst
ixpk= 3, nxpk= 0, iat= 381, 349, r1= 2.75, r2= 3.25, r3= 4.96, r4= 5.46, &end
#
# 12 DC3 H6 12 DC3 H1' 3.020 3.780 (#81 3.020 3.580 )
&rst
ixpk= 3, nxpk= 0, iat= 381, 378, r1= 2.52, r2= 3.02, r3= 3.78, r4= 4.28, &end
#
# 12 DC3 H6 12 DC3 H3' 2.700 3.220 (#134 2.800 3.220 )
&rst
ixpk= 2, nxpk= 0, iat= 381, 392, r1= 2.20, r2= 2.70, r3= 3.22, r4= 3.72, &end
#
# 12 DC3 H5 11 DT H1' 2.900 3.920 (#44,45,55,56,60,64,74 2.700 3.120 )

```

```

&rst
ixpk= 2, nxpk= 0, iat= 383, 346, r1= 2.40, r2= 2.90, r3= 3.92, r4= 4.42, &end
#
# 12 DC3 H5 11 DT H2'2 3.680 4.910
&rst
ixpk= 2, nxpk= 0, iat= 383, 365, r1= 3.18, r2= 3.68, r3= 4.91, r4= 5.41, &end
#
# 12 DC3 H5 11 DT H2'1 2.970 3.830 (#88,104 3.170 3.830 )
&rst
ixpk= 3, nxpk= 0, iat= 383, 364, r1= 2.47, r2= 2.97, r3= 3.83, r4= 4.33, &end
#
# 12 DC3 H5 11 DT H6 3.040 3.770 (#13,26 3.040 3.570)
&rst
ixpk= 3, nxpk= 0, iat= 383, 349, r1= 2.54, r2= 3.04, r3= 3.77, r4= 4.27, &end
#
# 12 DC3 H5 11 DT Q5 3.600 4.610
&rst
ixpk= 3, nxpk= 0, iat= 383, -1, r1= 3.10, r2= 3.60, r3= 5.54, r4= 6.04,
igr2= 352, 353, 354,
&end
#
# 12 DC3 H5 12 DC3 H3' 3.230 5.660
&rst
ixpk= 3, nxpk= 0, iat= 383, 392, r1= 2.73, r2= 3.23, r3= 5.66, r4= 6.16, &end
#
# 13 DG5 H3' 13 DG5 H1' 3.130 5.400
&rst
ixpk= 3, nxpk= 0, iat= 424, 407, r1= 2.63, r2= 3.13, r3= 5.40, r4= 5.90, &end
#
# 13 DG5 H3' 13 DG5 H2'2 2.400 4.420 (#near ws 54,92 IQG3.dist2.600 4.420 )
&rst
ixpk= 3, nxpk= 0, iat= 424, 427, r1= 1.90, r2= 2.40, r3= 4.42, r4= 4.92, &end
#
# 13 DG5 H3' 13 DG5 H2'1 2.700 4.360 (#41,42,57,93 3.100 4.360 )
&rst
ixpk= 3, nxpk= 0, iat= 424, 426, r1= 2.20, r2= 2.70, r3= 4.36, r4= 4.86, &end
#
# 13 DG5 H8 13 DG5 H1' 2.750 4.240
&rst
ixpk= 3, nxpk= 0, iat= 410, 407, r1= 2.25, r2= 2.75, r3= 4.24, r4= 4.74, &end
#
# 14 DA H8 13 DG5 H1' 2.410 3.600 (#102,103 2.410 3.300 )
&rst
ixpk= 2, nxpk= 0, iat= 443, 407, r1= 1.91, r2= 2.41, r3= 3.60, r4= 4.10, &end
#
# 14 DA H8 13 DG5 H2'1 2.100 4.130 (#141 2.200 4.130 )
&rst
ixpk= 2, nxpk= 0, iat= 443, 426, r1= 1.60, r2= 2.10, r3= 4.13, r4= 4.63, &end
#
# 14 DA H8 14 DA H1' 2.730 3.840 (#op )
&rst
ixpk= 2, nxpk= 0, iat= 443, 440, r1= 2.23, r2= 2.73, r3= 3.84, r4= 4.34, &end
#
# 14 DA H8 14 DA H3' 2.330 4.520 (#21 2.330 4.020 )
&rst

```

```

ixpk= 2, nxpk= 0, iat= 443, 456, r1= 1.83, r2= 2.33, r3= 4.52, r4= 5.02, &end
#
# 14 DA H8 14 DA H5'2 2.800 6.490
&rst
ixpk= 2, nxpk= 0, iat= 443, 435, r1= 2.30, r2= 2.80, r3= 6.49, r4= 6.99, &end
#
# 15 DT H2'2 15 DT H1' 1.960 3.020 (#4,7,10,11,18,30,60 1.960 2.320)
&rst
ixpk= 1, nxpk= 0, iat= 491, 472, r1= 1.46, r2= 1.96, r3= 3.02, r4= 3.52, &end
#
# 15 DT H2'1 15 DT H1' 2.270 3.570
&rst
ixpk= 1, nxpk= 0, iat= 490, 472, r1= 1.77, r2= 2.27, r3= 3.57, r4= 4.07, &end
#
# 15 DT H3' 15 DT H2'2 2.250 3.330 (#op 26,32,66,70,81 2.750 3.330 )
&rst
ixpk= 26, nxpk= 0, iat= 488, 491, r1= 1.75, r2= 2.25, r3= 3.33, r4= 3.83, &end
#
# 15 DT H3' 15 DT H2'1 2.710 3.650 (#105 2.810 3.650 )
&rst
ixpk= 2, nxpk= 0, iat= 488, 490, r1= 2.21, r2= 2.71, r3= 3.65, r4= 4.15, &end
#
# 15 DT H6 14 DA H1' 2.350 3.690 (#104,114 2.350 3.390)
&rst
ixpk= 2, nxpk= 0, iat= 475, 440, r1= 1.85, r2= 2.35, r3= 3.69, r4= 4.19, &end
#
# 15 DT H6 14 DA H2'2 2.550 3.880
&rst
ixpk= 2, nxpk= 0, iat= 475, 459, r1= 2.05, r2= 2.55, r3= 3.88, r4= 4.38, &end
#
# 15 DT H6 14 DA H2'1 2.180 3.570
&rst
ixpk= 2, nxpk= 0, iat= 475, 458, r1= 1.68, r2= 2.18, r3= 3.57, r4= 4.07, &end
#
# 15 DT H6 15 DT H1' 2.680 3.880 (#21 2.680 3.380 )
&rst
ixpk= 2, nxpk= 0, iat= 475, 472, r1= 2.18, r2= 2.68, r3= 3.88, r4= 4.38, &end
#
# 15 DT H6 15 DT H2'2 2.220 3.720 (#14 2.320 3.720 )
&rst
ixpk= 2, nxpk= 0, iat= 475, 491, r1= 1.72, r2= 2.22, r3= 3.72, r4= 4.22, &end
#
# 15 DT H6 15 DT H3' 3.450 5.630 (#op 97 3.550 5.630 )
&rst
ixpk= 97, nxpk= 0, iat= 475, 488, r1= 2.95, r2= 3.45, r3= 5.63, r4= 6.13, &end
#
# 15 DT Q5 14 DA H1' 2.800 4.460
&rst
ixpk= 97, nxpk= 0, iat= -1, 440, r1= 2.30, r2= 2.80, r3= 5.36, r4= 5.86,
igr1= 478, 479, 480,
&end
#
# 15 DT Q5 14 DA H2'2 2.740 4.880
&rst
ixpk= 97, nxpk= 0, iat= -1, 459, r1= 2.24, r2= 2.74, r3= 5.86, r4= 6.36,

```

```

igr1= 478, 479, 480,
&end
#
# 15 DT Q5  14 DA H2'1 3.130 4.720 (#103 3.230 4.720 )
&rst
ixpk= 3, nxpk= 0, iat= -1, 458, r1= 2.63, r2= 3.13, r3= 5.67, r4= 6.17,
igr1= 478, 479, 480,
&end
#
# 15 DT Q5  14 DA H8  2.160 4.290
&rst
ixpk= 3, nxpk= 0, iat= -1, 443, r1= 1.66, r2= 2.16, r3= 5.15, r4= 5.65,
igr1= 478, 479, 480,
&end
#
# 15 DT Q5  15 DT H1' 3.090 6.090
&rst
ixpk= 3, nxpk= 0, iat= -1, 472, r1= 2.59, r2= 3.09, r3= 7.31, r4= 7.81,
igr1= 478, 479, 480,
&end
#
# 15 DT Q5  15 DT H2'2 3.140 6.490
&rst
ixpk= 3, nxpk= 0, iat= -1, 491, r1= 2.64, r2= 3.14, r3= 7.79, r4= 8.29,
igr1= 478, 479, 480,
&end
#
# 15 DT Q5  15 DT H6  2.400 2.990
&rst
ixpk= 3, nxpk= 0, iat= -1, 475, r1= 1.90, r2= 2.40, r3= 3.59, r4= 4.09,
igr1= 478, 479, 480,
&end
#
# 16 DG H3' 16 DG H1' 2.780 4.450
(#16 DG H3' 15 DT Q5  3.110 4.300 #22,23,31,33,35,38 3.110 3.600 )
&rst
ixpk= 3, nxpk= 0, iat= 521, 504, r1= 2.28, r2= 2.78, r3= 4.45, r4= 4.95, &end
#
# 16 DG H8  15 DT H1' 4.440 5.210
&rst
ixpk= 3, nxpk= 0, iat= 507, 472, r1= 3.94, r2= 4.44, r3= 5.21, r4= 5.71, &end
#
# 16 DG H8  15 DT H2'2 2.620 3.180 (#64 2.620 3.080 )
&rst
ixpk= 2, nxpk= 0, iat= 507, 491, r1= 2.12, r2= 2.62, r3= 3.18, r4= 3.68, &end
#
# 16 DG H8  15 DT H2'1 2.490 3.650 (#60,61,63,72,117 2.990 3.650 )
&rst
ixpk= 2, nxpk= 0, iat= 507, 490, r1= 1.99, r2= 2.49, r3= 3.65, r4= 4.15, &end
#
# 16 DG H8  15 DT H6  3.720 5.290
&rst
ixpk= 2, nxpk= 0, iat= 507, 475, r1= 3.22, r2= 3.72, r3= 5.29, r4= 5.79, &end
#
# 16 DG H8  16 DG H1' 2.720 3.910 (#16 2.720 3.310 ci)

```

```

&rst
ixpk= 2, nxpk= 0, iat= 507, 504, r1= 2.22, r2= 2.72, r3= 3.91, r4= 4.41, &end
#
# 16 DG H8 16 DG H3' 2.870 5.570
&rst
ixpk= 2, nxpk= 0, iat= 507, 521, r1= 2.37, r2= 2.87, r3= 5.57, r4= 6.07, &end
#
# 16 DG H8 16 DG H4' 4.380 6.650
&rst
ixpk= 2, nxpk= 0, iat= 507, 501, r1= 3.88, r2= 4.38, r3= 6.65, r4= 7.15, &end
#
# 16 DG H8 16 DG H5'1 2.980 4.100 (#82,93,95,96,101,113,119 2.980 3.300 )
&rst
ixpk= 2, nxpk= 0, iat= 507, 498, r1= 2.48, r2= 2.98, r3= 4.10, r4= 4.60, &end
#
# 17 DG H1' 7 DKA H19 3.430 5.060 (#17,26,28,36,37,97 3.430 4.360 )
&rst
ixpk= 3, nxpk= 0, iat= 537, 217, r1= 2.93, r2= 3.43, r3= 5.06, r4= 5.56, &end
#
# 17 DG H2'2 17 DG H1' 1.730 3.160 (#op 11,13,92 1.730 2.360 ci)
&rst
ixpk= 11, nxpk= 0, iat= 557, 537, r1= 1.23, r2= 1.73, r3= 3.16, r4= 3.66, &end
#
# 17 DG H2'1 16 DG H1' 2.900 5.410 (#broad 53,57,67,69,79,83 2.800 3.810 )
&rst
ixpk= 53, nxpk= 0, iat= 556, 504, r1= 2.40, r2= 2.90, r3= 5.41, r4= 5.91, &end
#
# 17 DG H2'1 17 DG H1' 2.110 3.750
&rst
ixpk= 53, nxpk= 0, iat= 556, 537, r1= 1.61, r2= 2.11, r3= 3.75, r4= 4.25, &end
#
# 17 DG H3' 17 DG H1' 2.980 5.180
&rst
ixpk= 53, nxpk= 0, iat= 554, 537, r1= 2.48, r2= 2.98, r3= 5.18, r4= 5.68, &end
#
# 17 DG H3' 17 DG H2'2 2.170 3.880
&rst
ixpk= 53, nxpk= 0, iat= 554, 557, r1= 1.67, r2= 2.17, r3= 3.88, r4= 4.38, &end
#
# 17 DG H3' 17 DG H2'1 2.160 2.960
&rst
ixpk= 53, nxpk= 0, iat= 554, 556, r1= 1.66, r2= 2.16, r3= 2.96, r4= 3.46, &end
#
# 17 DG H8 16 DG H1' 2.690 3.620 (#100,130 2.690 3.320 )
&rst
ixpk= 2, nxpk= 0, iat= 540, 504, r1= 2.19, r2= 2.69, r3= 3.62, r4= 4.12, &end
#
# 17 DG H8 17 DG H1' 2.670 3.790 (#71 2.670 3.590 )
&rst
ixpk= 2, nxpk= 0, iat= 540, 537, r1= 2.17, r2= 2.67, r3= 3.79, r4= 4.29, &end
#
# 17 DG H8 17 DG H3' 3.340 5.580
&rst
ixpk= 2, nxpk= 0, iat= 540, 554, r1= 2.84, r2= 3.34, r3= 5.58, r4= 6.08, &end
#

```

```

# 18 DC H2'2 7 DKA H19 2.770 4.460 (#op 3,10,14,22,24,25,88 2.470 3.060 )
&rst
ixpk= 3, nxpk= 0, iat= 587, 217, r1= 2.27, r2= 2.77, r3= 4.46, r4= 4.96, &end
#
# 18 DC H2'2 17 DG H1' 3.310 5.200
&rst
ixpk= 3, nxpk= 0, iat= 587, 537, r1= 2.81, r2= 3.31, r3= 5.20, r4= 5.70, &end
#
# 18 DC H2'2 18 DC H1' 2.090 3.330 (#ci 2.090 2.430 )
&rst
ixpk= 2, nxpk= 0, iat= 587, 570, r1= 1.59, r2= 2.09, r3= 3.33, r4= 3.83, &end
#
# 18 DC H2'1 7 DKA H19 2.880 5.520 (#23,45,50,53 3.180 4.920 )
&rst
ixpk= 3, nxpk= 0, iat= 586, 217, r1= 2.38, r2= 2.88, r3= 5.52, r4= 6.02, &end
#
# 18 DC H2'1 18 DC H1' 2.290 5.070 (#170 2.390 5.170 )
&rst
ixpk= 2, nxpk= 0, iat= 586, 570, r1= 1.79, r2= 2.29, r3= 5.07, r4= 5.57, &end
#
# 18 DC H3' 18 DC H1' 3.730 5.320
&rst
ixpk= 2, nxpk= 0, iat= 584, 570, r1= 3.23, r2= 3.73, r3= 5.32, r4= 5.82, &end
#
# 18 DC H5'2 18 DC H1' 2.170 4.750 (#18, 20 2.170 3.550 ci)
&rst
ixpk= 20, nxpk= 0, iat= 565, 570, r1= 1.67, r2= 2.17, r3= 4.75, r4= 5.25, &end
#
# 18 DC H6 17 DG H1' 2.760 3.960 (#51,57,68,81,107,110 2.760 3.160 )
&rst
ixpk= 2, nxpk= 0, iat= 573, 537, r1= 2.26, r2= 2.76, r3= 3.96, r4= 4.46, &end
#
# 18 DC H6 17 DG H2'2 3.360 5.350
&rst
ixpk= 2, nxpk= 0, iat= 573, 557, r1= 2.86, r2= 3.36, r3= 5.35, r4= 5.85, &end
#
# 18 DC H6 17 DG H2'1 3.510 5.760 (#73,95,111 3.810 5.760 )
&rst
ixpk= 3, nxpk= 0, iat= 573, 556, r1= 3.01, r2= 3.51, r3= 5.76, r4= 6.26, &end
#
# 18 DC H6 17 DG H3' 3.330 4.620 (#30,45,46,74,87,112 3.330 3.820 )
&rst
ixpk= 3, nxpk= 0, iat= 573, 554, r1= 2.83, r2= 3.33, r3= 4.62, r4= 5.12, &end
#
# 18 DC H6 18 DC H1' 2.770 3.980 (#9 2.770 3.180 ci)
&rst
ixpk= 2, nxpk= 0, iat= 573, 570, r1= 2.27, r2= 2.77, r3= 3.98, r4= 4.48, &end
#
# 18 DC H6 18 DC H2'2 2.450 4.020 (#36,77 2.650 4.020 )
&rst
ixpk= 2, nxpk= 0, iat= 573, 587, r1= 1.95, r2= 2.45, r3= 4.02, r4= 4.52, &end
#
# 18 DC H6 18 DC H2'1 2.760 4.010 (#2,29,31,52,117 2.760 3.310)
&rst
ixpk= 2, nxpk= 0, iat= 573, 586, r1= 2.26, r2= 2.76, r3= 4.01, r4= 4.51, &end

```



```

#
# 18 DC H6  18 DC H3'  3.420  4.920
&rst
ixpk= 2, nxpk= 0, iat= 573, 584, r1= 2.92, r2= 3.42, r3= 4.92, r4= 5.42, &end
#
# 18 DC H6  18 DC H4'  3.660  4.650
&rst
ixpk= 2, nxpk= 0, iat= 573, 567, r1= 3.16, r2= 3.66, r3= 4.65, r4= 5.15, &end
#
# 18 DC H6  18 DC H5'1  3.480  5.610
&rst
ixpk= 2, nxpk= 0, iat= 573, 564, r1= 2.98, r2= 3.48, r3= 5.61, r4= 6.11, &end
#
# 18 DC H6  18 DC H5'2  2.650  4.690 (#98,101,103,109,115 3.350  4.690 )
&rst
ixpk= 3, nxpk= 0, iat= 573, 565, r1= 2.15, r2= 2.65, r3= 4.69, r4= 5.19, &end
#
# 18 DC H5  17 DG H1'  3.930  5.440 (#1,21,32,39,54,59,60,70 2.930  3.440 )
&rst
ixpk= 2, nxpk= 0, iat= 575, 537, r1= 3.43, r2= 3.93, r3= 5.44, r4= 5.94, &end
#
# 18 DC H5  17 DG H3'  3.380  4.520 (#96,100,121 3.380  4.220 )
&rst
ixpk= 3, nxpk= 0, iat= 575, 554, r1= 2.88, r2= 3.38, r3= 4.52, r4= 5.02, &end
#
# 19 DG H2'2 19 DG H1'  1.960  3.060 (#op 92 1.960  2.960 )
&rst
ixpk= 92, nxpk= 0, iat= 620, 600, r1= 1.46, r2= 1.96, r3= 3.06, r4= 3.56, &end
#
# 19 DG H2'1 19 DG H1'  2.240  3.250
&rst
ixpk= 92, nxpk= 0, iat= 619, 600, r1= 1.74, r2= 2.24, r3= 3.25, r4= 3.75, &end
#
# 19 DG H3'  7 DKA H19  3.240  4.640 (#op 95 3.240  4.540 )
&rst
ixpk= 95, nxpk= 0, iat= 617, 217, r1= 2.74, r2= 3.24, r3= 4.64, r4= 5.14, &end
#
# 19 DG H3'  18 DC H1'  3.110  5.170
&rst
ixpk= 95, nxpk= 0, iat= 617, 570, r1= 2.61, r2= 3.11, r3= 5.17, r4= 5.67, &end
#
# 19 DG H3'  18 DC H6  4.480  6.180 (#102,104,125 4.480  5.880 )
&rst
ixpk= 4, nxpk= 0, iat= 617, 573, r1= 3.98, r2= 4.48, r3= 6.18, r4= 6.68, &end
#
# 19 DG H3'  19 DG H2'1  2.810  3.510 (#75 2.910  3.510 )
&rst
ixpk= 2, nxpk= 0, iat= 617, 619, r1= 2.31, r2= 2.81, r3= 3.51, r4= 4.01, &end
#
# 19 DG H8  7 DKA H19  2.930  3.890 (#114 2.930  3.790 )
&rst
ixpk= 2, nxpk= 0, iat= 603, 217, r1= 2.43, r2= 2.93, r3= 3.89, r4= 4.39, &end
#
# 19 DG H8  18 DC H1'  2.870  5.230
&rst

```

```

ixpk= 2, nxpk= 0, iat= 603, 570, r1= 2.37, r2= 2.87, r3= 5.23, r4= 5.73, &end
#
# 19 DG H8 18 DC H2'2 3.850 5.120 (#93 3.850 4.920 )
&rst
ixpk= 3, nxpk= 0, iat= 603, 587, r1= 3.35, r2= 3.85, r3= 5.12, r4= 5.62, &end
#
# 19 DG H8 19 DG H2'1 1.960 3.520 (#op 64,76,90,91,99 1.960 2.820 )
&rst
ixpk= 64, nxpk= 0, iat= 603, 619, r1= 1.46, r2= 1.96, r3= 3.52, r4= 4.02, &end
#
# 19 DG H8 19 DG H3' 3.870 6.470
&rst
ixpk= 64, nxpk= 0, iat= 603, 617, r1= 3.37, r2= 3.87, r3= 6.47, r4= 6.97, &end
#
# 20 DC H2'2 20 DC H1' 1.860 3.030 (#op 1,3,22,26,34,56,66 1.760 2.130)
&rst
ixpk= 1, nxpk= 0, iat= 650, 633, r1= 1.36, r2= 1.86, r3= 3.03, r4= 3.53, &end
#
# 20 DC H2'1 20 DC H1' 2.250 4.050 (#4,11,15,16,24 2.750 4.950)
&rst
ixpk= 2, nxpk= 0, iat= 649, 633, r1= 1.75, r2= 2.25, r3= 4.05, r4= 4.55, &end
#
# 20 DC H3' 20 DC H1' 3.380 5.460
&rst
ixpk= 2, nxpk= 0, iat= 647, 633, r1= 2.88, r2= 3.38, r3= 5.46, r4= 5.96, &end
#
# 20 DC H3' 20 DC H2'2 2.210 3.200
&rst
ixpk= 2, nxpk= 0, iat= 647, 650, r1= 1.71, r2= 2.21, r3= 3.20, r4= 3.70, &end
#
# 20 DC H6 19 DG H1' 2.780 3.150
&rst
ixpk= 2, nxpk= 0, iat= 636, 600, r1= 2.28, r2= 2.78, r3= 3.15, r4= 3.65, &end
#
# 20 DC H6 19 DG H2'2 2.690 3.910 (#30,42,43,48,60,94 2.690 3.110 )
&rst
ixpk= 2, nxpk= 0, iat= 636, 620, r1= 2.19, r2= 2.69, r3= 3.91, r4= 4.41, &end
#
# 20 DC H6 19 DG H8 3.140 4.480 (#79,81,85,87,96,98 2.940 3.480 )
&rst
ixpk= 2, nxpk= 0, iat= 636, 603, r1= 2.64, r2= 3.14, r3= 4.48, r4= 4.98, &end
#
# 20 DC H6 20 DC H1' 2.560 3.740 (#51,59,89 2.560 3.340 )
&rst
ixpk= 2, nxpk= 0, iat= 636, 633, r1= 2.06, r2= 2.56, r3= 3.74, r4= 4.24, &end
#
# 20 DC H6 20 DC H2'2 2.120 5.880 (#op 73 2.320 5.880 )
&rst
ixpk= 73, nxpk= 0, iat= 636, 650, r1= 1.62, r2= 2.12, r3= 5.88, r4= 6.38, &end
#
# 20 DC H6 20 DC H2'1 1.860 3.730 (#op 49,63,80,82,83,84 1.860 2.530 )
&rst
ixpk= 49, nxpk= 0, iat= 636, 649, r1= 1.36, r2= 1.86, r3= 3.73, r4= 4.23, &end
#
# 20 DC H6 20 DC H3' 3.860 6.310

```

```

&rst
ixpk= 49, nxpk= 0, iat= 636, 647, r1= 3.36, r2= 3.86, r3= 6.31, r4= 6.81, &end
#
# 20 DC H6  20 DC H4'  4.400  6.780
&rst
ixpk= 49, nxpk= 0, iat= 636, 630, r1= 3.90, r2= 4.40, r3= 6.78, r4= 7.28, &end
#
# 20 DC H6  20 DC H5'1  3.650  6.020
&rst
ixpk= 49, nxpk= 0, iat= 636, 627, r1= 3.15, r2= 3.65, r3= 6.02, r4= 6.52, &end
#
# 20 DC H6  20 DC H5'2  3.970  5.060 (#61,65,68,72 3.570 4.660 )
&rst
ixpk= 3, nxpk= 0, iat= 636, 628, r1= 3.47, r2= 3.97, r3= 5.06, r4= 5.56, &end
#
# 20 DC H5  19 DG H2'1  3.000  4.390 (#17,27,40 3.000 3.990 )
&rst
ixpk= 3, nxpk= 0, iat= 638, 619, r1= 2.50, r2= 3.00, r3= 4.39, r4= 4.89, &end
#
# 20 DC H5  19 DG H8   3.370  4.930 (#95 3.470 4.930 )
&rst
ixpk= 3, nxpk= 0, iat= 638, 603, r1= 2.87, r2= 3.37, r3= 4.93, r4= 5.43, &end
#
# 20 DC H5  20 DC H2'2  3.270  4.770
&rst
ixpk= 3, nxpk= 0, iat= 638, 650, r1= 2.77, r2= 3.27, r3= 4.77, r4= 5.27, &end
#
# 20 DC H5  20 DC H2'1  3.410  5.530 (#100,103 3.410 5.330 )
&rst
ixpk= 3, nxpk= 0, iat= 638, 649, r1= 2.91, r2= 3.41, r3= 5.53, r4= 6.03, &end
#
# 21 DC H2'1 21 DC H1'  2.010  2.600
(#21 DC H1' 20 DC H5  3.140  4.350 #2,3,4,38,41,42,70 3.140 3.450 )
&rst
ixpk= 3, nxpk= 0, iat= 679, 663, r1= 1.51, r2= 2.01, r3= 2.60, r4= 3.10, &end
#
# 21 DC H3' 21 DC H2'2  2.280  2.810
&rst
ixpk= 3, nxpk= 0, iat= 677, 680, r1= 1.78, r2= 2.28, r3= 2.81, r4= 3.31, &end
#
# 21 DC H3' 21 DC H2'1  2.510  4.230
&rst
ixpk= 3, nxpk= 0, iat= 677, 679, r1= 2.01, r2= 2.51, r3= 4.23, r4= 4.73, &end
#
# 21 DC H6  20 DC H2'2  2.140  2.950
(#21 DC H6  20 DC H1'  2.540  4.130 #10,14,19,23,29,32,35 2.640 3.630 )
&rst
ixpk= 3, nxpk= 0, iat= 666, 650, r1= 1.64, r2= 2.14, r3= 2.95, r4= 3.45, &end
#
# 21 DC H6  20 DC H2'1  2.400  3.930 (#31 2.500 3.930 )
&rst
ixpk= 2, nxpk= 0, iat= 666, 649, r1= 1.90, r2= 2.40, r3= 3.93, r4= 4.43, &end
#
# 21 DC H6  20 DC H6   3.100  4.290 (#107,119 3.100 4.090 )
&rst

```

```

ixpk= 3, nxpk= 0, iat= 666, 636, r1= 2.60, r2= 3.10, r3= 4.29, r4= 4.79, &end
#
# 21 DC H6  21 DC H1'  2.860  4.170
&rst
ixpk= 3, nxpk= 0, iat= 666, 663, r1= 2.36, r2= 2.86, r3= 4.17, r4= 4.67, &end
#
# 21 DC H6  21 DC H2'2  2.110  4.140 (#op 55 2.210  4.140  )
&rst
ixpk= 55, nxpk= 0, iat= 666, 680, r1= 1.61, r2= 2.11, r3= 4.14, r4= 4.64, &end
#
# 21 DC H6  21 DC H2'1  1.770  3.290 (#28,33,43,57,74,75,105 1.770  2.290  )
&rst
ixpk= 1, nxpk= 0, iat= 666, 679, r1= 1.27, r2= 1.77, r3= 3.29, r4= 3.79, &end
#
# 21 DC H6  21 DC H3'  2.960  4.530 (#13,18,20,46,65,97 2.960  3.630  )
&rst
ixpk= 2, nxpk= 0, iat= 666, 677, r1= 2.46, r2= 2.96, r3= 4.53, r4= 5.03, &end
#
# 21 DC H5  20 DC H2'2  2.380  3.790
(#21 DC H5  20 DC H1'  3.300  6.010 #25,30,36,45,47,49,50,62 3.300  #5.210  )
&rst
ixpk= 2, nxpk= 0, iat= 668, 650, r1= 1.88, r2= 2.38, r3= 3.79, r4= 4.29, &end
#
# 21 DC H5  20 DC H2'1  2.770  4.600 (#69 2.770  4.500  )
&rst
ixpk= 2, nxpk= 0, iat= 668, 649, r1= 2.27, r2= 2.77, r3= 4.60, r4= 5.10, &end
#
# 21 DC H5  20 DC H6  3.020  3.650 (#114 3.020  3.550  )
&rst
ixpk= 3, nxpk= 0, iat= 668, 636, r1= 2.52, r2= 3.02, r3= 3.65, r4= 4.15, &end
#
# 21 DC H5  20 DC H5  3.690  5.980 (#78,79,92,93 4.090  5.980  )
&rst
ixpk= 4, nxpk= 0, iat= 668, 638, r1= 3.19, r2= 3.69, r3= 5.98, r4= 6.48, &end
#
# 21 DC H5  21 DC H2'2  2.910  4.530
&rst
ixpk= 4, nxpk= 0, iat= 668, 680, r1= 2.41, r2= 2.91, r3= 4.53, r4= 5.03, &end
#
# 21 DC H5  21 DC H2'1  2.820  5.150 (#45,48,51,59,101,109,154 2.620  4.450  )
&rst
ixpk= 2, nxpk= 0, iat= 668, 679, r1= 2.32, r2= 2.82, r3= 5.15, r4= 5.65, &end
#
# 22 DG H2'2  22 DG H1'  1.680  3.030 (#op 22,27,42,63 1.680  2.530  )
&rst
ixpk= 22, nxpk= 0, iat= 713, 693, r1= 1.18, r2= 1.68, r3= 3.03, r4= 3.53, &end
#
# 22 DG H2'1  22 DG H1'  2.130  3.800
&rst
ixpk= 22, nxpk= 0, iat= 712, 693, r1= 1.63, r2= 2.13, r3= 3.80, r4= 4.30, &end
#
# 22 DG H3'  22 DG H1'  2.910  3.950
&rst
ixpk= 22, nxpk= 0, iat= 710, 693, r1= 2.41, r2= 2.91, r3= 3.95, r4= 4.45, &end
#

```

```

# 22 DG H8 21 DC H1' 2.610 3.540
&rst
ixpk= 22, nxpk= 0, iat= 696, 663, r1= 2.11, r2= 2.61, r3= 3.54, r4= 4.04, &end
#
# 22 DG H8 21 DC H2'2 2.620 4.370 (#40,116,167 2.620 4.070 )
&rst
ixpk= 2, nxpk= 0, iat= 696, 680, r1= 2.12, r2= 2.62, r3= 4.37, r4= 4.87, &end
#
# 22 DG H8 21 DC H2'1 2.400 4.090 (#25,60,85,125 2.800 4.090 )
&rst
ixpk= 2, nxpk= 0, iat= 696, 679, r1= 1.90, r2= 2.40, r3= 4.09, r4= 4.59, &end
#
# 22 DG H8 21 DC H3' 3.600 5.020
&rst
ixpk= 2, nxpk= 0, iat= 696, 677, r1= 3.10, r2= 3.60, r3= 5.02, r4= 5.52, &end
#
# 22 DG H8 22 DG H1' 2.570 3.870
(#22 DG H8 21 DC H6 3.300 5.120 #72,91,95,96,99,110 3.300 4.120 )
&rst
ixpk= 2, nxpk= 0, iat= 696, 693, r1= 2.07, r2= 2.57, r3= 3.87, r4= 4.37, &end
#
# 22 DG H8 22 DG H3' 2.730 4.830 (#op 32,37,53,57,68,89 2.730 4.130 )
&rst
ixpk= 32, nxpk= 0, iat= 696, 710, r1= 2.23, r2= 2.73, r3= 4.83, r4= 5.33, &end
#
# 23 DA H2'2 23 DA H1' 1.970 3.070 (#22,26,52,112 1.970 2.570 )
&rst
ixpk= 1, nxpk= 0, iat= 745, 726, r1= 1.47, r2= 1.97, r3= 3.07, r4= 3.57, &end
#
# 23 DA H2'1 23 DA H1' 2.330 4.500 (#82 2.430 4.500 )
&rst
ixpk= 2, nxpk= 0, iat= 744, 726, r1= 1.83, r2= 2.33, r3= 4.50, r4= 5.00, &end
#
# 23 DA H8 22 DG H1' 2.570 3.350
&rst
ixpk= 2, nxpk= 0, iat= 729, 693, r1= 2.07, r2= 2.57, r3= 3.35, r4= 3.85, &end
#
# 23 DA H8 22 DG H3' 3.920 6.440
&rst
ixpk= 2, nxpk= 0, iat= 729, 710, r1= 3.42, r2= 3.92, r3= 6.44, r4= 6.94, &end
#
# 23 DA H8 23 DA H1' 2.580 4.010 (#9,19 2.580 3.210 ci)
&rst
ixpk= 2, nxpk= 0, iat= 729, 726, r1= 2.08, r2= 2.58, r3= 4.01, r4= 4.51, &end
#
# 23 DA H8 23 DA H2'2 2.270 2.900
&rst
ixpk= 2, nxpk= 0, iat= 729, 745, r1= 1.77, r2= 2.27, r3= 2.90, r4= 3.40, &end
#
# 23 DA H8 23 DA H3' 3.050 4.530 (#20 3.050 4.430)
&rst
ixpk= 3, nxpk= 0, iat= 729, 742, r1= 2.55, r2= 3.05, r3= 4.53, r4= 5.03, &end
#
# 23 DA H8 23 DA H4' 3.910 5.890
&rst

```

```

ixpk= 3, nxpk= 0, iat= 729, 723, r1= 3.41, r2= 3.91, r3= 5.89, r4= 6.39, &end
#
# 23 DA H8 23 DA H5'1 3.320 6.040
&rst
ixpk= 3, nxpk= 0, iat= 729, 720, r1= 2.82, r2= 3.32, r3= 6.04, r4= 6.54, &end
#
# 23 DA H8 23 DA H5'2 3.610 5.680
&rst
ixpk= 3, nxpk= 0, iat= 729, 721, r1= 3.11, r2= 3.61, r3= 5.68, r4= 6.18, &end
#
# 24 DG3 H2'2 24 DG3 H1' 2.110 3.010 (#op 12,16,18,54 2.110 2.610 )
&rst
ixpk= 12, nxpk= 0, iat= 778, 758, r1= 1.61, r2= 2.11, r3= 3.01, r4= 3.51, &end
#
# 24 DG3 H3' 24 DG3 H1' 2.820 3.820
&rst
ixpk= 12, nxpk= 0, iat= 775, 758, r1= 2.32, r2= 2.82, r3= 3.82, r4= 4.32, &end
#
# 24 DG3 H8 23 DA H1' 1.860 3.310 (#op 66,67,70,71,84,93,94* 1.760 2.210 )
&rst
ixpk= 66, nxpk= 0, iat= 761, 726, r1= 1.36, r2= 1.86, r3= 3.31, r4= 3.81, &end
#
# 24 DG3 H8 23 DA H2'2 2.420 3.810 (#15,17,31,41,73 2.420 3.210)
&rst
ixpk= 2, nxpk= 0, iat= 761, 745, r1= 1.92, r2= 2.42, r3= 3.81, r4= 4.31, &end
#
# 24 DG3 H8 23 DA H3' 3.440 5.890
&rst
ixpk= 2, nxpk= 0, iat= 761, 742, r1= 2.94, r2= 3.44, r3= 5.89, r4= 6.39, &end
#
# 24 DG3 H8 23 DA H8 3.410 5.300
&rst
ixpk= 2, nxpk= 0, iat= 761, 729, r1= 2.91, r2= 3.41, r3= 5.30, r4= 5.80, &end
#
# 24 DG3 H8 24 DG3 H1' 2.690 3.890
&rst
ixpk= 2, nxpk= 0, iat= 761, 758, r1= 2.19, r2= 2.69, r3= 3.89, r4= 4.39, &end
#
# 24 DG3 H8 24 DG3 H2'2 1.930 2.930 (#op 32 1.930 2.830 )
&rst
ixpk= 32, nxpk= 0, iat= 761, 778, r1= 1.43, r2= 1.93, r3= 2.93, r4= 3.43, &end
#
# 24 DG3 H8 24 DG3 H3' 2.950 6.050
&rst
ixpk= 32, nxpk= 0, iat= 761, 775, r1= 2.45, r2= 2.95, r3= 6.05, r4= 6.55, &end

```

IQ at G¹

```
#
# 1 DC5 H2'1 1 DC5 H1' 2.210 3.980
&rst
ixpk= 0, nxpk= 0, iat= 26, 10, r1= 1.71, r2= 2.21, r3= 3.98, r4= 4.48,
rk2=20.0, rk3=20.0, ir6=1, ialtd=0,
&end
#
# 1 DC5 H3' 1 DC5 H1' 3.450 5.910
&rst
ixpk= 0, nxpk= 0, iat= 24, 10, r1= 2.95, r2= 3.45, r3= 5.91, r4= 6.41, &end
#
# 1 DC5 H3' 1 DC5 H2'2 2.380 4.610 (#1 3.080 4.610 )
&rst
ixpk= 3, nxpk= 0, iat= 24, 27, r1= 1.88, r2= 2.38, r3= 4.61, r4= 5.11, &end
#
# 1 DC5 H3' 1 DC5 H2'1 2.320 2.620
&rst
ixpk= 3, nxpk= 0, iat= 24, 26, r1= 1.82, r2= 2.32, r3= 2.62, r4= 3.12, &end
#
# 1 DC5 H6 1 DC5 H1' 3.000 5.700
&rst
ixpk= 3, nxpk= 0, iat= 13, 10, r1= 2.50, r2= 3.00, r3= 5.70, r4= 6.20, &end
#
# 1 DC5 H6 1 DC5 H2'1 2.950 5.310 (#1,7,8,57 3.850 5.310 )
&rst
ixpk= 3, nxpk= 0, iat= 13, 26, r1= 2.45, r2= 2.95, r3= 5.31, r4= 5.81, &end
#
# 1 DC5 H6 1 DC5 H3' 4.290 5.580 (#1,28,59 5.390 6.580 )
&rst
ixpk= 5, nxpk= 0, iat= 13, 24, r1= 3.79, r2= 4.29, r3= 5.58, r4= 6.08, &end
#
# 1 DC5 H5 1 DC5 H6 2.100 2.600 (#ma )
&rst
ixpk= 5, nxpk= 0, iat= 15, 13, r1= 1.60, r2= 2.10, r3= 2.60, r4= 3.10, &end
#
# 2 DT H2'2 2 DT H1' 2.120 2.960 (#1,5 2.120 2.360 )
&rst
ixpk= 2, nxpk= 0, iat= 59, 40, r1= 1.62, r2= 2.12, r3= 2.96, r4= 3.46, &end
#
# 2 DT H2'1 2 DT H1' 2.350 3.630 (#1 2.650 3.630 )
&rst
ixpk= 2, nxpk= 0, iat= 58, 40, r1= 1.85, r2= 2.35, r3= 3.63, r4= 4.13, &end
#
# 2 DT H3' 2 DT H1' 3.620 5.210
&rst
ixpk= 2, nxpk= 0, iat= 56, 40, r1= 3.12, r2= 3.62, r3= 5.21, r4= 5.71, &end
#
# 2 DT H3' 2 DT H2'2 2.340 3.360 (#15,41 2.540 3.360 )
&rst
ixpk= 2, nxpk= 0, iat= 56, 59, r1= 1.84, r2= 2.34, r3= 3.36, r4= 3.86, &end
#
# 2 DT H3' 2 DT H2'1 2.300 2.740 (#34,53 2.300 2.640 )
```

```

&rst
ixpk= 2, nxpk= 0, iat= 56, 58, r1= 1.80, r2= 2.30, r3= 2.74, r4= 3.24, &end
#
# 2 DT H4' 2 DT H1' 2.650 3.220 (#61 2.650 2.920 )
&rst
ixpk= 2, nxpk= 0, iat= 37, 40, r1= 2.15, r2= 2.65, r3= 3.22, r4= 3.72, &end
#
# 2 DT H6 1 DC5 H1' 1.480 3.140 (#op 1,18,46,61 1.480 1.940 )
&rst
ixpk= 1, nxpk= 0, iat= 43, 10, r1= 0.98, r2= 1.48, r3= 3.14, r4= 3.64, &end
#
# 2 DT H6 1 DC5 H3' 3.100 4.670 (#22,59 3.100 4.470 )
&rst
ixpk= 3, nxpk= 0, iat= 43, 24, r1= 2.60, r2= 3.10, r3= 4.67, r4= 5.17, &end
#
# 2 DT H6 2 DT H1' 3.050 5.770
&rst
ixpk= 3, nxpk= 0, iat= 43, 40, r1= 2.55, r2= 3.05, r3= 5.77, r4= 6.27, &end
#
# 2 DT H6 2 DT H3' 3.210 5.240
&rst
ixpk= 3, nxpk= 0, iat= 43, 56, r1= 2.71, r2= 3.21, r3= 5.24, r4= 5.74, &end
#
# 2 DT Q5 1 DC5 H1' 2.530 4.500
&rst
ixpk= 3, nxpk= 0, iat= -1, 10, r1= 2.03, r2= 2.53, r3= 5.40, r4= 5.90,
igr1= 46, 47, 48,
&end
#
# 2 DT Q5 1 DC5 H3' 3.270 4.350 (#1,61 3.270 3.750 )
&rst
ixpk= 3, nxpk= 0, iat= -1, 24, r1= 2.77, r2= 3.27, r3= 5.22, r4= 5.72,
igr1= 46, 47, 48,
&end
#
# 2 DT Q5 1 DC5 H6 3.390 5.100
&rst
ixpk= 3, nxpk= 0, iat= -1, 13, r1= 2.89, r2= 3.39, r3= 6.12, r4= 6.62,
igr1= 46, 47, 48,
&end
#
# 2 DT Q5 1 DC5 H5 3.200 3.840 (#53,59 3.200 3.540 )
&rst
ixpk= 3, nxpk= 0, iat= -1, 15, r1= 2.70, r2= 3.20, r3= 4.61, r4= 5.11,
igr1= 46, 47, 48,
&end
#
# 2 DT Q5 2 DT H6 2.310 5.320
&rst
ixpk= 3, nxpk= 0, iat= -1, 43, r1= 1.81, r2= 2.31, r3= 6.39, r4= 6.89,
igr1= 46, 47, 48,
&end
#
# 2 DT Q5 1 DC5 H2'2 2.500 3.500 (#ma )
&rst

```



```

ixpk= 3, nxpk= 0, iat= -1, 27, r1= 2.00, r2= 2.50, r3= 4.20, r4= 4.70,
igr1= 46, 47, 48,
&end
#
# 3 DC H2'2 3 DC H1' 2.030 3.030 (#1,51 2.330 2.530 )
&rst
ixpk= 2, nxpk= 0, iat= 89, 72, r1= 1.53, r2= 2.03, r3= 3.03, r4= 3.53, &end
#
# 2 DT Q5 2 DT H1' 4.900 6.160 (#1,4,6,27,33 3.900 5.360 ca 3 H2' )
&rst
ixpk= 3, nxpk= 0, iat= -1, 40, r1= 4.40, r2= 4.90, r3= 7.40, r4= 7.90,
igr1= 46, 47, 48,
&end
#
# 3 DC H2'1 3 DC H1' 2.460 3.790 (#1,32 3.060 5.790 )
&rst
ixpk= 3, nxpk= 0, iat= 88, 72, r1= 1.96, r2= 2.46, r3= 3.79, r4= 4.29, &end
#
# 3 DC H6 2 DT H1' 3.540 4.320 (#30,37 3.540 4.120 )
&rst
ixpk= 3, nxpk= 0, iat= 75, 40, r1= 3.04, r2= 3.54, r3= 4.32, r4= 4.82, &end
#
# 3 DC H6 2 DT H2'1 2.260 4.440 (#1,23,24 3.060 4.440)
&rst
ixpk= 3, nxpk= 0, iat= 75, 58, r1= 1.76, r2= 2.26, r3= 4.44, r4= 4.94, &end
#
# 3 DC H6 3 DC H1' 3.390 3.760 (#53 3.390 3.560 )
&rst
ixpk= 3, nxpk= 0, iat= 75, 72, r1= 2.89, r2= 3.39, r3= 3.76, r4= 4.26, &end
#
# 3 DC H6 3 DC H2'1 2.300 3.660 (#10,35,59,62 2.300 2.560 )
&rst
ixpk= 2, nxpk= 0, iat= 75, 88, r1= 1.80, r2= 2.30, r3= 3.66, r4= 4.16, &end
#
# 3 DC H6 3 DC H3' 4.170 5.630
&rst
ixpk= 2, nxpk= 0, iat= 75, 86, r1= 3.67, r2= 4.17, r3= 5.63, r4= 6.13, &end
#
# 3 DC H5 2 DT H1' 3.910 4.940
&rst
ixpk= 2, nxpk= 0, iat= 77, 40, r1= 3.41, r2= 3.91, r3= 4.94, r4= 5.44, &end
#
# 3 DC H5 2 DT H2'1 3.070 3.970 (#op 17,61 3.070 3.870 )
&rst
ixpk= 17, nxpk= 0, iat= 77, 58, r1= 2.57, r2= 3.07, r3= 3.97, r4= 4.47, &end
#
# 3 DC H5 2 DT Q5 3.030 5.150 (#1,21,38 3.030 3.250 ca 3 H2')
&rst
ixpk= 3, nxpk= 0, iat= 77, -1, r1= 2.53, r2= 3.03, r3= 6.18, r4= 6.68,
igr2= 46, 47, 48,
&end
#
# 3 DC H5 3 DC H6 2.100 2.600 (#ma )
&rst
ixpk= 3, nxpk= 0, iat= 77, 75, r1= 1.60, r2= 2.10, r3= 2.60, r4= 3.10, &end

```

```

#
# 4 DKA H2'2 4 DKA H1' 2.070 3.060 (#op 1,42 2.070 2.460 )
&rst
ixpk= 1, nxpk= 0, iat= 105, 102, r1= 1.57, r2= 2.07, r3= 3.06, r4= 3.56, &end
#
# 4 DKA H2'1 4 DKA H1' 2.390 4.490 (#br 1,14,59 3.090 4.490 )
&rst
ixpk= 1, nxpk= 0, iat= 104, 102, r1= 1.89, r2= 2.39, r3= 4.49, r4= 4.99, &end
#
# 4 DKA H3' 4 DKA H1' 3.780 5.540 (#11 3.880 5.540 )
&rst
ixpk= 3, nxpk= 0, iat= 145, 102, r1= 3.28, r2= 3.78, r3= 5.54, r4= 6.04, &end
#
# 4 DKA H3' 4 DKA H2'1 2.470 2.780
&rst
ixpk= 3, nxpk= 0, iat= 145, 104, r1= 1.97, r2= 2.47, r3= 2.78, r4= 3.28, &end
#
# 4 DKA H19 4 DKA H20 2.370 2.750
&rst
ixpk= 3, nxpk= 0, iat= 125, 127, r1= 1.87, r2= 2.37, r3= 2.75, r4= 3.25, &end
#
# 4 DKA H11 4 DKA H1' 2.820 3.580
&rst
ixpk= 3, nxpk= 0, iat= 118, 102, r1= 2.32, r2= 2.82, r3= 3.58, r4= 4.08, &end
#
# 4 DKA H11 4 DKA H2'2 3.300 6.090 (#br 1,20,43 3.300 4.690 )
&rst
ixpk= 1, nxpk= 0, iat= 118, 105, r1= 2.80, r2= 3.30, r3= 6.09, r4= 6.59, &end
#
# 4 DKA H11 4 DKA H2'1 5.110 6.060 (#53,61,62 5.410 6.560 )
&rst
ixpk= 5, nxpk= 0, iat= 118, 104, r1= 4.61, r2= 5.11, r3= 6.06, r4= 6.56, &end
#
# 4 DKA Q13 4 DKA H11 2.970 3.500 (#1,61 3.370 3.500)
&rst
ixpk= 3, nxpk= 0, iat= -1, 118, r1= 2.47, r2= 2.97, r3= 4.20, r4= 4.70,
igr1= 136, 137, 138,
&end
#
# 4 DKA Q13 4 DKA H1' 3.400 4.800 (#ma )
&rst
ixpk= 3, nxpk= 0, iat= -1, 102, r1= 2.90, r2= 3.40, r3= 5.76, r4= 6.26,
igr1= 136, 137, 138,
&end
#
# 4 DKA H18 4 DKA H19 2.330 2.530
&rst
ixpk= 3, nxpk= 0, iat= 123, 125, r1= 1.83, r2= 2.33, r3= 2.53, r4= 3.03, &end
#
# 4 DKA H8 3 DC H1' 3.920 4.180 (#61 3.920 4.180 )
&rst
ixpk= 3, nxpk= 0, iat= 143, 72, r1= 3.42, r2= 3.92, r3= 4.18, r4= 4.68, &end
#
# 4 DKA H8 3 DC H2'2 3.000 4.550 (#1,25 3.000 3.150 )
&rst

```

```

ixpk= 3, nxpk= 0, iat= 143, 89, r1= 2.50, r2= 3.00, r3= 4.55, r4= 5.05, &end
#
# 4 DKA H8 3 DC H2'1 2.350 4.040 (#1,36,61,63 3.350 4.040 )
&rst
ixpk= 3, nxpk= 0, iat= 143, 88, r1= 1.85, r2= 2.35, r3= 4.04, r4= 4.54, &end
#
# 4 DKA H8 3 DC H6 4.330 5.260 (#40,63 4.330 5.060 )
&rst
ixpk= 4, nxpk= 0, iat= 143, 75, r1= 3.83, r2= 4.33, r3= 5.26, r4= 5.76, &end
#
# 4 DKA H8 4 DKA H1' 3.340 3.960 (#53 3.340 3.760 )
&rst
ixpk= 3, nxpk= 0, iat= 143, 102, r1= 2.84, r2= 3.34, r3= 3.96, r4= 4.46, &end
#
# 4 DKA H8 4 DKA H2'2 2.200 5.440 (#1,13 2.900 5.440 )
&rst
ixpk= 2, nxpk= 0, iat= 143, 105, r1= 1.70, r2= 2.20, r3= 5.44, r4= 5.94, &end
#
# 4 DKA H8 4 DKA H3' 3.350 4.570 (#1,26 3.350 3.970 )
&rst
ixpk= 3, nxpk= 0, iat= 143, 145, r1= 2.85, r2= 3.35, r3= 4.57, r4= 5.07, &end
#
# 5 DG H1' 4 DKA Q13 4.290 5.650 (#59 4.390 5.650 )
&rst
ixpk= 4, nxpk= 0, iat= 158, -1, r1= 3.79, r2= 4.29, r3= 6.79, r4= 7.29,
igr2= 136, 137, 138,
&end
#
# 5 DG H2'2 5 DG H1' 2.250 3.050
&rst
ixpk= 4, nxpk= 0, iat= 178, 158, r1= 1.75, r2= 2.25, r3= 3.05, r4= 3.55, &end
#
# 5 DG H2'1 5 DG H1' 2.350 3.970 (#op 1,19 2.650 3.970 )
&rst
ixpk= 1, nxpk= 0, iat= 177, 158, r1= 1.85, r2= 2.35, r3= 3.97, r4= 4.47, &end
#
# 5 DG H3' 5 DG H1' 3.610 4.900
&rst
ixpk= 1, nxpk= 0, iat= 175, 158, r1= 3.11, r2= 3.61, r3= 4.90, r4= 5.40, &end
#
# 5 DG H8 4 DKA H1' 4.030 4.640
&rst
ixpk= 1, nxpk= 0, iat= 161, 102, r1= 3.53, r2= 4.03, r3= 4.64, r4= 5.14, &end
#
# 5 DG H8 4 DKA Q13 4.540 5.340
&rst
ixpk= 1, nxpk= 0, iat= 161, -1, r1= 4.04, r2= 4.54, r3= 6.41, r4= 6.91,
igr2= 136, 137, 138,
&end
#
# 5 DG H8 5 DG H1' 3.440 3.850 (#53 3.440 3.750 )
&rst
ixpk= 3, nxpk= 0, iat= 161, 158, r1= 2.94, r2= 3.44, r3= 3.85, r4= 4.35, &end
#
# 5 DG H8 5 DG H2'1 2.520 3.610 (#op 1 2.320 2.810 )

```

```

&rst
ixpk= 1, nxpk= 0, iat= 161, 177, r1= 2.02, r2= 2.52, r3= 3.61, r4= 4.11, &end
#
# 5 DG H8 5 DG H3' 3.680 5.150
&rst
ixpk= 1, nxpk= 0, iat= 161, 175, r1= 3.18, r2= 3.68, r3= 5.15, r4= 5.65, &end
#
# 5 DG H8 4 DKA H2'1 3.800 5.000 (#ma )
&rst
ixpk= 1, nxpk= 0, iat= 161, 104, r1= 3.30, r2= 3.80, r3= 5.00, r4= 5.50, &end
#
# 6 DC H2'1 6 DC H1' 2.120 3.080 (#op 1 2.120 2.780 )
&rst
ixpk= 1, nxpk= 0, iat= 207, 191, r1= 1.62, r2= 2.12, r3= 3.08, r4= 3.58, &end
#
# 6 DC H2'2 6 DC H1' 2.400 4.810 (#1,6,45 3.000 4.810 )
&rst
ixpk= 3, nxpk= 0, iat= 208, 191, r1= 1.90, r2= 2.40, r3= 4.81, r4= 5.31, &end
#
# 6 DC H6 5 DG H3' 5.360 6.840 (#wk 2,34,59 6.260 6.840 )
&rst
ixpk= 2, nxpk= 0, iat= 194, 175, r1= 4.86, r2= 5.36, r3= 6.84, r4= 7.34, &end
#
# 6 DC H6 5 DG H8 4.480 5.930 (#61 4.580 6.930 )
&rst
ixpk= 4, nxpk= 0, iat= 194, 161, r1= 3.98, r2= 4.48, r3= 5.93, r4= 6.43, &end
#
# 6 DC H6 6 DC H2'2 2.180 3.040 (#op 22,30 2.180 2.640)
&rst
ixpk= 22, nxpk= 0, iat= 194, 208, r1= 1.68, r2= 2.18, r3= 3.04, r4= 3.54, &end
#
# 6 DC H6 6 DC H3' 4.300 5.000 (#ma 6,62 4.700 6.000 )
&rst
ixpk= 6, nxpk= 0, iat= 194, 205, r1= 3.80, r2= 4.30, r3= 5.00, r4= 5.50, &end
#
# 6 DC H5 5 DG H1' 4.500 5.420
&rst
ixpk= 6, nxpk= 0, iat= 196, 158, r1= 4.00, r2= 4.50, r3= 5.42, r4= 5.92, &end
#
# 6 DC H5 5 DG H2'2 3.270 4.240 (#1 3.270 3.840 )
&rst
ixpk= 3, nxpk= 0, iat= 196, 178, r1= 2.77, r2= 3.27, r3= 4.24, r4= 4.74, &end
#
# 6 DC H5 5 DG H2'1 3.620 4.570 (#53 3.620 4.270 )
&rst
ixpk= 3, nxpk= 0, iat= 196, 177, r1= 3.12, r2= 3.62, r3= 4.57, r4= 5.07, &end
#
# 6 DC H5 5 DG H8 3.730 4.100
&rst
ixpk= 3, nxpk= 0, iat= 196, 161, r1= 3.23, r2= 3.73, r3= 4.10, r4= 4.60, &end
#
# 6 DC H5 6 DC H2'2 3.540 5.260
&rst
ixpk= 3, nxpk= 0, iat= 196, 208, r1= 3.04, r2= 3.54, r3= 5.26, r4= 5.76, &end
#

```

```

# 7 DG H8 6 DC H1' 3.320 4.400 (#op 17 3.520 4.400)
&rst
ixpk= 17, nxpk= 0, iat= 224, 191, r1= 2.82, r2= 3.32, r3= 4.40, r4= 4.90, &end
#
# 7 DG H8 6 DC H2'2 3.100 3.900 (#ma )
&rst
ixpk= 17, nxpk= 0, iat= 224, 208, r1= 2.60, r2= 3.10, r3= 3.90, r4= 4.40, &end
#
# 8 DC H2'2 8 DC H1' 1.790 3.100 (#1,38 1.790 2.300 )
&rst
ixpk= 1, nxpk= 0, iat= 271, 254, r1= 1.29, r2= 1.79, r3= 3.10, r4= 3.60, &end
#
# 8 DC H2'1 8 DC H1' 2.450 3.690 (#1,10 3.150 3.590 )
&rst
ixpk= 3, nxpk= 0, iat= 270, 254, r1= 1.95, r2= 2.45, r3= 3.69, r4= 4.19, &end
#
# 8 DC H3' 8 DC H1' 3.670 5.480 (#7 3.870 5.480 )
&rst
ixpk= 3, nxpk= 0, iat= 268, 254, r1= 3.17, r2= 3.67, r3= 5.48, r4= 5.98, &end
#
# 8 DC H3' 8 DC H2'2 2.390 3.450 (#1,2,3,32 2.790 3.450 )
&rst
ixpk= 2, nxpk= 0, iat= 268, 271, r1= 1.89, r2= 2.39, r3= 3.45, r4= 3.95, &end
#
# 8 DC H3' 8 DC H2'1 2.500 2.920
&rst
ixpk= 2, nxpk= 0, iat= 268, 270, r1= 2.00, r2= 2.50, r3= 2.92, r4= 3.42, &end
#
# 8 DC H6 7 DG H1' 3.050 4.300 (#op 1,19,23,59 2.050 2.500 )
&rst
ixpk= 1, nxpk= 0, iat= 257, 221, r1= 2.55, r2= 3.05, r3= 4.30, r4= 4.80, &end
#
# 8 DC H6 7 DG H2'2 2.420 3.270 (#op 1 2.420 3.070 )
&rst
ixpk= 1, nxpk= 0, iat= 257, 241, r1= 1.92, r2= 2.42, r3= 3.27, r4= 3.77, &end
#
# 8 DC H6 7 DG H2'1 2.480 4.400 (#op 1,61 2.780 5.400 )
&rst
ixpk= 1, nxpk= 0, iat= 257, 240, r1= 1.98, r2= 2.48, r3= 4.40, r4= 4.90, &end
#
# 8 DC H6 7 DG H8 3.640 4.430
(#8 DC H6 7 DG H3' 5.090 6.040 #br 29 5.190 6.840 )
&rst
ixpk= 1, nxpk= 0, iat= 257, 224, r1= 3.14, r2= 3.64, r3= 4.43, r4= 4.93, &end
#
# 8 DC H6 8 DC H1' 2.870 3.770 (#op 1,25 1.870 2.470 )
&rst
ixpk= 1, nxpk= 0, iat= 257, 254, r1= 2.37, r2= 2.87, r3= 3.77, r4= 4.27, &end
#
# 8 DC H6 8 DC H2'2 2.090 4.250 (#op 1 2.890 4.250 )
&rst
ixpk= 1, nxpk= 0, iat= 257, 271, r1= 1.59, r2= 2.09, r3= 4.25, r4= 4.75, &end
#
# 8 DC H6 8 DC H2'1 1.830 3.320 (#br 1,11,14,40,61 1.830 2.420 )
&rst

```

```

ixpk= 1, nxpk= 0, iat= 257, 270, r1= 1.33, r2= 1.83, r3= 3.32, r4= 3.82, &end
#
# 8 DC H6 8 DC H3' 3.710 6.030
&rst
ixpk= 1, nxpk= 0, iat= 257, 268, r1= 3.21, r2= 3.71, r3= 6.03, r4= 6.53, &end
#
# 8 DC H5 7 DG H1' 4.850 5.450 (#53 3.850 5.350 )
&rst
ixpk= 3, nxpk= 0, iat= 259, 221, r1= 4.35, r2= 4.85, r3= 5.45, r4= 5.95, &end
#
# 8 DC H5 7 DG H2'2 3.090 3.900 (#op 1 3.090 3.500 )
&rst
ixpk= 1, nxpk= 0, iat= 259, 241, r1= 2.59, r2= 3.09, r3= 3.90, r4= 4.40, &end
#
# 8 DC H5 7 DG H2'1 3.500 4.970
&rst
ixpk= 1, nxpk= 0, iat= 259, 240, r1= 3.00, r2= 3.50, r3= 4.97, r4= 5.47, &end
#
# 8 DC H5 7 DG H8 3.510 4.330 (#op 53 3.610 4.330 )
&rst
ixpk= 53, nxpk= 0, iat= 259, 224, r1= 3.01, r2= 3.51, r3= 4.33, r4= 4.83, &end
#
# 8 DC H5 8 DC H2'2 2.940 6.700
&rst
ixpk= 53, nxpk= 0, iat= 259, 271, r1= 2.44, r2= 2.94, r3= 6.70, r4= 7.20, &end
#
# 8 DC H5 8 DC H2'1 3.370 5.280
&rst
ixpk= 53, nxpk= 0, iat= 259, 270, r1= 2.87, r2= 3.37, r3= 5.28, r4= 5.78, &end
#
# 8 DC H5 8 DC H6 2.000 2.600 (#ma )
&rst
ixpk= 53, nxpk= 0, iat= 259, 257, r1= 1.50, r2= 2.00, r3= 2.60, r4= 3.10, &end
#
# 9 DC H2'2 9 DC H1' 2.200 3.010 (#1,5 2.200 2.410 )
&rst
ixpk= 2, nxpk= 0, iat= 301, 284, r1= 1.70, r2= 2.20, r3= 3.01, r4= 3.51, &end
#
# 9 DC H2'1 9 DC H1' 2.470 5.080 (#1 3.170 5.580 )
&rst
ixpk= 3, nxpk= 0, iat= 300, 284, r1= 1.97, r2= 2.47, r3= 5.08, r4= 5.58, &end
#
# 9 DC H6 8 DC H1' 4.050 4.660
&rst
ixpk= 3, nxpk= 0, iat= 287, 254, r1= 3.55, r2= 4.05, r3= 4.66, r4= 5.16, &end
#
# 9 DC H6 8 DC H3' 4.740 5.630 (#53 4.840 6.630 )
&rst
ixpk= 4, nxpk= 0, iat= 287, 268, r1= 4.24, r2= 4.74, r3= 5.63, r4= 6.13, &end
#
# 9 DC H6 9 DC H1' 3.290 3.460
&rst
ixpk= 4, nxpk= 0, iat= 287, 284, r1= 2.79, r2= 3.29, r3= 3.46, r4= 3.96, &end
#
# 9 DC H6 9 DC H2'1 2.160 2.560 (#59 2.160 2.460 )

```

```

&rst
ixpk= 2, nxpk= 0, iat= 287, 300, r1= 1.66, r2= 2.16, r3= 2.56, r4= 3.06, &end
#
# 9 DC H5 8 DC H2'2 3.300 4.870
&rst
ixpk= 2, nxpk= 0, iat= 289, 271, r1= 2.80, r2= 3.30, r3= 4.87, r4= 5.37, &end
#
# 9 DC H5 8 DC H2'1 3.010 4.010
&rst
ixpk= 2, nxpk= 0, iat= 289, 270, r1= 2.51, r2= 3.01, r3= 4.01, r4= 4.51, &end
#
# 9 DC H5 8 DC H6 3.340 4.380 (#61 3.340 4.280 )
&rst
ixpk= 3, nxpk= 0, iat= 289, 257, r1= 2.84, r2= 3.34, r3= 4.38, r4= 4.88, &end
#
# 9 DC H5 9 DC H2'1 3.460 4.750 (#53,59 3.460 4.550)
&rst
ixpk= 3, nxpk= 0, iat= 289, 300, r1= 2.96, r2= 3.46, r3= 4.75, r4= 5.25, &end
#
# 9 DC H5 9 DC H6 2.000 2.600 (#ma )
&rst
ixpk= 3, nxpk= 0, iat= 289, 287, r1= 1.50, r2= 2.00, r3= 2.60, r4= 3.10, &end
#
# 10 DA H2'1 10 DA H1' 2.260 3.450
&rst
ixpk= 3, nxpk= 0, iat= 332, 314, r1= 1.76, r2= 2.26, r3= 3.45, r4= 3.95, &end
#
# 10 DA H3' 10 DA H1' 3.250 4.990
&rst
ixpk= 3, nxpk= 0, iat= 330, 314, r1= 2.75, r2= 3.25, r3= 4.99, r4= 5.49, &end
#
# 10 DA H3' 10 DA H2'2 2.320 3.450 (#op 12,41 2.520 3.450 )
&rst
ixpk= 12, nxpk= 0, iat= 330, 333, r1= 1.82, r2= 2.32, r3= 3.45, r4= 3.95, &end
#
# 10 DA H8 9 DC H1' 2.980 3.600 (#24,37 3.280 3.600 )
&rst
ixpk= 3, nxpk= 0, iat= 317, 284, r1= 2.48, r2= 2.98, r3= 3.60, r4= 4.10, &end
#
# 10 DA H8 9 DC H2'2 3.850 5.100 (#1,8 2.950 3.100 )
&rst
ixpk= 2, nxpk= 0, iat= 317, 301, r1= 3.35, r2= 3.85, r3= 5.10, r4= 5.60, &end
#
# 10 DA H8 9 DC H2'1 3.340 5.120 (#1,53,59 3.740 6.120 )
&rst
ixpk= 3, nxpk= 0, iat= 317, 300, r1= 2.84, r2= 3.34, r3= 5.12, r4= 5.62, &end
#
# 10 DA H8 9 DC H6 4.480 5.660
&rst
ixpk= 3, nxpk= 0, iat= 317, 287, r1= 3.98, r2= 4.48, r3= 5.66, r4= 6.16, &end
#
# 10 DA H8 10 DA H3' 4.150 6.080
&rst
ixpk= 3, nxpk= 0, iat= 317, 330, r1= 3.65, r2= 4.15, r3= 6.08, r4= 6.58, &end
#

```

```

# 11 DT H2'1 11 DT H1' 2.330 3.310 (#1 2.730 3.310 )
&rst
ixpk= 2, nxpk= 0, iat= 364, 346, r1= 1.83, r2= 2.33, r3= 3.31, r4= 3.81, &end
#
# 11 DT H6 10 DA H1' 3.320 3.860
&rst
ixpk= 2, nxpk= 0, iat= 349, 314, r1= 2.82, r2= 3.32, r3= 3.86, r4= 4.36, &end
#
# 11 DT H6 10 DA H2'2 2.460 3.210 (#5,10,33 2.460 2.710 )
&rst
ixpk= 2, nxpk= 0, iat= 349, 333, r1= 1.96, r2= 2.46, r3= 3.21, r4= 3.71, &end
#
# 11 DT H6 10 DA H2'1 2.220 4.090 (#op 1,15 2.720 4.090 )
&rst
ixpk= 1, nxpk= 0, iat= 349, 332, r1= 1.72, r2= 2.22, r3= 4.09, r4= 4.59, &end
#
# 11 DT H6 10 DA H8 4.640 6.090 (#29 4.740 6.090 )
&rst
ixpk= 4, nxpk= 0, iat= 349, 317, r1= 4.14, r2= 4.64, r3= 6.09, r4= 6.59, &end
#
# 11 DT H6 11 DT H1' 3.300 3.740 (#4 3.300 3.540 )
&rst
ixpk= 3, nxpk= 0, iat= 349, 346, r1= 2.80, r2= 3.30, r3= 3.74, r4= 4.24, &end
#
# 11 DT H6 11 DT H2'2 2.410 4.370 (#1,6,61 2.910 4.370 )
&rst
ixpk= 2, nxpk= 0, iat= 349, 365, r1= 1.91, r2= 2.41, r3= 4.37, r4= 4.87, &end
#
# 11 DT H6 11 DT H2'1 2.540 3.880 (#op 1 2.040 2.580 )
&rst
ixpk= 1, nxpk= 0, iat= 349, 364, r1= 2.04, r2= 2.54, r3= 3.88, r4= 4.38, &end
#
# 11 DT Q5 10 DA H2'1 3.400 3.550 (#53 3.500 3.550 )
&rst
ixpk= 3, nxpk= 0, iat= -1, 332, r1= 2.90, r2= 3.40, r3= 4.26, r4= 4.76,
igr1= 352, 353, 354,
&end
#
# 11 DT Q5 10 DA H3' 3.880 4.350
&rst
ixpk= 3, nxpk= 0, iat= -1, 330, r1= 3.38, r2= 3.88, r3= 5.22, r4= 5.72,
igr1= 352, 353, 354,
&end
#
# 11 DT Q5 10 DA H8 2.830 3.080
&rst
ixpk= 3, nxpk= 0, iat= -1, 317, r1= 2.33, r2= 2.83, r3= 3.70, r4= 4.20,
igr1= 352, 353, 354,
&end
#
# 11 DT Q5 11 DT H6 2.740 3.100 (#22 2.840 3.100)
&rst
ixpk= 2, nxpk= 0, iat= -1, 349, r1= 2.24, r2= 2.74, r3= 3.72, r4= 4.22,
igr1= 352, 353, 354,
&end

```



```

#
# 11 DT Q5 10 DA H2'2 3.000 4.500 (#ma )
&rst
ixpk= 2, nxpk= 0, iat= -1, 333, r1= 2.50, r2= 3.00, r3= 5.40, r4= 5.90,
igr1= 352, 353, 354,
&end
#
# 12 DC3 H3' 12 DC3 H1' 3.760 5.680 (#1 4.060 5.680 )
&rst
ixpk= 4, nxpk= 0, iat= 392, 378, r1= 3.26, r2= 3.76, r3= 5.68, r4= 6.18, &end
#
# 12 DC3 H6 11 DT H2'2 2.660 3.150
&rst
ixpk= 4, nxpk= 0, iat= 381, 365, r1= 2.16, r2= 2.66, r3= 3.15, r4= 3.65, &end
#
# 12 DC3 H6 11 DT H2'1 2.260 3.680 (#1,16,18,31 3.060 3.680 )
&rst
ixpk= 3, nxpk= 0, iat= 381, 364, r1= 1.76, r2= 2.26, r3= 3.68, r4= 4.18, &end
#
# 12 DC3 H6 12 DC3 H1' 3.300 5.450
&rst
ixpk= 3, nxpk= 0, iat= 381, 378, r1= 2.80, r2= 3.30, r3= 5.45, r4= 5.95, &end
#
# 12 DC3 H5 11 DT H1' 3.850 4.930 (#20,56,59 3.850 4.630 )
&rst
ixpk= 3, nxpk= 0, iat= 383, 346, r1= 3.35, r2= 3.85, r3= 4.93, r4= 5.43, &end
#
# 12 DC3 H5 11 DT H2'2 3.200 4.120 (#op 21 3.400 4.120 )
&rst
ixpk= 21, nxpk= 0, iat= 383, 365, r1= 2.70, r2= 3.20, r3= 4.12, r4= 4.62, &end
#
# 12 DC3 H5 11 DT H2'1 3.370 3.700
&rst
ixpk= 21, nxpk= 0, iat= 383, 364, r1= 2.87, r2= 3.37, r3= 3.70, r4= 4.20, &end
#
# 12 DC3 H5 11 DT H6 3.640 3.950
&rst
ixpk= 21, nxpk= 0, iat= 383, 349, r1= 3.14, r2= 3.64, r3= 3.95, r4= 4.45, &end
#
# 12 DC3 H5 11 DT Q5 4.070 4.500
&rst
ixpk= 21, nxpk= 0, iat= 383, -1, r1= 3.57, r2= 4.07, r3= 5.40, r4= 5.90,
igr2= 352, 353, 354,
&end
#
# 12 DC3 H5 12 DC3 H6 2.000 2.600 (#ma )
&rst
ixpk= 21, nxpk= 0, iat= 383, 381, r1= 1.50, r2= 2.00, r3= 2.60, r4= 3.10, &end
#
# 13 DG5 H2'2 13 DG5 H1' 2.050 3.090 (#op 1 2.050 2.490 )
&rst
ixpk= 1, nxpk= 0, iat= 427, 407, r1= 1.55, r2= 2.05, r3= 3.09, r4= 3.59, &end
#
# 13 DG5 H2'1 13 DG5 H1' 2.350 2.920
&rst

```

```

ixpk= 1, nxpk= 0, iat= 426, 407, r1= 1.85, r2= 2.35, r3= 2.92, r4= 3.42, &end
#
# 13 DG5 H8 13 DG5 H1' 3.130 3.940 (#1,63 3.130 3.540 )
&rst
ixpk= 3, nxpk= 0, iat= 410, 407, r1= 2.63, r2= 3.13, r3= 3.94, r4= 4.44, &end
#
# 13 DG5 H8 13 DG5 H2'2 2.670 4.390 (#op 7,32,59 3.170 4.390 )
&rst
ixpk= 7, nxpk= 0, iat= 410, 427, r1= 2.17, r2= 2.67, r3= 4.39, r4= 4.89, &end
#
# 10 DA H1' 11 DT Q5 3.300 4.250 (#58,61 3.300 4.050 )
&rst
ixpk= 3, nxpk= 0, iat= 314, -1, r1= 2.80, r2= 3.30, r3= 5.10, r4= 5.60,
igr2= 352, 353, 354,
&end
#
# 14 DA H2'1 14 DA H1' 2.340 3.660 (#op 26 2.540 3.660 )
&rst
ixpk= 26, nxpk= 0, iat= 458, 440, r1= 1.84, r2= 2.34, r3= 3.66, r4= 4.16, &end
#
# 14 DA H3' 14 DA H1' 3.190 4.600
&rst
ixpk= 26, nxpk= 0, iat= 456, 440, r1= 2.69, r2= 3.19, r3= 4.60, r4= 5.10, &end
#
# 14 DA H3' 14 DA H2'2 2.340 3.260 (#op 11,14 2.540 3.260 )
&rst
ixpk= 11, nxpk= 0, iat= 456, 459, r1= 1.84, r2= 2.34, r3= 3.26, r4= 3.76, &end
#
# 14 DA H8 13 DG5 H1' 2.980 3.790 (#40 3.180 3.690 )
&rst
ixpk= 3, nxpk= 0, iat= 443, 407, r1= 2.48, r2= 2.98, r3= 3.79, r4= 4.29, &end
#
# 14 DA H8 14 DA H3' 3.330 5.060
&rst
ixpk= 3, nxpk= 0, iat= 443, 456, r1= 2.83, r2= 3.33, r3= 5.06, r4= 5.56, &end
#
# 15 DT H2'2 15 DT H1' 2.170 2.980 (#1 2.170 2.480 )
&rst
ixpk= 2, nxpk= 0, iat= 491, 472, r1= 1.67, r2= 2.17, r3= 2.98, r4= 3.48, &end
#
# 15 DT H2'1 15 DT H1' 2.200 5.590 (#1 3.000 5.590 )
&rst
ixpk= 3, nxpk= 0, iat= 490, 472, r1= 1.70, r2= 2.20, r3= 5.59, r4= 6.09, &end
#
# 15 DT H6 14 DA H1' 3.420 3.860 (#62 3.420 3.860 )
&rst
ixpk= 3, nxpk= 0, iat= 475, 440, r1= 2.92, r2= 3.42, r3= 3.86, r4= 4.36, &end
#
# 15 DT H6 14 DA H2'2 2.590 3.060 (#53 2.590 2.760 )
&rst
ixpk= 2, nxpk= 0, iat= 475, 459, r1= 2.09, r2= 2.59, r3= 3.06, r4= 3.56, &end
#
# 15 DT H6 14 DA H2'1 2.200 4.210 (#op 1,57 3.000 4.210 )
&rst
ixpk= 1, nxpk= 0, iat= 475, 458, r1= 1.70, r2= 2.20, r3= 4.21, r4= 4.71, &end

```

```

#
# 15 DT H6 14 DA H8 4.570 6.190
&rst
ixpk= 1, nxpk= 0, iat= 475, 443, r1= 4.07, r2= 4.57, r3= 6.19, r4= 6.69, &end
#
# 15 DT H6 15 DT H1' 3.280 3.800 (#9,59 3.280 3.500 )
&rst
ixpk= 3, nxpk= 0, iat= 475, 472, r1= 2.78, r2= 3.28, r3= 3.80, r4= 4.30, &end
#
# 15 DT H6 15 DT H2'2 2.550 4.720 (#13,18,30,34,36,38,59 3.350 4.720 )
&rst
ixpk= 3, nxpk= 0, iat= 475, 491, r1= 2.05, r2= 2.55, r3= 4.72, r4= 5.22, &end
#
# 15 DT H6 15 DT H2'1 2.330 4.400 (#1 2.330 2.500 )
&rst
ixpk= 2, nxpk= 0, iat= 475, 490, r1= 1.83, r2= 2.33, r3= 4.40, r4= 4.90, &end
#
# 15 DT Q5 14 DA H1' 3.890 5.020
&rst
ixpk= 2, nxpk= 0, iat= -1, 440, r1= 3.39, r2= 3.89, r3= 6.03, r4= 6.53,
igr1= 478, 479, 480,
&end
#
# 15 DT Q5 14 DA H2'1 3.250 4.110
&rst
ixpk= 2, nxpk= 0, iat= -1, 458, r1= 2.75, r2= 3.25, r3= 4.94, r4= 5.44,
igr1= 478, 479, 480,
&end
#
# 15 DT Q5 14 DA H3' 4.400 4.860
&rst
ixpk= 2, nxpk= 0, iat= -1, 456, r1= 3.90, r2= 4.40, r3= 5.84, r4= 6.34,
igr1= 478, 479, 480,
&end
#
# 15 DT Q5 14 DA H8 3.280 5.570
&rst
ixpk= 2, nxpk= 0, iat= -1, 443, r1= 2.78, r2= 3.28, r3= 6.69, r4= 7.19,
igr1= 478, 479, 480,
&end
#
# 15 DT Q5 15 DT H6 2.770 3.070 (#20 2.870 3.070)
&rst
ixpk= 2, nxpk= 0, iat= -1, 475, r1= 2.27, r2= 2.77, r3= 3.69, r4= 4.19,
igr1= 478, 479, 480,
&end
#
# 15 DT Q5 14 DA H2'2 2.900 4.300 (#ma )
&rst
ixpk= 2, nxpk= 0, iat= -1, 459, r1= 2.40, r2= 2.90, r3= 5.16, r4= 5.66,
igr1= 478, 479, 480,
&end
#
# 16 DG H2'2 16 DG H1' 2.160 3.060 (#op 1 2.160 2.460 )
&rst

```

```

ixpk= 1, nxpk= 0, iat= 524, 504, r1= 1.66, r2= 2.16, r3= 3.06, r4= 3.56, &end
#
# 16 DG H3' 16 DG H1' 3.240 4.300
&rst
ixpk= 1, nxpk= 0, iat= 521, 504, r1= 2.74, r2= 3.24, r3= 4.30, r4= 4.80, &end
#
# 16 DG H8 15 DT H1' 4.030 5.130 (#1,25,61 4.030 4.330 )
&rst
ixpk= 4, nxpk= 0, iat= 507, 472, r1= 3.53, r2= 4.03, r3= 5.13, r4= 5.63, &end
#
# 16 DG H8 15 DT H2'2 3.000 3.130
&rst
ixpk= 4, nxpk= 0, iat= 507, 491, r1= 2.50, r2= 3.00, r3= 3.13, r4= 3.63, &end
#
# 16 DG H8 15 DT H2'1 3.000 3.900 (#1 3.300 3.900 )
&rst
ixpk= 3, nxpk= 0, iat= 507, 490, r1= 2.50, r2= 3.00, r3= 3.90, r4= 4.40, &end
#
# 16 DG H8 15 DT H6 4.460 5.190
&rst
ixpk= 3, nxpk= 0, iat= 507, 475, r1= 3.96, r2= 4.46, r3= 5.19, r4= 5.69, &end
#
# 16 DG H8 16 DG H1' 3.330 3.890 (#37 3.330 3.690 )
&rst
ixpk= 3, nxpk= 0, iat= 507, 504, r1= 2.83, r2= 3.33, r3= 3.89, r4= 4.39, &end
#
# 16 DG H8 16 DG H2'2 2.280 3.310 (#op 10,12 2.580 4.310 )
&rst
ixpk= 10, nxpk= 0, iat= 507, 524, r1= 1.78, r2= 2.28, r3= 3.31, r4= 3.81, &end
#
# 16 DG H8 16 DG H2'1 2.040 3.200 (#op 8,17,29,63 2.040 2.600 )
&rst
ixpk= 8, nxpk= 0, iat= 507, 523, r1= 1.54, r2= 2.04, r3= 3.20, r4= 3.70, &end
#
# 16 DG H8 16 DG H3' 3.820 6.200
&rst
ixpk= 8, nxpk= 0, iat= 507, 521, r1= 3.32, r2= 3.82, r3= 6.20, r4= 6.70, &end
#
# 17 DG H2'1 17 DG H1' 2.360 3.760 (#op 1,14 2.460 3.460 )
&rst
ixpk= 1, nxpk= 0, iat= 556, 537, r1= 1.86, r2= 2.36, r3= 3.76, r4= 4.26, &end
#
# 17 DG H8 16 DG H1' 2.940 3.430
&rst
ixpk= 1, nxpk= 0, iat= 540, 504, r1= 2.44, r2= 2.94, r3= 3.43, r4= 3.93, &end
#
# 17 DG H8 17 DG H1' 2.670 3.880 (#op 1,22,60 2.670 2.880 )
&rst
ixpk= 1, nxpk= 0, iat= 540, 537, r1= 2.17, r2= 2.67, r3= 3.88, r4= 4.38, &end
#
# 17 DG H8 17 DG H2'1 2.170 3.830 (#op 1,23 2.170 2.530 )
&rst
ixpk= 1, nxpk= 0, iat= 540, 556, r1= 1.67, r2= 2.17, r3= 3.83, r4= 4.33, &end
#
# 17 DG H8 17 DG H3' 3.220 5.290

```

```

&rst
ixpk= 1, nxpk= 0, iat= 540, 554, r1= 2.72, r2= 3.22, r3= 5.29, r4= 5.79, &end
#
# 18 DC H2'2 18 DC H1' 1.920 3.080 (#op 1,24 1.920 2.480 )
&rst
ixpk= 1, nxpk= 0, iat= 587, 570, r1= 1.42, r2= 1.92, r3= 3.08, r4= 3.58, &end
#
# 18 DC H2'1 18 DC H1' 2.420 4.200 (#1,61 2.820 4.200 )
&rst
ixpk= 2, nxpk= 0, iat= 586, 570, r1= 1.92, r2= 2.42, r3= 4.20, r4= 4.70, &end
#
# 18 DC H3' 18 DC H1' 3.680 5.610 (#wk 1 4.080 5.610 )
&rst
ixpk= 1, nxpk= 0, iat= 584, 570, r1= 3.18, r2= 3.68, r3= 5.61, r4= 6.11, &end
#
# 18 DC H3' 18 DC H2'2 2.320 3.560 (#1 2.820 3.560 )
&rst
ixpk= 2, nxpk= 0, iat= 584, 587, r1= 1.82, r2= 2.32, r3= 3.56, r4= 4.06, &end
#
# 18 DC H3' 18 DC H2'1 2.620 2.950
&rst
ixpk= 2, nxpk= 0, iat= 584, 586, r1= 2.12, r2= 2.62, r3= 2.95, r4= 3.45, &end
#
# 18 DC H6 17 DG H1' 3.180 4.480
&rst
ixpk= 2, nxpk= 0, iat= 573, 537, r1= 2.68, r2= 3.18, r3= 4.48, r4= 4.98, &end
#
# 18 DC H6 17 DG H8 3.930 5.920
&rst
ixpk= 2, nxpk= 0, iat= 573, 540, r1= 3.43, r2= 3.93, r3= 5.92, r4= 6.42, &end
#
# 18 DC H6 18 DC H2'1 2.150 3.130 (#op 3,42,57,62 2.150 2.530 )
&rst
ixpk= 3, nxpk= 0, iat= 573, 586, r1= 1.65, r2= 2.15, r3= 3.13, r4= 3.63, &end
#
# 18 DC H6 18 DC H3' 4.310 6.130
&rst
ixpk= 3, nxpk= 0, iat= 573, 584, r1= 3.81, r2= 4.31, r3= 6.13, r4= 6.63, &end
#
# 18 DC H5 17 DG H1' 3.570 4.490 (#15,20,31,59 3.570 3.890 )
&rst
ixpk= 3, nxpk= 0, iat= 575, 537, r1= 3.07, r2= 3.57, r3= 4.49, r4= 4.99, &end
#
# 18 DC H5 17 DG H2'2 3.100 3.420
&rst
ixpk= 3, nxpk= 0, iat= 575, 557, r1= 2.60, r2= 3.10, r3= 3.42, r4= 3.92, &end
#
# 18 DC H5 17 DG H2'1 3.380 5.460 (#1 3.680 5.460 )
&rst
ixpk= 3, nxpk= 0, iat= 575, 556, r1= 2.88, r2= 3.38, r3= 5.46, r4= 5.96, &end
#
# 18 DC H5 17 DG H8 3.700 4.100
&rst
ixpk= 3, nxpk= 0, iat= 575, 540, r1= 3.20, r2= 3.70, r3= 4.10, r4= 4.60, &end
#

```

```

# 18 DC H5 18 DC H2'2 4.460 4.990 (#1,6,13 5.360 5.990 )
&rst
ixpk= 5, nxpk= 0, iat= 575, 587, r1= 3.96, r2= 4.46, r3= 4.99, r4= 5.49, &end
#
# 18 DC H5 18 DC H2'1 3.900 5.240 (#5,27,33,61 3.400 4.840 )
&rst
ixpk= 3, nxpk= 0, iat= 575, 586, r1= 3.40, r2= 3.90, r3= 5.24, r4= 5.74, &end
#
# 19 DG H8 18 DC H1' 3.530 4.240
&rst
ixpk= 3, nxpk= 0, iat= 603, 570, r1= 3.03, r2= 3.53, r3= 4.24, r4= 4.74, &end
#
# 19 DG H8 18 DC H3' 5.020 6.580
&rst
ixpk= 3, nxpk= 0, iat= 603, 584, r1= 4.52, r2= 5.02, r3= 6.58, r4= 7.08, &end
#
# 19 DG H8 18 DC H6 3.420 3.820 (#53 3.520 3.820)
&rst
ixpk= 3, nxpk= 0, iat= 603, 573, r1= 2.92, r2= 3.42, r3= 3.82, r4= 4.32, &end
#
# 19 DG H8 18 DC H2'1 3.000 3.500 (#ma )
&rst
ixpk= 3, nxpk= 0, iat= 603, 586, r1= 2.50, r2= 3.00, r3= 3.50, r4= 4.00, &end
#
# 20 DC H1' 4 DKA H19 2.620 3.250
&rst
ixpk= 3, nxpk= 0, iat= 633, 125, r1= 2.12, r2= 2.62, r3= 3.25, r4= 3.75, &end
#
# 20 DC H2'2 4 DKA H19 2.340 4.880 (#op 1 2.340 3.180 )
&rst
ixpk= 1, nxpk= 0, iat= 650, 125, r1= 1.84, r2= 2.34, r3= 4.88, r4= 5.38, &end
#
# 20 DC H2'2 4 DKA H18 3.080 5.070 (#1,23,32,35,38 3.080 4.370 )
&rst
ixpk= 3, nxpk= 0, iat= 650, 123, r1= 2.58, r2= 3.08, r3= 5.07, r4= 5.57, &end
#
# 20 DC H2'1 4 DKA H19 2.590 3.770
&rst
ixpk= 3, nxpk= 0, iat= 649, 125, r1= 2.09, r2= 2.59, r3= 3.77, r4= 4.27, &end
#
# 20 DC H2'1 4 DKA H18 3.340 4.610
&rst
ixpk= 3, nxpk= 0, iat= 649, 123, r1= 2.84, r2= 3.34, r3= 4.61, r4= 5.11, &end
#
# 20 DC H2'1 20 DC H1' 2.430 3.820 (#op 1,17 2.730 3.820 )
&rst
ixpk= 1, nxpk= 0, iat= 649, 633, r1= 1.93, r2= 2.43, r3= 3.82, r4= 4.32, &end
#
# 20 DC H3' 20 DC H2'1 2.540 2.870
&rst
ixpk= 1, nxpk= 0, iat= 647, 649, r1= 2.04, r2= 2.54, r3= 2.87, r4= 3.37, &end
#
# 20 DC H6 4 DKA H19 2.900 3.770
&rst
ixpk= 1, nxpk= 0, iat= 636, 125, r1= 2.40, r2= 2.90, r3= 3.77, r4= 4.27, &end

```

```

#
# 20 DC H6 4 DKA H18 3.430 4.500
&rst
ixpk= 1, nxpk= 0, iat= 636, 123, r1= 2.93, r2= 3.43, r3= 4.50, r4= 5.00, &end
#
# 20 DC H6 19 DG H1' 3.210 4.720 (#1,19 3.210 3.620 )
&rst
ixpk= 3, nxpk= 0, iat= 636, 600, r1= 2.71, r2= 3.21, r3= 4.72, r4= 5.22, &end
#
# 20 DC H6 19 DG H2'2 2.480 2.970 (#63 2.580 2.970 )
&rst
ixpk= 2, nxpk= 0, iat= 636, 620, r1= 1.98, r2= 2.48, r3= 2.97, r4= 3.47, &end
#
# 20 DC H6 19 DG H2'1 2.670 4.440 (#1 3.270 4.840 )
&rst
ixpk= 3, nxpk= 0, iat= 636, 619, r1= 2.17, r2= 2.67, r3= 4.44, r4= 4.94, &end
#
# 20 DC H6 19 DG H8 3.980 4.590
&rst
ixpk= 3, nxpk= 0, iat= 636, 603, r1= 3.48, r2= 3.98, r3= 4.59, r4= 5.09, &end
#
# 20 DC H6 20 DC H1' 3.230 3.530 (#62 3.230 3.430 )
&rst
ixpk= 3, nxpk= 0, iat= 636, 633, r1= 2.73, r2= 3.23, r3= 3.53, r4= 4.03, &end
#
# 20 DC H6 20 DC H2'2 2.230 3.060 (#1,7,16,34,50 3.330 5.660 )
&rst
ixpk= 3, nxpk= 0, iat= 636, 650, r1= 1.73, r2= 2.23, r3= 3.06, r4= 3.56, &end
#
# 20 DC H6 20 DC H2'1 2.350 2.520
&rst
ixpk= 3, nxpk= 0, iat= 636, 649, r1= 1.85, r2= 2.35, r3= 2.52, r4= 3.02, &end
#
# 20 DC H5 4 DKA H18 4.380 5.180 (#1,2,26,28,37,61 3.380 3.680 )
&rst
ixpk= 3, nxpk= 0, iat= 638, 123, r1= 3.88, r2= 4.38, r3= 5.18, r4= 5.68, &end
#
# 20 DC H5 19 DG H1' 3.800 5.380 (#op 1,39 3.800 4.680 )
&rst
ixpk= 1, nxpk= 0, iat= 638, 600, r1= 3.30, r2= 3.80, r3= 5.38, r4= 5.88, &end
#
# 20 DC H5 19 DG H2'2 3.240 3.540
&rst
ixpk= 1, nxpk= 0, iat= 638, 620, r1= 2.74, r2= 3.24, r3= 3.54, r4= 4.04, &end
#
# 20 DC H5 19 DG H2'1 3.460 4.220 (#op 29,53,62 3.460 3.920 )
&rst
ixpk= 29, nxpk= 0, iat= 638, 619, r1= 2.96, r2= 3.46, r3= 4.22, r4= 4.72, &end
#
# 20 DC H5 19 DG H8 3.440 4.090
&rst
ixpk= 29, nxpk= 0, iat= 638, 603, r1= 2.94, r2= 3.44, r3= 4.09, r4= 4.59, &end
#
# 20 DC H5 20 DC H2'1 3.500 4.710 (#br 1 3.500 4.110)
&rst

```

```

ixpk= 1, nxpk= 0, iat= 638, 649, r1= 3.00, r2= 3.50, r3= 4.71, r4= 5.21, &end
#
# 20 DC H5 20 DC H6 2.100 2.700 (#ma )
&rst
ixpk= 1, nxpk= 0, iat= 638, 636, r1= 1.60, r2= 2.10, r3= 2.70, r4= 3.20, &end
#
# 21 DC H1' 4 DKA H19 2.300 3.050 (#op 1,47 2.500 3.350 )
&rst
ixpk= 1, nxpk= 0, iat= 663, 125, r1= 1.80, r2= 2.30, r3= 3.05, r4= 3.55, &end
#
# 21 DC H1' 4 DKA H18 2.910 4.260 (#53 2.910 4.060 )
&rst
ixpk= 2, nxpk= 0, iat= 663, 123, r1= 2.41, r2= 2.91, r3= 4.26, r4= 4.76, &end
#
# 21 DC H2'2 4 DKA H19 3.540 6.110
&rst
ixpk= 2, nxpk= 0, iat= 680, 125, r1= 3.04, r2= 3.54, r3= 6.11, r4= 6.61, &end
#
# 21 DC H2'2 21 DC H1' 2.300 3.040 (#1,9,40 2.300 2.540 )
&rst
ixpk= 2, nxpk= 0, iat= 680, 663, r1= 1.80, r2= 2.30, r3= 3.04, r4= 3.54, &end
#
# 21 DC H2'1 4 DKA H19 3.300 4.570 (#56 )
&rst
ixpk= 2, nxpk= 0, iat= 679, 125, r1= 2.80, r2= 3.30, r3= 4.57, r4= 5.07, &end
#
# 21 DC H2'1 21 DC H1' 2.370 5.210 (#1 3.070 5.210 )
&rst
ixpk= 3, nxpk= 0, iat= 679, 663, r1= 1.87, r2= 2.37, r3= 5.21, r4= 5.71, &end
#
# 21 DC H3' 21 DC H1' 3.890 5.380 (#60,61 4.090 5.380 )
&rst
ixpk= 4, nxpk= 0, iat= 677, 663, r1= 3.39, r2= 3.89, r3= 5.38, r4= 5.88, &end
#
# 21 DC H3' 21 DC H2'2 2.340 3.540 (#op 1,25 2.640 3.840 )
&rst
ixpk= 1, nxpk= 0, iat= 677, 680, r1= 1.84, r2= 2.34, r3= 3.54, r4= 4.04, &end
#
# 21 DC H3' 21 DC H2'1 2.480 2.900 (#ws 6 2.480 2.700 )
&rst
ixpk= 6, nxpk= 0, iat= 677, 679, r1= 1.98, r2= 2.48, r3= 2.90, r4= 3.40, &end
#
# 21 DC H4' 4 DKA H19 3.340 3.880 (#6 3.340 3.680 )
&rst
ixpk= 3, nxpk= 0, iat= 660, 125, r1= 2.84, r2= 3.34, r3= 3.88, r4= 4.38, &end
#
# 21 DC H4' 21 DC H1' 2.940 3.620 (#1 3.340 3.620 )
&rst
ixpk= 3, nxpk= 0, iat= 660, 663, r1= 2.44, r2= 2.94, r3= 3.62, r4= 4.12, &end
#
# 21 DC H5'1 21 DC H1' 2.680 4.390 (#1,4,21 2.680 3.190)
&rst
ixpk= 2, nxpk= 0, iat= 657, 663, r1= 2.18, r2= 2.68, r3= 4.39, r4= 4.89, &end
#
# 21 DC H5'1 4 DKA H19 4.000 5.500 (#ma )

```



```

&rst
ixpk= 2, nxpk= 0, iat= 657, 125, r1= 3.50, r2= 4.00, r3= 5.50, r4= 6.00, &end
#
# 21 DC H5'2 4 DKA H19 2.980 5.510 (#30 2.980 5.410 )
&rst
ixpk= 2, nxpk= 0, iat= 658, 125, r1= 2.48, r2= 2.98, r3= 5.51, r4= 6.01, &end
#
# 21 DC H6 20 DC H1' 3.470 4.210 (#br 53 3.470 4.010 )
&rst
ixpk= 53, nxpk= 0, iat= 666, 633, r1= 2.97, r2= 3.47, r3= 4.21, r4= 4.71, &end
#
# 21 DC H6 20 DC H2'2 3.340 4.260 (#op 3 3.340 3.960 )
&rst
ixpk= 3, nxpk= 0, iat= 666, 650, r1= 2.84, r2= 3.34, r3= 4.26, r4= 4.76, &end
#
# 21 DC H6 20 DC H2'1 2.860 6.040 (#br 1 4.260 6.740 )
&rst
ixpk= 1, nxpk= 0, iat= 666, 649, r1= 2.36, r2= 2.86, r3= 6.04, r4= 6.54, &end
#
# 21 DC H6 20 DC H3' 2.960 3.250 (#53 2.960 3.150 )
&rst
ixpk= 2, nxpk= 0, iat= 666, 647, r1= 2.46, r2= 2.96, r3= 3.25, r4= 3.75, &end
#
# 21 DC H6 21 DC H1' 3.380 3.620
&rst
ixpk= 2, nxpk= 0, iat= 666, 663, r1= 2.88, r2= 3.38, r3= 3.62, r4= 4.12, &end
#
# 21 DC H6 21 DC H2'2 2.780 4.190
&rst
ixpk= 2, nxpk= 0, iat= 666, 680, r1= 2.28, r2= 2.78, r3= 4.19, r4= 4.69, &end
#
# 21 DC H6 21 DC H2'1 3.050 4.000 (#1,24,49 2.250 2.600 )
&rst
ixpk= 2, nxpk= 0, iat= 666, 679, r1= 2.55, r2= 3.05, r3= 4.00, r4= 4.50, &end
#
# 21 DC H6 21 DC H3' 3.560 4.410
&rst
ixpk= 2, nxpk= 0, iat= 666, 677, r1= 3.06, r2= 3.56, r3= 4.41, r4= 4.91, &end
#
# 21 DC H6 21 DC H4' 4.240 5.660 (#22 4.340 5.660 )
&rst
ixpk= 4, nxpk= 0, iat= 666, 660, r1= 3.74, r2= 4.24, r3= 5.66, r4= 6.16, &end
#
# 21 DC H6 21 DC H5'1 3.020 3.820 (#10,52,57,63 3.120 3.320 )
&rst
ixpk= 3, nxpk= 0, iat= 666, 657, r1= 2.52, r2= 3.02, r3= 3.82, r4= 4.32, &end
#
# 21 DC H6 21 DC H5'2 3.860 5.900
&rst
ixpk= 3, nxpk= 0, iat= 666, 658, r1= 3.36, r2= 3.86, r3= 5.90, r4= 6.40, &end
#
# 21 DC H5 20 DC H3' 3.070 3.650 (#53 3.170 3.650 )
&rst
ixpk= 3, nxpk= 0, iat= 668, 647, r1= 2.57, r2= 3.07, r3= 3.65, r4= 4.15, &end
#

```

```

# 21 DC H5 21 DC H2'1 3.770 5.750 (#wk,27 1 3.770 5.150)
&rst
ixpk= 1, nxpk= 0, iat= 668, 679, r1= 3.27, r2= 3.77, r3= 5.75, r4= 6.25, &end
#
# 21 DC H5 20 DC H2'2 4.000 5.300
&rst
ixpk= 1, nxpk= 0, iat= 668, 650, r1= 3.50, r2= 4.00, r3= 5.30, r4= 5.80, &end
#
# 21 DC H5 21 DC H6 2.100 2.700 (#ma )
&rst
ixpk= 1, nxpk= 0, iat= 668, 666, r1= 1.60, r2= 2.10, r3= 2.70, r4= 3.20, &end
#
# 22 DG H1' 4 DKA H20 3.660 4.400 (#op 53 3.660 4.000 )
&rst
ixpk= 53, nxpk= 0, iat= 693, 127, r1= 3.16, r2= 3.66, r3= 4.40, r4= 4.90, &end
#
# 22 DG H2'2 22 DG H1' 2.250 3.050 (#1 2.250 2.450 )
&rst
ixpk= 2, nxpk= 0, iat= 713, 693, r1= 1.75, r2= 2.25, r3= 3.05, r4= 3.55, &end
#
# 22 DG H2'1 22 DG H1' 2.330 3.760 (#1,31 2.830 3.760 )
&rst
ixpk= 2, nxpk= 0, iat= 712, 693, r1= 1.83, r2= 2.33, r3= 3.76, r4= 4.26, &end
#
# 22 DG H3' 22 DG H1' 3.850 5.170 (#1 4.050 5.170 )
&rst
ixpk= 4, nxpk= 0, iat= 710, 693, r1= 3.35, r2= 3.85, r3= 5.17, r4= 5.67, &end
#
# 22 DG H3' 22 DG H2'2 2.310 4.030 (#ws 1,14 2.710 4.030 )
&rst
ixpk= 1, nxpk= 0, iat= 710, 713, r1= 1.81, r2= 2.31, r3= 4.03, r4= 4.53, &end
#
# 22 DG H3' 22 DG H2'1 2.470 2.930
&rst
ixpk= 1, nxpk= 0, iat= 710, 712, r1= 1.97, r2= 2.47, r3= 2.93, r4= 3.43, &end
#
# 22 DG H8 4 DKA H19 3.350 4.590 (#1 3.350 3.690 )
&rst
ixpk= 3, nxpk= 0, iat= 696, 125, r1= 2.85, r2= 3.35, r3= 4.59, r4= 5.09, &end
#
# 22 DG H8 21 DC H1' 2.890 3.660 (#1,59 3.390 3.660 )
&rst
ixpk= 3, nxpk= 0, iat= 696, 663, r1= 2.39, r2= 2.89, r3= 3.66, r4= 4.16, &end
#
# 22 DG H8 21 DC H3' 4.850 6.550
&rst
ixpk= 3, nxpk= 0, iat= 696, 677, r1= 4.35, r2= 4.85, r3= 6.55, r4= 7.05, &end
#
# 22 DG H8 22 DG H1' 3.600 4.190
&rst
ixpk= 3, nxpk= 0, iat= 696, 693, r1= 3.10, r2= 3.60, r3= 4.19, r4= 4.69, &end
#
# 22 DG H8 21 DC H2'2 4.300 5.300 (#ma )
&rst
ixpk= 3, nxpk= 0, iat= 696, 680, r1= 3.80, r2= 4.30, r3= 5.30, r4= 5.80, &end

```

```

#
# 23 DA H2'2 23 DA H1' 2.180 3.060 (#1,7,57 2.180 2.360 )
&rst
ixpk= 2, nxpk= 0, iat= 745, 726, r1= 1.68, r2= 2.18, r3= 3.06, r4= 3.56, &end
#
# 23 DA H2'1 23 DA H1' 2.280 3.410 (#1 2.580 3.500 )
&rst
ixpk= 2, nxpk= 0, iat= 744, 726, r1= 1.78, r2= 2.28, r3= 3.41, r4= 3.91, &end
#
# 23 DA H3' 23 DA H2'2 2.280 3.500
&rst
ixpk= 2, nxpk= 0, iat= 742, 745, r1= 1.78, r2= 2.28, r3= 3.50, r4= 4.00, &end
#
# 23 DA H8 22 DG H1' 3.620 4.960 (#1,12 3.620 4.160 )
&rst
ixpk= 3, nxpk= 0, iat= 729, 693, r1= 3.12, r2= 3.62, r3= 4.96, r4= 5.46, &end
#
# 23 DA H8 22 DG H2'2 2.270 2.830 (#13,18 2.670 2.830 )
&rst
ixpk= 2, nxpk= 0, iat= 729, 713, r1= 1.77, r2= 2.27, r3= 2.83, r4= 3.33, &end
#
# 23 DA H8 22 DG H2'1 3.180 4.220
&rst
ixpk= 2, nxpk= 0, iat= 729, 712, r1= 2.68, r2= 3.18, r3= 4.22, r4= 4.72, &end
#
# 23 DA H8 22 DG H3' 3.950 4.460
&rst
ixpk= 2, nxpk= 0, iat= 729, 710, r1= 3.45, r2= 3.95, r3= 4.46, r4= 4.96, &end
#
# 23 DA H8 23 DA H1' 3.390 3.860
&rst
ixpk= 2, nxpk= 0, iat= 729, 726, r1= 2.89, r2= 3.39, r3= 3.86, r4= 4.36, &end
#
# 23 DA H8 23 DA H2'2 2.570 4.640 (#1,33 2.770 4.640 )
&rst
ixpk= 2, nxpk= 0, iat= 729, 745, r1= 2.07, r2= 2.57, r3= 4.64, r4= 5.14, &end
#
# 23 DA H8 23 DA H3' 3.540 5.240
(#23 DA H8 23 DA H2'1 2.660 3.920 #op 1,48,61 2.060 2.420 )
&rst
ixpk= 2, nxpk= 0, iat= 729, 742, r1= 3.04, r2= 3.54, r3= 5.24, r4= 5.74, &end
#
# 24 DG3 H2'2 24 DG3 H1' 2.650 4.670
&rst
ixpk= 2, nxpk= 0, iat= 778, 758, r1= 2.15, r2= 2.65, r3= 4.67, r4= 5.17, &end
#
# 24 DG3 H2'1 24 DG3 H1' 2.060 2.320
&rst
ixpk= 2, nxpk= 0, iat= 777, 758, r1= 1.56, r2= 2.06, r3= 2.32, r4= 2.82, &end
#
# 24 DG3 H3' 24 DG3 H1' 3.440 4.210
&rst
ixpk= 2, nxpk= 0, iat= 775, 758, r1= 2.94, r2= 3.44, r3= 4.21, r4= 4.71, &end
#
# 24 DG3 H3' 24 DG3 H2'2 2.210 2.630 (#62 2.310 2.630 )

```

```

&rst
ixpk= 2, nxpk= 0, iat= 775, 778, r1= 1.71, r2= 2.21, r3= 2.63, r4= 3.13, &end
#
# 24 DG3 H3' 24 DG3 H2'1 2.530 3.700
&rst
ixpk= 2, nxpk= 0, iat= 775, 777, r1= 2.03, r2= 2.53, r3= 3.70, r4= 4.20, &end
#
# 24 DG3 H8 23 DA H2'2 2.770 3.160 (#20,23 2.770 2.960 )
&rst
ixpk= 2, nxpk= 0, iat= 761, 745, r1= 2.27, r2= 2.77, r3= 3.16, r4= 3.66, &end
#
# 24 DG3 H8 23 DA H2'1 2.650 3.510 (#1,59 3.050 3.510 )
&rst
ixpk= 3, nxpk= 0, iat= 761, 744, r1= 2.15, r2= 2.65, r3= 3.51, r4= 4.01, &end
#
# 24 DG3 H8 23 DA H3' 4.410 6.120
&rst
ixpk= 3, nxpk= 0, iat= 761, 742, r1= 3.91, r2= 4.41, r3= 6.12, r4= 6.62, &end
#
# 24 DG3 H8 23 DA H8 3.770 4.260
&rst
ixpk= 3, nxpk= 0, iat= 761, 729, r1= 3.27, r2= 3.77, r3= 4.26, r4= 4.76, &end
#
# 24 DG3 H8 24 DG3 H2'2 2.360 3.740
&rst
ixpk= 3, nxpk= 0, iat= 761, 778, r1= 1.86, r2= 2.36, r3= 3.74, r4= 4.24, &end
#
# 24 DG3 H8 24 DG3 H3' 3.110 4.620
&rst
ixpk= 3, nxpk= 0, iat= 761, 775, r1= 2.61, r2= 3.11, r3= 4.62, r4= 5.12, &end

```

REFERENCES

- (1) Dickerson, R.; Drew, H.; Conner, B.; Wing, R.; Fratini, A.; Kopka, M. *Science* **1982**, *216*, 475.
- (2) Watson, J.; Crick, F. *Nature* **1953**, *171*, 737.
- (3) Watson, J.; Crick, F. *Nature* **1953**, *171*, 964.
- (4) Wilkins, M.; Stokes, A.; Wilson, H. *Nature* **1953**, *171*, 738.
- (5) Paleček, E.; Rašovská, E.; Boublíková, P. *Biochem. Biophys. Res. Comm.* **1988**, *150*, 731.
- (6) Jiang, H.; Zacharias, W.; Amirhaeri, S. *Nucl. Acids Res.* **1991**, *19*, 6943.
- (7) Lua, X.; Shakked, Z.; Olson, W. *J. Mol. Biol.* **2000**, *300*, 819.
- (8) Wahl, M.; Sundaralingam, M. *Biopolymers* **1997**, *44*, 45.
- (9) Pohl, F.; Jovin, T. *J. Mol. Biol.* **1972**, *67*, 375.
- (10) Oh, D.; Kim, Y.; Rich, A. *Proc. Natl. Acad. U.S.A.* **2002**, *99*, 16666.
- (11) Wang, A.; Quigley, G.; Kolpak, F.; Crawford, J.; Boom, J. v.; Marel, G. v. d.; Rich, A. *Nature* **1979**, *282*, 680.
- (12) Muller, J. *Metallomics* **2010**, *2*, 318.
- (13) Sinden, R. *DNA Structure and Function*; Elsevier, 2012.
- (14) Thomas, D.; Roberts, J.; Sabatino, R.; Meyers, T.; Tan, C.; Downey, K.; So, A.; Bambara, A.; Kunkel, T. *Biochem.* **1991**, *30*, 11751.
- (15) Schaaper, R. *J. Biol. Chem.* **1993**, *268*, 23762.
- (16) Garg, P.; Burgers, P. *Crit. Rev. Mol. Biol.* **2005**, *40*, 115.
- (17) Johnson, A.; O'Donnel, M. *Annu. Rev. Biochem.* **2005**, *74*, 283.
- (18) Kool, E. *Annu. Rev. Biochem.* **2002**, *71*, 191.
- (19) Goodman, M.; Creighton, S.; Bloom, L.; Petruska, J. *Crit. Rev. Biochem. Mol. Biol.* **1993**, *28*, 83.
- (20) Washington, M.; Helquist, S.; Prakash, L.; Prakash, S. *Mol. Cell Biol.* **2003**, *23*, 5107.
- (21) Echols, H.; Goodman, M. *Annu. Rev. Biochem.* **1991**, *60*, 477.
- (22) Kunkel, T.; Bebenek, K. *Annu. Rev. Biochem.* **2000**, *69*, 487.
- (23) Goodman, M. *Proc. Natl. Acad. U.S.A.* **1997**, *94*, 10493.
- (24) Johnson, S.; Beese, L. *Cell* **2004**, *116*, 803.
- (25) Altieri, F.; Grillo, C.; Maceroni, M.; Chichiarelli, S. *Antioxid. Redox Signaling* **2008**, *10*, 891.

- (26) Gupta, R.; Lutz, W. *Mutat. Res* **1999**, *424*, 1.
- (27) Iyer, R.; Pluciennik, A.; Burdett, V.; Modrich, P. *Chem. Rev.* **2006**, *106*, 302.
- (28) Kim, Y.; Wilson, D. *Curr. Mol. Pharmacol.* **2012**, *5*, 3.
- (29) Sancar, A. *Annu. Rev. Biochem.* **1996**, *65*, 43.
- (30) Spivak, G. *Mutat. Res* **2008**, *577*, 162.
- (31) Masutani, C.; Sugasawa, K.; Yanagisawa, J.; Sonoyama, T.; Ui, M.; Enomoto, T.; Takio, K.; Tanaka, K.; Spek, P. v. d.; Bootsma, D. *EMBO J.* **1994**, *13*, 1831.
- (32) Nishi, R.; Okuda, Y.; Watanabe, E.; Mori, T.; Iwai, S.; Masutani, C.; Sugasawa, K.; Hanaoka, F. *Mol. Cell Biol.* **2005**, *25*, 5664.
- (33) Chu, G.; Chang, E. *Science* **1988**, *242*, 564.
- (34) Wakasugi, M.; Kawashima, A.; Morioka, H.; Linn, S.; Sancar, A.; Mori, T.; Nikaido, O.; Matsunaga, T. *J. Biol. Chem.* **2002**, *277*, 1637.
- (35) Scrima, A.; Konickova, R.; Czyzewski, B.; Kawasaki, Y.; Jeffrey, P.; Groisman, R.; Nakatani, Y.; Iwai, S.; Pavletich, N.; Thoma, N. *Cell* **2008**, *135*, 1213.
- (36) Sugasawa, K.; Okamoto, T.; Shimizu, Y.; Masutani, C.; Iwai, S.; Hanaoka, F. *Genes Dev.* **2001**, *15*, 507.
- (37) Yokoi, M.; Masutani, C.; Maekawa, T.; Sugasawa, K.; Ohkuma, Y.; Hanaoka, F. *J. Biol. Chem.* **2000**, *275*, 9870.
- (38) Compe, E.; Egly, J. *Nature Rev. Mol. Cell Biol.* **2012**, *13*, 343.
- (39) Camenisch, U.; Dip, R.; Schumacher, S.; Schuler, B.; Naegeli, H. *Nature Struct. and Mol. Biol.* **2006**, *13*, 278.
- (40) Sugasawa, K.; Akagi, J.; Nishi, R.; Iwai, S.; Hanaoka, F. *Mol. Cell Biol.* **2009**, *36*, 642.
- (41) Wolski, S.; Kuper, J.; Hanzelmann, P.; Truglio, J.; Croteau, D.; Houten, B.; Kisker, C. *PLoS Biol* **2008**, *6*.
- (42) Matheiu, N.; Kaczmarek, N.; Ruthemann, P.; Luch, A.; Naegeli, H. *Curr. Biol.* **2013**, *23*, 2014.
- (43) Coin, F.; Oksenysh, V.; Mocquet, V.; Groh, S.; Blattner, C.; Egly, J. *Mol. Cell Biol.* **2008**, *31*, 9.
- (44) Fagbemi, A.; Orelli, B.; Scharer, O. *DNA Repair* **2011**, *10*, 722.
- (45) Mocquet, V.; Laine, J.; Riedl, T.; Yajin, Z.; Lee, M.; Egly, J. *EMBO J.* **2008**, *27*, 155.
- (46) Orelli, B.; McClendon, T.; Tsodikov, O.; Ellenberger, T.; Niedernhofer, L.; Scharer, O. *J. Biol. Chem.* **2010**, *285*.
- (47) Dunand-Sauthier, I.; Hohl, M.; Thorel, F.; Jaquier-Gubler, P.; Clarkson, S.; Scharer, O. *J. Biol. Chem.* **2005**, *280*, 7030.

- (48) Staresincic, L.; Fagbemi, A.; Enzlin, J.; Gourdin, A.; Wijgers, N.; Dunand-Sauthier, I.; Giglia-Mari, G.; Clarkson, S.; Vermeulen, W.; Scharer, O. *EMBO J.* **2009**, *28*, 1111.
- (49) Ogi, T.; Limsirichaikul, S.; Overmeer, R.; Volker, M.; Takenaka, K.; Cloney, R.; Nakazawa, Y.; Niimi, A.; Miki, Y.; Jaspers, N.; Mullenders, L.; Yamashita, S.; Fousteri, M.; Lehmann, A. *Mol Cell Biol* **37**, *37*, 714.
- (50) Marteiijn, J.; Lans, H.; Vermeulen, W.; Hoeijmakers, J. *Nature Rev. Mol. Cell Biol.* **2014**, *15*, 465.
- (51) Somoza, V.; Fogliano, V. *J. Agric. Food Chem.* **2013**, *61*, 10197.
- (52) Hodge, J. *J. Agric. Food Chem.* **1953**, *1*, 928.
- (53) Doll, R.; Peto, R. *J. Natl. Cancer Inst* **1981**, *66*, 1191.
- (54) Parkin, D. *Lancet Oncol.* **2001**, *2*, 533.
- (55) Anderson, K.; Mongin, S.; Sinha, R.; Stolzenberg-Solomon, R.; Gross, M.; Ziegler, R.; Mabie, J.; Risch, A.; Kazin, S.; Church, T. *Mol. Carcinog.* **2011**, *51*, 128.
- (56) Lang, N.; Butler, M.; Massengill, J.; Lawson, M.; Stotts, R.; Hauer-Jenson, M.; Kadlubar, F. *Cancer Epidemiol. Biomarkers Prev.* **1994**, *3*.
- (57) Snyderwine, E. *Cancer Res.* **1994**, *74*, 1070.
- (58) Shirai, T.; Sano, M.; Tamano, S.; Takahashi, S.; Hirose, M.; Futakuchi, M.; Hasegawa, R.; Imaida, K.; Matsumoto, K.; Wakabayashi, K. *Cancer Res.* **1997**, *57*, 195.
- (59) Persson, E.; Sjöholm, I.; Skog, K. *J. Agric. Food Chem.* **2003**, *51*, 4472.
- (60) Salmon, C.; Kinze, M.; Panteleakos, F.; Wu, R.; Nelson, D.; Felton, J. *J. Natl. Cancer Inst* **2000**, *92*, 1773.
- (61) Felton, J.; Jägerstad, M.; Knize, M.; Skog, K.; Wakabayashi, K. In *Food borne carcinogens: Heterocyclic amines*; Nagao M, S. T., e, Ed.; John Wiley & Sons Ltd.: Chichester, 2000, p 31.
- (62) Stofer, E.; Lavery, R. *Biopolymers* **1994**, *34*, 337.
- (63) Smith, J.; Ameri, F.; Gadgil, P. *J. Food Sci.* **2008**, *73*, T100.
- (64) IARC *World Health Organization* **1993**, *56*, 165.
- (65) Tanaka, T.; Barnes, W.; Williams, G.; Weisburger, J. *Gann* **1985**, *76*, 570.
- (66) Adamson, R.; Thorgeirsson, U.; Snyderwine, E.; Thorgeirsson, S.; Reeves, J.; Dalgard, D.; Takayama, S.; Sugimura, T. *Jpn. J. Canc. Res.* **1990**, *81*, 10.
- (67) Turesky, R. *Current Drug Metabolism*; Bentham Science Publishers; Vol. 5.
- (68) Koutros, S.; Berndt, S.; Sinha, R.; Ma, X.; Chatterjee, N.; Alavanja, M.; Zheng, T.; Huang, W.; Hayes, R.; Cross, A. *Cancer Res.* **2009**, *69*, 1877.
- (69) Milhe, C.; Fuchs, R.; Lefevre, J. *Eur. J. Biochem.* **1996**, *235*, 120.
- (70) Koehl, P.; Burnouf, D.; Fuchs, R. *Environ. Sci. Res.* **1990**, *40*, 105.
- (71) Jain, N.; Li, Y.; Zhang, L.; Meneni, S.; Cho, B. *Biochem.* **2007**, *46*, 13310.

- (72) Koffel-Schwartz, N.; Fuchs, R. *Mol. Gen. Genet.* **1989**, *215*, 306.
- (73) Okada, Y.; Streisinger, G.; Owen, J.; Newton, J.; Tsugita, A.; Inouye, M. *Nature* **1972**, *236*, 338.
- (74) Prinbow, D.; Sigurdson, D.; Gold, L.; Singer, B.; Napoli, C.; Brosius, J.; Dull, T.; Noller, H. *J. Mol. Biol.* **1981**, *149*, 337.
- (75) Farabaugh, P.; Schmeissner, U.; Hofer, M.; Miller, J. *J. Mol. Biol.* **1978**, *126*, 847.
- (76) Broschard, T.; Koffel-Schwartz, N.; Fuchs, R. *J. Mol. Biol.* **1999**, *288*, 191.
- (77) Sodergren, E.; DeMoss, J. *J. Bacteriol.* **1988**, *170*, 1721.
- (78) Streisinger, G.; Okada, Y.; Emrich, J.; Newton, J.; Tsugita, A.; Terzaghi, E.; Inoye, M. *Cold Spring Harb. Symp. Quant. Biol.* **1966**, *31*, 77.
- (79) Drake, J.; Glickman, B.; Ripley, L. *Am. Scient.* **1983**, *71*, 621.
- (80) Streisinger, G.; Owen, J. *Genetics* **1985**, *109*, 6330.
- (81) Oliveira, E.; Padua, J.; Zucchi, M.; Vencovsky, R.; Viera, M. *Genet. Mol. Biol.* **2006**, *29*.
- (82) Jain, V.; Hilton, B.; Patnaik, S.; Zou, Y.; Chiarelli, M.; Cho, B. *Nucl. Acids Res.* **2012**, *40*, 3939.
- (83) Grishaev, A.; Tugarinov, V.; Kay, L.; Trewella, J.; Bax, A. *J. Biomol. NMR* **2008**, *40*, 95.
- (84) Bragg, W. *Proc. R. Soc. Lond.* **1913**, *A89*, 248.
- (85) Kendrew, J.; Bodo, G.; Dintzis, H.; Parrish, R.; Wyckoff, H. *Nature* **1958**, *181*, 662.
- (86) Bioinformatics, R. C. f. S. 2014.
- (87) Ducruix, A.; Giege, R. *Crystallization of nucleic acids and proteins. A practical approach*; Oxford University Press: New York, 1992.
- (88) Yaffe, M. *Critical Care Medicine* **2005**, *33*, S435.
- (89) Taylor, G. *Acta Cryst.* **2003**, *D 59*.
- (90) Rossmann, M. *Acta Cryst. A.* **1990**, *46*, 73.
- (91) Ealick, S. *Curr. Opin. Struct. Biol.* **2000**, *4*, 495.
- (92) Hendrickson, W. *Trans. ACA* **1985**, *21*.
- (93) Rice, L.; Earnest, T.; Brunger, A. *Acta Cryst. D. Biol. Crystallogr.* **2000**, *56*, 1413.
- (94) Wells, A. F. *Structural Inorganic Chemistry*; 5 ed.; Oxford University Press, 1984.
- (95) Kleywegt, G.; Brunger, A. *Structure* **1996**, *15*, 897.
- (96) Bhattacharya, A. *Nature* **2010**, *463*, 605.

- (97) Marion, D.; Wuthrich, K. *Biochem. Biophys. Res. Comm.* **1983**, *113*, 967.
- (98) Broido, M.; Zon, G.; James, T. *Biochem. Biophys. Res. Comm.* **1984**, *119*, 663.
- (99) Scheek, R.; Russo, N.; Boelens, R.; Kaptein, R.; Boom, J. V. *J. Am. Chem. Soc.* **1983**, *105*, 2914.
- (100) Boelens, R.; Scheek, R.; Dijkstra, K.; Kaptein, R. *J. Magn. Reson.* **1985**, *62*, 378.
- (101) Borgias, B.; James, T. *Meth. in Enzymol.* **1989**, *176*, 169.
- (102) Borgias, B.; James, T. *J. Magn. Reson.* **1990**, *87*, 475.
- (103) Bassolino-Klimas, D.; Tejero, R.; Krystek, S.; Metzler, W.; Montelione, G.; Bruccoleri, R. *Protein Sci.* **1996**, *5*, 593.
- (104) P. Khandelwal; Panchal, S.; Hosur, R. *Nucl. Acids Res.* **2001**, *29*, 499.
- (105) James, T.; Basus, V. *Annu. Rev. Phys. Chem.* **1991**, *42*, 501.
- (106) Schmitz, U.; Pearlman, D.; James, T. *J. Mol. Biol.* **1991**, *221*, 271.
- (107) Madrid, M.; Llinas, E.; Llinas, M. *J. Magn. Reson.* **1991**, *93*, 329.
- (108) Lavery, R.; Sklenar, H. *J. Biomol. Struct. Dyn.* **1989**, *6*, 655.
- (109) Lu, X.; Olson, W. *Nucl. Acids Res.* **2003**, *31*, 5108.
- (110) Bishop, G.; Chaires, J. *Current Protocols in Nucleic Acid Chemistry* **2003**, *11:7.11:7.11.1–7.11.8*.
- (111) Polavarapu, P.; Zhao, C. *Fresenius J. Anal. Chem.* **2000**, *366*, 727.
- (112) Stover, J.; Rizzo, C. *Chem. Res. Toxicol.* **2007**, *20*, 1972.
- (113) Wu, Y.; Ghosh, A.; Szyperski, T. *J. Struct. Funct. Genomics* **2009**, *10*, 227.
- (114) Piotto, M.; Saudek, V.; Sklenar, V. *J. Biomol. NMR* **1992**, *2*, 661.
- (115) Goddard, T.; Kneller, D. University of California, San Francisco, 2006.
- (116) James, T. *Curr. Opin. Struct. Biol.* **1991**, *1*, 1042.
- (117) Keepers, J.; James, T. *J. Magn. Reson.* **1984**, *57*, 404.
- (118) Arnott, S. H., D. W. L. *Biochem. Biophys. Res. Comm.* **1972**, *47*, 1504.
- (119) Frisch, M. J. T., G. W.; Schlegel, H. B.; Scuseria, G. E.; Robb, M. A.; Cheeseman, J. R.; Montgomery, J. A.; Vreven, T.; Kudin, K. N.; Burant, J. C.; Millam, J. M.; Iyengar, S. S.; Tomasi, J.; Barone, V.; Mennucci, B.; Cossi, M.; Scalmani, G.; Rega, N.; Petersson, G. A.; Nakatsuji, H.; Hada, M.; Ehara, M.; Toyota, K.; Fukuda, R.; Hasegawa, J.; Ishida, M.; Nakajima, T.; Honda, Y.; Kitao, O.; Nakai, H.; Klene, M.; Li, X.; Knox, J. E.; Hratchian, H. P.; Cross, J. B.; Adamo, C.; Jaramillo, J.; Gomperts, R.; Stratmann, R. E.; Yazyev, O.; Austin, A. J.; Cammi, R.; Pomelli, C.; Pomelli, J.; Ochterski, W.; Ayala, P. Y.; Morokuma, K.; Voth, G. A.; Salvador, P.; Dannenberg, J. J.; Zakrzewska, V. G.; Daniels, A. D.; Farkas, O.; Rabuck, A. D.; Raghavachari, K.; Ortiz, J. V. Wallingford, CT, 2004.
- (120) Kirkpatrick, S. G., C. D., Jr.; Vecchi, M. P. *Science* **1983**, *220*, 671.

- (121) Wang, J.; Wolf, R.; Caldwell, J.; Kollman, P.; Case, D. *J. Comput. Chem.* **2004**, *25*, 1157.
- (122) Case, D.; Darden, T.; Cheatham, T.; III, C. S.; Wang, J.; Duke, R.; Luo, R.; Crowley, M.; Walker, R.; Zhang, W.; Merz, K.; B.Wang; Hayik, S.; Roitberg, A.; Seabra, G.; Kolossváry, I.; Wong, K.; Paesani, F.; Vanicek, J.; Wu, X.; Brozell, S.; Steinbrecher, T.; Gohlke, H.; Yang, L.; Tan, C.; Mongan, J.; Hornak, V.; Cui, G.; Mathews, D.; Seetin, M.; Sagui, C.; Babin, V.; Kollman, P. University of California, San Francisco, 2008.
- (123) Bashford, D.; Case, D. *Annu. Rev. Phys. Chem.* **2000**, *51*, 129.
- (124) Lavery, R.; Moakher, M.; Maddocks, J.; Petkeviciute, D.; Zakrzewska, K. *Nucl. Acids Res.* **2009**, *37*, 5917.
- (125) Blanchet, C.; Pasi, M.; Zakrzewska, K.; Lavery, R. *Nucl. Acids Res.* **2011**, *39*, W68.
- (126) Pace, C. N.; Vajdos, F.; Fee, L.; Grimsley, G. *Protein Sci.* **1995**, *4*, 2411.
- (127) R. Eoff, A. I., K. Angel, M. Egli, F. Guengerich *J. Biol. Chem.* **2007**, *282*.
- (128) Eoff, R.; Irmia, A.; Angel, K.; Egli, M.; Guengerich, F. *J. Biol. Chem.* **2007**, *282*, 19831.
- (129) Otwinowski, Z.; Minor, W. *Meth. in Enzymol.* **1997**, *276*, 307.
- (130) Zang, H.; Irimia, A.; Choi, J.; Angel, K.; Loukachevitch, L.; Egli, M.; Guengerich, F. *J. Biol. Chem.* **2006**, *281*, 2358.
- (131) Brunger, A.; Adams, P.; Clore, G.; Delano, W.; Gros, P.; Grosse-Kunstleve, R.; Jiang, J.; Krahn, J.; Kuszewski, J.; Nilges, M.; Pannu, N.; Read, R.; Rice, L.; Schroeder, G.; Simonson, T.; Warren, G. *Acta Cryst.* **1998**, *54*, 905.
- (132) Brunger, A. *Nature Protocols* **2007**, *2*, 2728.
- (133) Emsley, P.; Lohkamp, B.; Scott, W.; Cowtan, K. *Acta Crystal. Section D - Biol. Crystallog.* **2010**, *66*, 486.
- (134) DeLano, W.; DeLano Scientific, LLC: Palo Alto, CA, 2008.
- (135) Stover, J. S.; Rizzo, C. J. *Chem. Res. Toxicol.* **2007**, *20*, 1972.
- (136) Patel, D. J.; Shapiro, L.; Hare, D. *Q. Rev. Biophys.* **1987**, *20*, 35.
- (137) Reid, B. R. *Q. Rev. Biophys.* **1987**, *20*, 2.
- (138) Elmquist, E.; Wang, F.; Stover, J.; Stone, M.; Rizzo, C. *Chem. Res. Toxicol.* **2007**, *20*, 445.
- (139) Arnott, S.; Hukins, D. W. L. *Biochem. Biophys. Res. Comm.* **1972**, *47*, 1504.
- (140) Keepers, J. W.; James, T. L. *J. Magn. Reson.* **1984**, *57*, 404.
- (141) Borgias, B. A.; James, T. L. *J. Magn. Reson.* **1990**, *87*, 475.
- (142) Bashford, D.; Case, D. A. *Annu. Rev. Phys. Chem.* **2000**, *51*, 129.
- (143) James, T. L. *Curr. Opin. Struct. Biol.* **1991**, *1*, 1042.

- (144) Turesky, R. J.; Markovic, J.; Aeschlimann, J. M. *Chem. Res. Toxicol.* **1996**, *9*, 397.
- (145) Fuchs, R. P.; Schwartz, N.; Daune, M. P. *Nature* **1981**, *294*, 657.
- (146) Koffel-Schwartz, N.; Verdier, J. M.; Bichara, M.; Freund, A. M.; Daune, M. P.; Fuchs, R. P. *J. Mol. Biol.* **1984**, *177*, 33.
- (147) Koehl, P.; Burnouf, D.; Fuchs, R. P. *J. Mol. Biol.* **1989**, *207*, 355.
- (148) Koehl, P.; Valladier, P.; Lefevre, J. F.; Fuchs, R. P. *Nucleic Acids Res.* **1989**, *17*, 9531.
- (149) Broschard, T. H.; Koffel-Schwartz, N.; Fuchs, R. P. *J. Mol. Biol.* **1999**, *288*, 191.
- (150) Hoffmann, G. R.; Fuchs, R. P. *Chem. Res. Toxicol.* **1997**, *10*, 347.
- (151) Choi, J. Y.; Stover, J. S.; Angel, K. C.; Chowdhury, G.; Rizzo, C. J.; Guengerich, F. *P. J. Biol. Chem.* **2006**, *281*, 25297.
- (152) Zaliznyak, T.; Bonala, R.; Johnson, F.; de los Santos, C. *Chem. Res. Toxicol.* **2006**, *19*, 745.
- (153) Grad, R.; Shapiro, R.; Hingerty, B. E.; Broyde, S. *Chem. Res. Toxicol.* **1997**, *10*, 1123.
- (154) Brown, K.; Hingerty, B. E.; Guenther, E. A.; Krishnan, V. V.; Broyde, S.; Turteltaub, K. W.; Cosman, M. *Proc. Natl. Acad. Sci. USA* **2001**, *98*, 8507.
- (155) Shibutani, S.; Grollman, A. P. *Chem. Res. Toxicol.* **1993**, *6*, 819.
- (156) Wang, F.; Demuro, N. E.; Elmquist, C. E.; Stover, J. S.; Rizzo, C. J.; Stone, M. P. *J. Am. Chem. Soc.* **2006**, *128*, 10085.
- (157) Turesky, R. J.; Box, R. M.; Markovic, J.; Gremaud, E.; Snyderwine, E. G. *Mutat. Res.* **1997**, *376*, 235.
- (158) Gunz, D.; Hess, M. T.; Naegeli, H. *J. Biol. Chem.* **1996**, *271*, 25089.
- (159) Batty, D. P.; Wood, R. D. *Gene* **2000**, *241*, 193.
- (160) Sugawara, K.; Okamoto, T.; Shimizu, Y.; Masutani, C.; Iwai, S.; Hanaoka, F. *Genes Dev.* **2001**, *15*, 507.
- (161) Geacintov, N. E.; Broyde, S.; Buterin, T.; Naegeli, H.; Wu, M.; Yan, S.; Patel, D. J. *Biopolymers* **2002**, *65*, 202.
- (162) Yeo, J. E.; Khoo, A.; Fagbemi, A. F.; Scharer, O. D. *Chem. Res. Toxicol.* **2012**, *25*, 2462.
- (163) Cai, Y.; Geacintov, N. E.; Broyde, S. *Biochemistry* **2012**, *51*, 1486.
- (164) Reeves, D. A.; Mu, H.; Kropachev, K.; Cai, Y.; Ding, S.; Kolbanovskiy, A.; Kolbanovskiy, M.; Chen, Y.; Krzeminski, J.; Amin, S.; Patel, D. J.; Broyde, S.; Geacintov, N. E. *Nucleic Acids Res.* **2011**, *39*, 8752.
- (165) Kosakarn, P.; Halliday, J. A.; Glickman, B. W.; Josephy, P. D. *Carcinogenesis* **1993**, *14*, 511.

- (166) Watanabe, M.; Ohta, T. *Carcinogenesis* **1993**, *14*, 1149.
- (167) Stover, J. S.; Chowdhury, G.; Zang, H.; Guengerich, F. P.; Rizzo, C. J. *Chem. Res. Toxicol.* **2006**, *19*, 1506.
- (168) Ling, H.; Boudsocq, F.; Woodgate, R.; Yang, W. *Cell* **2001**, *107*, 91.
- (169) Stover, J.; Chowdhury, G.; Zang, H.; Guengerich, F.; Rizzo, C. *Chem. Res. Toxicol.* **2006**, *19*, 1506.
- (170) Zang, H.; Goodenough, A.; Choi, J.; Irimia, A.; Loukachevitch, L.; Kozekov, I.; Angel, K.; Rizzo, C.; Egli, M.; Guengerich, F. *J. Biol. Chem.* **2005**, *280*, 29750.
- (171) Elmquist, C.; Stover, J.; Wang, Z.; Rizzo, C. *J. Am. Chem. Soc.* **2004**, *126*, 11189.
- (172) IARC **1993**, *56*, 245.
- (173) Poirier'pt, M.; Beland, F. *Chem. Res. Toxicol.* **1992**, *5*, 749.
- (174) Choi, J.; Stover, J.; Angel, K.; Chowdhury, G.; Rizzo, C.; Guengerich, F. *J. Biol. Chem.* **2006**, *281*, 25297.
- (175) Stavros, K.; Hawkins, E.; Rizzo, C.; Stone, M. *Nucl. Acids Res.* **2014**, *42*, 3450.
- (176) Ruan, Q.; Kolbanovskiy, A.; Zhuang, P.; Chen, J.; Krzeminski, J.; Amin, S.; Geacintov, N. *Chem. Res. Toxicol.* **2002**, *15*, 249.
- (177) Cosman, M.; Hingerty, B.; Luneva, N.; Amin, S.; Geacintov, N.; Broyde, S.; Patel, D. *Biochem.* **1996**, *35*, 9850.
- (178) Wang, F.; Elmquist, C.; Stover, J.; Rizzo, C.; Stone, M. *Biochemistry* **2007**, *46*, 8498.
- (179) Rechkoblit, O.; Malinina, L.; Cheng, Y.; Geacintov, N.; Broyde, S.; Patel, D. *Structure* **2009**, *17*, 725.
- (180) Biertumpfel, C.; Zhao, Y.; Kondo, Y.; Ramon-Maiques, S.; Gregory, M.; Lee, J.; Masutani, C.; Lehmann, A.; Hanaoka, F.; Yang, W. *Nature* **2010**, *465*, 1044.